UNCLASSIFIED

AD 296 762

Reproduced
by the

ARMED SERVICES TECHNICAL INFORMATION AGENCY
ARLINGTON HALL STATION
ARLINGTON 12, VIRGINIA

UNCLASSIFIED

NOTICE: When government or other drawings, specifications or other data are used for any purpose other than in connection with a definitely related government procurement operation, the U. S. Government thereby incurs no responsibility, nor any obligation whatsoever; and the fact that the Government may have formulated, furnished, or in any way supplied the said drawings, specifications, or other data is not to be regarded by implication or otherwise as in any manner licensing the holder or any other person or corporation, or conveying any rights or permission to manufacture, use or sell any patented invention that may in any way be related thereto.

63-2-4

296 762

296762

CATALOGED BY ASTIA
AS AD NO. _____

DEPARTMENT OF THE ARMY
CORPS OF ENGINEERS

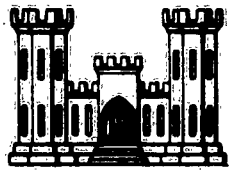

T-1490 a-c

BLINOV, V.I. AND KHUDYAKOV, G. N.

DIFFUSION BURNING OF LIQUIDS

ASTIA
DEC 26 1963

221 pp

U S Army

Engineer Research And

Development Laboratories

FORT BELVOIR, VIRGINIA

DIFFUSION BURNING OF LIQUIDS

[redacted]

T-1490a-c

by

V.I. Blinov and G.N. Khudyakov

Izdatel'stvo Akademii Nauk SSSR, Moscow, 1961

Translated by

RESEARCH INFORMATION SERVICE
Div. of Pergamon International Corp.
122 East 55th Street
New York 22, N. Y.

for

U.S. Army Engineer Research
and Development Laboratories
Information Resources Branch
Translation Analysis Section
Fort Belvoir, Virginia

T - 1490
(a - c)

DIFFUSION BURNING OF LIQUIDS

By

V. I. Blinov and G. N. Khudyakov

Moscow, Academy of Sciences, 1961

208 pages

Contents

(cont'd)

AUTHORS' NOTE

The diffusion burning of liquids is of great theoretical interest and of considerable importance to the national economy. The authors have confined themselves to a discussion of the diffusion burning of liquids in tanks.

In the last fifteen years a considerable amount of experimental and some theoretical material bearing on the physics of the combustion of liquids in tanks has been accumulated; unfortunately, it has not been widely published. Accordingly, there arose a need for collecting and generalizing the results obtained. In writing this book the authors have made use of all the material on the subject with which they are familiar.

The first part of the book is devoted to questions connected with the flammability and ignition of liquids. In this section an important place is occupied by a description of the properties of mixtures of liquids. Without this information it would not be possible to explain a number of phenomena observed in the ignition and burning of mixtures of liquids. The same knowledge is also necessary for the correct interpretation of certain laws governing temperature distribution in burning liquids.

The second part is devoted to the burning of liquids. The problems investigated include those connected with the shape and dimensions of the flame, pulsations, temperature, radiation and various combustion regimes. A description is given of the change in the composition of liquids during combustion and the results of measurements of burnup rates are discussed. An important place in this second part is occupied by an examination of the temperature distribution in burning liquids and by an explanation of the reasons for the appearance and development of a hot homothermic layer in burning gasoline, petroleum and certain other liquids. This section concludes with a consideration of the results of investigations into the problem of the ejection of a burning liquid during combustion and the serious consequences that may ensue.

The third part of the book consists of a discussion of the mechanism of extinguishing the flames from liquids in tanks by means of foam, sprays of water and combinations of various means.

A considerable part of the data reproduced in this monograph was obtained in current research at the laboratory for the intensification of fuel processes of the Energetics Institute of the AS USSR and at the heat physics laboratory of the Central Scientific Research Institute for Fire-Fighting (TsNIIPO).

In addition to the authors this group of workers includes: I.I. Petrov, V.Ch. Reutt, L.A. Volodina, I.V. Gerasimov and N.V. Obukhova.

Our monograph makes use of the work of G.N. Khudyakov, carried out in the ENIN, of V.I. Blinov and coworkers at the Leningrad Institute of Aviation Instrumentation and of recent work by V.I. Blinov and G.N. Khudyakov.

It also utilizes the results of a series of investigations into the extinction of flames from liquids carried out by I.I. Petrov, V.Ch. Reutt and coworkers of the heat physics laboratory of the TsNIIPO.

Finally, the book also incorporates the work of the Bakinsk laboratory of the TsNIIPO and investigations carried out abroad.

The first part of the book was written by V.I. Blinov alone, the second and third parts by him in co-authorship with G.N. Khudyakov.

Part One

THE FLASHING AND IGNITION OF LIQUIDS

1. Flash Point and Ignition Temperature of a Liquid

The burning of a liquid is preceded by flashing and ignition. We shall therefore begin by examining the fundamental characteristics of these phenomena.

If isoamyl alcohol is poured into a test tube and slowly heated and a small flame is then approached, at a certain temperature the mixture of alcohol vapor and air will flash. This temperature is ordinarily called the flash point. It defines the lower limit of flashing.

If the alcohol is heated further and a flame again approached, the mixture will again catch fire. The lowest temperature of the liquid ϑ_B, at which the mixture continues to burn, is called the ignition point of the liquid.

If the source of heat is removed, the flame forming at the ignition point is not extinguished. The temperature at the surface of the liquid rises owing to the heat from the flame and reaches a definite value. We shall call this temperature the temperature of the burning liquid. The temperature of the liquid during burning ϑ_b is close to the boiling point of the liquid ϑ_k, but somewhat lower than the latter.

If a combustible liquid is heated in a closed vessel, the cover lifted slightly from time to time and a flame brought up to the opening, then on reaching the flash point the mixture of vapor and air will flash. If the experiment is continued, then flashing will occur even at higher temperatures, until the upper limit of flashing ϑ_{BC} is reached. At temperatures above this limit, the mixture of vapor and air in the vessel will not ignite, but a flame of burning vapor may form at the opening. The vapors of burning liquids and air form mixtures which at given concentrations explode. At concentrations below the lower limit the mixture does not flash and does not burn, within the concentration limits flashing is observed, while above the upper limit we get mixtures that do not explode but may burn in air when $\vartheta > \vartheta'_{BC}$.

Thus, ϑ_{BC}, the flash point, is lower than the ignition point ϑ_B. The ignition point is lower than the temperature of the burning liquid ϑ_b. The upper limit of flashing ϑ'_{BC} is also lower than ϑ_b. As already pointed out, the temperature of the liquid during burning is close to the boiling point of the liquid

$$\vartheta_{BC} < \vartheta_B < \vartheta_r, \quad \vartheta_{BC} < \vartheta'_{BC} < \vartheta_r.$$

If the flash point is low, the ignition point will only be slightly different. If the flash point is high, the ignition temperature may considerably exceed the latter. This is obvious from the data given below (in °C) for gasoline and lubricating oil:

	Gasoline			
Boiling point	60-70	70-88	80-115	100-150
Flash point	-39	-45	-21	+10
Ignition point	-34	-42	-19	+16

	Lubricating Oil			
Flash point	185	150	215	285
Ignition point	212	186	265	344
Difference	27	36	50	59

Note also the flash, boiling and ignition points (in °C) of ethyl alcohol, n-butyl alcohol and acetone:

	Flash point	Upper limit of flashing	Ignition point	Boiling point
Ethyl alcohol	+10	+41	69-76	78
n-butyl alcohol	+34	+61	105	117
Acetone	-20	+7.5	55	56

2. Instruments for Determing Flash and Ignition Points

The same instruments are usually used for determining both flash and ignition points /1,2/. Since these points depend on the experimental conditions, the latter are kept strictly constant.

The ignition and flash points are sometimes determined by the Brenken method (Fig. 1). This requires a porcelain crucible 6.4 cm in diameter and 4.7 cm deep. The test liquid is poured into the crucible, until the level is 1.2 cm below its edge. The crucible is then placed in a sand bath. Between the bottom of the crucible and the bath there must be a thick layer of sand and the level of the liquid in the crucible and that of the sand in the bath must be the same. A thermometer is introduced into the liquid. The bath is heated so that the temperature in the crucible rises at not more than 3-4° a minute. Every half minute a small flame 4-5 mm long is moved towards the edge of the crucible. The flame must remain at the edge of the crucible for no more than 2 seconds. The temperature at which flashing is observed is the flash point of the liquid in question. If heating is continued, on reaching the ignition point a flame will be formed.

By means of special instruments the flash and ignition points can be determined with greater precision. The Abel-Pensky instrument is

used if the flash point is less than 50°, and the Pensky-Martens instrument if the flash point is greater than 50°. In these instruments the liquid is heated in closed vessels with small openings in the lids. These openings are closed with a slide. During the test the slide is opened and a small flame moved up to the opening. The vessels are fitted with agitators for mixing liquids.

The flash points of lubricating oils are determined in a Markusson instrument, similar to the Brenken apparatus but with a different size of cup.

Flash points determined by closed cup methods are always somewhat lower than the corresponding points (in °C) obtained by open cup techniques. Thus,

	Flash Point	
	Closed Cup	Open Cup
Petroleum	30	46
Mazut	96	119
Solar oil	148	160
Machine oil	196	212
Cylinder oil	215	236

The flash points of many substances will be found in reference works /3,4/.

We must again stress the fact that the flash and ignition points depend on the experimental conditions. ϑ_{BC} and ϑ_{B} cannot be treated as if they were physical constants.

3. Flash Point of Liquids and Limits of Ignition of Mixtures

In mixtures of vapor and air over a liquid, formed at temperatures of the liquid below the flash point and above the upper limit of flashing a flame cannot spread and embrace the entire mixture. Thus, the temperatures ϑ_{BC} and ϑ'_{BC} are connected with the concentration limits of ignition of mixtures of vapor and air or, in other words, with the limits of flame propagation in mixtures. It is easy to establish the relation connecting ϑ_{BC} and ϑ'_{BC} and the limits of ignition k.

The limit of ignition k of a mixture can be determined from the formula:

$$k = \frac{V_v}{V_v + V_B} \cdot 100, \qquad (1.1)$$

where V_v is the volume of vapor and V_B the volume of air for a mixture of limiting composition.

If by p_v and p_B we denote the partial pressures of vapor and air in the mixture, by p_o the atmospheric pressure and by V_o the volume of mixture obtained for the pressure p_o, then, in accordance with the Boyle-Mariotte

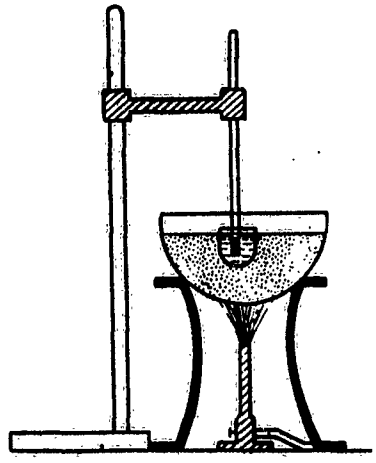

Fig. 1: Brenken apparatus for determining the flash and ignition points of liquids.

law, we can write:

$$p_V V_0 = p_0 V_V \quad \text{and} \quad p_B V_0 = p_0 V_B \tag{1.1a}$$

From (1.1) and (1.1a) it follows that the limit of ignition k is equal to

$$k = \frac{p_V}{p_V + p_B} \cdot 100. \tag{1.2}$$

But

$$p_V + p_B = p_0,$$

and the partial pressure of the vapor is equal to the saturated vapor pressure π at the flash point. If p_0 = 760 mm, then

$$\pi = 7.6\ k \tag{1.3}$$

i.e. the saturated vapor pressure at the flash point is equal (at normal atmospheric pressure) to 7.6 k.

Table 1.1 shows that relation (1.3) is in good agreement with experiment.

4. Autoignition and Forced Ignition of Gas Mixtures

The flashing of liquids is a special case of the ignition of mixtures of gases. Experience shows that two kinds of ignition are possible. In the first the whole of a given mixture is brought to a certain temperature, above which it ignites spontaneously. In the second a cold mixture

Table 1.1*

	Lower limit of ignition k_H, exper.	Lower limit of flashing		Upper limit of ignition k_B	Upper limit of flashing	
		exper.	from (1.3)		exper.	from (1.3)
Benzene	1.3	-12	-11.5	6.75	+12	+12
Methyl alcohol	3.5	- 1	- 1.5	-	-	-
Ethyl "	2.6	+10	+ 8	-	-	-
Butyl "	1.7	+35	+35	8.0	+62	+60
Acetone	2.55	-19.8	-20	-	-	-
Toluene	1.3	+ 5	+ 6	7.0	+38	+38
Aniline	1.58	+71	+71	-	-	-
Diethyl ether	1.2	-45	-49	-	-	-

* all temperatures in °C.

is ignited only at a certain point in space by means of a high-temperature source and the rest of the mixture ignites without outside interference thanks to the spreading of the combustion zone. Thus, we can talk about spontaneous and forced ignition.

Flashing is usually brought about by means of some kind of source and may therefore be classed as an example of forced ignition.

The theory of forced ignition has been sufficiently well explored. Before discussing it, we shall return to the question of autoignition of gas mixtures, since even forced ignition involves spontaneous ignition in the first stage.

The thermal theory of autoignition was first proposed by Academician N.N. Semenov /5/. This theory consists in the following. Suppose the inflammable liquid under investigation is placed in a vessel of volume V and the temperature T_o of the walls of the vessel is kept constant. A chemical reaction will take place in the mixture. We shall assume that the temperature in the vessel is everywhere the same and equal to T and that the reaction velocity ω

$$w = k_0 c^n e^{-\frac{E}{RT}}, \tag{1.4}$$

where c is the oxygen concentration;
n the order of the reaction;
R the universal gas constant;
E the activation energy;
T the temperature of the gas.

If the thermal effect of the reaction is q, the rate of liberation of heat in the vessel will be equal to

$$q_1 = q k_0 c^n \exp\left(-\frac{E}{RT}\right) \cdot v. \tag{1.5}$$

Part of the heat, liberated as a result of the reaction, goes to heating the mixture and part is released into the surrounding medium. The amount of heat lost will be equal to

$$q_2 = \alpha (T - T_0) S, \tag{1.6}$$

where α is the heat-transfer coefficient;
S the surface area of the vessel walls.

In order to explain under what conditions the mixture will ignite spontaneously, we turn to Fig. 2, in which the temperature T is plotted against the quantity of heat liberated and removed per unit of time q. The three curves $q_2(T)$ correspond to different values of T_o.

Under steady-state conditions q_1 will be equal to q_2 and the corresponding temperature will be equal to the abscissa of the points of intersection of the curves $q_1(T)$ and $q_2(T)$. It is clear from the figure that in certain cases the curves intersect in two points and sometimes in one.

Let us consider the first of these two possibilities. The mixture is heated from an initial temperature T_o. Heating is interrupted and the mixture enters a state of equilibrium when the temperature of the gas is equal to T_a, corresponding to the lower point of intersection "a" of the curves q_1 and q_2. This regime will be a stable one. The second point of intersection "b" lies in a region of higher temperatures and in this case the thermal regime, as it is easy to see, will be unstable: on departing from the state corresponding to point "b", the system does not return to "b", but moves further away from this state.

When the temperature T_o of the walls of the vessel is raised, the curve q_2 will be displaced to the right, and the value of the stationary temperature T_a will increase smoothly and continuously. At a certain wall temperature T_{OB} the curves $q_1(T)$ and $q_2(T)$ will touch, as with the center curve in Fig. 2. The tangent point c of the curves will be the point marking the limit of existence of the stationary regime. If there is an increase in the wall temperature above T_{OB}, no matter how small, stationary conditions will not be preserved and there will be a sharp rise in the temperature and hence in the rate of combustion of the mixture. The phenomenon consisting in the transition from a slowly proceeding reaction, accompanied by insignificant heating, to a violent, progressively accelerating combustion of the mixture will also be a phenomenon of autoignition or a "thermal explosion".

We would get a picture similar to that described, if the heat transfer conditions remained invariable and the reaction velocity changed with changes in the concentration c or the pressure p (Fig. 3).

Let us know consider the quantitative relations characterizing the phenomenon of autoignition of gas mixtures.

At the tangent point q_1 and q_2 and their temperature derivatives are equal. Thus, for the critical condition the following relations will hold:

$$k_0 V q c^n \exp\left(-\frac{E}{RT_s}\right) = \alpha (T_s - T_0) s \tag{1.7}$$

and

$$k_0 V q c^n \frac{E}{RT_s^2} \exp\left(-\frac{E}{RT_s}\right) = \alpha s. \tag{1.8}$$

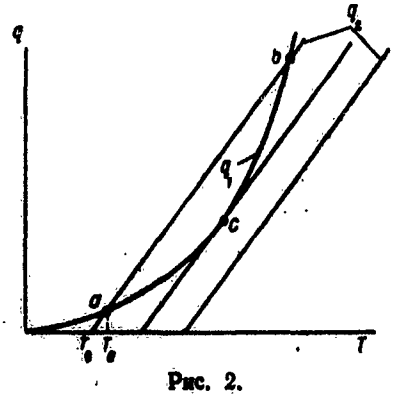

Рис. 2.
Fig. 2

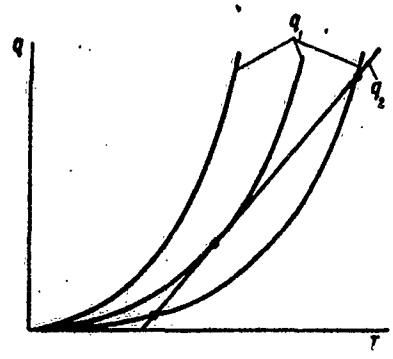

Рис. 3.
Fig. 3

On dividing the left hand and right hand sides of these equations, we get

$$\frac{E}{RT_s^2}(T_s - T_0) = 1$$

or

$$T_s^2 - \frac{E}{R} T_s + \frac{E}{R} T_0 = 0.$$

Whence

$$T_s = \frac{E}{2R}\left(1 \pm \sqrt{1 - \frac{4R}{E} T_0}\right).$$

In the last formula the minus sign in front of the square root corresponds to the ignition point.

Since usually $T_0 \ll \frac{E}{2R}$, the expression under the root sign can be replaced with a series expansion and we can limit ourselves to its first three terms. We shall then have

$$T_B = \frac{E}{2R}\left[1 - \left(1 - \frac{2RT_0}{E} - \frac{2R^2T_0^2}{E^2}\right)\right]$$

and finally

$$T_B = T_0 + \frac{RT_0^2}{E}. \qquad (1.9)$$

From (1.9) it is clear that the autoignition point T_B differs only slightly from the temperature T_0 of the medium. In certain cases, therefore, we can take T_0 instead of T_B, without too serious an error. We shall use T_0 in (1.8), rewriting it in the form:

$$qk_0Vc^n e^{-\frac{E}{RT_0}} = \frac{\alpha s R T_0^2}{E}. \qquad (1.10)$$

This last relation links the composition of the mixture with the ignition point. If we put n = 2, $T_B(c)$ will give a curve (Fig. 4) representing the boundary of the explosive region. Thus, it follows from the theory, in full accord with experiment, that not every mixture can ignite and that the only mixtures that do are those, the composition of which lies within the corresponding limits of concentration. These limiting concentrations, moreover, correspond to the upper and lower limits of flashing of liquids.

Fig. 4: Ignition point as a function of the percentage composition of the mixture for constant pressure. Top: "explosive region".

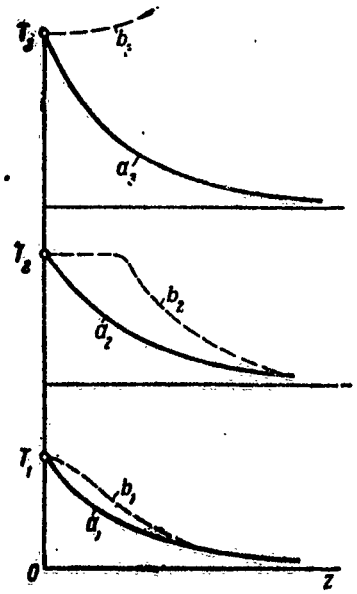

Fig. 5

The phenomenon of autoigniti... an also be explained in terms of the so-called chain theory. This theory was developed by N.N. Semenov and his coworkers and is discussed in Semenov's monograph /5/.

An analysis of the experimental data shows that in certain cases autoignition has a thermal character and in others a chain character. In what follows we shall confine ourse... s to questions relating to the thermal theory of ignition.

In forced ignition only a small volume of the medium is heated. This is done by introducing into the mixture either an incandescent body, a flame or a spark. Essentially the process of autoignition and that of forced ignition are the same, but the latter is more complex. In forced ignition the critical conditions are also linked with the properties of the source and the conditions of propagation of the flame.

For an explanation of the mechanism of the ignition of a mixture by an incandescent body let us turn to the reasoning of van't Hoff /6/. We shall assume that the temperature T_1 at the surface of a body, immersed in a gaseous medium and acting as a source of ignition, is higher than the temperature of the gas, but lower than the temperature at which the mixture ignites. In an inert medium the distribution of temperature T close to the wall is depicted by curve a_1 (Fig. 5). In a medium, in which a chemical reaction can proceed, the curve T(z) will lie (owing to the liberation of heat) somewhat above a_1 and will have a shape similar to that of b_1 in Fig. 5.

If the temperature of the body is raised, then in an inert medium it will fall more quickly than in the preceding case and is represented by the curve a_2, similar to a_1, while in a reactive medium, owing to the increase in reaction velocity with increase in temperature, the curve T(z) at the wall will fall more slowly than in the preceding case, and there will exist a temperature T_2 of the body, at which the temperature of the reacting gas will not fall on moving away from the source, even close to the latter, and the curve T(z) will then run parallel to the abscissa. If the temperature of the hot body is further increased, the temperature of the reacting medium will progressively rise with increase in z, until the combustible mixture of gases ceases to ignite. The temperature T_2 will be the critical temperature, analogous to the ignition point in the process of autoignition.

Thus, as Ya.B. Zel'dovich /7/ also shows, the limiting critical condition of forced ignition should be written in the form:

$$\left(\frac{dT}{dz}\right)_{\text{CT}} = 0, \tag{1.11}$$

where CT indicates that the temperature gradient relates to the layer at the surface of the wall (source). This condition shows that from the moment the temperature of the source reaches a certain critical value, the source ceases to take part in the process, which is now determined by the conditions in the layer of gas in contact with the very hot body.

Experimental data show that in f ..d ignition the critical temperature may exceed the autoignition point of the mixture. This is because the gas temperature quickly falls as one moves away from the surface of the hot body, and the concentration of combustible substance close to its surface is lower than in the rest of the medium (owing to the chemical reaction). There are cases where a reaction proceeds at the hot body, but the flame is not propagated.

Convincing proof of the important part played by the impoverishment of the combustible layer close to the incandescent body is to be found in the fact that gas mixtures are harder to ignite with a body that acts as a catalyst for the mixture in question. In this case the surface reaction is more intense, and the concentration of reacting gases close to the surface falls more sharply than it would for a noncatalytic surface. Accordingly, the temperature of the surface rises significantly, but the distribution of temperature and concentration in the gas are such that the ignition conditions become less favorable.

In forced ignition the critical temperature depends on the dimensions of the source. This was the subject of investigations by Silver and Paterson /8,9/, who studied the ignition of gas mixtures by means of balls of different diameters dropped into the mixture. Fig. 6 shows the results of Silver's experiments with illuminating gas. It is evident from the figure that the ignition temperature falls with increase in the diameter of the balls. Paterson has shown that the ignition point essentially depends on the rate of fall of the balls.

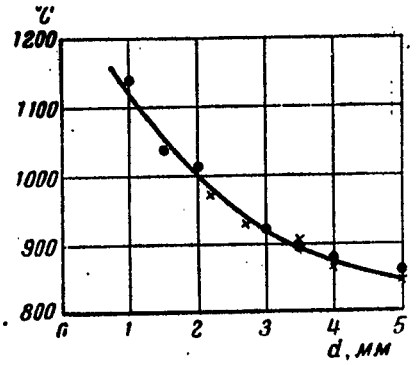

Fig. 6: Ignition point as a function of the diameter of the ball.

These results may be attributed to the fact that the temperature distribution close to the source depends on the size and rate of motion of the latter.

The first attempt to provide a theory of the ignition of gas mixtures by a hot body was made by Silver. Ya.B. Zel'dovich /7/ has offered a more rigorous solution of the problem.

We shall consider the problem for the very simple case in which a combustible gas mixture lies between two infinite plane parallel walls. We shall assume that one wall is at the temperature T_s, while the other is

held at the temperature T_0 and that $T_s > T_0$. The temperature distribution in the gas will only be steady, if the temperature of the heated wall does not exceed the critical value. As already noted, under critical conditions

$$\left(\frac{dT}{dz}\right)_{CT} = 0.$$

We shall find the temperature distribution in the gas by solving the equation of thermal conductivity, which in this case for the steady state can be written in the following form:

$$\lambda \frac{d^2T}{dz^2} + qw = 0, \tag{1.12}$$

where λ is the thermal conductivity of the gas, q the Q-value and w the reaction velocity.

$$w = k_0 c^n \exp\left(-\frac{E}{RT}\right).$$

We shall introduce the new variable

$$y = \frac{dT}{dz}$$

and write equation (1.12) so that

$$y \frac{dy}{dT} = -\frac{qw}{\lambda}. \tag{1.13}$$

On integrating, we get

$$y = \sqrt{\frac{2}{\lambda} q \int_T^{T_s} w(T)\, dT}.$$

Whence it follows that the heat flux in the gas

$$q_z = \lambda \frac{dT}{dz} = \lambda \sqrt{\frac{2}{\lambda} q \int_T^{T_s} w\, dT}.$$

Since the reaction velocity w depends heavily on the temperature, the reaction in the gas between the walls will be practically limited to a narrow layer δ adjacent to the heated wall. Inside this layer, under conditions close to the critical, $T_s - T$ will be small compared with T; accordingly, without too serious an error we can assume that

$$\frac{1}{T} = \frac{1}{T_s\left(1 - \frac{T_s - T}{T_s}\right)} = \frac{1}{T_s}\left(1 + \frac{T_s - T}{T_s}\right)$$

and that

$$e^{-\frac{E}{RT}} = e^{-\frac{E}{RT_s}} e^{-\frac{E}{RT_s^2}(T_s - T)} \qquad (1.14)$$

Substituting (1.14) in (1.13), integrating and bearing in mind that under critical conditions condition (1.11) must be fulfilled, we get

$$y = \frac{dT}{dz} = \sqrt{\frac{2q}{\lambda} w(T_s) \frac{RT_s^2}{E} \left[1 - e^{-\frac{(T_s - T)}{RT_s^2} E}\right]}.$$

When $T_s - T$ varies by tens of degrees, $\exp\left[-\frac{(T_s - T)\,E}{RT_s^2}\right]$ changes from 1 to 0.4. Hence outside the zone δ the value of y differs little from

$$y = \sqrt{\frac{2q}{\lambda} w(T_s) \frac{RT_s^2}{E}}.$$

Thus, the heat flux from the reaction zone will be equal to

$$q_2 = \lambda \sqrt{\frac{2q}{\lambda} w(T_s) \frac{RT_s^2}{E}}.$$

Under steady-state conditions this heat flux can be represented, without serious error, by

$$q_1 = \lambda \frac{T_s - T}{d}.$$

Hence it follows that for steady-state conditions

$$\sqrt{\frac{2q}{\lambda} w(T_s) \frac{RT_s^2}{E}} = \frac{T_s - T}{d}. \qquad (1.15)$$

Relation (1.15) establishes the dependence of the critical parameters and the conditions, under which ignition occurs, on the dimensions of the vessel.

A more complete and rigorous theory of ignition has recently been advanced by L.N. Khitrin and S.A. Gol'denberg /10/.

Spark ignition is a more complex phenomenon than hot-body ignition. A spark is characterized by intense local excitation of the molecules, which become ionized. At the same time a spark causes a sharp local increase in the temperature of the gas. A spark may be considered as a special kind of gaseous incandescent body. This is the reason for the

existence of two theories of spark ignition, the ionic and the thermal. It is clear that the thermal aspect of the phenomenon has great importance, since the conditions at the flame front, remote from the source of ignition, are decisive.

In spark ignition for each mixture there is a certain minimum spark power, starting from which the mixture will ignite. This power depends on the composition of the mixture, the pressure and the temperature. The nature of the dependence of the spark power on the composition of the mixture is shown in Fig. 7. For each gas there is a minimum of the minimum powers, for which a given gas cannot be ignited for any mixture of itself and air. For a given spark power, in excess of the minimum, there are two values of the composition of the mixture that are limiting values. Outside these limits ignition is impossible, and between these limits any mixture will ignite.

As the spark power increases, the limits of ignition progressively spread, as shown in Fig. 8, and tend to a certain limiting value. The spark, for which the critical conditions of ignition are not dependent on a further increase in power, is called the saturation spark.

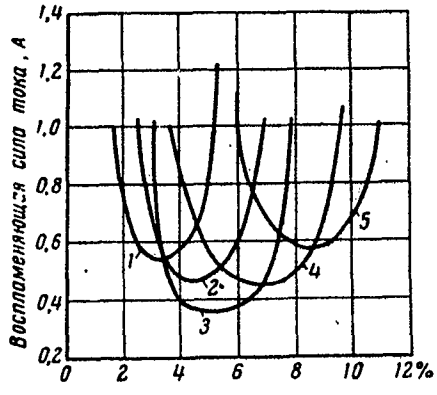

Fig. 7: Minimum spark power capable of igniting mixture as a function of mixture composition.

1 - hexane; 2 - butane; 3 - propane; 4 - ethane; 5 - methane. Ordinate: current (amps).

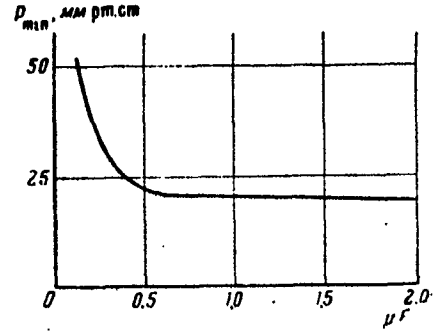

Fig. 8: Mininum ignition pressure as a function of spark power. Ordinate: mm Hg.

The literature contains a great deal of experimental data on the forced ignition of combustible gas mixtures. Particularly important is the information published on the concentration limits of ignition. Certain results in this area are reproduced in Table 1.2.

Table 1.2

Liquid	Limits, vol-%		Liquid	Limits, vol-%	
	lower	upper		lower	upper
Benzene	1.41	6.75	Ethyl alcohol	3.28	18.95
Toluene	1.27	6.75	Propyl "	2.55	-
o-xylene	1.00	6.00	Isopropyl "	2.65	-
Acetone	2.55	12.80	Butyl "	1.70	-
Ethyl ether	1.85	36.50	Isobutyl "	1.68	-
Methyl alcohol	6.62	36.50	Amyl "	1.19	-

The pressure, temperature and the presence of admixtures in the gas have an important influence on the limits of ignition. These questions, and others relating to ignition, will be found discussed in the literature /6/.

All the fundamental laws and theoretical results relating to spontaneous and forced ignition of gas mixtures can also be extended to the flashing of liquids, bearing in mind that in flashing the concentration of vapor in the mixture depends on the temperature of the liquid.

5. Flame Propagation in Combustible Gas Mixtures

In the forced ignition of mixtures a particularly important part is played by flame propagation. The first and most important contribution to this question was that of V.A. Michelson in 1889 /11/.

In the last twenty years the theory of normal flame propagation has been developed by N.N. Semenov /12/, Ya.B. Zel'dovich, D.A. Frank-Kamenetskiy and a number of others /12,13/.

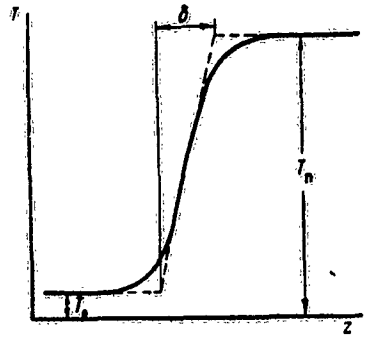

Fig. 9: Temperature distribution in a gas mixture through which a flame is being propagated.

In its simplest form the modern theory of flame propagation goes somewhat as follows. Let us assume that a flame is being propagated in a gas mixture. In front of the flame there will be fresh mixture and behind it the products of combustion. Let the gas move towards the flame at a rate equal to the rate of propagation of the flame. Then the flame will be fixed. The temperature distribution in the gas is represented schematically by the curve shown in Fig. 9. We shall denote the temperature of the mixture remote from the flame by T_o and the temperature of the combustion products T_p.

We shall substitute for the curve T(z) a broken line consisting of the straight segments $T = T_o$, $T = T_p$ and the tangent to the curve T(z) at the point of inflection.

The quantity of heat

$$q = \lambda \frac{T_p - T_o}{\delta}, \tag{1.15a}$$

is delivered by thermal conduction from unit surface of the flame per unit of time, where λ is the thermal conductivity and δ the nominal thickness of the flame front. This heat is expended in warming the mixture from the initial temperature T_o to the temperature T_p. Thus,

$$q = uc\rho (T_p - T_0), \tag{1.15b}$$

where u is the flow velocity of the gas, equal to the rate of propagation of the flame, c is the specific heat and ρ the density of the mixture.

From (1.15a) and (1.15b) it follows that

$$u = \frac{\lambda}{c\rho\delta} = \frac{a}{\delta}, \tag{1.16}$$

where $a = \lambda/c\rho$ is the average value of the thermal diffusivity.

Since the reaction velocity increases very strongly with increase in temperature, the combustion of the bulk of the mixture proceeds in a region, the temperature of which is close to the maximum T_p, and the reaction zone ξ is less than δ. We may assume that the width of the reaction zone ξ is equal to the product of the velocity u and the residence time of the mixture in the combustion zone τ

$$\xi = u\tau, \tag{1.16a}$$

and that the time τ is inversely proportional to the reaction velocity $k = k_o \exp\left(-\frac{E}{RT_p}\right)$, i.e.

$$\tau = \frac{1}{k} = \tau_0 e^{\frac{E}{RT_n}}. \tag{1.16b}$$

Here E is the activation energy of the reaction, R is the universal gas constant.

We shall put

$$\xi = b\delta, \tag{1.16c}$$

where b is a dimensionless multiplier less than unity; the numerical value of b is determined by the form of the kinetics of the combustion reaction.

Using (1.16a,b,c) we get

$$u = \sqrt{b\frac{a}{\tau_0}e^{-\frac{E}{RT_p}}} = b_0 e^{-\frac{E}{2RT_p}}, \tag{1.17}$$

where b_o is a quantity depending on the properties of the mixture.

Heat removal from the flame reduces the combustion temperature and hence the rate of propagation of the flame. If the heat losses are sufficiently great, combustion will be interrupted, the flame will go out and will no longer be propagated through the mixture. By taking into account the effect of heat losses on the maximum temperature and the rate of flame propagation and the reciprocal effect of the rate of flame propagation on the heat losses, we can determine the limits of flame propagation. The theory of the limits of flame propagation proposed by Zel'dovich /12,14/ is based on these considerations.

On examining the heat losses in flame propagation, Zel'dovich came to the conclusion that the reduction in the maximum flame temperature T_p with respect to the theoretical T_{theor} is inversely proportional to the square of the rate of flame propagation

$$T_{theor} - T_p = \frac{\alpha}{u^2}, \tag{1.18}$$

where α is the heat transfer coefficient.

By simultaneously solving (1.17) and (1.18) we get the rate of flame propagation for the given conditions.

Equations (1.17) and (1.18) can be solved graphically. For this it is necessary to take a rectangular system of coordinates, plot T_p along the abscissa and the rate of flame propagation u along the ordinate and use (1.17) and (1.18) to construct the corresponding curves; the coordinates of the points of intersection of these curves give the values of u and T_p sought.

In Fig. 10 curves 1, 2 and 3 are based on (1.18). In plotting these curves the values of T_{theor} were assumed to be the same, and those of α different for the different curves ($\alpha_1 > \alpha_2 > \alpha_3$). Curve 4 graphically represents the connection between u and T_p given by equation (1.17). Curves 3 and 4 intersect at points a and b. The coordinates of these points give

values of u and T_p satisfying equations (1.17) and (1.18). It is easy to see that point a corresponds to an unstable regime and point b to a stable regime, when combustion proceeds at a temperature close to the theoretical. When heat transfer and hence the coefficient α increases, the points of intersection of the curves will approach and the temperature T_p and the rate of propagation of the flame, corresponding to stable conditions, will fall. For a value of α corresponding to curve 2 the curves corresponding to equations (1.17) and (1.18) will have a common tangent in the point b. With a further increase in α these curves will cease to intersect and the flame will not be propagated in the mixture; it will go out, because in these conditions the removal of heat from the combustion zone is large. It is clear that the point b determines the limit of ignition of the mixture. We shall compute the values of T_p and u corresponding to this limit.

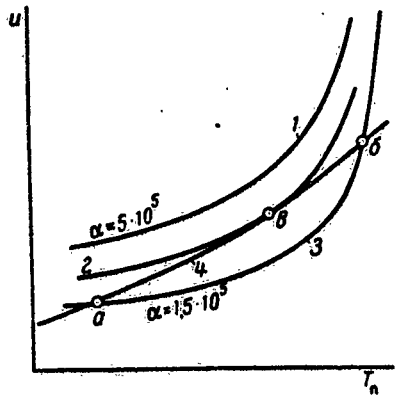

Fig. 10: Curves illustrating computation of ignition temperature.

It follows from (1.17) that

$$\frac{du}{dT_p} = b_0 \frac{E}{2RT_p^2} \exp\left(-\frac{E}{2RT_p}\right) = \frac{uE}{2RT_p^2},$$

and from (1.18) that

$$\frac{du}{dT_p} = \frac{u^3}{2\alpha} = \frac{1}{2} \frac{u}{T_{theor} - T_p}.$$

At point b the tangents to the curves coincide and hence the derivatives du/dT_p are equal. Equating them, we find that the limiting value of T_p (T_{lim}) is equal to:

$$T_{lim} = T_{theor} - \frac{RT_{lim}^2}{E}$$

or, approximately,

$$T_{lim} = T_{theor} - \frac{RT^2_{theor}}{E}. \qquad (1.19)$$

It is also easy to find the limiting rate of flame propagation u_{lim}. For this we first transform the exponent in (1.17), putting $T_p = T_{lim}$

$$\frac{E}{2RT_{theor}} = \frac{E}{2R\left(T_{theor} - \frac{RT^2_{theor}}{E}\right)} = \frac{E}{2RT_{theor}\left(\frac{1 - RT_{theor}}{E}\right)}.$$

Since RT_{theor} does not exceed several thousands and E is ordinarily equal to several tens of thousands, RT_{theor}/E is considerably less than unity, and without serious error we can write:

$$\frac{E}{2RT_{lim}} = \frac{E}{2RT_{theor}}\left(1 + \frac{RT_{theor}}{E}\right),$$

$$u_{lim} = b_0 \exp\left(-\frac{E}{2RT_{lim}}\right) = b_0 \exp\left(-\frac{E}{2RT_{theor}} - \frac{1}{2}\right).$$

From the last relation it follows that

$$u_{lim} = \frac{u_{max}}{\sqrt{e}}. \qquad (1.20)$$

Here u_{max} is the maximum rate of flame propagation in a mixture of the given composition:

$$u_{max} = b_o \exp\left(-\frac{E}{2RT_{theor}}\right).$$

(1.19) shows that the flame cannot spread through the entire mixture, if the flame temperature is lower than the theoretical by an amount exceeding $\frac{RT^2_{theor}}{E}$.

In flame propagation in narrow tubes, the reduction in combustion temperature is due to heat transfer to the walls of the tube. In flame propagation in broad tubes the reduction in flame temperature is due to radiative heat losses.

6. Flame Propagation on the Surface of a Combustible Liquid

When a liquid is flashed, the flame is propagated over the liquid. This phenomenon has been studied by P.G. Ipatov /15/, who has contributed a very clear account of the mechanism.

Ipatov carried out three series of experiments. In the first he used a setup consisting of two identical horizontal glass tubes A and B (Fig. 11), connected together and forming part of a closed system, into which he also introduced a pump H and an evaporator E containing the test liquid. The tubes were 52 cm long and 3.3 cm in diameter. In tube A was a thin layer of the combustible test liquid. The pump H circulated the vapor-air mixture through the system and made it possible to saturate the air in A and B with vapor relatively quickly. The tubes were mounted in a thermostat, the temperature of which could be varied.

After the temperature in the thermostat had been brought to the required value, and the air in the tubes was saturated with vapor, the stoppers a and b were removed and the mixture at the open end of the tube ignited with an electric spark supplied by a small induction coil. The flame was photographed with the aid of a "Kiev" camera, in front of the objective of which a disc with circular openings slowly rotated. In this way a series of successive images of the flame were obtained. The photographs were used to compute the rate of displacement and the normal velocity of propagation of the flame.

Fig. 12 shows the results of the experiments with ethyl alcohol. The temperature is plotted along the abscissa and the normal rate of propagation of the flame in the tubes along the ordinate. The hollow circles indicate data for tube A (with the liquid) and the solid circles data for tube B (without liquid). It is clear from the figure that the rate of flame propagation in the tubes with and without liquid was the same and that a flame developed and spread, only when the temperature of the system was within the flash limits.

The experiments showed that the temperature at the surface of a liquid in a tube does not change when a flame passes. Similar results were obtained for benzene and acetone.

The second series of experiments, employing the same setup, was designed to investigate flame propagation in tubes with and without liquid at system temperatures lower than the flash point of the liquid and for an igniter in the form of a strongly heated metal spiral. During the experiment the tubes were opened at one end, where the ignition spirals were introduced. In tube A the spiral was placed close to the surface of the liquid. In tube B there was no flame even at the maximum igniter temperature. A flame developed in tube A some time after switching on the current in the spiral (the flame began to spread through the tube when the temperature of the liquid near the spiral was close to the flash point) and after progressing a certain distance went out. At temperatures below a certain limit there was no flame in tube A.

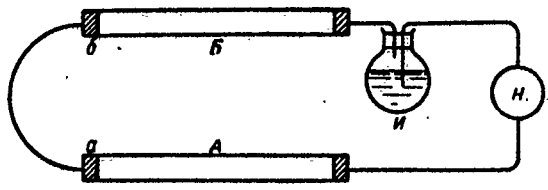

Fig. 11: Ipatov's apparatus.

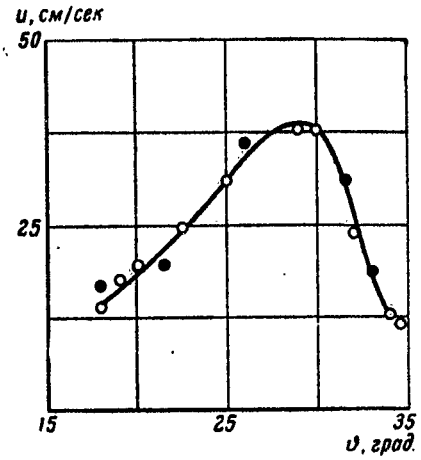

Fig. 12: Normal rate of flame propagation at the surface of ethyl alcohol as a function of the temperature. u in cm/sec; in degrees.

Table 1.3 gives the results of the second series with ethyl alcohol. Here ϑ is the temperature of the liquid; l the distance covered by the flame in the tube; t the time during which the flame was propagated, in sec; v the mean rate of displacement of the flame, in cm/sec.

Table 1.3

ϑ, °C	l, см	t, сек	$\bar{v}$, см/сек	ϑ, °C	l, см	t, сек	$\bar{v}$, см/сек
0	0	0	0	5,1	21	4	5
1,0	0	0	0	6,5	32	5,3	6
2,3	0	0	0	8,0	52	5,5	9,4
3,3	10	4	2,5	10,0	52	5	10,4
4,0	15	4	3,7				

It is clear from the table that between 2° and 10° the increase in l was proportional to the increase in temperature ϑ and that in this case the limiting temperature was 2°, i.e. when $\vartheta < 2°$ no flame developed in the tube with liquid. It should be noted that the flash point of ethyl alcohol is close to 10°.

The third series was devoted to a study of the propagation of a flame at the surface of a liquid poured into an open trough 5 cm wide and 52 cm long. The liquid was ignited by means of an incandescent metal spiral, close to its surface at the end of the trough. The time taken by

the flame to pass along the trough was determined by means of a stopwatch. Butyl, isoamyl and ethyl alcohol, toluene and two mixtures of ethyl alcohol and toluene were tested. The results are shown in Fig. 13, where the abscissa represents the temperature of the liquid and the ordinate the rate of displacement of the flame; the hollow circles denote experimental data. The flash point of the corresponding liquids is marked by a broken line. The figure also shows some results for the rate of flame displacement in ethyl alcohol vapor in tubes.

From Fig. 13 we can conclude that at a temperature ϑ of the liquid, not exceeding the flash point ϑ_{BC}, the flame velocity along the length of the trough is small and increases with increase in v; at temperatures exceeding ϑ_{BC} the flame is propagated with a velocity close to the rate of displacement of a flame in a tube.

At temperatures below the flash point a flame develops not immediately after the spiral has become hot, but after a certain time lag, which is the greater the lower the temperature of the liquid.

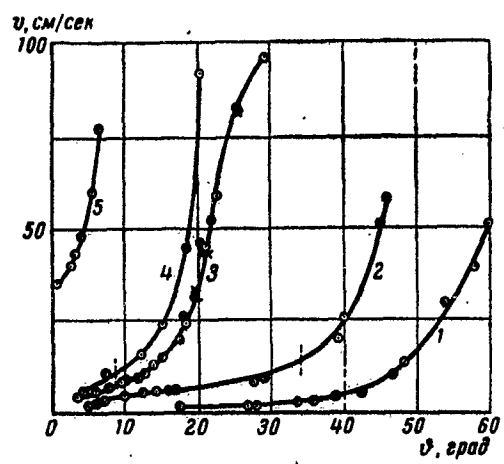

Fig. 13: Rate of flame displacement at the surface of various liquids as a function of the liquid temperature. v in cm/sec; in degrees.

1 - isoamyl alcohol; 2 - butyl alcohol; 3 - ethyl alcohol; 4 - toluene; 5 - mixture, 0.69 molar fraction ethyl alcohol.

The results of Ipatov's experiments show that at low liquid temperatures an important part in flame propagation is played by the heating of the liquid by the flame. It is obvious that for $\vartheta < \vartheta_{BC}$ a flame develops in a mixture of vapor and air, when the concentration of the latter near the spiral reaches a value corresponding to the flash point. The flame warms

the adjacent layers of liquid, the concentration of vapor over which increases, the mixture in the same region ignites, the displaced flame warms up the next layer of liquid and so on. At temperatures above the flash point of the liquid the part played by heating in flame propagation is relatively small; the flame is propagated through the mixture already available.

It should be noted, however, that in the propagation of a flame over the surface of a liquid in an open vessel an upper flash limit is not observed. In fact, if the concentration of vapor at the surface of the liquid exceeds the concentration corresponding to the upper limit, then at a certain distance from the liquid the latter will not exceed the limit, owing to the fall in concentration.

Returning to Fig. 13, it should be noted that there is a special relation between the rates of displacement of a flame over ethyl alcohol, toluene and a mixture of these liquids. $\bar{v}$ for the mixture is considerably greater than that for the starting liquids at the same temperatures. This is due to the vapor pressure over mixtures of liquids differing from that over the pure components.

7. Ignition of Liquids

A flame will not go out, if vapor and oxygen are supplied to the combustion zone at a suitable rate. Vapor is fed to the flame by molecular diffusion and molecular migration from the layer adjacent to the liquid. The rate of supply of vapor to the combustion zone depends on the vapor pressure at the surface of the liquid and hence on the liquid temperature. The lowest liquid temperature at which a flame will not go out is the ignition temperature of the liquid ϑ_B.

The ignition temperature can easily be determined theoretically /16/.

Let us suppose that the liquid is in a cylindrical glass tube. We shall heat the liquid and at short intervals advance a small flame to the end of the tube. If the liquid temperature is equal to the ignition temperature, a flame will form at the end of the tube. As experiments show, this flame will be almost flat.

Let us denote by N the number of moles of vapor supplied to 1 cm^2 of flame per second, and by D and u the diffusion coefficient and rate of flow of vapor respectively. If the z-axis runs along the axis of the tube from the surface of the liquid towards the flame, then we can write:

$$-D\frac{dn}{dz} + un = N, \tag{1.20a}$$

where n is the number of moles of vapor per unit volume, i.e. the molar concentration.

During burning in air nitrogen will be found between the liquid and the flame. Here the oxygen concentration will be zero. Let us denote the molar concentration of nitrogen by n_a. The distribution of nitrogen concentration in the tube over the liquid will then satisfy the equation

$$-D\frac{n_a}{dz}+un_a=0. \qquad (1.20b)$$

If by p and p_a we denote the partial pressures of the vapor and the nitrogen, then, in accordance with the Mendeleyev-Clapeyron law we can write:

$$p=nRT \text{ and } p_a=n_aRT. \qquad (1.20c)$$

It is clear that the sum of p and p_a is equal to the atmospheric pressure p_o

$$p + p_a = p_o. \qquad (1.20d)$$

Adding (1.20a) and (1.20b) and bearing in mind (1.20c) and (1.20d) we get:

$$-D\frac{d}{dz}\left(\frac{p_0}{RT}\right)+u\frac{p_0}{RT}=N.$$

We shall neglect the variation in temperature in the layer of vapor. Then the first term on the LHS of the last equation will be equal to zero and

$$u\frac{p_0}{RT}=N. \qquad (1.20e)$$

Using relations (1.20c) and (1.20e) we can rewrite (1.20a) in the following form:

$$-\frac{D}{RT}\frac{dp}{dz}+N\frac{p}{p_0}=N.$$

Whence

$$-\frac{dp}{dz}=\frac{RT}{D}N\left(1-\frac{p}{p_0}\right). \qquad (1.20f)$$

The pressure of the vapor in the layer adjacent to the liquid will be equal to the saturated vapor pressure π for the given temperature. Thus, if the origin is at the surface of the liquid, when $z = 0$, $p = \pi$.

A consideration of the processes in the combustion zone suggests that the fluxes of vapor and oxygen, directed towards the combustion surface, are in a stoichiometric ratio and that the concentration of fuel and oxygen in the flame is very small /17,18/. Accordingly, if the distance from the liquid to the flame is taken as h, we can write that when $z = h$ $p = 0$.

For the boundary conditions formulated above the solution of (1.20f) can be written in the form:

$$\pi=p_0(1-e^{-bh}), \qquad (1.21)$$

where

$$b=\frac{RT_B}{p_0}\frac{N}{D}. \qquad (1.21a)$$

In flame theory it has been proved /19/ that the height of a flame is determined by

$$\delta = \beta \frac{N}{4D_к n_к} r^2, \tag{1.21b}$$

where β is the number of moles of oxygen required to burn 1 mole of vapor; r is the radius of the tube in which the liquid is burned; D_k is the coefficient of diffusion of oxygen through the layer of combustion products and nitrogen; n_k is the molar concentration of oxygen in the air.

Substituting the value of N from (1.21b) in (1.21a), we get:

$$b = 4 \frac{RT_в}{p_0} \delta \frac{D_к}{D} \frac{n_к}{\beta r^2}. \tag{1.21c}$$

It is known that the diffusion coefficient is proportional to T^2. Thus, we can write:

$$D = D_0 \frac{T_в^2}{273^2},$$

where D_o is the diffusion coefficient for T = 273°K. Taking this last relation into account, we get:

$$b = 4 \cdot 273^2 \frac{R}{p_0} \delta \frac{D_к n_к}{r^2} \frac{1}{D_0 T_в \beta}. \tag{1.21d}$$

Equation (1.21) relates the saturation vapor pressure π of the liquid at the ignition temperature with the quantities p_o, b and h; b is determined from (1.21d).

In Fig. 14 the ignition temperature is plotted along the abscissa and the distance h between the flame and the surface of the liquid in the tube along the ordinate; the circles denote the results of experiments with benzene, ethyl alcohol, toluene and amyl alcohol and are taken from /16/ (a glass tube 3 mm in diameter was used); the lines are drawn from formula (1.21). In constructing these curves values of π were taken from tables, and values of b were chosen so that the theoretical curves corresponded as closely as possible with the experimental data. The values of b found in this way are given below:

	b, cm	$D_o \beta T_B$
Benzene	1.08	205
Ethyl alcohol	2.3	238
Toluene	1.14	260
Amyl alcohol	1.20	197

Fig. 14 shows that formula (1.21) agrees with experiment.

If on the RHS of (1.21d) we substitute the values of the quantities occurring in it and take δ equal to 0.1 cm, then for ethyl alcohol we find b = 2.0 cm^{-1}. The latter agrees closely with the experimental value of b = 2.3 cm^{-1}.

Figure 14:

(Legend not translated)

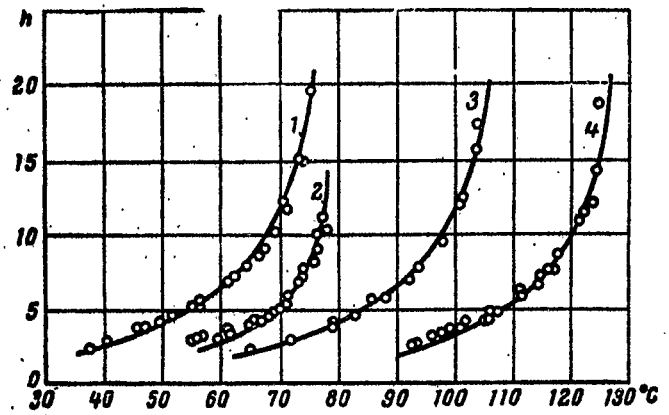

Рис. 14. Зависимость температуры воспламенения жидкостей в трубке от расстояния конца трубки до поверхности жидкости

1 — бензол; *2* — этиловый спирт; *3* — толуол; *4* — амиловый спирт

Let us consider certain consequences that flow from formulas (1.21) and (1.21d).

From (1.21d) it follows that for invariable values of p_0, δ and r the product $D_0\beta T_B b$ must be the same for different liquids. In fact,

$$D_0\beta T_B b = 4\cdot 273^2 \frac{R}{p_0}\delta D_K \frac{n_K}{r^2} = \text{const} = b_0. \tag{1.21e}$$

It was shown above that the relation (1.21e) is confirmed by experiment. The value of b_0 for toluene is a little different, but this is evidently due to the fact that the incompleteness of combustion was not allowed for in the calculations.

If bh is small compared with unity, then we can write

$$e^{-bh} = 1 - bh.$$

In this case

$$\pi = p_0 bh. \tag{1.21f}$$

It is known that the saturated vapor pressure of liquids varies with the temperature in accordance with the law:

$$\pi = \pi_0 e^{-\frac{rQ}{RT}}, \tag{1.21g}$$

where Q is the heat of vaporization, referred to a gram-molecule of substance. If the value of π from (1.21g) is substituted in (1.21f) and logarithms are taken, then

$$-\frac{Q}{RT_B}\lg e = \lg h + \lg\frac{rp_0 b}{\pi_0}.$$

Whence it follows that

$$-\frac{Q}{R}\left(\frac{1}{T_1} - \frac{1}{T_2}\right)\lg e = \lg\frac{h_1}{h_2}, \tag{1.21h}$$

where h_1, h_2 are the distances of the flame from the liquid at ignition temperatures T_1 and T_2.

Making use of formula (1.21) and the experimental data we can compute Q. The results of such computations are given below:

	$Q_{theor.}$	$Q_{exper.}$
Benzene	8,700	7,200
Ethyl alcohol	9,600	10,000
Toluene	8,000	8,000
Amyl alcohol	11,500	11,500

The values of c_p were taken from technical manuals. The results obtained by calculation agree with those determined experimentally.

Furthermore, for the same instrument, if h is constant and bh substantially less than unity, π will be equal to

$$\pi = p_0 bh = \frac{b_0 h p_0}{D_0 \beta T_B} = \frac{A}{D_0 \beta T_B}. \qquad (1.22)$$

The quantity A does not depend on the nature of the liquid and is a constant for the instrument.

Formula (1.22) shows that at the ignition temperature the saturated vapor pressure π of the liquid in question is equal to $A/D_0\beta T_B$. If we know the instrument constant and have information about the quantities D_0, β and π, we can find the ignition temperature of the liquid from formula (1.22).

Unfortunately, the literature is almost totally lacking in experimental data on ignition temperatures and therefore it is difficult to test the applicability of formula (1.22) for a large number of substances. But there is a way out. In fact, it was pointed out above that the ignition temperature differs only slightly from the flash point, if the latter is not high. Therefore, if relation (1.22) gives satisfactory results for the flash point, it must also give satisfactory results for the ignition temperature. Below we give the flash points (in °C) for a number of substances, both as determined experimentally and as calculated from formula (1.22):

	Theor.	Exper.		
Methyl alcohol	+4.5	from - 1	to	+32
Ethyl "	+11	+ 9		+32
Propyl "	+25	+22		+45
Butyl "	+40	+35		+36
Benzene	-10	-12		+10
Toluene	+ 9	+ 6		+30
Ethyl ether	-43	-41		-20
Ethyl formate	-18.5	-19.5		
Ethyl propionate	+13	-12.5		
Methyl butyrate	+14	-14		

The constant A was determined for the flash point of acetic acid.

The data show that the theoretical and experimental values of the flash point are in satisfactory agreement.

Thus, a number of consequences of formulas (1.21) and (1.21d) are confirmed by experiment. This also serves as evidence in support of the hypotheses about the ignition of liquids and the fundamental relations obtained above.

It should be stressed that the ignition temperature is not a physicochemical constant of a substance, but, as follows from (1.21) and (1.21d), largely depends on the conditions under which it is determined. It is inter-

esting to note that ϑ_B is equal to the boiling point of the liquid for an external pressure p' equal to π .

/1,2/ give a formula recommended for calculating the flash points of liquids. Using the above notation, this formula may be written in the form:

$$\pi = B\frac{p_0}{\beta}, \tag{1.22a}$$

where π is the saturated vapor pressure of the liquid at the flash point, and B is a constant depending on the type of instrument.

Formula (1.22a) can be obtained from (1.10) by taking

$$B = \frac{b_0 h}{D_0 T_B}.$$

Table 1.4

Liquid	Жидкость	β	D_0	T_B	D_0T_B
Methyl alcohol	Метиловый спирт	1,5	0,132	272	36
Ethyl "	Этиловый спирт	3,0	0,102	283	29
n-propyl "	Нормальный пропиловый спирт	4,5	0,085	295	25
n-butyl "	Н. бутиловый спирт	6,0	0,070	307	21
n-amyl "	Н. амиловый спирт	7,5	0,059	319	19
Benzene	Бензол	7,5	0,077	261	20
Toluene	Толуол	9,0	0,071	278	20
Xylene	Ксилол	10,5	0,060	296	18
Carbon bisulfide	Сероуглерод	3,0	0,089	230	20

Table 1.4 shows that the coefficient β varies much more strongly than the product D_0T_B. Since the vapor pressure quickly rises with increase in temperature, a deviation of D_0T_B from the mean involves a small change in the temperature determined from (1.22a) compared with the value of T obtained from (1.22).

The flash and ignition points of mixtures of liquids are also of considerable interest. Before turning to this question, it will be convenient to devote some space to the consideration of certain properties of liquid solutions, confining ourselves in this case to binary mixtures.

8. Ideal Solutions

An ideal or simple solution of a liquid is one in which the partial pressures of the components in the vapor phase are proportional to the molar fractions of the components in the liquid phase.

Note that the molar fraction of a component k, x_k, is a quantity equal to the number of moles N_k of the given component divided by the

total number of moles in the system

$$x_{\kappa} = \frac{N_{\kappa}}{\Sigma N_{\kappa}}.$$

It is evident that

$$x_1 + x_2 + \ldots = 1.$$

Thus, if by p_1 and p_2 we denote the partial pressures and by $p_{1,0}$ and $p_{2,0}$ the vapor pressure of the pure components of a binary ideal mixture and by x_1 and x_2 the molar fractions of the components of the solution, then

$$p_1 = p_{1,0}x_1 \text{ and } p_2 = p_{2,0}x_2.$$

The total vapor pressure of the solution will be equal to:

$$p = p_1 + p_2 = p_{1,0}x_1 + p_{2,0}x_2$$

or, since $x_1 + x_2 = 1$,

$$p = p_{1,0} + (p_{2,0} - p_{1,0})\, x_2. \tag{1.23}$$

The total vapor pressure of an ideal solution is a linear function of the molar composition of the liquid phase. If we take a rectangular system of coordinates and plot the molar fraction of a component along the abscissa and the total vapor pressure of the ideal solution along the ordinate, then given constant temperature the dependence $P(x_2)$ will be represented by a straight line.

The connection between the molar fraction of the components in the vapor and liquid phases of an ideal solution is easily established. Let us denote by N_1', N_2', y_1 and y_2 the number of moles and the molar fractions of the first and second components in the vapor phase, and by N_1, N_2, x_1 and x_2 the number of moles and the molar fractions of the first and second components in the liquid phase. It is evident that

$$y_2 = \frac{N_2'}{N_1' + N_2'}.$$

Using Mendeleyev's equation, according to which

$$p_1 v = N_1' RT \text{ and } p_2 v = N_2' RT,$$

and the relations for p_1 and p_2, we get:

$$y_2 = \frac{p_2}{p_1 + p_2} = \frac{p_{2,0}x_2}{p_{1,0}x_1 + p_{2,0}x_2} = \frac{\alpha x_2}{1 + (\alpha - 1)\, x_2}. \tag{1.24}$$

where $\alpha = \frac{p_{2,0}}{p_{1,0}}$.

In Fig. 15 x_2 is plotted along the abscissa and y_2 along the ordinate. Curve 1 gives the connection between y and x when $\alpha = 3$, curve 2 is for $\alpha = 1$ and curve 3 for $\alpha = 0.3$. It is easy to see that when $\alpha > 1$ and $y_2 > x_2$, the vapor phase is richer in the second component than the liquid phase; when $\alpha = 1$, $y_2 = x_2$, i.e. the vapor and the liquid have the same composition; when $\alpha < 1$, $y_2 < x_2$ and, consequently, the vapor phase is richer in the first component than the liquid phase. In other words, the vapor phase is richer in the component, the vapor pressure of which is greater at the given temperature.

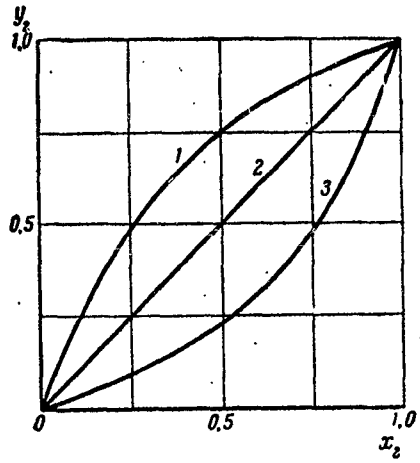

Fig. 15: Composition of the liquid and vapor phases of liquid solutions for different α.

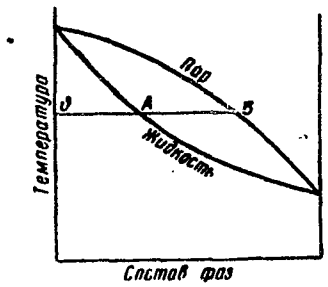

Fig. 16: Boiling point of ideal mixtures of liquids as a function of composition at constant pressure. Ordinate: temp.; abscissa: phase composition; top: vapor; bottom: liquid.

A point that will be of interest later on is the dependence of the boiling point of mixtures of liquids on the composition. We shall find this dependence, if we take the total vapor pressure p of the solution in (1.23) as constant and if for each molar fraction x we find the temperature at which

$$p_{1,0} + (p_{2,0} - p_{1,0})x_2 = p = \text{const.}$$

This dependence is shown for ideal mixtures in Fig. 16, where the molar fraction of the low boiling component is plotted along the abscissa and the boiling point for constant pressure along the ordinate. The lower

curve links the boiling point and the composition of the solution and the upper curve the b.p. and the composition of the vapor over the boiling liquid.

If at a distance ϑ from the abscissa we draw a straight line parallel to the latter, this straight line will intersect the lower curve in a point A and the upper curve in a point B; the abscissa of point A defines the molar fraction x of the low-boiling component in the solution, the b.p. of which is equal to ϑ; the abscissa of B gives the molar fraction of the low-boiling component in the vapor y, in equilibrium with the boiling solution.

The figure shows that the molar fraction of the low-boiling component (i.e. the component with the lower b.p., or, in other words, with the higher vapor pressure) is greater in the vapor than in the liquid phase, "the vapor is enriched in that component, which, added to the liquid, increases the vapor pressure above it (or reduces the b.p.)". The statement thus formulated is called the first law of Konovalov and holds for any liquid solution /20,21/.

9. Classification of Mixtures of Liquids

The mutual solubility of two liquids varies within wide limits: from practically total insolubility to miscibility in any proportions to form a homogeneous solution. Thus, mixtures of two liquids can be divided into three basic groups: mixtures of liquids miscible in all proportions; mixtures of liquids that are partially miscible; mixtures of liquids that are practically mutually insoluble.

Organic liquids of related chemical structure and properties ordinarily mix in all proportions, forming homogeneous solutions. Examples of this are mixtures of benzene and toluene, ethyl and butyl alcohol, etc.

Mixtures of partially soluble liquids are of great importance. These include acetone and water, ether and water, isobutyl alcohol and water and many other liquids.

The third group includes mixtures of benzene and water, toluene and water, etc.

10. Mixtures of Liquids Miscible in All Proportions

Only some solutions of liquids miscible in all proportions behave like ideal solutions. As a rule, the behavior of bicomponent real solutions deviates from that of ideal solutions. Depending on the degree and nature of this deviation we can distinguish three types of solutions of liquids of unlimited mutual solubility.

The first type includes so-called normal solutions, for which the dependence of the pressure and boiling point on composition is represented by curves close to the corresponding curves for ideal solutions. A large number of substances with unlimited mutual solubility are of this type.

The second type includes solutions with isothermal total-pressure curves characterized by a maximum. A typical example of such a mixture

is a mixture of carbon bisulfide and acetone, experimental data for which are given in Fig. 17 for a temperature of 35.2°. Along the abscissa is plotted the molar fraction of carbon bisulfide and along the ordinate the total vapor pressure, measured in mm Hg. One curve characterizes the dependence of the composition of the liquid phase and the other that of the vapor phase on the vapor pressure.

It is clear from the figure that for mixtures with a molar fraction of carbon bisulfide less than 0.67 the vapor phase is richer in carbon bisulfide than the liquid phase, and that as the molar fraction of CS_2 in the solution increases, so does the total vapor pressure; for mixtures with a molar fraction of CS_2 greater than 0.67 the vapor phase is richer in acetone and adding CS_2 to the solution leads to a reduction in the vapor pressure p. Konovalov's law, defined above, holds here too.

The figure also reveals that the vapor above a solution with a molar fraction of CS_2 equal to 0.67 has the same composition as the solution itself. Mixtures with vapors having the same composition as the solution are called azeotropic.

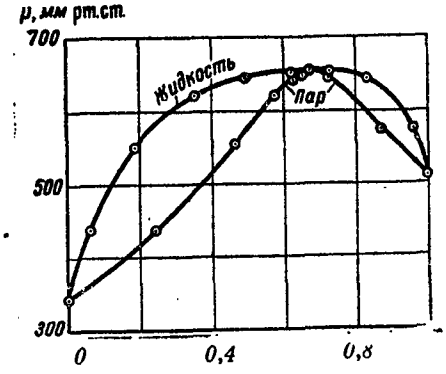

Fig. 17: Dependence of total vapor pressure (mm Hg) on composition of mixtures of carbon bisulfide and acetone at constant temperature. Left: liquid; right: vapor.

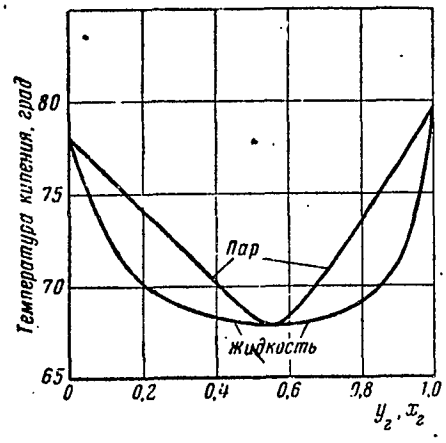

Fig. 18: Dependence of boiling point of mixtures of ethyl alcohol and benzene on phase composition at constant pressure. Ordinate: boiling point, degrees; Top: vapor; bottom: liquid.

Fig. 18 shows the dependence of the boiling point at constant pressure on the composition of a mixture of ethyl alcohol and benzene, a mixture of the second type. The molar fraction of benzene is plotted along the abscissa. The lower curve shows the dependence of the boiling point on the composition of the solution, and the upper its dependence on that of the

vapor, in equilibrium with the solution. It is easy to see that when benzene is added to the solution, the change in the boiling point of the mixture is non-monotone, and the dependence of the boiling point on the composition of the mixture is represented by a curve with a minimum. The composition of the solution with the minimum boiling point is the same as that of the vapor. The mixture corresponding to the minimum b.p. will be azeotropic.

The results shown in Figs. 17 and 18 illustrate Konovalov's second law, which states that "at extremes of vapor pressure or of boiling point the compositions of the liquid and vapor phases of mixtures coincide" /20,21/. The composition and boiling point of an azeotropic mixture depend on the pressure. This is evident from the data given below:

Mixture of ethanol and water

Pressure, mm Hg	100	150	200	400	760	1100	1450
B.P. of azeotrope, °C	34.2	42.0	47.8	62.8	78.1	87.8	95.3
Content of ethanol in azeotrope, mole %	99.6	96.2	93.8	91.4	90.0	89.3	89.1

Mixture of ethyl alcohol and ethyl acetate

Pressure, mm Hg	25	50	100	200	400	600	760	900	1200	1500
B.P. of azeotrope, °C	-1.4	10.6	23.8	38.4	54.9	65.4	71.8	76.5	85	91.8
Content of alcohol in azeotrope, mole %	22.1	24.6	28.2	33.4	39.6	43.6	46.4	48.5	52.2	55.4

The third type of infinitely miscible liquids includes mixtures with a total vapor pressure characterized by a minimum at constant temperature. An example of such a system is provided by a mixture of acetone and chloroform (see Fig. 19 for experimental data). Along the abscissa are plotted molar fractions of chloroform, and along the ordinate vapor pressure in mm Hg; the lower curve shows the dependence of the vapor pressure on the composition of the vapor phase, the upper curve the relation between the vapor pressure over the solution and the composition of the solution. The figure shows that the composition of the vapor over a solution, the molar fraction of chloroform in which is equal to 0.625, is the same as that of the solution; the liquid phase of a mixture, the molar fraction of chloroform in which is less than 0.625, is richer in chloroform than the vapor phase in equilibrium with it, while the opposite situation applies when the molar fraction of chloroform in the mixture is greater than 0.625.

Fig. 20 shows the dependence of the boiling point at constant pressure on the composition of a mixture of nitric acid and water, a mixture of the third type. The molar fraction of nitric acid is plotted along the abscissa. The curves in the figure, relating the b.p. and the compositions of the liquid and vapor phases, are characterized by maxima and have a common point, corresponding to an azeotropic mixture.

It is easy to see that mixtures of the third type obey both the

first and second of Konovalov's laws.

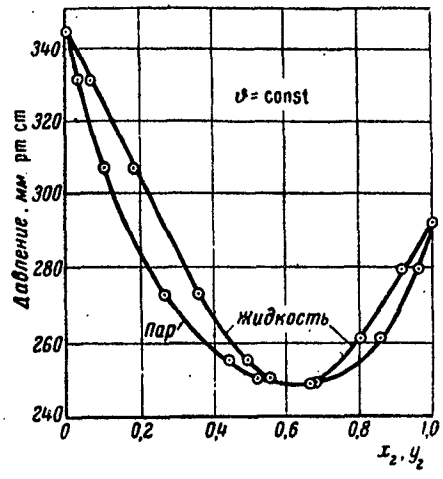

Fig. 19: Dependence of vapor pressure of a mixture of acetone and chloroform on phase composition at constant temperature. Ordinate: pressure, mm Hg; left: vapor; right: liquid.

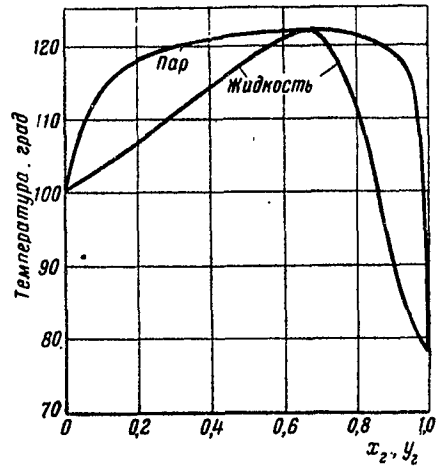

Fig. 20: Dependence of boiling point of mixtures of nitric acid and water on phase composition at constant pressure. Ordinate: temperature, degrees; left: vapor; right: liquid.

It is clear from Figs. 17, 18, 19 and 20 that the curves p(x) and p(y) have a dependence opposite to that of curves $\vartheta(x)$ and $\vartheta(y)$. The maximum of the total vapor pressure at constant temperature corresponds to a minimum of the boiling point at constant pressure and vice versa.

11. Mixtures of Liquids of Limited Miscibility

An example of a mixture of this type is a mixture of aniline and water, which up to a certain limiting concentration will give a homogeneous solution. If further water is added, on shaking the mixture separates into two layers: the lower consisting of aniline saturated with water and the upper consisting of water saturated with aniline; when the amount of water added becomes sufficiently large, a homogeneous solution is again obtained, but this will be a solution of aniline in water.

The mutual solubility of liquids with limited miscibility depends on the temperature. The classic investigations of V.F. Alekseyev have shown that the solubility of liquids increases in some systems with increase and in others with decrease in temperature. The solubility of aniline in water and of water in aniline increases with increase in temperature and at the critical point becomes unlimited. This unlimited solubility is

remains during further heating. Solubility in the system diethylamine-water increases with decrease in temperature and at temperatures below the critical the two liquids have unlimited miscibility. In certain mixtures two critical points are observed.

The composition and vapor pressure of a saturated solution of A in B (e.g. aniline in water) and a saturated solution of B in A (e.g. water in aniline) are the same at the same temperature. This can be proved. Let us take a ring-shaped tube and introduce into it two saturated solutions of the infinitely miscible liquids A and B (Fig. 21). The vapor pressures over the solutions in the tube must be the same.

Fig. 22 shows the dependence of the total vapor pressure of mixtures of infinitely soluble liquids 1 and 2 on the phase composition. Molar fractions of component 2 are plotted along the abscissa. The curve AC characterizes the vapor pressure over the solution of component 1, the point C corresponding to a saturated solution of component 2 in component 1; the length cut off by a perpendicular from point C along the abscissa gives the molar fraction x_2' of component 2 in this saturated solution. DB is the pressure curve for solutions of the first component 1 in component 2 and D corresponds to a saturated solution of component 1 in component 2; x_2'' represents the molar fraction of component 2 in the solution. The mixtures CD are heterogeneous; they break down into saturated solutions C and D.

Curves AE and EB give the dependence of the total vapor pressure on the composition of the vapor phase.

If we construct a diagram of composition v. boiling point for constant pressure, we get the picture shown in Fig. 23.

Hexane and methyl alcohol constitute a pair of substances corresponding to figures 22 and 23.

In certain circumstances two infinitely miscible liquids may give a picture different from that discussed above. In this case the dependence of the total vapor pressure at constant temperature on the phase composition is represented by the curves in Fig. 24. This case is characterized by the fact that the vapor E over the saturated solutions C and D has a composition lying within the interval x_2' x_2'' .

Fig. 25 gives the dependence of the boiling point at constant pressure on the phase composition for the second case.

12. Mixtures of Liquids with Slight Mutual Solubility

It is worth paying special attention to mixtures of liquids with slight mutual solubility. Examples of such mixtures are toluene-water, benzene-water, xylene-water, etc.

Fig. 26 shows the dependence of the total vapor pressure at constant temperature on the composition of the liquid phase of mixtures of liquids characterized by slight mutual solubility. The molar fraction of component 2 of the solution is plotted along the abscissa. Here x_2' is nearly zero and x_2'' nearly 1 .

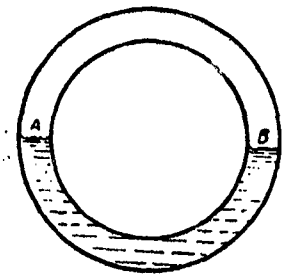

Fig. 21

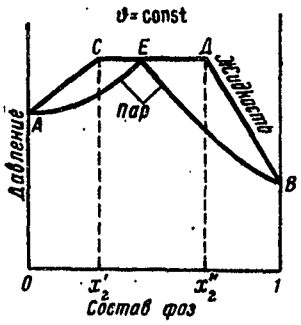

Fig. 22: Total vapor pressure of infinitely soluble liquids v. phase composition for constant temperature. Ord.: pressure; absc.: composition; center: vapor; diagonal: liquid.

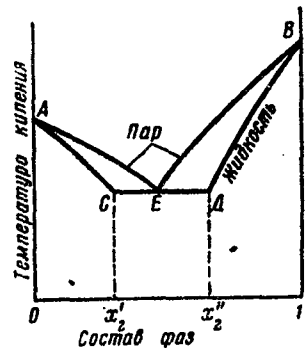

Fig. 23: Boiling point of infinitely soluble liquids v. phase composition for constant pressure. Ord.: b.p.; absc.: composition; center: vapor; diag.: liquid.

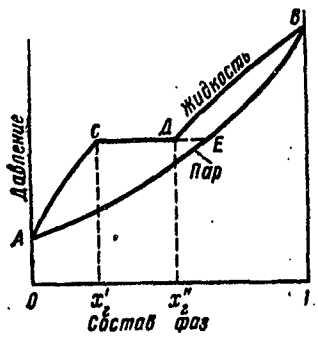

Fig. 24: Vapor pressure of infinitely miscible liquids v. phase composition for constant temperature. Cf. Fig. 22.

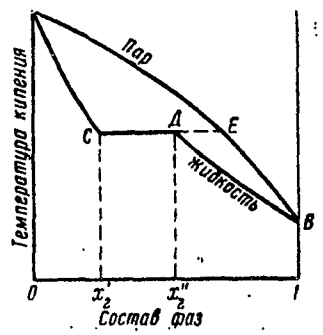

Fig. 25: Boiling point of infinitely soluble liquids v. phase composition (variant 2) for constant pressure. Cf. Fig. 23.

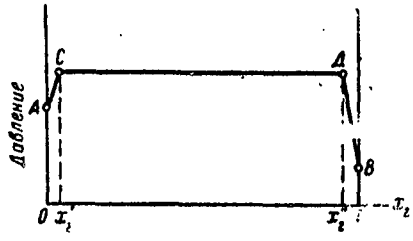

Fig. 26: Vapor pressure v. phase composition of mixtures of liquids with slight mutual solubility for fixed temperature. Ordinate: pressure.

In the region AC component 1 dominates the solution and should be considered the solvent. The partial pressure of the vapor of this component is defined by Raoult's law

$$p_1 = p_{1,0}x_1 = p_{1,0}(1 - x_2). \tag{1.24a}$$

In a solution belonging to the region AC component 2 represents an inconsiderable quantity. To determine the partial vapor pressure of this component, it is necessary to make use of Henry's law, according to which at constant temperature the concentration of a gas in a solution is proportional to the pressure of this gas. Thus, we can write:

$$p_2 = k_2x_2, \tag{1.24b}$$

where k_2 is a proportionality factor.

For a saturated solution C

$$p_1 = p_{1,0}(1 - x_2') \quad \text{and} \quad p_2 = k_2x_2'. \tag{1.24c}$$

In a solution corresponding to the region DB component 2 predominates and should be regarded as the solvent. In the region DB the partial vapor pressure of this component will be equal to

$$p_2 = p_{2,0}x_2. \tag{1.24d}$$

Component 1 is present in the solution in small quantities and thus its partial vapor pressure will be

$$p_1 = k_1x_1 = k_1(1 - x_2). \tag{1.24e}$$

For a saturated solution D

$$p_2 = p_{2,0}x_2'' \quad \text{and} \quad p_1 = k_1(1 - x_2''). \tag{1.24f}$$

From (1.24c) and (1.24f) we find:

$$k_2 = p_{2,0}\frac{x_2''}{x_2'}, \quad \text{and} \quad k_1 = p_{1,0}\frac{1 - x_2'}{1 - x_2''}. \tag{1.24g}$$

The total vapor pressure of the saturated solutions C and D will be

$$p = p_1 + p_2 = p_{1,0}(1 - x_2') + p_{2,0}x_2''. \qquad (1.24h)$$

Formula (1.24h) defines the vapor pressure not only of the solutions with concentrations x_2' and x_2'' but also of mixtures with a molar fraction of component 2 lying between x_2' and x_2''. Such mixtures may be regarded as mixtures of the saturated solutions C and D.

For mixtures of liquids with very slight mutual solubility the value of x_2' is close to zero, while x_2'' is close to unity; accordingly, with sufficient accuracy:

$$p = p_{1,0} + p_{2,0}, \qquad (1.24i)$$

i.e. the total pressure of vapor in equilibrium with mixtures of very slightly mutually soluble liquids is equal to the sum of the saturation vapor pressures for the pure components. In such cases the molar fraction of the second component in the vapor phase will be equal to

$$y_2 = \frac{p_{2,0}}{p_{1,0} + p_{2,0}}.$$

Since the boiling point of liquids is equal to the temperature, at which the saturated vapor pressure is equal to the external pressure, and the total vapor pressure over liquids with very slight mutual solubility is the sum of the saturated vapor pressures of the components of the mixtures, then the boiling points of such mixtures will always be lower than the boiling point of the pure components. Let us consider some examples.

The b.p. of benzene is 80.2° and that of a mixture of water and benzene 69.2°. The molar fraction of water in the vapor phase of the boiling mixture is then equal to 0.30.

Toluene boils at 110.7° and a mixture of toluene and water at 84.5°. In this case the molar fraction of water in the vapor is 0.56.

The b.p. of m-xylene is 139° and that of a mixture of xylene and water 92.5°. The molar fraction of water in the vapor phase of the mixture is 0.76.

These examples show that the molar fraction of water in the vapor phase of a mixture increases with increase in the boiling point of component 2.

13. Ignition Temperature of Binary Mixtures of Combustible Liquids

The ignition of binary mixtures of infinitely soluble combustible liquids has been investigated by P.G. Ipatov /22/. In Ipatov's experiments solutions of liquids were poured into a glass tube 3 mm in diameter and the ignition temperatures of the solutions determined for different distances from the surface of the liquid to the edge of the tube. Fig. 27 shows the results for toluene + benzene, which behaves like an ideal solution, Fig. 28

those for isoamyl + ethyl alcohol, a normal type with positive deviation of the pressure from that calculated in accordance with the laws of ideal solutions. Fig. 29 shows the results for imperfect mixtures of ethyl alcohol and benzene, for which the curve of total pressure has a maximum. The ignition temperature is plotted along the abscissas and the distance h between the level of the liquid in the tube and the flame along the ordinates.

The curve marked 1 in Fig. 27 shows $\vartheta_B(h)$ for pure benzene; curve 6 that for toluene, and curves 2, 3, 4 and 5 those for mixtures containing 0.8, 0.6, 0.4 and 0.2 molar fractions of benzene in the solution. It is clear from the figure that the curves for mixtures of benzene and toluene lie between the curves for the pure components and the further from the benzene curve the less the molar fraction of benzene in the mixture. This means that for a given h the ignition temperature of these mixtures varies uniformly with changes in their composition.

Fig. 30 shows the dependence of the ignition temperature of mixtures of toluene and benzene on the composition of the liquid (curve A) and vapor (curve B) phases for constant h. The figure shows that the temperature ϑ_B varies uniformly with changes in the concentration of the components in both the liquid and the vapor phases. The simplest dependence is that between the ignition temperature and the composition of the vapor phase: if by $\vartheta_{B.C.}$ we denote the ignition temperature of the mixture, by $\vartheta_{B.T.}$ and $\vartheta_{B.b.}$ the ignition temperatures of the toluene and the benzene, and by y the molar fraction of benzene in the vapor phase, then the experimental data satisfy the following relation:

$$\vartheta_{B.C} = \vartheta_{B.T} + (\vartheta_{B.6} - \vartheta_{B.T})\, y. \qquad (1.25)$$

The dependence of ϑ_B on the composition (analogous to Fig. 30) was also observed by Ipatov for mixtures of benzene and ethyl ether, ethyl and methyl alcohol, ethylene chloride and benzene and benzene and acetone. All these can be regarded as ideal mixtures. The ignition temperature varies linearly with variation in the molar fraction of one or the other component in the vapor phase.

Fig. 28 shows that the curves $v_B(h)$ of mixtures of ethyl and isoamyl alcohol follow in order of increasing molar fraction x of ethyl alcohol in the solution (as with the mixtures of benzene and toluene). Fig. 31 gives the dependence of the ignition temperature on the phase composition of these mixtures. In this case the relationship is graphically represented by curves. The same thing is observed for mixtures of toluene and acetone, mixtures of the normal type with a positive deviation of the pressure from that of ideal mixtures.

It is clear from Fig. 29 that the curves $\vartheta_B(h)$ for mixtures of ethyl alcohol and benzene lie to the left of the corresponding curves for the pure components. This order of the components confirms the fact that the ignition temperature of these mixtures does not vary monotonically

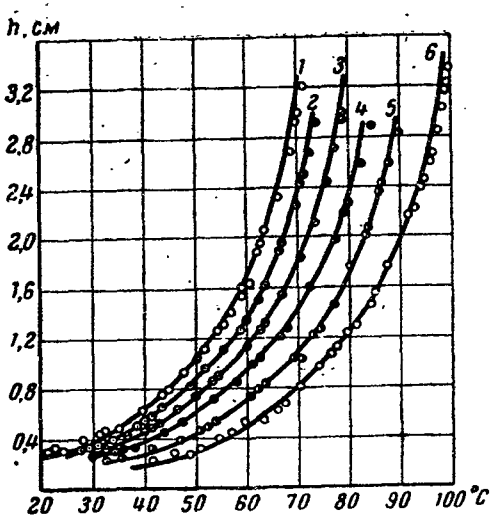

Fig. 27: Ignition temperature v. distance h for mixtures of toluene and benzene.

1 - benzene; 2,3,4,5 - mixtures containing 0.8,0.6,0.4 and 0.2 molar fractions of benzene; 6 - toluene

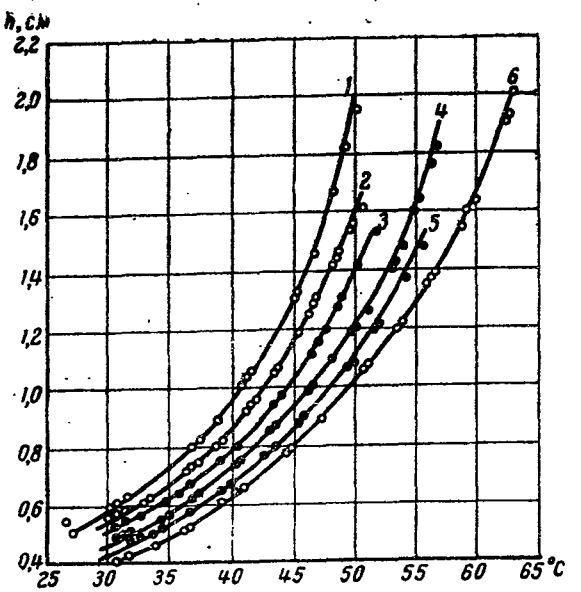

Fig. 28: Ignition temperature v. distance h for mixtures of ethyl and isoamyl alcohol.

1 - ethyl alcohol; 2,3,4,5 - mixtures containing 0.8,0.6, 0.4 and 0.2 molar fractions of ethyl alcohol; 6 - isoamyl alcohol

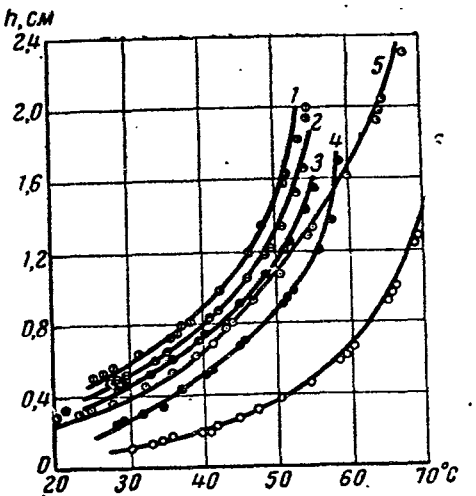

Fig. 29: Ignition temperature v. distance h for mixtures of ethyl alcohol and benzene.

1,2,3,4 - mixtures containing 0.8,0.6,0.4 and 0.2 molar fractions of benzene; 5 - benzene; 6 - ethyl alcohol

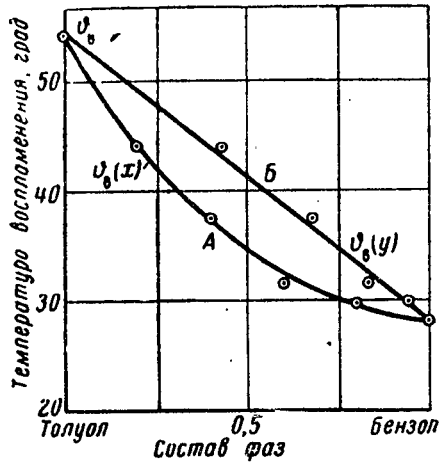

Fig. 30: Dependence of ignition temperature of mixtures of toluene and benzene on phase composition. Ordinate: ignition temperature, degrees; abscissa: phase composition; left: toluene; right: benzene.

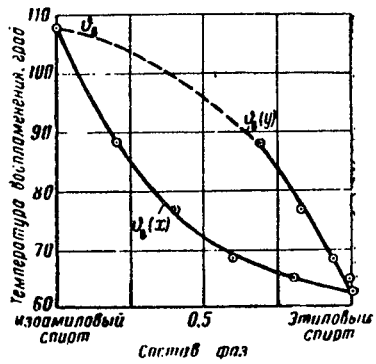

Fig. 31: Dependence of ignition temperature of mixtures of ethyl and isoamyl alcohol on phase composition. Ordinate: ignition temperature, degrees; absc.: phase composition; left: isoamyl; right: ethyl alcohol.

with variation in the phase composition. The ignition temperature of some mixtures is lower than that of the pure components. An analogous picture is observed in connection with mixtures of toluene and ethyl alcohol and methyl alcohol and benzene, imperfect mixtures with a pressure maximum.

We may assume that $\vartheta_B(x)$ and $\vartheta_B(y)$ for imperfect mixtures with a pressure minimum will form curves with maxima, and that the ignition temperature of some of these mixtures will be higher than that of the pure components.

The laws governing the ignition of mixtures of combustible liquids can be explained on the basis of the same assumptions as were made in describing the ignition of individual liquids and with reference to the theory of solutions. This can be done as follows /22/.

Having appeared, a flame will not go out, if vapor and oxygen are supplied to it at a sufficiently high rate. The vapor will enter the combustion zone as a result of diffusion and molecular motion. If by N_1 and N_2 we denote the number of moles of the first and second components entering 1 sq. cm of flame per second, by n_1 and n_2 the molar concentrations of the components in the vapor phase, by D_1 and D_2 the coefficients of diffusion of vapors of the components of the mixture and let the z-axis run along the axis of the tube from the liquid to the flame, then we can write:

$$-D_1\frac{dn_1}{dz}+un_1=N_1,\quad -D_2\frac{dn_2}{dz}+un_2=N_2. \tag{1.25a}$$

Between the flame and the liquid there will be nitrogen, the distribution of which is given by:

$$-D\frac{dn_3}{dz}+un_3=0, \tag{1.25b}$$

where u is the rate of flow of the vapor.

If, instead of molar concentrations, we introduce into (1.25a) the molar fractions y_1 and y_2 of the components in the vapor phase and bear in mind that

$$y_1=\frac{n_1}{n_1+n_2},\qquad y_2=\frac{n_2}{n_1+n_2},$$

then, adding the left hand and right hand sides of equations (a) and (b) and using Mendeleyev's law, we get

$$-\frac{d}{dz}\left\{[(D_1y_1+D_2y_2)(p_1+p_2)+Dp_3]\cdot\frac{1}{RT}\right\}+u\frac{p_1+p_2+p_3}{RT}=N. \tag{1.25c}$$

Here p_1, p_2 and p_3 are partial pressures of the components of the mixture and of nitrogen and

$$N=N_1+N_2.$$

It is clear that

$$p_1+p_2+p_3=p_0,$$

where p_o is the atmospheric pressure.

$D_1y_1 + D_2y_2$ may be regarded as a quantity playing the part of diffusion coefficient for the vapors of the mixture /23/. Thus, we can assume that

$$D=D_1y_1+D_2y_2. \tag{1.25d}$$

Now equation (1.25c) can be rewritten in the form:

$$-\frac{d}{dz}\left(D\frac{p_0}{RT}\right)+u\frac{p_0}{RT}=N. \tag{1.25e}$$

Neglecting variation in temperature in the region between the liquid and the flame, we get:

$$u=N\frac{RT}{p_0}. \tag{1.25f}$$

Adding equations (1.25a), bearing in mind (1.25c) and (1.25d) and using Mendeleyev's law, we get:

$$-\frac{dp}{dz}=\frac{RT}{D}N\left(1-\frac{p}{p_0}\right), \tag{1.25g}$$

where $p = p_1 + p_2$.

If the origin of the coordinates is put at the surface of the liquid, and the distance from the liquid to the flame denoted by h, the boundary conditions may be written as follows: when $z = 0$, $p = \pi$, where π is the saturated vapor pressure of the solution; when $z = h$, $p = 0$.

For these boundary conditions the solution of (1.25g) will have the form:

$$\pi = p_0 (1 - e^{-bh}), \tag{1.26}$$

where

$$b = \frac{RT_в}{p_0} \frac{N}{D}. \tag{1.26a}$$

Equation (1.26) expresses the relationship between the saturated vapor pressure of the mixture at the ignition temperature and the quantities b and h. This equation is the same as the corresponding equation for an individual liquid.

During the combustion of mixtures of liquids the height of the flame will be equal to:

$$\delta = \frac{N_0}{4D_к n_к} r^2,$$

where N_o is the number of moles of oxygen entering the flame per sq. cm per sec; D_k and n_k are the diffusion coefficient and molar concentration of the oxygen; r is the radius of the tube.

It is evident that for complete combustion

$$N_0 = \beta_1 N_1 + \beta_2 N_2 = \beta N, \tag{1.26b}$$

where β_1 and β_2 are the numbers of moles of oxygen required for the combustion of a mole of the first and second components respectively.

From (1.26b) it follows that

$$\beta = \beta_1 y_1 + \beta_2 y_2. \tag{1.26c}$$

Taking into account (1.26a), (1.26b) and the dependence of D on the temperature, we get:

$$b = 4.273^2 \frac{R}{p_0} \delta \frac{D_к n_к}{r^2} \frac{1}{D_0 \beta T_в}. \tag{1.26d}$$

Equation (1.26) is in satisfactory agreement with experiment. Figs. 27, 28 and 29 show curves drawn in accordance with this formula. In plotting these curves values of π were taken from tables, and values of b were chosen so that the curve would correspond as closely as possible to the experimental data.

For mixtures of liquids with fairly similar ignition temperatures it

is possible to assume that for fixed values of r, δ, p_0 and n_k

$$4.273^2 \frac{R}{p_0} \delta \frac{D_k n_k}{r^2} \cdot \frac{1}{T_n} = a_0 = \text{const}$$

and

$$b = \frac{a_0}{D_0 \beta} \tag{1.26e}$$

Table 1.5 gives values of $a_0 = b_{ex} D_0 \beta$ * for a series of mixtures and for the conditions under which Ipatov's experiments were carried out.

As the Table shows, there is little change in a_0 when the composition of the mixture is varied. Hence, if we take a mean value of $a_0 = 0.254$ and values of D_0 and β, then with sufficient accuracy we can use (1.26e) to find the value of b for the mixtures in which we are interested, and, having information about the saturated vapor pressure of the mixture, we can also determine, making use of (1.26), the ignition temperature of the mixture under the given conditions.

Where bh is small compared with unity, instead of (1.26) we can write:

$$\pi = p_0 bh.$$

For constant h we get:

$$\pi = \frac{A}{D_0 \beta}, \tag{1.27}$$

where D is a constant for a given instrument;
β is determined from (1.26b);
D_0 is the diffusion coefficient for the mixture, found from (1.25d) and taken for 0°.

Table 1.6 gives values of the coefficients b, computed from (1.26e) and found by experiment. In computing b the value of a_0 was taken equal to the mean value in Table 1.5. In Table 1.6 the computed values are given in the numerator, the experimental values in the denominator.

These results show that the ignition points of mixtures of liquids are not constants of the mixtures but depend on the corresponding conditions.

We shall now examine the dependence of the ignition point on the composition of the mixture.

At the ignition temperature the saturated vapor pressure of mixtures of liquids is found from equations (1.26) and (1.27). It is clear that the ignition point of mixtures is equal to their boiling point for an external pressure

$$p' = p_0 (1 - e^{-bh}). \tag{1.28}$$

Relation (1.28) permits a number of conclusions.

If the quantity b entering into (1.26), (1.27) and (1.28) does not

---

* b_{ex} is the value of b found by experiment.

Table 1.5

Components A	Components B	Molar fractions of component B: 0	0,2	0,4	0,6	0,8	1,0	Mean a_0
Toluene	Benzene	0,242	0,246	0,238	0,246	0,249	0,243	0,243
Benzene	Ethyl ether	0,243	0,222	0,222	0,239	0,262	0,270	0,243
Ethyl alcohol	Methyl alcohol	0,263	0,252	0,234	0,222	0,223	0,238	0,240
Ethylene chloride . . .	Benzene	0,270	0,272	0,266	0,268	0,265	0,243	0,264
Isoamyl alcohol . . .	Ethyl alcohol	0,263	0,260	0,257	0,250	0,260	0,264	0,260
Benzene	Acetone	0,243	0,262	0,260	0,263	0,264	0,268	0,260
Toluene	Acetone	0,242	0,252	0,245	0,252	0,244	0,268	0,250
Ethyl alcohol . . .	Benzene	0,263	0,262	0,268	0,258	0,238	0,243	0,255
Toluene	Ethyl alcohol	0,242	0,271	0,234	0,262	0,259	0,262	0,256

Table 1.6

Components A	Components B	Molar fractions of component B: 0	0,2	0,4	0,6	0,8	1,0
Toluene	Benzene	*0,38	0,40	0,41	0,41	0,42	0,42
		**0,38	0,40	0,40	0,42	0,43	0,42
Benzene	Ethyl alcohol	0,42	0,47	0,49	0,51	0,52	0,52
		0,42	0,43	0,45	0,50	0,56	0,58
Ethylene chloride	Benzene	1,17	0,88	0,70	0,59	0,52	0,45
		1,12	0,90	0,71	0,60	0,52	0,42
Benzene	Acetone	0,45	0,53	0,62	0,69	0,75	0,81
		0,42	0,54	0,62	0,70	0,76	0,84
Toluene	Acetone	0,39	0,54	0,65	0,71	0,76	0,78
		0,38	0,54	0,64	0,72	0,74	0,84
Ethyl alcohol	Methyl alcohol	0,78	0,86	0,93	1,03	1,10	1,21
		0,86	0,90	0,91	0,96	1,03	1,12
Isoamyl alcohol	Ethyl alcohol	0,59	0,63	0,76	0,83	0,84	0,85
		0,60	0,63	0,75	0,80	0,83	0,86
Ethyl alcohol	Benzene	0,83	0,60	0,54	0,51	0,49	0,44
		0,86	0,62	0,57	0,52	0,46	0,42
Toluene	Ethyl alcohol	0,40	0,53	0,58	0,63	0,69	0,83
		0,38	0,56	0,58	0,65	0,70	0,86
Chloroform	Acetone	—	—	1,04	0,92	0,87	0,83
				1,05	0,90	0,88	0,84

* Coefficient b computed (numerator)

** Coefficient b experimental (denominator)

depend on the composition of the mixture, then for a given value of h for a mixture of two known components

$$p' = \pi = \text{const.}$$

In this case the dependence of the ignition temperature ϑ_B on the composition of the liquid and vapor phases of the mixture is graphically represented by curves coinciding with the curves giving the relationship between the boiling point ϑ_K and the phase composition for constant pressure, determined from (1.28) for bh = const.

If b depends on the composition of the mixture, then for constant $h = h_o$ curves $\vartheta_B(x)$ and $\vartheta_B(y)$ will coincide with curves $\vartheta_K(x)$ and $\vartheta_K(y)$ provided that the external pressure p' is determined from formula (1.28), in which b is a corresponding function of the composition.

It is clear that curves $\vartheta_B(x)$ and $\vartheta_B(y)$ for variable b differ from the curves giving ϑ_K as a function of x and y for constant pressure, this difference being the greater the more strongly b depends on the composition of the mixture, but the nature of the curves showing the dependence of ϑ_B and ϑ_K at constant pressure on the phase composition will be the same.

Thus, with imperfect mixtures of the type characterized by the presence of a minimum in curves $\vartheta_K(x)$ and $\vartheta_K(y)$ for p' = const., there must be a minimum in the curves $\vartheta_B(x)$ and $\vartheta_B(y)$. Such curves have been obtained by Ipatov in his investigations into the ignition of imperfect mixtures of the second type.

In the case of imperfect mixtures with isobaric curves $\vartheta_K(x)$ and $\vartheta_K(y)$ characterized by a maximum, the dependence of ϑ_B on x and y must be represented by curves with maxima. The addition of one component to the other must then lead to the formation of mixtures with ignition points higher than those of the pure components.

Obviously, minima and maxima in the ignition curves must correspond to azeotropic mixtures.

It should be noted that with variation in the ignition conditions the curves $\vartheta_B(x)$ and $\vartheta_B(y)$ and the positions of the maxima and minima will change.

Let us now look more closely at the dependence of the ignition point of ideal mixtures on the composition of the vapor phase. We shall limit the discussion to cases where b may be considered constant and the ignition points of the components are fairly close.

For ideal mixtures relation (1.23) holds and this can be rewritten in the form:

$$\pi = \pi_{1,0} + (\pi_{2,0} - \pi_{1,0})\, x_2, \tag{1.28a}$$

where π is the total vapor pressure of the mixture;

$\pi_{1,0}$ and $\pi_{2,0}$ are the saturated vapor pressures of the pure components at the ignition temperature of the mixture;

x_2 is the molar fraction of the second component in the solution.

From (1.24) it follows that

$$x_2 = \frac{\alpha' y^2}{1 + (\alpha' - 1) y_2}. \qquad (1.28b)$$

where y_2 is the molar fraction of the second component in the vapor phase, and

$$\alpha' = \frac{\pi_{1.0}}{\pi_{2.0}}.$$

Substituting the value of x_2 from (1.28b) in (1.28a), we find that for ideal mixtures:

$$\pi = \frac{\alpha' \pi_{2,0}}{1 + (\alpha' - 1) y_2}.$$

If by T_c and T_2 we denote the ignition temperatures of the mixture and the second component, measured in degrees on the absolute scale, and by ϑ the difference between these temperatures, then

$$T_c = T_2 + \vartheta = T_2\left(1 + \frac{\vartheta}{T_2}\right).$$

Since ϑ/T_2 is small compared with unity,

$$\frac{1}{T_c} = \frac{1}{T_2\left(1 + \frac{\vartheta}{T_2}\right)} = \frac{1}{T_2}\left(1 - \frac{\vartheta}{T_2}\right) = \frac{1}{T_2} - \frac{\vartheta}{T_2^2},$$

and

$$\pi_{2,0} = ae^{-\frac{Q}{RT_c}} = \Pi e^{\frac{Q}{RT_2^2}\vartheta},$$

where

$$\Pi = ae^{-\frac{Q}{RT_2}}$$

and is equal to the saturated vapor pressure of the second component at the ignition temperature of this component;

Q is the heat of vaporization of a mole of the liquid.

If $\frac{Q}{RT_2^2}\vartheta$ is significantly less than unity, then with sufficient accuracy:

$$e^{\frac{Q\vartheta}{RT_2^2}} = 1 + \frac{Q}{RT_2^2}\vartheta$$

and

$$\pi_{2.0} = \Pi\left(1 + \frac{Q}{RT_2^2}\vartheta\right).$$

Thus, with the assumptions made above, we can write

$$\pi = \prod \left(1 + \frac{Q}{RT_c^2}\vartheta\right) \cdot {}^{\alpha'}_{1+(\alpha'-1)y_2} = \text{const.} \qquad (1.28c)$$

Since α' varies slowly with change in temperature, it follows from (1.28c) that

$$\vartheta = \varepsilon_1 + \varepsilon_2 y_2,$$

where ε_1 and ε_2 are corresponding constants, the value of which is easy to determine. In fact, when $y_2 = 0$, $\vartheta = T_1 - T_2 = \vartheta_1 - \vartheta_2$, and when $y_2 = 1$, $T_c = T_2$ and, hence, $\vartheta = 0$. Whence

$$\varepsilon_1 = \vartheta_1 - \vartheta_2, \quad \varepsilon_1 + \varepsilon_2 = 0$$

and

$$\vartheta_c = \vartheta_1 + (\vartheta_2 - \vartheta_1)\, y_2. \qquad (1.28d)$$

Here ϑ_c, ϑ_1 and ϑ_2 are the ignition temperatures in °C of the mixture and the first and second components. Accordingly, where b is practically independent of the composition of the mixture and the ignition points of the components are close, the ignition temperature of an ideal mixture of the liquids is a linear function of the molar fraction of a component in the vapor phase.

These conditions are satisfied by mixtures of benzene and toluene. Ipatov's experiments show that the ignition temperatures of such mixtures actually obey relation (1.28d).

14. Ignition Points of Mixtures of Combustible and Incombustible Liquids

There are no data in the literature concerning the ignition points of mixtures of combustible and incombustible liquids. We shall therefore confine ourselves to certain theoretical considerations, which we shall test indirectly.

We shall assume that we have a homogeneous mixture of a combustible and an incombustible liquid (e.g. a mixture of ethyl alcohol and water) contained in a cylindrical tube and at a temperature equal to the ignition temperature. Suppose now that a flame is brought up to the end of the tube.

The distribution of concentrations of the components and nitrogen in the region lying between the liquid and the flame will be determined by the solution of the equations:

$$-D_1\frac{dn_1}{dz} + un_1 = N_1, \quad -D_2\frac{dn_2}{dz} + un_2 = N_2, \quad -D_3\frac{dn_3}{dz} + un_3 = 0. \qquad (1.29)$$

Here the subscript 1 refers to the combustible, 2 to the incombustible liquid and 3 to nitrogen; the notation is the same as in the previous section.

If we assume that

$$D_1 = D_2 = D_3 = D,$$

then it is easy to arrive at the equation

$$-\frac{dp}{dz} = \frac{RT}{D} N\left(1 - \frac{p}{p_0}\right), \tag{1.29a}$$

in which

$$p = p_1 + p_2.$$

In this case the boundary conditions may be written as follows: at the surface of the mixture ($z = 0$) $p = \pi = \pi_1 + \pi_2$, where π is the total saturated vapor pressure of the mixture at the ignition temperature, and π_1 and π_2 are the partial pressures of the components of the mixture; when $z = h$ (in the flame) $p_1 = 0$, and $p_2 = \gamma\pi_2$, where γ is a factor close to unity.

For these boundary conditions the solution of (1.29a) may be written:

$$\pi_1 = p_0 - \pi_2 - (p_0 - \gamma\pi_2)\, e^{-bh}. \tag{1.29b}$$

where

$$b = \frac{RT_c N}{p_0 D}.$$

If $\gamma = 1$,

$$\pi_1 = (p_0 - \pi_2)\,(1 - e^{-bh}) \tag{1.29c}$$

and

$$un_2 = u\frac{\pi_2}{RT_s} = N_2,$$

and since

$$u = (N_1 + N_2)\frac{RT_s}{p_0},$$

$$u\frac{\pi_2}{RT_s} = (N_1 + N_2)\frac{\pi_2}{p_0} = N_2. \tag{1.29d}$$

The height of the flame

$$\delta = \frac{N_0 r^2}{4D_K n_K},$$

and

$$N_0 = \beta N_1.$$

Hence,

$$N_1 = 4D_K n_K \frac{\delta}{\beta r^2}. \tag{1.29e}$$

From (1.29d) and (1.29e) it follows that

$$N = N_1 + N_2 = 4D_K n_K \frac{\delta}{\beta r^2}\frac{p_0}{p_0 - \pi_2}.$$

Thus

$$b = 4\frac{RT_в}{Dp_0} D_к n_к \frac{\delta}{\beta r^3} \frac{p_0}{p_0 - \pi_2}. \qquad (1.29f)$$

In this case, when bh is small compared with unity,

$$\pi_1 = (p_0 - \pi_2)\, bh = \frac{B}{D_0 \beta T_в}, \qquad (1.29g)$$

where

$$B = 4.273^2 RD_к n_к \frac{\delta h}{r^3}.$$

For the two liquids in question, when n_k, δ, h and r are fixed, if the variation in concentration is small, we can assume that

$$\frac{B}{D_0 \beta T_в} = \text{const} = C, \qquad (1.30)$$

and

$$\pi_1 = C.$$

From (1.30) it follows that the ignition temperature of homogeneous mixtures of combustible and incombustible liquids is equal (with the assumptions made above) to the temperature, at which the partial pressure π_1 of the vapor of the combustible component over a solution of the given composition is equal to C.

As already noted, the literature contains no data relating to the ignition of mixtures of combustible and incombustible liquids. However, we do have certain information about the flash points of such mixtures. Since the ignition temperatures are close to the flash points, we shall use the latter to test our theoretical conclusions.

In Fig. 32 the triangles denote the results of determinations of the flash points of solutions of ethyl alcohol in water; the curve is based on relation (1.30). The constant C has been chosen so that (1.30) closely corresponds with the experimental data. The figure shows that in this case the theory is in satisfactory agreement with experiment.

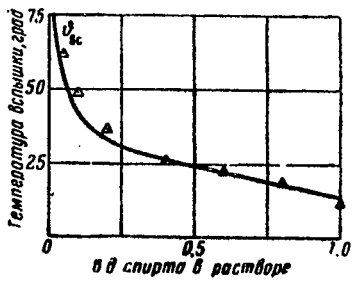

Fig. 32: Dependence of flash point on composition of mixtures of ethyl alcohol and water. Ordinate: flash point, degrees; abscissa: proportion of ethyl alcohol in the solution.

The literature does contain data about the dependence of the flash points of mixtures of ethyl alcohol and water or carbon tetrachloride, but since the partial vapor pressures for these mixtures at different temperatures are not given it is not possible to compare the results obtained from equation (1.30) with the experimental data in question.

We still do not know whether in such cases formula (1.29g) agrees with experiment.

15. Flash Points of Binary Mixtures of Combustible Liquids

In order to compute the lower flash limit, and hence the lowest flash point for a liquid, we make use of Le Chatelier's rule. This rule is an application of the displacement law to mixtures of combustible gases and can be written in the form

$$k = \frac{1}{\frac{y_1}{k_1} + \frac{1-y_1}{k_2}}, \tag{1.31}$$

where k is the limit of ignition of the mixture;

k_1, k_2 the limits of ignition of the components;

y_1 the molar fraction of the first component in the vapor phase.

In a number of cases this rule gives results close to those obtained by experiment. This is evident from Table 1.7, which gives Ipatov's experimental data /24/ and values of the flash limit k_b computed from (1.31). In the table y denotes the molar fraction of benzene in the vapor phase.

"Naturally, for fuels that strongly influence each other in burning we cannot expect that this rule will be fulfilled even approximately. Therefore we should not look for a special explanation either for very large or for very small infractions of the rule. On the other hand, we would need an explanation, if we unexpectedly found that Le Chatelier's rule was generally fulfilled. In this case we would be the better justified, the more similar the substances in question. In practical terms, the most interesting instance is that of a mixture of substances with parallel (similar) properties. Here Le Chatelier's rule can often be useful for a preliminary evaluation." This is how Jost /13/ characterizes Le Chatelier's rule.

Since the flash point is close to the ignition point, in computing flash points and limits of ignition we can use results obtained for the ignition temperature. This technique has proved successful both for individual liquids and for mixtures of ethyl alcohol and water. It is also convenient to work in this way in relation to mixtures of combustible liquids. We then make use of formula (1.27), determine the constant A and compute the limit of ignition k of the mixture from (1.3).

In Fig. 33 the hollow circles denote the results of Ipatov's experiments with mixtures of benzene and toluene; the solid circles denote experimental data relating to mixtures of ethyl alcohol and benzene and the triangles experimental data for mixtures of acetone and benzene. The curves are based on (1.27) and (1.30). The same value of A was used for all three.

Table 1.7

Ethyl alcohol and benzene			Benzene and toluene			Acetone and benzene		
Этиловый спирт с бензолом			Бензол с толуолом			Ацетон с бензолом		
y	k	$k_в$	y	k	$k_в$	y	k	$k_в$
0	4,40	4,40	0	2,13	2,13	0	3,10	3,10
0,37	3,10	3,40	0,34	2,18	2,23	0,44	2,80	2,78
0,59	2,64	2,99	0,55	2,28	2,30	0,70	2,68	2,62
0,71	2,47	2,81	0,73	2,32	2,35	0,88	2,58	2,51
1,10	2,45	2,45	0,91	2,40	2,42	1,00	2,45	2,45
—	—	—	1,00	2,45	2,45	—	—	—

The required values of D_o were taken from the corresponding tables. The figure shows that in these cases formula (1.27) satisfactorily describes the experimental data. It should be noted that in describing the results of these experiments we used only one constant found experimentally. In computing the limits of ignition for an examination of mixtures in accordance with Le Chatelier's formula six constants are used.

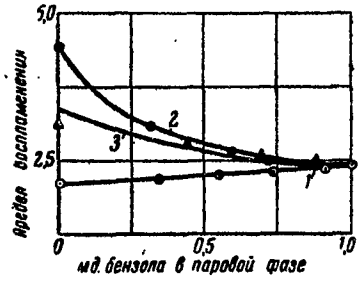

Fig. 33: Dependence of limit of ignition on benzene content of vapor phase for: 1 - benzene + toluene; 2 - ethyl alcohol + benzene; 3 - acetone + benzene. Ordinate: limit of ignition; absc.: molar fraction of benzene in vapor phase.

References

1. B.G. Tideman and D.B. Stsiborskiy. Khimiya goreniya (Chemistry of Combustion). M., Gostranizdat. 1935.
2. P.G. Demidov. Osnovy goreniya veshchestv (Fundamentals of Combustion). M., publ. by MKKh RSFSR, 1951.

3. P.T. Bezuglov. Spravochnaya tablitsa ogneopasnykh veshchestv (Reference Table of Inflammable Substances). M., Gostoptekhizdat. 1950.
4. M.G. Godzhello et al. Legkovosplamenyayushchiyesya i goryuchiye zhidkosti (Easily Inflammable and Combustible Liquids). Manual. M., publ. by MKKh RSFSR, 1956.
5. N.N. Semenov. Tsennye reaktsii (Valuable Reactions). L., Goskhimizdat. 1934.
6. L.N. Khitrin. Fizika goreniya i vzryva (Physics of Combustion and Explosions). Publ. Moscow State University (MSU), 1957.
7. Ya.B. Zel'dovich. Teoriya zazhiganiya nakalennoy poverkhnost'yu (Theory of Ignition by an Incandescent Surface). ZhETF (J. of Exp. and Theor. Phys.), 9 (1939) No 12.
8. R.S. Silver. Ignition of Gaseous Mixtures by Hot Particles. Phil. Mag., 23 (1933) No 156.
9. S. Paterson. Ignition of Inflammable Gases by Hot Moving Particles. Phil. Mag., 28 (1939) 186, 30 (1940) 203.
10. L.N. Khitrin and S.A. Gol'denberg. Teplovaya teoriya zazhiganiya gazovykh smesey i predel'nye yavleniya (Thermal Theory of Ignition of Gas Mixtures and Limit Phenomena). Izv. AN SSSR, OTN, 3 (1957).
11. V.A. Michelson. O normal'noy skorosti vosplameneniya gremuchikh gazovykh smecey (Normal Rate of Ignition of Detonating Gas Mixtures). Coll. works. Vol 1, M., Novyy agronom press. 1930.
12. N.N. Semenov. Osnovye voprosy sovremennoy teorii gomogennogo goreniya odnorodnykh gazovykh sistem (Basic Problems of Modern Theory of Uniform Combustion of Homogeneous Gaseous Systems). Izv. AN SSSR, OTN, (1953) No 5.
13. A.G. Geydon and Kh.G. Vol'fgard. Plamya, ego struktura, izlucheniye i temperatura (Flames, their Structure, Radiation and Temperature). M., Metallurgizdat. 1959
B. Lewis and G. Elbe. Combustion, Flames and Explosions in Gases. For. Lit. Publ. Ho. 1948.
W. Jost. Explosions and Combustion in Gases. For. Lit. Publ. Ho. 1952.
14. Ya.B. Zel'dovich. Teoriya predela rasprostraneniya tikhogo plameni (Theory of the Limit Of Propagation of a Still Flame). ZhETF, 11 (1941) No 1.
15. P.G. Ipatov. O rasprostranenii plameni po poverkhnosti goryuchikh zhidkostey (Propagation of Flames over the Surface of Combustible Liquids). IFZh (Engineering Physics Journal) (1960) No 12.
16. V.I. Blinov. O temperature vosplameneniya zhidkostey (The Ignition Point of Liquids). Dokl. AN SSSR, 52 (1946) No 9.
17. Ya.B. Zel'dovich. K teorii goreniya neperemeshannykh gazov (Theory of Combustion of Unmixed Gases). ZhTF, 19 (1949) No 10.
18. V.A. Shvab. Svyaz' mezhdu temperaturnymi i skorostnymi polyami gazovogo fakela (Connection between the Temperature and Velocity Fields of a Gas Flame). Symp. Issledovaniye protsessov goreniya natural'nogo topliva (Investigation of the Combustion Processes of Natural Fuel). M.-L., Gosenergoizdat. 1948.
19. V.I. Blinov. O trekh rezhimakh goreniya zhidkostey v rezervuarakh (Three Regimes of Combustion of Liquids in Tanks). Izv. AN SSSR, OTN,

(1956) No 4.
20. D.P. Konovalov. Ob uprugosti para rastvorov (Vapor Pressure of Solutions). L., 1928.
21. A.I. Brodskiy. Fizicheskaya khimiya (Physical Chemistry). M.-L., Goskhimizdat. 1948.
S.A. Bogaturov. Kurs teorii peregonki i rektefikatsii (Course in the Theory of Distillation and Rectification). M., Gostoptekhizdat. 1954.
22. P.G. Ipatov. Vosplameneniye sovershennykh i nesovershennykh binarnykh smecey zhidkikh goryuchikh veshchestv (Ignition of Perfect and Imperfect Mixtures of Combustible Liquids). Inform. sb. TsNIIPO (Bulletin of Central Scientific Research Institute for Fire-Fighting). Moscow, publ. MKKh. 1952.
23. A.S. Irisov. Isparyaemost topliv dlya porshnevykh dvigateley i metody eye issledovaniya (Evaporability of Fuels for Piston Engines and Methods of Investigating It). M., Gostoptekhizdat. 1955.
24. P.G. Ipatov. Opredeleniye nizhnikh predelov vosplameneniya smecey zhidkikh goryuchikh veshchestv (Determination of Lower Limits of Ignition for Liquid Combustible Substances). Trudy Leningr. inst. aviatsionnogo priborostroyeniya (LIAP) (Proc. Leningrad Inst. of Aviation Instrumentation) (1954) No 7.
25. L.A. Vulis. Teplovoy rezhim goreniya (Thermal Conditions of Combustion). M.-L., Gosenergoizdat. 1954.
26. V.N. Kondrat'ev. Kinetika khimicheskikh gazovykh reaktsiy (Kinetics of Chemical Gaseous Reactions). Publ. Acad. Sci. USSR. 1958.

Part Two

BURNING OF LIQUIDS IN VESSELS

Flames from Liquids

A liquid burning in a vessel is, in effect, a stream of vapor burning in air; the flow of vapor is maintained by evaporation, whose rate is governed by the flow of heat from flame to liquid. The oxygen derives from the surrounding gas.

The flame is of diffusion type; the burning is a special case of the combustion of unmixed gases.

Shape and Size of Flame

The shape and size are very much dependent on the diameter of the burner or vessel, as Fig. 1 shows for flames from gasoline [1]. The flame has a clearly defined fixed conical shape

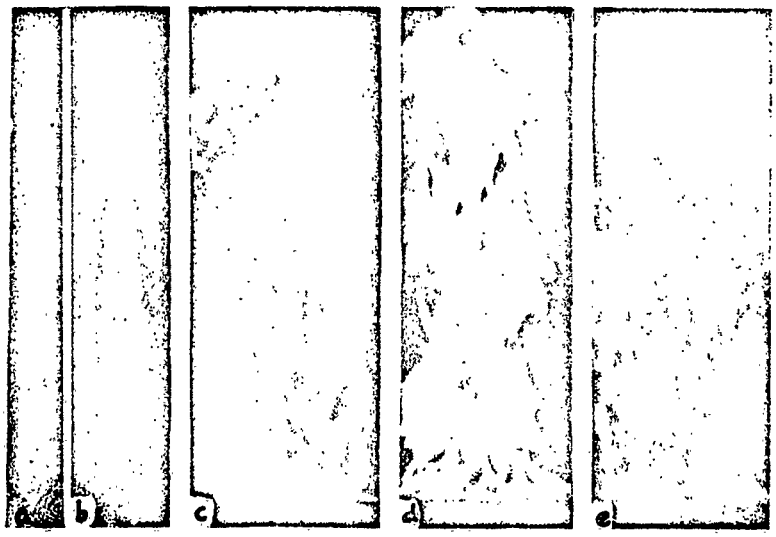

Fig. 1. Flames of gasoline burning in vessels of various diameters: a) 1.1 cm; b) 3.0 cm; c) 15 cm; d) 130 cm.

when the liquid is contained in tube not more than 10 mm in diameter; longitudinal pulsations appear as the diameter d increases, and the height oscillates with a low frequency (about 15 c/s). The flame begins to break up as d is increased further, and random turbulent motion is the sole effect for d > 15 cm.

Table 2.1

d, cm	I		II		III	
	δ	δ/d	δ	δ/d	δ	δ/d
0,37	—	—	3,0	8,1	3,6	10
0,50	—	—	3,9	7,7	5,4	11
0,60	9,5	16	4,3	7,2	6,3	10
0,71	9,7	13,5	5,0	7,0	6,3	9
1,14	11,9	10,4	7,8	6,8	9,6	8
1,97	20,3	10,3	13	6,5	15,3	8
2,98	24,2	8,1	19	6,4	20	7
4,7	31,4	6,7	27	5,7	29,5	6
8,0	—	—	40	5,0	41,3	5
14,8	—	—	—	—	68	5
30	100	3,3	—	—	—	—
130	300	2,3	220	1,7	208	1,6
260	440	1,7	31	1,2	—	—
2290	3900	1,7	—	—	—	—

Notes. I, automobile gasoline; II, diesel oil; III, tractor kerosene. All commas in numbers should be read as points.

It is found [1] that the height δ increases with d (see Table 2.1); at first δ/d decreases rapidly, but there is later little variation as d increases.

The structure and shape show that there are several modes of burning, namely laminar for d small and turbulent for d large [2].

Laminar Flames

The flame separates the region where there is oxygen but no vapor (the oxidative region) from the one where there is vapor but no oxygen (the reductive region); the two components react in the flame, which forms a very thin layer if the reaction rate is high. The concentrations of the reactants are zero at this surface or layer, as Fig. 2 [3] shows for hydrogen emerging from a burner into air. A stoichiometric mixture is burnt in the flame zone [4-6]; if we were to assume that the concentration of one reactant (say oxygen) at this surface is not zero, we would have that a combustible mixture could form away from this surface,

which mixture would burn at the prevailing high temperature, so the flame zone would be displaced. The result is that the flame migrates to a position where the fluxes correspond to the stoichiometric mixture and where the concentrations are zero.

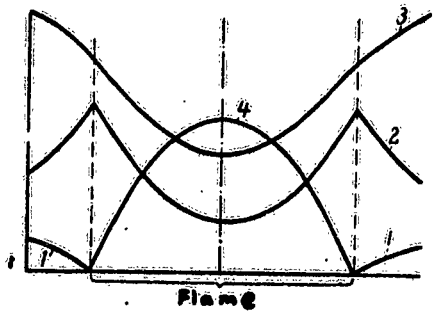

Fig. 2. Simplified model of concentrations in a diffusion flame: 1) oxygen; 2) reaction products; 3) nitrogen; 4) vapor.

Theory of Laminar Diffusion Flames

Burke and Schuman [7] first gave this theory in 1928; they considered the combustion of a jet of gas emerging from a cylinder into a coaxial cylinder carrying air flowing at the same speed. They derived an equation for the shape and size of the flame. This is a particular case, but some of their results have a more general significance; the theory is applicable to flames from liquids, so we deal briefly with it here.

The discussion is based on the mutual diffusion of fuel and oxygen in a cylindrical coordinate system (z,r), the z axis being the axis of the burner and the origin being at the center of the end, which has a radius R_1. The radius of the outer chamber is R_2, the oxygen concentration is c_k, the fuel concentration is c_f, the rate of consumption of oxygen is w_k (that for the fuel being w_2), the stoichiometry factor is β (since $w_2 = \beta w_k$), and the flow speeds are u. The process is steady, and the diffusion coefficients D for fuel and oxygen are the same.

The diffusion equations are

$$u\frac{\partial c_к}{\partial z} = D\left[\frac{\partial^2 c_к}{\partial z^2} + \frac{1}{r}\frac{\partial}{\partial r}\left(r\frac{\partial c_к}{\partial r}\right)\right] - w_к,$$
$$u\frac{\partial c_f}{\partial z} = D\left[\frac{\partial^2 c_f}{\partial z^2} + \frac{1}{r}\frac{\partial}{\partial r}\left(r\frac{\partial c_f}{\partial r}\right)\right] - w. \qquad (2.1)$$

The first equation is multiplied by β and is subtracted from the second, which, in conjunction with the notation

$$c = c_2 - \beta c_к$$

gives us that

$$u\frac{\partial c}{\partial z} = D\left(\frac{\partial^2 c}{\partial z^2} + \frac{\partial^2 c}{\partial r^2} + \frac{1}{r}\frac{\partial c}{\partial r}\right). \qquad (2.2)$$

The term in (2.2) for diffusion along the flame is small relative to the others; that is,

$$\frac{\partial^2 c}{\partial z^2} \ll \frac{\partial^2 c}{\partial r^2} + \frac{1}{r}\frac{\partial c}{\partial r},$$

and so we may put that

$$u\frac{\partial c}{\partial z} = D\left(\frac{\partial^2 c}{\partial r^2} + \frac{1}{r}\frac{\partial c}{\partial r}\right). \qquad (2.3)$$

The dimensionless coordinates

$$\bar{r} = \frac{r}{R_2}, \qquad \bar{z} = \frac{Dz}{uR_2^2},$$

enable us to put (2.3) as

$$\frac{\partial c}{\partial \bar{z}} = \frac{\partial^2 c}{\partial \bar{r}^2} + \frac{1}{\bar{r}}\frac{\partial c}{\partial \bar{r}}. \qquad (2.4)$$

The boundary conditions are $c = c_{of}$ for the gas in the tube at $z = 0$ and $\bar{r} < \bar{r}_0$ (here $\bar{r}_0 = R_1/R_2$), $c = c_{ok}$ for the oxygen at $z = 0$ and $\bar{r}_0 < \bar{r} < 1$, and $c/\bar{r} = 0$ at $\bar{r} = 0$ and $\bar{r} = 1$. Burke and Schuman's solution to (2.4) subject to these conditions is

$$\frac{c_f + \beta c_{ok}}{c_{of} + \beta c_{ok}} = \bar{r}_0^2\left[1 + \frac{2}{\bar{r}_0}\sum \frac{I_0(\mu_i \bar{r}_0)\, I_0(\mu_i \bar{r})}{\mu_i I_0^2(\mu_i)}\, e^{-\mu_i^2 \bar{z}}\right], \qquad (2.5)$$

in which I_0 and I_1 are Bessel functions of the first kind of orders zero and one, the μ_i being the roots of

$$I_1(\mu_i) = 0.$$

Now c_k and c_f are zero in the flame zone, so we put $c = 0$ in (2.5) to get the equation for the flame surface. Figure 3 shows results 1) for excess oxygen and 2) for deficit; experiment confirms that there are two types of flame, which have the shapes shown in Fig. 3.

With $c = 0$ and $\bar{r} = 0$ (excess oxygen) and $\bar{r} = 1$ (deficit), the $\bar{z}$ of (2.6) becomes the dimensionless height of the flame; for given $\bar{r}_0$ and c_{ok}/c_f we have that

$$z = \text{const} = k; \quad \delta = k\frac{uR_2^2}{D} \quad ; \quad \delta \propto \frac{uR_1^2}{D} \propto \frac{V}{D}, \qquad (2.6)$$

in which V is the flow of fuel. It is found that (2.6) agrees well with experiment.

Frank-Kamenetskii [8] has shown that the expression for

can be found without solving (2.4), if in this we insert the dimensionless concentration $\bar{c} = c/c_0$; the equation becomes dimensionless and free from parameters, while the boundary conditions contain $\bar{r}_0$. The solution to (2.4) can then be put as

$$\bar{c} = f(\bar{z}, \bar{r}, \bar{r}_0),$$

and the shape of the flame is given by

$$f(\bar{z}, \bar{r}, \bar{r}_0) = 0.$$

This implies that, for a given $\bar{r}_0$,

$$\delta \propto \frac{uR_2^2}{D} \propto \frac{uR_1^2}{D} \propto \frac{V}{D}.$$

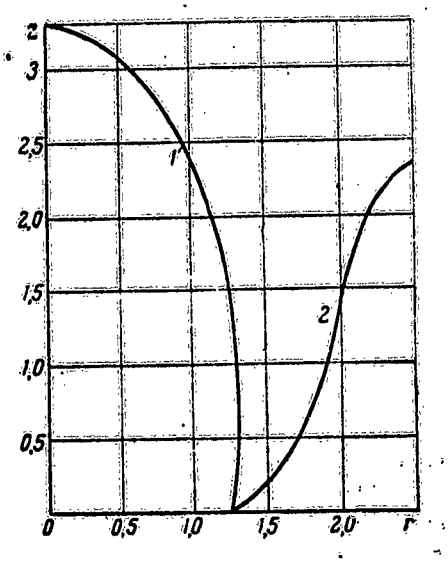

Fig. 3. Shape of a diffusion flame (Burke and Schuman): 1) cylindrical flame with excess oxygen; 2) the same with too little oxygen.

Burke and Schuman's results agree with experiment, which means that the mixing conditions govern the rate of combustion and that the detailed reaction kinetics play no important part (the slower process is the rate-limiting one). This applies also to vapors from liquids.

Barr [9] has considered this problem for flows differing in speed; Hottel and Gausorn [5] have discussed open laminar diffusion flames by using Burke and Schuman's approximation, (2.4) being solved subject to the modified boundary condition that dc/dr is zero at $r = \infty$, not at $\bar{r} = 1$. Their solution relates to the case in which the atmosphere moves with the speed of the gas in the burner; but it does satisfy one of the boundary conditions, so the problem remains unsolved.

There is a simpler way of solving this problem approximately for the flame from a liquid [10]. The amount dm of oxygen reaching an element of the steady flame equals the amount consumed in burning the vapor reaching the same element in the same period. We use the (z,r) system, with z along the flame and the angle formed by r with this axis; here ρ' and u are the density and speed of the vapor, g_1 and g_2 are the proportions (by weight) of the combustible components (assumed to number two),

and β_1 and β_2 are the amounts (g per g) of oxygen needed to burn these, so

$$dm = u\rho' (\beta_1 g_1 + \beta_2 g_2)\, r\,d\varphi\, dr = u\rho' [(\beta_2 - \beta_1) g_2 + \beta_1]\, r\,d\varphi\, dr. \qquad (2.7)$$

This dm may be found in another way. We isolate by means of two indefinitely close planes normal to z a layer in the flow of vapor at the surface of the liquid; this layer has the radius R of the burner or vessel. Let it move upwards at the speed u; it burns as it moves, and its radius r is that of the flame, which decreases. The width of the zone of combustion products increases. The oxygen reaches the flame via a circular layer of these products; if we assume that c in this layer is as for a steady state, then, with ξ denoting the distance from the z axis, we have that

$$D\left(\frac{d^2c}{d\xi^2} + \frac{1}{\xi}\frac{dc}{d\xi}\right) = 0.$$

Now c is c_0, the oxygen concentration in the surrounding atmosphere, at $\xi = R$ and is zero at $\xi = r$, so

$$dm = D\left(\frac{dc}{d\xi}\right)_{\xi=r} r\,d\varphi\, dz = \frac{Dc_0}{\ln R - \ln r} \cdot \frac{1}{r}\, r\,d\varphi\, dz. \qquad (2.8)$$

Then (2.7) and (2.8) give

$$\frac{Dc_0}{\rho' u [(\beta_2 - \beta_1) g_2 + \beta_1]}\, dz = r (\ln R - \ln r)\, dr. \qquad (2.9)$$

The origin may be placed at the surface of the liquid; $r = R$ at $z = 0$ and

$$\int r \ln r\, dr = r^2\left(\frac{1}{2}\ln r - \frac{1}{4}\right),$$

so (2.9) gives

$$-\frac{Dc_0}{\rho' u [(\beta_2 - \beta_1) g_2 + \beta_1]}\, z = \frac{1}{4}(r^2 - R^2) + \frac{r^2}{2}\ln\frac{R}{r}. \qquad (2.10)$$

Further, $\delta = z$ for $r = 0$, so (2.10) gives us that

$$\delta = \frac{\rho' u [(\beta_2 - \beta_1) g_2 + \beta_1]}{4Dc_0} R^2.$$

But $\rho' u$ is the amount evaporating per cm^2 per sec, so $\rho' u = \rho v$, in which ρ and v are the density and linear burning rate; then

$$\delta = \frac{\rho v [(\beta_2 - \beta_1) g_2 + \beta_1]}{4Dc_0} R^2. \qquad (2.11)$$

The dimensionless coordinates

$$\bar{z} = \frac{z}{\delta} \; ; \; \bar{r} = \frac{r}{R},$$

enable us to put (2.10) as

$$\bar{z} = 1 - \bar{r}^2 + \bar{r}^2 \ln \bar{r}^2. \quad (2.12)$$

Then (2.12) defines the shape of the flame.

If there is no second component, (2.11) becomes

$$\delta = \frac{\beta \rho v}{4Dc_0} R^2 = \frac{\beta \rho V}{4\pi Dc_0}. \quad (2.13)$$

This agrees fully with (2.6); Fig. 4 shows that the agreement with experiment is also good. Here z/δ is plotted against r/R; the various symbols denote results obtained with ethanol-water mixtures used in glass tubes ($d = 22$ mm). The full line represents (2.12); it fits the experimental points very closely.

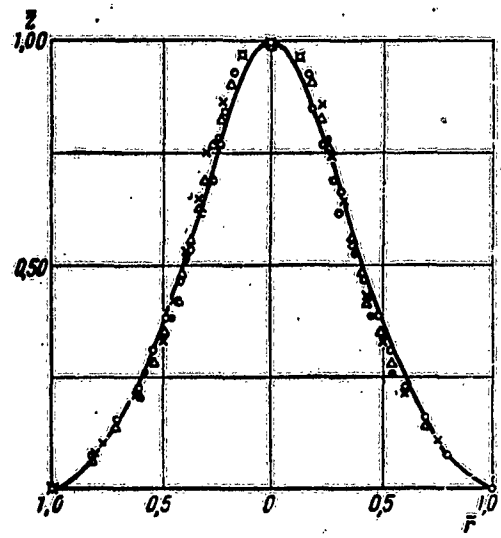

Fig. 4. Shapes of diffusion flames of ethanol in burners.

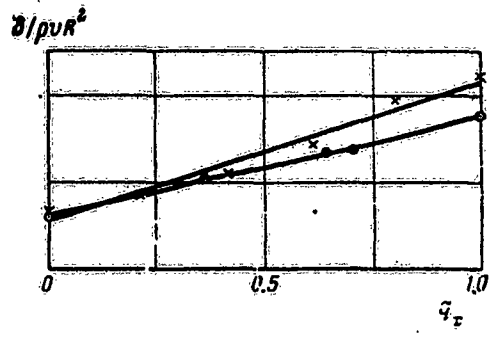

Fig. 5. Relation of $\delta/\rho v R^2$ to composition; glass, d = 7.7 mm.

Table 2.2 shows that (2.6) and (2.11) also fit experiments with ethanol in glass tubes of various diameters; here h is the distance from the free edge of the burner to the surface of the liquid and v is the linear burning rate for the liquid. The variations in δ/vR^2 with R and h lie within the limits of error of the measurements.

The following results [1] for $(\delta/v)/1000$ for steel burners show that (2.6) and (2.13) apply also to these more complex substances:

and β_1 and β_2 are the amounts (g per g) of oxygen needed to burn these, so

$$dm = u\rho' (\beta_1 g_1 + \beta_2 g_2)\, r\, d\varphi\, dr = u\rho' [(\beta_2 - \beta_1)\, g_2 + \beta_1]\, r\, d\varphi\, dr. \qquad (2.7)$$

This dm may be found in another way. We isolate by means of two indefinitely close planes normal to z a layer in the flow of vapor at the surface of the liquid; this layer has the radius R of the burner or vessel. Let it move upwards at the speed u; it burns as it moves, and its radius r is that of the flame, which decreases. The width of the zone of combustion products increases. The oxygen reaches the flame via a circular layer of these products; if we assume that c in this layer is as for a steady state, then, with ξ denoting the distance from the z axis, we have that

$$D\left(\frac{d^2c}{d\xi^2} + \frac{1}{\xi}\frac{dc}{d\xi}\right) = 0.$$

Now c is c_0, the oxygen concentration in the surrounding atmosphere, at $\xi = R$ and is zero at $\xi = r$, so

$$dm = D\left(\frac{dc}{d\xi}\right)_{\xi=r} r\, d\varphi\, dz = \frac{Dc_0}{\ln R - \ln r} \cdot \frac{1}{r}\, r\, d\varphi\, dz. \qquad (2.8)$$

Then (2.7) and (2.8) give

$$\frac{Dc_0}{\rho' u [(\beta_2 - \beta_1) g_2 + \beta_1]}\, dz = r (\ln R - \ln r)\, dr. \qquad (2.9)$$

The origin may be placed at the surface of the liquid; $r = R$ at $z = 0$ and

$$\int r \ln r\, dr = r^2\left(\frac{1}{2}\ln r - \frac{1}{4}\right),$$

so (2.9) gives

$$-\frac{Dc_0}{\rho' u [(\beta_2 - \beta_1) g_2 + \beta_1]}\, z = \frac{1}{4}(r^2 - R^2) + \frac{r^2}{2}\ln\frac{R}{r}. \qquad (2.10)$$

Further, $\delta = z$ for $r = 0$, so (2.10) gives us that

$$\delta = \frac{\rho' u [(\beta_2 - \beta_1) g_2 + \beta_1]}{4Dc_0} R^2.$$

But $\rho' u$ is the amount evaporating per cm^2 per sec, so $\rho' u = \rho v$, in which ρ and v are the density and linear burning rate; then

$$\delta = \frac{\rho v [(\beta_2 - \beta_1) g_2 + \beta_1]}{4Dc_0} R^2. \qquad (2.11)$$

The dimensionless coordinates

$$\bar{z} = \frac{z}{\delta} \; ; \; \bar{r} = \frac{r}{R},$$

enable us to put (2.10) as

$$\bar{z} = 1 - \bar{r}^2 + \bar{r}^2 \ln \bar{r}^2. \quad (2.12)$$

Then (2.12) defines the shape of the flame.

If there is no second component, (2.11) becomes

$$\delta = \frac{\beta \rho v}{4Dc_0} R^2 = \frac{\beta \rho V}{4\pi D c_0}. \quad (2.13)$$

This agrees fully with (2.6); Fig. 4 shows that the agreement with experiment is also good. Here z/δ is plotted against r/R; the various symbols denote results obtained with ethanol-water mixtures used in glass tubes (d = 22 mm). The full line represents (2.12); it fits the experimental points very closely.

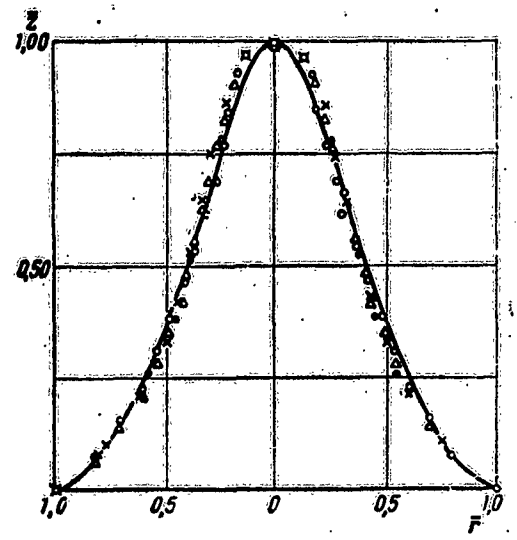

Fig. 4. Shapes of diffusion flames of ethanol in burners.

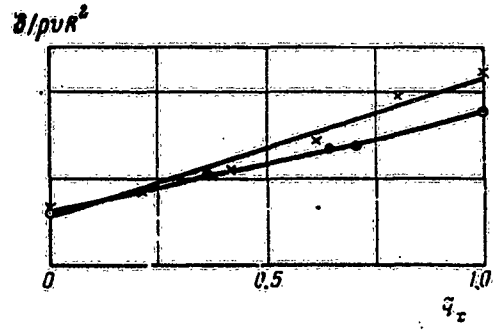

Fig. 5. Relation of $\delta/\rho v R^2$ to composition; glass, d = 7.7 mm.

Table 2.2 shows that (2.6) and (2.11) also fit experiments with ethanol in glass tubes of various diameters; here h is the distance from the free edge of the burner to the surface of the liquid and v is the linear burning rate for the liquid. The variations in δ/vR^2 with R and h lie within the limits of error of the measurements.

The following results [1] for $(\delta/v)/1000$ for steel burners show that (2.6) and (2.13) apply also to these more complex substances:

		$2R$, мм	3,7	5,0	6,0	7,1	11	20	30
Benzene	Бензин		—	—	1,1	1,1	1,4	1,1	0,9
Kerosene	Керосин		1,7	2,2	2,1	2,0	1,9	1,5	—
Solar oil	Соляровое масло		1,8	2,4	2,3	2,2	2,1	2,0	2,0

Table 2.2

$2R$, мм	2,15		4,6		9,4						15,1						
h, мм	4,2	5,0	4,2	6,5	0	1,8	4,2	6,0	8,0	10	0	1,8	4,2	6,0	8,0	10	12
$\frac{\delta}{\nu R^2} \cdot 10^3$, $\frac{мин}{мм^2}$	35	33	41	37	34	34	31	33	36	36	34	37	35	32	31	35	35

Figure 5 shows $\delta/\rho v R^2$ as a function of g, the proportion of the second component by weight in the liquid; the crosses represent results for mixtures of ethyl and isoamyl alcohols, and the circles ones for ethyl and butyl alcohols. The full lines represent (2.11), which clearly shows good agreement with the actual behavior of $\delta/\rho v R^2$.

Further, (2.13) implies that $\beta\rho v/\delta$ should be independent of the nature of the liquid for laminar burning, as is found; experiments [2] show that the mean $\rho v/\delta$ for ethanol in burners of d between 4.6 and 46.8 mm is 1.21 mg/cm.sec, and for butanol for d of 3 to 30 mm is 0.88 mg/cm.sec (the β for these compounds are 2.1 and 2.6 respectively). Then $\beta\rho v/\delta$ is 2.54 and 2.38 mg/cm.sec for these two alcohols; the two values are very similar.

The approximate theory is thus satisfactory, so the rate of combustion of vapor in laminar burning is governed by the rates of influx of reactants, not by the rate of the reaction (the latter is much higher than the rate of formation of the mixture).

Turbulent Flames

The flame from a liquid in a vessel over 30 cm in diameter is turbulent [1]; not much is known about this type of flame, but Table 2.1 shows that δ/d varies little with d, being about two, which is much less than for laminar flames. The explanation is simple; arguments similar to those for laminar flames [1,11] show that

$$\delta \propto \frac{V}{D},$$

But $D \propto ud \propto vd$ for turbulent flames, and so

$$\delta \propto d. \qquad (2.14)$$

The fall in δ/d is clearly a result of the increase in the

effective D for turbulent flames.

Pulsations in Flames

1. Long ago it was observed that the diffusion flame of a gas jet in air shows low-frequency fluctuations; these have been

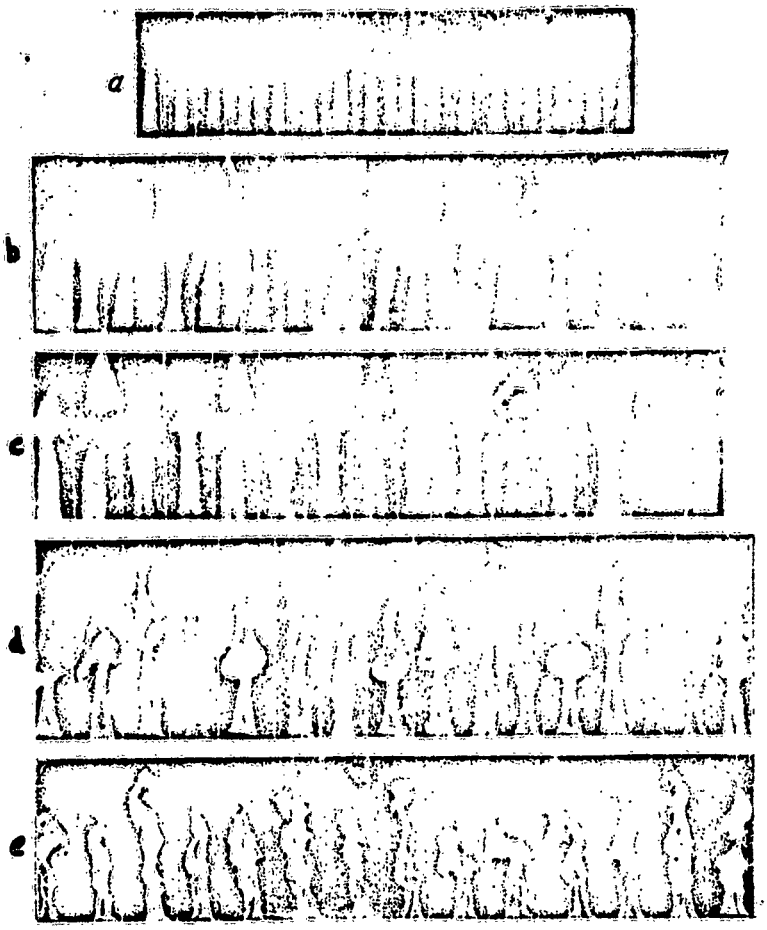

Fig. 6. Photographs of flames from automobile gasoline (Khudyakov) taken at 32 frames per sec; d: a) 11 mm; b) 20 mm; c) 30 mm; d) 47 mm; e) 80 mm.

studied by Maklakov [12]. The flame does not fluctuate if the rate of flow is low, but the length starts to fluctuate as the rate is increased. The critical flow speed u_c decreases as d increases, and it is also dependent on the nature of the gas.

The type of oscillation alters as the speed increases; the top part of the flame breaks away and completes its burning in isolation. The oscillations become complex at high speeds.

2. Flames from liquids resemble those from unmixed gases; the flame is stable if d is less than d_c, the critical diameter, but oscillations of frequency 10-15 c/s set in above that limit. Figure 6a shows the oscillations in a gasoline flame. The nature of the liquid affects d_c, which is about 1 cm. The type of oscillation also varies with d; the upper part tends to break away as d increases. The top elongates, a neck appears, and

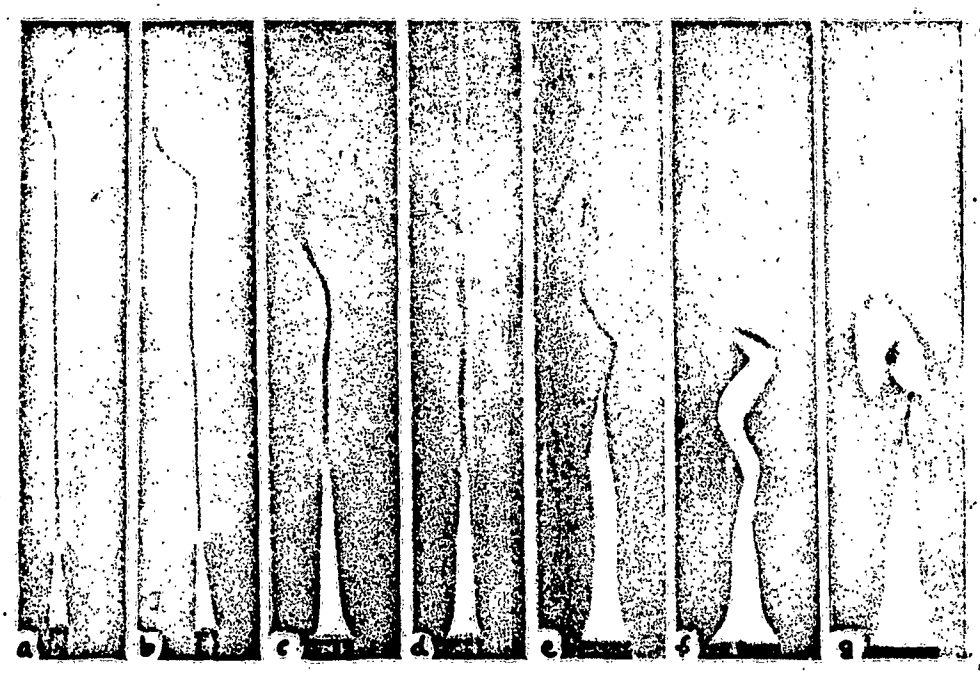

Fig. 7. Flames from solar oil in burners of diameters a) 5 mm; b) 12 mm; c) 15 mm; d) 20 mm; e) to g) 30 mm.

the top breaks away; the residual part is at first short, but it soon lengthens again, and the process is repeated. The lower part of the flame has a regular and simple shape (Fig. 6, b and c).

Further increase in d (Fig. 6d) gives rise to an upper part of complex shape; the oscillations encompass a large part of the flame. The whole flame begins to pulsate when d is very large, and we get the continuously changing forms of Fig. 6e. There is a general tendency for the oscillation frequency to decrease as d

increases.

3. These oscillations set in at Re much less than those for the transition from laminar to turbulent flow; for example, Maklakov finds that the flame of carbon monoxide flowing from a burner of diameter 4 mm starts to oscillate when the flow rate is only 8 cm^3/sec. The corresponding Re is 21, which is 1/100 of the critical Re. The same is found for flames from liquids. The causes of oscillation have been examined [13]; the onset of oscillation is closely associated with turbulence in the stream of gas from the flame.

Figure 7 shows flames of solar oil in glass cylinders of d between 5 and 30 mm; the soot-laden stream above the flame is clearly visible. The mode of flow of this stream is very much dependent on d; the stream is straight and has sharp outlines at first if $d < d_c$, but at a certain distance it begins to oscillate, the amplitude increasing with the distance from the tube. Finally, the stream is dispersed. Thus the flow is laminar near the flame but becomes turbulent after a certain distance. The entire flow is turbulent if $d > d_c$. Similar patterns are observed for kerosene and gasoline.

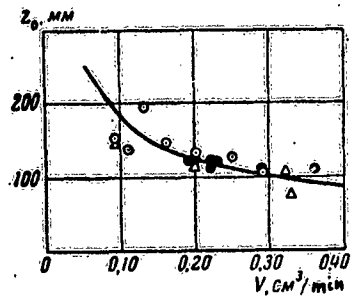

Fig. 8. Relation of z_0 to rate of consumption of liquid.

4. Kerosene in a tube with d = 22.6 mm gives a strongly pulsating flame; the pulsations weaken as the distance h between the liquid and the end of the tube increases, and they cease entirely if $h > h_c$.

It is found that the distance z_0 from the tube to the point of onset of oscillation decreases as d increases (if h is fixed) and as h increases (if d is fixed): this z_0 is related to V, the rate of consumption of the liquid. Figure 8 shows this for various (denoted by the different signs), the line being drawn in accordance with

$$z_0 = aV^{-1/2}. \qquad (2.15)$$

All the points lie near this curve, which means that z_0 is governed by V, not by d and h: moreover, a cannot vary much from one liquid to another.

5. It is known that δ increases with V, so $z_0 - \delta$ decreases as V increases, becoming zero at V_c, whereupon the top of the flame starts to oscillate. The oscillations extend into the

flame when $V > V_c$, and ultimately the motion becomes so vigorous that the top part of the flame breaks away (Fig. 6).

The oscillation in the flame starts when $d = d_c$ (for h fixed); further, the oscillations starts for $h < h_c$ if $d > d_c$. The critical rate $V = V_c$ is given by

$$z_0 = aV_c^{-1/5} = \delta = bV_c.$$

so

$$V_c = \left(\frac{a}{b}\right)^{-5/4} = k. \qquad (2.16)$$

The V_c for solar oil, kerosene, and gasoline are 0.35 cm^3/min; (2.16) is confirmed by Table 2.3, which gives the d_c and h_c calculated from experimental results. Here (-) denotes no

Table 2.3

d, мм	Solar oil		Kerosene				Gasoline						
	14,6	20,3	12	14,6	22,6		5,2	10,9			22,6		
h, мм	0	0	0	0	2,5	4,5	0	2,5	4,5	6,5	6,5	8,5	12,5
$V \cdot 10^2$, $\frac{см^3}{мин}$	39	44	29	36	50	36	38	50	32	17	46	31	15
	—	+	—	+	+	—	+	+	*	—	+	*	—
d_c, мм	17,5		14,5				4,5						
h_c, мм					4,2				4,2			7,9	

* Signs of incipient oscillation.

oscillation in the flame; (+), the presence of oscillation.

6. Zel'dovich [14] made a theoretical study of the transition from laminar to turbulent flow in the gas rising from a flame as long ago as 1937; he gave an approximate expression for the limiting behavior. Prandtl [15] has subsequently made a detailed analysis of some aspects. The following is a summary of Zel'dovich's work.

The heat flux (not the momentum) is conserved in the freely rising convective stream above the flame; then, at large distances from the flame (where the process is self-modeling), we

have (apart from a constant factor) that

$$Q = \bar{u}\bar{\vartheta}c\rho b^2, \tag{2.17}$$

in which Q is the heat produced per sec, b is the width of the stream, c is the thermal capacity of the gas, whose mean speed, temperature, and density are $\bar{u}$, $\bar{\vartheta}$, and ρ. The equation of motion for laminar flow is

$$u\frac{\partial u}{\partial z} = \nu\frac{\partial^2 u}{\partial r^2} + g\beta\vartheta,$$

in which z and r are as above, ν is the kinematic viscosity, g is the acceleration due to gravity, and β is the coefficient of thermal expansion.

Self-modeling behavior gives us that

$$\frac{\bar{u}^2}{z} = \nu\frac{\bar{u}}{b^2} = g\beta\vartheta$$

The latter relation gives us that

$$\mathrm{Re} = \frac{\bar{u}b}{\nu} = \sqrt{\frac{\bar{u}z}{\nu}},$$

but

$$\bar{u} = \frac{g\beta\vartheta b^2}{\nu} = \frac{g\beta\vartheta Q}{\nu\bar{u}\vartheta c\rho}. \tag{2.18}$$

so

$$\mathrm{Re} = \left(\frac{g\beta Qz^2}{\nu c\rho}\right)^{1/4}. \tag{2.19}$$

That is, (2.19) shows that Re increases with z, so the laminar flow must terminate at a certain height, as the photographs show.

7. The Re given by (2.19) for the transition point is about 150, which is about a tenth of the usual critical Re. This is not unexpected, for the transition occurs at low Re in convective flows generally; for example, Re is 400-500 for the flow around a heated vertical plate [15]. The low Re are consequent on the special shape of the velocity profile for the plate; the very low critical Re for flames can be understood on this basis. Of course, the above value for Re may be somewhat too low, for (2.19) is only approximate.

Further, (2.19) gives us the transition point as

$$z_0 \propto \frac{1}{\sqrt{Q}} \propto \frac{1}{\sqrt{V}} \quad \text{or} \quad z_0 = aV^{-1/2}.$$

This last relation is simply (2.15), so Zel'dovich's conclusions

may be applied to the experiments quoted above; his theory enables us to understand and explain the causes of oscillation, although many features remain unexplained.

Shape and Structure of the Flame from a Vertical Tube Surrounded by a Rising Air Current

Here an interesting pattern may be observed. The tube containing the liquid (gasoline) is coaxial with the air tube; the air speed and liquid level are varied. The top of the burner tube may be above or below the bottom of the air tube. It is found that the flame is extinguished at quite low air speeds when

Fig. 9. Shape and structure of flame from gasoline in a tube (d = 9 mm) inside an air tube (d = 13.7 mm); air flow rate (l/min): a) 2; b) 4; c) 8; d) 10; e) 14.

the liquid fills the tube, but it is not extinguished even at high speeds if $h \neq 0$.

The flame is always conical if the air is at rest; it is then strongly luminous and is attached to the tube. Figure 9 shows the effects of air when the liquid is slightly below the top edge of the tube. At 2 l/min (Fig. 9a) the flame is detached from the tube and is still strongly luminescent, except at the base. The luminous part becomes very small at 4 l/min; the flame is still conical, but now with a rim, and its various parts have different colors. The outline becomes diffuse, and the flame starts to roar, at higher speeds; Fig. 9, c-e, illustrates the behavior.

It is difficult to give a full explanation of this behavior; it is clear that the flame becomes detached on account of dilution with air (see Zel'dovich [4] on the extinction of the flame). The low luminosity is clearly the result of an increased rate of influx of oxygen.

1. These features are very important to the theory and practice of liquid combustion, but our information on them is rather scanty. Reliable measurements are difficult to make, especially for turbulent flames; the problem is made more difficult by the rapid and considerable fluctuations if the vessel is of fairly large size.

The luminous flame is of the main interest to us; this contains many very small carbon particles. Schak [16] has shown that these particles differ in temperature from the gas by only a fraction of a degree: the emission comes principally from the particles.

Thermocouples and optical pyrometers can be used to measure the temperature, provided that the readings are suitably corrected. It is best to use two thermocouples of different (known) sizes. The disappearing-filament pyrometer is also convenient, but this reads only the brightness temperature (that of an absolutely black body having the same brightness at the chosen wavelength), which can differ by several hundred degrees from the true temperature (the degree of blackness is the controlling factor). Several methods have been proposed [17,18] for measuring the true temperature and degree of blackness conveniently; one of these is to measure the brightness temperature at two wavelengths, and another is to use a temperature lamp. We describe the latter in detail.

The temperature lamp is a strip-filament lamp whose brightness temperature is known as a function of current; this enables one to read the temperature in terms of the current. The brightness temperature of the flame, s_f, is measured; the current is adjusted to make s_l, the brightness temperature of the lamp, some 200-300° more than s_f. Then a measurement is made of s_{lf}, the brightness temperature of the lamp as seen through the flame. The readings enable one to deduce the temperature T and degree of blackness ϵ by means of the following formulas.

Let B_f be the brightness of the flame as measured at wavelength λ; then Planck's law gives us that

$$B_f = C\lambda^{-5} \exp\left(-\frac{C_2}{\lambda s}\right) = \varepsilon\, C\lambda^{-5} \exp\left(-\frac{C_2}{\lambda T}\right),$$

in which C_1 and C_2 are constants. Let B_l and B_{lf} be the brightness of the filament as seen directly and via the flame; then

$$B_l = C\lambda^{-5} \exp\left(-\frac{C_2}{\lambda s_l}\right)$$

and

$$B_{1f} = C\lambda^{-5}\exp\left(-\frac{C_2}{\lambda s_{1f}}\right) = \varepsilon\, C\lambda^{-5}\exp\left(-\frac{C_2}{\lambda T}\right) + \varepsilon\, C(1-\varepsilon)\,\lambda^{-5}\exp\left(-\frac{C_2}{\lambda T}\right).$$

These equations give us that

$$\frac{1}{T} = \frac{1}{s_f} + \frac{\lambda}{C_2}\ln\varepsilon \tag{2.20}$$

$$\varepsilon = 1 + \exp\left[-\frac{C_2}{\lambda}\left(\frac{1}{s_f} - \frac{1}{s_1}\right)\right] - \exp\left[-\frac{C_2}{\lambda}\left(\frac{1}{s_{f1}} - \frac{1}{s_1}\right)\right], \tag{2.21}$$

It is usual to use a red filter of effective wavelength 0.65 μ in the pyrometer; then C_2/λ is 2.18×10^4. These two equations (2.20) and (2.21) give T (in °K) and ε for this wavelength.

A more precise result is obtained if T and ε are found by adjusting the lamp current I in the measurements on s_1 and s_{1f}; the point where $s_1(I)$ meets $s_{1f}(I)$ gives T, for if

$$B_{1f} = B_f + B_1(1-\varepsilon) = B_1,$$

then

$$B_1 = C\lambda^{-5}\exp\left(-\frac{C_2}{\lambda s_1}\right) = \frac{B_f}{\varepsilon} = C\lambda^{-5}\exp\left(-\frac{C_2}{\lambda T}\right)$$

and

$$T = s_1.$$

The following two cases are encountered. If $B_{1f} < B_1$, then $B_f < B_1\varepsilon$ and $s_1 > T$; if $B_{1f} > B_1$, $B_f > B_1\varepsilon$ and $s_1 < T$.

Hottel and Brayton have measured T by reference to s_f for wavelengths in the red and green regions as isolated by means of filters [18]; the final results are

$$\frac{1}{T}\left(\frac{1}{\lambda_1} - \frac{1}{\lambda_2}\right) = \left(\frac{1}{\lambda_1 s_1} - \frac{1}{\lambda_2 s_2}\right) - \frac{1}{C_2}\ln\frac{\varepsilon_2}{\varepsilon_1} \tag{2.22}$$

$$\frac{\varepsilon_2}{\varepsilon_1} = -C_2\left(\frac{1}{\lambda_2 s_2} - \frac{1}{\lambda_1 s_1}\right). \tag{2.23}$$

Here λ_1 and λ_2 are known, and s_1 and s_2 are measured, so T is readily found. Special nomograms have been compiled to simplify the calculations.

Line-reversal methods have been used for nonluminous flames

[19], but the methods are not applicable to luminous flames. (See [19] for a detailed review of methods of measuring flame temperatures.)

2. Thermopiles, bolometers, and so on are used to measure radiation from flames. In one case [20] the previously calibrated thermopile and galvanometer were placed at some distance from the tank containing the burning liquid (oil product). A double metal screen with a circular aperture was placed between the pile and the tank; the hole was such as to allow the pile to see only the central part of the flame. The emissivity E of the flame is calculated as follows.

Let $\Delta\phi$ be the radiation flux reaching the detector, which views the flame at right angles and which has a sensitive area s_0; the area of flame viewed is s', which lies at a distance r_0. The screen is at a distance r, and the hole has an area s; B is the brightness of the flame. Then

$$\Delta\Phi = BS\,\frac{s_0}{r_0^2} = Bs_0\,\frac{s}{r_0^2} = Bs_0\,\frac{s'}{r^2}.$$

This implies that

$$B = \frac{r^2\Delta\Phi}{s_0 s'}. \qquad (2.24)$$

It is easy to measure s/r^2; $\Delta\phi/s_0$ is deduced from the reading of the galvanometer, and so B is found. Then

$$E = \pi B$$

gives us E. But

$$E = \varepsilon_0\sigma T_n^4, \qquad (2.25)$$

in which σ is Stefan's constant and T is as above; this gives us ε_0, the integral degree of blackness of the flame.

3. The following ε_0 are for the central part of the flame of gasoline in tanks:

Run	1	2	3	4
Diameter, cm	130	130	260	260
T, °K	1390	1393	1403	1447
ε_0	0.75	0.86	0.91	1.0

Clearly, the degree of blackness is close to one for the tank of diameter 260 cm.

The absorptivity is defined by

$$\varepsilon_\lambda = 1 - e^{-k_\lambda l}, \qquad (2.26)$$

in which l is the depth of the absorbing layer and k_λ is the

absorption coefficient at wavelength λ. This latter coefficient is governed by the size and number of the carbon particles for a luminous flame; k_λ decreases as the particle size increases if the proportion of carbon is constant, and ε_λ may become almost one if the flame is of considerable depth and low reflectivity. The emission from the flame is then precisely that from a black body at the same temperature.

4. The following interesting deduction may be made from (2.26). If we have two flames, one twice the thickness of the other, whose absorptivities are ε_1 and ε_2, then

$$(1-\varepsilon_1)^2 = 1-\varepsilon_2. \tag{2.27}$$

This fits the results given above; if we take ε as 0.8 for the 130 cm tank, then $\varepsilon = 0.96$ for the 260 cm one, which is in agreement with the mean value. This implies that ε will be extremely close to unity for a tank of diameter 520 cm or more.

There is a general tendency for k_λ to fall as λ increases: Hottel et al [18] assume that

$$k_\lambda = k_0\lambda^{-n}, \tag{2.28}$$

in which n takes the values 1.39 up to 0.8 μ and 0.95 between 0.8 and 10 μ. It has been observed [19,23] that the finely divided carbon in a flame differs in its optical parameters from massive carbon; in particular, the variation of ε_λ with wavelength is very much more rapid. This means that results obtained with thermopiles should be checked, in order to establish to which spectral region they apply.

5. Great interest attaches to any estimate of the heat lost by radiation. Consider a tank (radius R) not less than 5 m in diameter; the ε for the flame is close to one, and the height is about 2d, while the linear rate of burning is almost independent of d. The heat lost as radiation per unit time is then

$$q_2 = \sigma T^4 S = 4\pi R^2 \sigma T^4,$$

The heat produced by combustion is

$$q_1 = \pi R^2 v \rho q,$$

in which q is the heat of reaction and v is the linear rate of burning. Now

$$\frac{q_2}{q_1} = \frac{4\sigma T^4}{v\rho q}.$$

For gasoline, v = 4 mm/min, ρ = 0.75 g/cm^3, q = 11 kcal/g,

and T ≈ 1400°K. Then

$$\frac{q_2}{q_1} = 0{,}4.$$

Gasoline does not burn completely in these flames, so about half of the heat is lost by radiation. The temperature is therefore well below the maximum possible.

The carbon particles produce most of the emission from a luminous flame; there are many papers on their formation, which

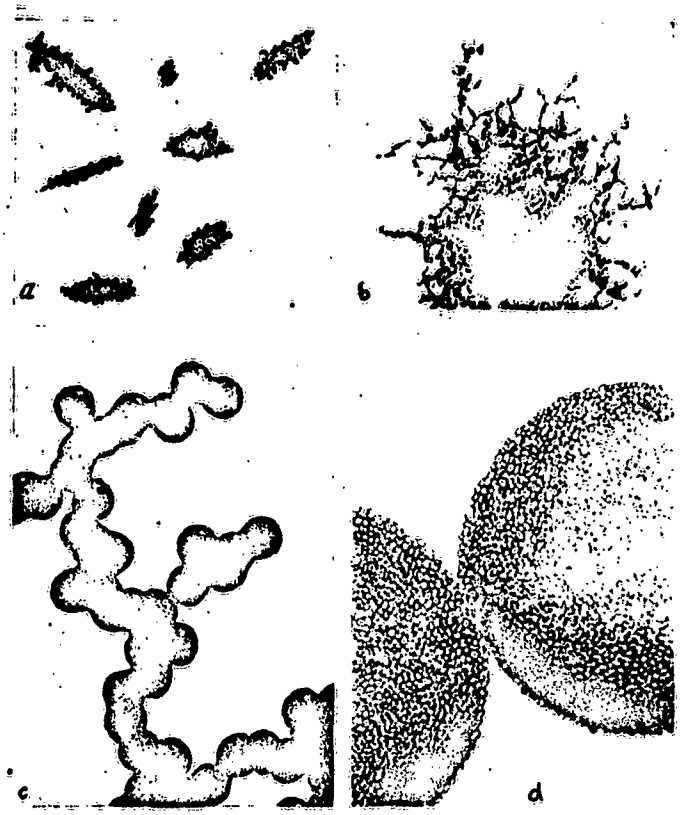

Fig. 10. Structure of soot particles: a) x 100; b) x 1000; c) x 100 000; d) structure of a spherical particle.

have been reviewed [19,21]. The following section deals mainly with the structure.

Figure 10 [21] shows some structures; at low magnification (Fig. 10a) the particles are seen as being composite and elongated, while at x 1000 they are seen to consist of very small particles (Fig. 10b). At x 100 000 they are seen to consist of filaments and clumps of particles more or less equal in size (Fig. 10c).

The diffraction patterns of hydrocarbon smoke and of amorphous lampblack show that the spherical particles revealed by the electron microscope in fact consist of crystallites about 20 Å in size; these are randomly linked together (Fig. 10d). Each crystallite consists of several layers of carbon atoms with hexagonal packing; the layers lie parallel in the order found in graphite, but are twisted one relative to another. The crystallites in smoke resemble sheets of graph paper stacked with their edges at random angles. The soot particles produced by diffusion flames are very small and are complex in structure.

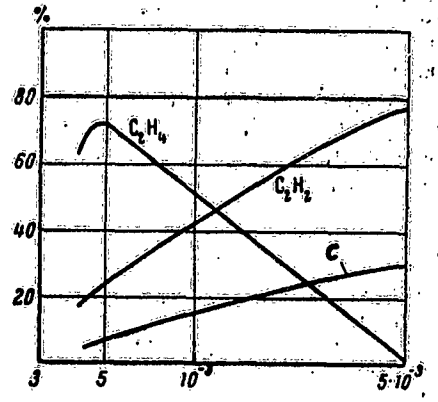

Fig. 11. Pyrolysis products from ethane at 1400°.

The proportion of the carbon appearing as soot varies with the fuel and the conditions; some liquids (e.g., ethanol) burning in narrow tubes give flames luminous at the apex only, with the proportion of luminous flame increasing with the diameter. Other liquids (e.g., benzene) give highly luminous flames even in tubes a few mm in diameter. Here soot starts to appear at the apex as the diameter increases (Fig. 7). The minimum flame height at which soot is formed is sometimes used as a measure of the tendency to produce soot, but it would be better to use the degree of blackness for this purpose.

The carbon in a diffusion flame is formed when the fuel passes through the zone of heating [22]; pure hydrocarbons were passed at high flow rates through a tube 0.3 mm in diameter (transit time a few msec), the temperature being 1100 to 1400°. Figure 11 shows results for ethane (abscissa: time spent in tube), which indicate that the pyrolysis is very rapid; the time spent in the hot part of the flame is quite adequate.

Thermal Conditions in Flames

1. A flame produces heat by reaction and loses it by radiation and convection; the temperature is determined by the amounts of heat produced and lost per unit time, q_1 and q_2. The temperature could be predicted if q_1 and q_2 were known as functions of the various parameters, but here we lack a proper knowledge of conditions in flames; all we can give are some general arguments. Here we deal with laminar flames.

The surface of a laminar flame divides the region having

oxygen but no fuel from that having fuel but no oxygen. The rate at which the vapor burns is very much dependent on the supply of oxygen; the same is true for the burning of solids such as carbon. Of course, the analogy is far from complete, but we can utilize some results on the burning of carbon (and on heterogeneous burning generally) [24-26], provided care is taken.

2. Let k_s be the amount of oxygen consumed in unit time at the surface; let c and c_0 be the oxygen concentrations in the combustion zone and in the surrounding atmosphere. Further, let α' be the gas-exchange factor, k the rate constant, E the activation energy, T the flame temperature, and R the gas constant. We assume that the reaction rate is proportional to c. Then we have for the flame from a liquid that

$$k_s = \alpha' (c_0 - c) = kc = k_0 c e^{-\frac{E}{RT}}.$$

This gives us that

$$k_s = \frac{c_0}{\frac{1}{\alpha'} + \frac{1}{k}}. \tag{2.28a}$$

This shows that the specific reaction rate is governed by the rates of diffusion and reaction; now k is large relative to α' at high temperatures, so

$$k_s = \alpha' c_0 \left(1 - \frac{\alpha'}{k}\right). \tag{2.29}$$

This shows that the rate of supply of oxygen controls the rate of burning; this mode of burning is called diffusion burning. In this case c is almost zero in the flame, and the specific rate of burning varies little with T.

The heat q_1 produced per unit area in unit time is $k_s q$, in which q is the heat of reaction; curve 1 of Fig. 12 shows $q_1(T)$. The heat lost per unit time from unit area of flame is

$$q_2 = \alpha (T - T_0) + \varepsilon\sigma (T^4 - T_0^4), \tag{2.30}$$

in which α is the heat-transfer factor, s is the degree of blackness of the flame, σ is Stefan's constant, and T_0 is the temperature of the surroundings. Curve 2 of Fig. 12 shows $q_2(T)$. In the steady state

$$q_1 = q_2. \tag{2.31}$$

The solution to (2.31) gives us the steady-state T; it is best found graphically from the intersection of the curves for q_1 and q_2.

3. The effect of altering c_o is to change $q_1(T)$, which becomes lower as qc_o decreases. Figure 13 shows that the curves for q_1 and q_2 then meet further to the left; the curves become tangential at a certain qc_o. The point of contact gives the temperature at which the flame goes out, so T falls as qc_o is reduced, there being a limiting qc_o at which the flame cannot persist.

Practical extinction measures include the addition of inert gases or fine sprays of nicombustible liquids; the droplets absorb heat in evaporating, while the vapor dilutes the oxygen and the fuel.

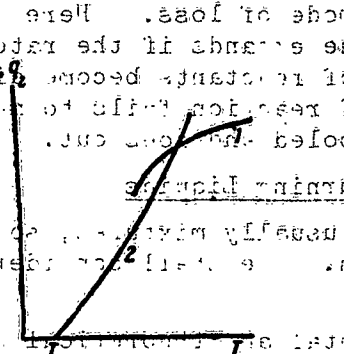

Fig. 12. Graphs of $q_1(T)$ and $q_2(T)$.

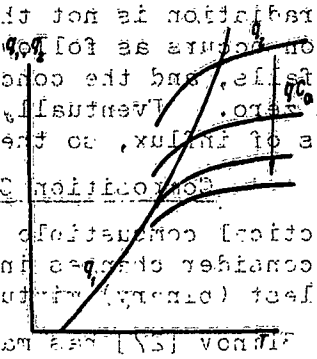

Fig. 13. Relation of flame temperature to qc_o.

The derivatives of q_1 and q_2 are equal at the extinction temperature, so

$$q_1 = q_2, \quad \frac{dq_1}{dT} = \frac{dq_2}{dT}. \tag{2.32}$$

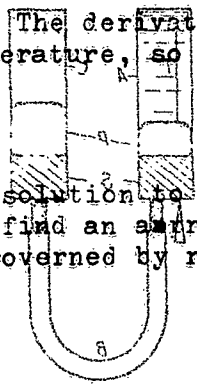

The solution to (2.32) gives us the corresponding T and qc_o. We can find an approximate solution to (2.32) if we assume that q_2 is governed by radiation; then

$$\alpha q c_0 \left(1 - \frac{\alpha}{k_0} e^{\frac{E}{RT}}\right) = \sigma \varepsilon T^4, \tag{2.33}$$

and, since αqc_o may be taken as constant,

$$\frac{\alpha^2 q c_0}{k_0} \cdot \frac{E}{RT^2} e^{\frac{E}{RT}} = 4\varepsilon\sigma T^3. \tag{2.34}$$

Let $RT/E = \theta$; the second term in the bracket in (2.33) is much less than one, so (2.33) and (2.34) may be replaced by

$$\frac{\alpha}{k_0} e^{\frac{1}{\theta}} = 40, \quad qc_0 = \varepsilon\sigma \left(\frac{E}{R}\right)^4 \theta^4. \tag{2.35}$$

This system gives us θ and · for this case.

The burning zone expands if qc_0 falls, because the rate of combustion is lower.

The main conclusions for the thermal conditions in laminar flames are applicable also to turbulent flames.

4. Zel'dovich [4] has shown that the flame goes when the temperature in the burning zone has fallen to

$$T_M - T \approx \frac{RT_M^2}{E},$$

even if radiation is not the dominant mode of loss. Here extinction occurs as follows. The zone expands if the rate of burning falls, and the concentrations of reactants become different from zero. Eventually the rate of reaction fails to match the rates of influx, so the flame is cooled and goes out.

Composition Changes in Burning Liquids

Practical combustible liquids are usually mixtures, so we have to consider changes in composition. We shall consider only the simplest (binary) mixtures.

1. Blinov [27] has made experimental and theoretical studies on binary mixtures, as have others [28]. Hall [35], Burgoyne and Katan [29], and Pavlov and Khovanova [30,31] have studied the effects for crude oil.

Figure 14 shows an apparatus that has been used: here A is a cylinorical glass burner, C is a container allowing of vertical movement, B is a rubber tube joining A to C, the S are bungs, and F is mercury. The mixture is poured into A; C is raised slowly and continuously to keep the surface of the liquid at the top of the tube. The flame is extinguished when the set proportion of liquid has been burned; the liquid is removed and is examined with a refractometer. A calibration curve for the mixture then gives the composition.

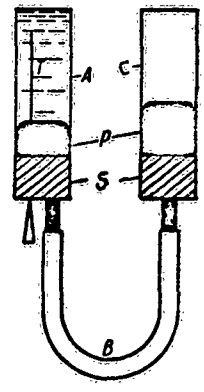

Fig. 14. Apparatus for examining composition changes in burning binary liquids.

In some cases the burner was fitted with a small thin-walled tube T whose tip lay 3-4 mm below the surface; the lower end was closed during the burning, but afterwards it was opened to allow the upper layer of liquid to run down into a test-tube. Then it was closed again, tube C was raised to restore the level of the

liquid, another sample was taken in a second test-tube, and so on. All samples were examined as before. Table 2.4 gives results for some tests in which the first component was always ethanol. Here A was 7.7 mm in diameter, and the initial depth h_0 was always 50 mm; g_0 and g denote the proportions (by weight) of the

Table 2.4

Water			Benzene $h = 13$		Isoamyl alc., $h = 12$		Propyl alc., $h = 10$		n-Butyl alc., $h = 13$	
g_0	g	h	g_0	g	g_0	g	g_0	g	g_0	g
0,04	0,04	13	0,13	0,08	0,21	0,36	0,24	0,30	0,36	0,51
0,11	0,11	13	0,25	0,19	0,41	0,68	0,29	0,56	0,64	0,78
0,24	0,33	13	0,51	0,43	0,61	0,83	0,75	0,80	0,70	0,81
0,40	0,58	13	0,72	0,72	,80	0,91	—	—	—	—
0,57	0,76	30	0,84	0,86	—	—	—	—	—	—
0,62	0,77	40	0,97	0,98	—	—	—	—	—	—
0,70	0,76	40	—	—	—	—	—	—	—	—

second component before and after the burning, h being the depth of the residual liquid. The mixtures containing the three higher alcohols always became depleted in ethanol, but ethanol-rich mixtures with water did not change in composition. Those containing more than 11 wt.% water became enriched in water. The mixtures with benzene became depleted in the second component if $g_0 < 0.72$, but enriched if $g_0 > 0.72$, the 0.72 composition being invariant.

The reason for this behavior is that the equilibrium vapor does not, in general, have the composition of the liquid, with the exception of azeotropic mixtures. We have discussed this question of composition in part one, so here we deal only with aspects essential to the explanation of these effects. Figure 15 shows the boiling points as functions of composition (weight proportion of the second component) of vapor (upper line) and liquid (lower line). The vapor is clearly enriched in ethanol, and so the liquid becomes enriched in the second component. The other two alcohols show similar effects.

Figure 16 shows the special behavior of mixtures containing water, which are imperfect mixtures of the second kind (the azeotropic composition contains 10.6 mole% of water and boils at 78.15°). Alcohol-rich mixtures give a vapor having the composition of the liquid; all other mixtures give a vapor enriched in alcohol. This feature explains the results of Table 2.4.

Figure 18 of part one gives these curves for the benzene-ethanol mixtures at constant pressure; these show that the vapor is enriched in benzene if the mole% of that corround is less than that for the azeotropic mixture, and vice versa. This explains why some mixtures become enriched in ethanol, and others in benzene.

In general, the liquid becomes enriched in the component under-represented in the vapor; Konovalov's first law [32,33] enables us to put this as: a mixture of two liquids in burning becomes enriched in the corponent whose addition reduces the vapor pressure (or raises the boiling point). (This deduction is also applicable to mixtures containing more than two components.)

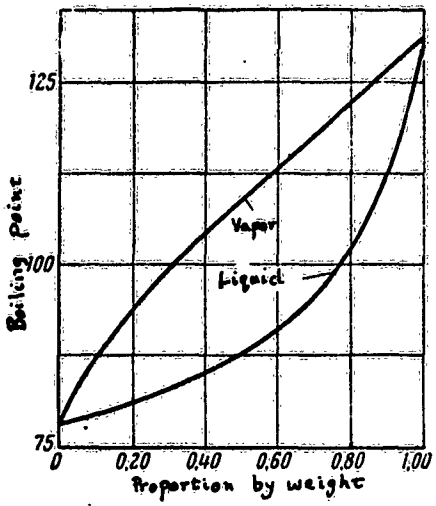

Fig. 15. Boiling points of mixtures of ethanol with isoamyl alcohol at constant pressure.

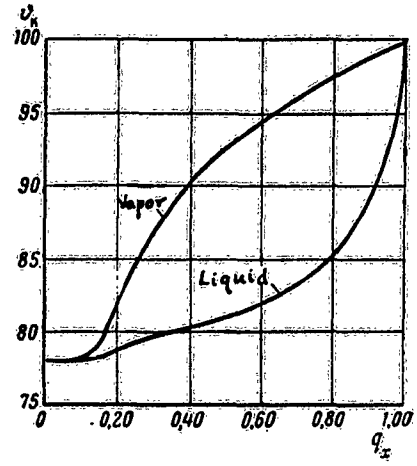

Fig. 16. Boiling points of ethanol-water mixtures as functions of composition.

The composition does not alter if the vapor has the composition of the liquid; Konovalov's second law indicates that this composition corresponds to a turning point on the curve for the vapor pressure (or boiling point).

The change in composition is the greater the larger the proportion consumed, as Table 2.5 shows for mixtures in which ethanol was the first component. Here g_o is as before (except that it is expressed in %), h_o is the initial depth, and d is the diameter of the tube.

The composition change, $\Delta g = g_o - g$, is dependent on the combustion conditions, as Table 2.5 shows for burner diameter and

Table 2.6 shows for mixtures containing 41% of the second component as burned in tubes of glass and iron (diameters 21 mm; wall thickness: iron 2mm, glass 1.5 mm). The iron burner produces the greater change in composition.

The nature of the mixture also affects the variation in composition as between layers, as Table 2.7 shows for mixtures in which ethanol was the first component. Here the burner was a glass tube (d = 29.5 mm), v is the rate of combustion (mm/min), and z is the distance from the surface (mm). The mixtures with

Table 2.5

	g_0	h_0	d						
	21	50	7,7	*12 / **22	23 / 23	42 / 26	60 / 30	79 / 39	86 / 47	90 / 54
Isoamyl alcohol	33	54	7,7	45 / 39	71 / 46	91 / 70	95 / 92	97 / 96		
	33	56	30	71 / 39	87 / 49					
	20	52	7,7	26 / 19	78 / 18	91 / 17	96 / 10			
	48	53	7,7	60 / 49	87 / 52	90 / 61	95 / 61	97 / 78		
Toluene	79	52	7,7	23 / 84	40 / 87	53 / 89	59 / 91	78 / 98	89 / 100	
	90	52	7,7	45 / 92	58 / 93	73 / 95	84 / 99			
Water	26	61	30	48 / 39	56 / 40	66 / 46	81 / 63	87 / 84		
	26	53	7,7	38 / 35	63 / 42	83 / 54	92 / 76			

* Top line: ξ, the % of the liquid consumed in the test.
** Bottom line: q, the % of the second component remaining.

the two higher alcohols show changes in composition only in the top 25 mm, whereas aniline and water show changes at all levels. These differences are caused by the density variations. The alcohols are very similar in density, and the top layer shows vigorous circultaion; the lower layer shows no appreciable flow. The top layer was 7-9 mm deep in a 7,7 mm burner, and 4-5 mm in a 30 mm one. Water and aniline differ greatly in density from ethanol, and here the circulation covers the entire volume; the

Table 2.6

		Glass				Iron			
Isoamyl and ethyl alcohols	ε	28	59	90	99	35	65	86	93
	Δg	1,8	2,2	8,5	37	7,6	14	28	46
Butyl and ethyl alcohols	ε	28	54	81	92	25	53	82	—
	Δg	1,6	3,1	11	28	5	16	33	—

circulation arises because the ethanol-depleted layer is denser than the original mixture.

Oil products also change in composition as they burn (Table 2.8); here Δn denotes the change in refractive index. The

Table 2.7

Isoamyl alcohol v=1,6; g_0=33; h_0=117; s=42		Butanol v=1,7; g_0=55; h_1=109; s=45		Aniline v=1,5; g_0=8; h_0=107; s=41		Water v=1,1; g_0=26; h_0=94; s=49		g_0=53; h_0=110; s=63	
z, мм	Δg	z, мм	Δg	z, мм	Δg	z, мм	Δg	z, мм	Δg
2,0	14,3	2,0	7,7	2,0	4,6	2,0	9,0	2,0	27
6,6	7,5	6,2	2,7	7,3	3,7	5,6	9,0	11,0	27
12,3	3,8	9,4	1,4	13,2	3,7	10,2	9,0	19,0	27
18,2	1,7	12,6	0,9	19,7	3,4	16,5	9,0	29,0	27
25,5	0	19,0	0,4	26,0	3,3	22,3	9,0	35,0	27
36,3	0	25,0	0,1	39,0	3,3	31,6	9,0	—	—
61,0	0	32,0	0	59,0	3,5	37,9	9,0	—	—

components were in every case used in equal volumes; ε is the proportion (%) burned. The change increases with ε; the extent is indicated by the Δn for benzene and kerosene (both pure), which is 0.0407. The Δn for solar oil and kerosene is 0.0250. The effect has been described elsewhere [29-31]; some of the results are collected in Table 2.9. These relate to Karachukhur crude oil, and they show that the more volatile components are consumed preferentially.

Now we turn to the quantitative aspects of the changes for binary mixtures. The following are some possible cases.

a. We assume that the circulation is vigorous; let a mass

Table 2.8

Benzine $d=17$; $h_0=108$		Kerosene $d=17$; $h_0=108$		Solar oil, $d=22$; $h_0=59$		Benzine + kerosene		Benzine with transformer oil		Benzine with solar oil	
						$d=21$ $h_0=65$					
ε	$\Delta n \cdot 10^4$	ε	$\Delta n \cdot 10^4$	ε	$\Delta n \cdot 10^4$	ε	$\Delta n \cdot 10^4$	ε	$\Delta n \cdot 10^4$	ε	$\Delta n \cdot 10^4$
20	23	20	25	24	20	25	100	25	150	25	140
39	61	39	75	49	45	50	210	50	270	50	260
59	97	59	120	75	113	75	280	75	340	75	340
78	147	78	160	91	210	90	370	90	370	90	410
94	213	94	263	—	—	—	—	—	—	—	—

Table 2.9

	Acetate	Burning time, hr			
		1	2	3	4
Density at 20° C, g/cm³	0,907	0,926	0,933	0,946	0,955
Viscosity, °E, at 100 °C	1,56	2,48	3,13	5,6	6,06
T_f (flash point) °C	102	138	148	162	165
T_i (ignition point) in °C	113	150	180	215	249
Water content, in %	0,65	0,25	0,35	0,3	0,1
Tar content, in % .	14,31	20,13	22,25	27,4	28,85

dm evaporate, to give a vapor containing a weight proportion of the second component g_y and a liquid specified similarly by g_x. Then

$$g_y\,dm = mg_x - (m - dm)(g_x - dg_x) = m\,dg_x + g_x\,dm.$$

This gives us that

$$\ln\frac{m}{m_0} = \int_{g_{0,x}}^{g_x} \frac{dg_x}{g_y - g_x}, \qquad (2.36)$$

in which m_0 is the initial amount of mixture and g_{0x} is the initial g_x. This relates g_x fo m/m_0 for perfect mixing; we need to know the relation of g_y to g_x for this purpose.

Table 2.5 (section for water) confirms this equation;

Fig. 17 shows this in terms of $g_x - g_{ox}$, in which the circles denote the experimental results and the line corresponds to (2.36). The g_y needed in the graphical integration were taken from tables. These mixtures actually do show a circulation that produces good mixing*.

b. The composition alters only in the top layer (depth z_o). Here

$$h\overline{\rho g_x} = \int_0^h \rho g_x dz = \int_0^{z_0} \rho g_x dz + \int_{z_0}^h \rho_0 g_{0x} dz = (h - z_0)\,\rho_0 g_{0x} + \int_0^{z_0} \rho g_x\, dz, \qquad (2.36a)$$

in which ρ is density, z is distance below the surface, h is the total depth, $\overline{\rho}$ is the mean density, and $\overline{g}_x$ is the mean g_x. In

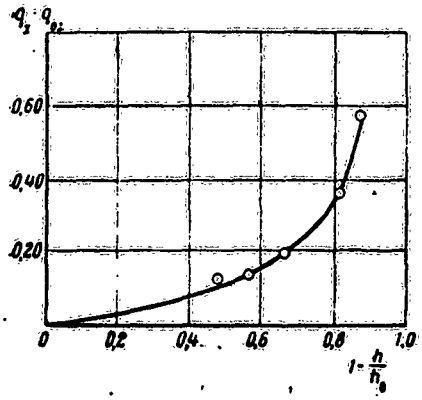

Fig. 17. Effect of burning on the composition of aqueous alcohol.

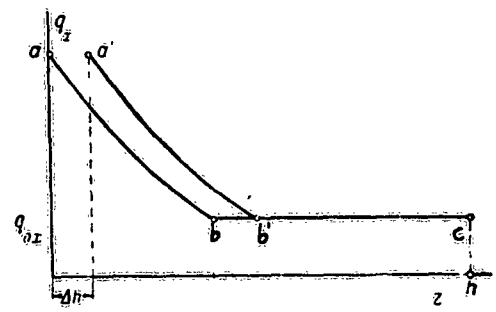

Fig. 18. Concentration curves for a burning liquid (case b).

the steady state

$$I = \int_0^{z_0} \rho g_x\, dz$$

will be constant. Let

$$A = I - z_0 \rho_0 g_{0x} = \text{const.}$$

---

* It is readily shown that (2.36) applies also to groups of similar components in a complex mixture, provided that this is well stirred.

Then

$$\overline{\rho g}_x = \rho_0 g_{0,x} + \frac{A}{h}. \tag{2.37}$$

If ρ is independent of g_x, we have

$$\bar{g}_x = g_{0,x} + \frac{k}{h}, \quad k = \frac{A}{\rho}. \tag{2.38}$$

It is readily shown that g_y is the same as g_{ox} in the steady state. Consider a rectangular coordinate system whose axis of abscissas is z and whose axis of ordinates is g_x; let the distribution of the second component at the time when the depth is h be represented by abc (Fig. 18)*. After a time Δt, when the depth is $h - \Delta h$, the distribution is represented by a'b'c, in which b'c is shorter than bc by Δh. The effect, in the steady state, is that a layer having the initial composition is lost, for sections ab and a'b' are identical; then in time dt

$$dm = vdt = \rho_0 sdh.$$

The change in the mass of the second component in the mixture in this time is

$$d(hs\overline{\rho g}_x) = \rho_0 g_{0,x} sdh = g_{0,x}\, dm.$$

But the amount of that component passing to the vapor in time dt is $g_y dm$, so

$$d(hs\overline{\rho g}_x) = g_{0,x} dm = g_y dm$$

and

$$g_y = g_{0,x}. \tag{2.38a}$$

That is, if the composition alters only in a surface layer of depth $z_0 < h$, then $g_y = g_{ox}$ in the steady state.

Further, (2.38a) enables us to deduce g_x for the surface. For this purpose we plot g horizontally and the boiling point ϑ vertically (Fig. 19); point a corresponds to the initial composition, whose ϑ is ϑ'. Through a we draw a horizontal straight line to meet the curve for the vapor at b; this defines the initial g_y. Similarly, a vertical line through a gives us point c, which defines the composition of the vapor over the burning liquid. The abscissa of point d gives us g_s, the g_x for the surface of the mixture, and ϑ'', the boiling point corresponding to

*The precise shape of the curve is without significance in what follows.

g_s. The same procedure may be used, of course, for imperfect mixtures.

The A and k of (2.37) and (2.38) are readily found when the law followed by g_x in the top layer is known. For example, the top layer may be perfectly stirred, in which case $\rho = \rho_0$ at all points in it, so

$$A = (g - g_{0,x})\,\rho_0 z_0$$

and

$$\bar{g}_x = g_{0,x} + \frac{g - g_{0,x}}{h} z_0. \qquad (2.39)$$

The z_0 given by (2.39) is close to that for the layer of

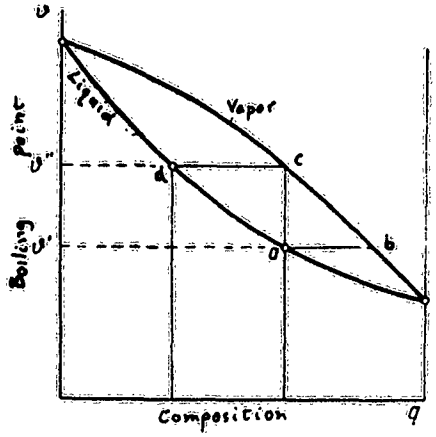

Fig. 19. Graphical determination of the composition of the surface layer and of the vapor at constant pressure.

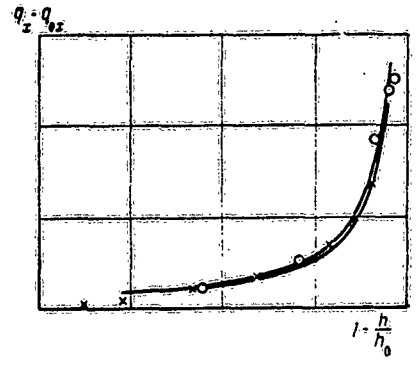

Fig. 20. Composition changes in two mixtures of ethyl and isoamyl alcohols.

vigorous circulation noted above. Table 2.7 shows that the alcohols give distributions of this type (their densities differ little); (2.38) describes these mixtures adequately, as Fig. 20 shows. Here the ordinates are $(\bar{g}_x - g_{0x})$, the points represent experimental results for two different mixtures, and the lines derive from (2.38).

c. Some oil products (benzine, crude oil) give rise to layers having vigorous circulation [54,55]; here the temperature and g_x are those for the surface, and z_0 increases with t up to some limit. We may represent the system as one of two liquids, namely liquid 1 (composition invariant, but not g_{0x}) and liquid 2 (also invariant, g_{0x}), the first lying above the second. We need to know how the composition of liquid 1 changes as z_0 increases. Let v be the thickness of the layer burned in unit

time (the specific burning rate) and let u be the rate of increase in the thickness of this homothermal layer. The mixture is assumed to consist of two mutually soluble components, the second one being the more volatile.

Let a mass Δm be burned; th...

$$g_y \Delta m = s\Delta\,(h\overline{\rho g}),$$

but

$$m = s\,[\rho z_0 + \rho_0 (h - z_0)]\,, \quad h\overline{\rho g}_x = \rho g_x z_0 + (h - z_0)\,\rho_0 g_{0,x}.$$

These equations imply that

$$g_y\,[(\rho - \rho_0)(z_{0,2} - z_{0,1}) + \rho_0 (h_2 - h_1)] = (\rho g_x - \rho_0 g_{0,x})(z_{0,2} - z_{0,1}) + \rho_0 g_{0,x} (h_2 - h_1),$$

in which subscripts 1 and 2 relate to different instants. But

$$z_{0,2} - z_{0,1} = u\Delta t, \quad h_1 - h_2 = v\Delta t,$$

in which Δt is a short time interval; then

$$g_y = \frac{\rho u g_x - (u + v)\,\rho_0 g_{0,x}}{\rho u - \rho_0 (u + v)}\,. \tag{2.40}$$

The two liquids differ little in density, so we may put $\rho = \rho_0$, whereupon

$$g_y = g_{0,x} + (g_{0,x} - g_x)\,\varphi, \quad \varphi = \frac{u}{v}\,. \tag{2.41}$$

This shows that g_y is dependent on u/v. Now $g_{ox} > g_x$, so $g_y > g_{ox}$ at all times.

If $u \gg v$, $g_x \approx g_{ox}$, so g_y takes the value corresponding to g_{ox}; g_y decreases with φ, and $g_y = g_{ox}$ when $\varphi = 0$.

d. Convection is absent; only diffusion occurs. The diffusion equation in this case is

$$D\frac{\partial^2 g_x}{\partial z^2} + v\frac{\partial g_x}{\partial z} = \frac{g c_x}{\partial t}\,,$$

in which D is the diffusion coefficient, the other symbols being as before. The boundary conditions are $g_x = g_{ox}$ for all z at $t = 0$ and for $z = \infty$ for $t > 0$; v is assumed to be constant.

The solution is then

$$g_x - g_{0,x} = A\int_0^t \exp\left\{-\frac{[z+v(t-\tau)]^2}{4D(t-\tau)}\right\}\frac{d\tau}{\sqrt{t-\tau}},$$

in which τ is a parameter and A is a constant.

The new variable

$$\psi = v\sqrt{\frac{t-\tau}{4D}},$$

enables us to put the solution as

$$g_x - g_{0,x} = 4A\sqrt{\frac{D}{v^2}}\,e^{-\frac{vz}{2D}}\int_0^{\sqrt{v^2t/4D}} \cdot \exp\left\{-\psi^2 - \frac{b^2}{\psi^2}\right\}d\psi, \quad b = \frac{vz}{4D}.$$

The steady state corresponds to $t = \infty$, in which case the integral on the right becomes

$$\int_0^\infty \exp\left\{-\psi^2 - \frac{b^2}{\psi^2}\right\}d\psi = \frac{\sqrt{\pi}}{2}\exp\left(-\frac{vz}{4D}\right).$$

and the steady state has

$$g_x - g_{0,x} = (g_s - g_{0,x})\exp\left(-\frac{vz}{2D}\right), \qquad (2.42)$$

in which g_s is the g_x for the surface.

Published values indicate that D is about 10^{-5} cm^2/sec; if v is 0.004 cm/sec (2.4 mm/min), $g_x = g_{ox}$ even for z = 0.2 mm.

These results show that the composition hardly alters if convection is absent; any change in composition points to vigorous convection, which is dependent on the composition and on the conditions. The same is true for $\Delta g = g_x - g_{ox}$. The above examples cover all possible cases.

The conclusions can be extended to mixtures such as crude petroleum and oil products, which may be treated roughly as binary mixtures of a volatile component with one of high boiling point. There is no maximum or minimum on the boiling-point curve, and the solutions are probably close to ideal. The above analysis enables us to explain the effects observed for oil products burning in large tanks (Burgoyne and Katan, Pavlov and Khovanova), but lack of details prevents us from performing a

strict quantitative analysis.

Burgoyne and Katan [29] conclude that Δg equals v/u, but we have shown that Δg is much less than v/u, so additional assumptions are needed. In fact, (2.41) shows that Δg does not equal $1/\varphi$. Burgoyne and Katan's conclusion about Δg and v/u is based on a wrong picture of the mechanism whereby the heated layer becomes deeper.

References

1. V. I. Blinov and G. N. Khudyakov. O nekotorykh zakonomernosti diffuzionnogo goreniya zhidkostei (Some Laws of Diffusion Burning for Liquids). Dokl. Akad. Nauk SSSR, 113, No. 5, 1957; Sb. "Nekotorye voprosy goreniya" (Coll.: 'Some Aspects of Combustion'), publ. Acad. Sci. USSR, 1958.
2. V. I. Blinov. O trekh rezhimakh goreniya zhidkostei v rezervuarakh (Three Modes of Burning of Liquids in Tanks). Izv. Akad. Nauk SSSR, OTN, No. 4, 1956, 115.
3. H. Hottel and W. Hausorn. Diffusion in a Flame in a Laminar Flow. Sb. "Voprosy goreniya" (Coll. 'Problems of Combustion'), vol. 1, Moscow, publ. Inost. Lit., 1953.
4. Ya. B. Zel'dovich. K teorii goreniya neperemeshannykh gazov (Theory of the Burning of Unmixed Gases). Zh. Tekh. Fiz., 19, No. 10, 1959.
5. V. A. Shvab. Svyaz' mezhdu temperaturnymi i skorostnymi polyami gazovogo fakela. Sb. "Issledovanie protsessov goreniya natural'nogo topliva" (The Relation between the Temperature and Velocity Distributions of a Gas Flame. Coll. 'Studies on Combustion Processes for Natural Fuel'). Moscow-Leningrad, publ. Gosenergoizdat, 1948.
6. L. A. Vulis. Teplovoi rezhim goreniya (Thermal Conditions of Combustion), Moscow-Leningrad, publ. Gosenergoizdat, 1954.
7. S. Burke and T. Schuman. The Diffusion Flame. Ind. Eng. Chem., No. 20, 1928, 998-1009.
8. D. A. Frank-Kamenetskii. Laminarnoe diffuzionnoe plamya. Dopolnerie redaktora k knige L'yuisa i El'be "Goreniye, plamya i vzryvy v gazakh" (The Laminar Diffusion Flame. Editor's supplement to Lewis and Elbe's 'Combustion, Flames and Explosions of Gases'). Moscow, publ. Inost. Lit., 1948.
9. J. Barr. Combustion in an Atmosphere with a Reduced Oxygen Content. Fuel, 27, No. 9, 1949.
10. V. I. Blinov. O skorosti goreniya binarnykh smesei zhidkostei. Trudy Leningr. in-ta aviatsionnogo priborostroeniya (LIAP) [Combustion Rates of Binary Mixtures of Liquids. Transactions of Leningrad Institute of Aviation Instrumentation (LIAP)], No. 7, 1954.
11. W. Hausorn, D. Didell, and H Hottel. Mixing and Combustion in Turbulent Gas Flows. Sb. "Voprosy goreniya" (Coll.

'Problems of Combustion'), vol. 1, Moscow, publ. Inost. Lit., 1953.
12. A. I. Maklakov. Izuchenie ustoichivosti otkrytykh laminarnykh diffuzionnykn plamen (A Study of Stability for Open Laminar Diffusion Flames). Dissertation, Kazan University, 1955.
Idem. Kolebaniya diffuzionnykh plamen, voznikayushchikh pri laminarnom istechenii goryuchego (Oscillations in Diffusion Flames Produced by Laminar Efflux of the Fuel). Zh. Fiz. Khim., 30, No. 3, 1956.
13. V. I. Blinov. K voprosu o pulsatsiyakh diffuzionnykh plamen (The Pulsations of Diffusion Flames). Inzh. Fiz. Zh., 2, No. 8, 1959.
14. Ya. B. Zel'dovich. Predel'nye zakony svobodno voskhodyashchikh konvektivnykh potokov (Limiting Laws for Freely Rising Convective Flows). Zh. Eksper. Teoret. Fiz., 7, No. 12, 1937.
15. L. Prandtl and O. G. Tietjens, Hydro- and Aeromechanics. Moscow-Leningrad, publ. ONTI, 1935.
16. A. Schak. Z. Tech. Fiz., 1925, No. 6, 530-540.
17. A. I. Gordov, A. S. Arzhanov, and others. Metody izmereniya temperatur v promyshlennosti (Industrial Methods of Measuring Temperature). Moscow, publ. Gosmetallurgizdat, 1952.
18. H. C. Hottel and F. Brighton. Determination of the True Temperature and Total Radiation of Luminous Gas Flames. Ind. Eng. Chem., 24, No. 2, 1932.
19. A. G. Gaydon and H. G. Wolfhard. Flames: their Structure, Radiation and Temperature. Moscow, publ. Gosmetallurgizdat, 1959.
20. V. I. Blinov, G. N. Khudyakov, and I. I. Petrov. Izuchenie goreniya nefteproduktov (Study of the Burning of Oil Products). Trudy ENIN and TsNIIPO, No. 17, 16, 1955.
21. NACA Report No. 1186, 1954.
22. H. Tropsch and G. Egloff. Ind. Eng. Chem., 27, 1063, 1935.
23. K. Schafer and F. Matossi. Infrared Spectra. Moscow-Leningrad, publ. ONTI, 1935.
24. V. I. Blinov. O temperature shara, reagiruyushchego s kislorodom okruzhayushchei gazovoi sredi. Trudy Voronezhskogo gos. un-ta (VGU) [The Temperature of a Sphere Reacting with the Oxygen in the Surrounding Gas. Proc. Voronezh Univ. (VGU)], No. 1, fiz.-mat. otdel., 1939.
25. Idem. O vosplamenenii uglerodnogo shara. (Ignition of a Carbon Sphere). Ibid., 1939.
26. D. A. Frank-Kamenstskii. Diffuziya i teploperedacha v khimicheskoi kinetike (Diffusion and Heat Transfer in Chemical Kinetics). Moscow, publ. Acad. Sci. USSR, 1947.
27. V. I. Blinov. Ob izmenenii sostava binarnykh smesei zhidkostei pri gorenii (Composition Changes in Binary Mixtures

of Burning Liquids). Dokl. Akad. Nauk SSSR, 89, No. 1, 1953.
28. G. N. Khudyakov. O temperaturnom pole zhidkosti, goryashchei so svobodnoi poverkhnosti, i o fakale nad nei (Temperature Distribution in a Liquid Burning from a Free Surface, and the Flame Above). Izv. Akad. Nauk SSSR, OTN, No. 7, 1951.
29. J. Burgoyne and L. Katan. Burning of Petroleum Products in Open Tanks. J. Inst. Petroleum, 33, No. 279, 1947.
30. P. P. Pavlov and A. M. Khovanova. O gorenii neftei i nefteproduktov so svobodnoi poverkhnosti (Burning of Petroleum and Oil Products from a Free Surface). Baku, 1955.
31. Idem. O teploperedache v nefteproduktakh pri gorenii so svobodnoi poverkhnosti (Heat Transfer in Oil Products Burning from a Free Surface). Inform. sbornik TsNIIPO (Bulletin of the Central Research Institute for Fire-Fighting), Moscow, publ. MKKh, 1954.
32. D. P. Konovalov. Ob uprugosti para rastvorov (The Vapor Pressures of Solutions). Leningrad, 1928.
33. S. A. Bogaturov. Kurs teorii peregonki i rektifikatsii (Textbook on the Theory of Distillation and Rectification). Moscow, publ. Gostoptekhizdat, 1954.
34. V. I. Blinov, G. N. Khudyakov, and I. I. Petrov. O raspredelenii temperaturi v nefteproduktakh, sgorayushchikh v rezervuarakh (Temperature Distributions in Oil Products Burning in Tanks). Inform. sbornik TsNIIPO (Bulletin of the Central Research Institute for Fire-Fighting), Moscow, publ. MKKh, 1954.
35. Hall. Boiling-over of Crude Petroleum Burning in Tanks. Mech. Eng., 47, No. 7, 1925.

Rates of Combustion of Liquids in Tanks

1. Figure 14 shows the apparatus used to measure the rate of combustion for vessels of small diameter.

The rate in a large vessel was measured by connecting the vessel to a level indicator (trarsparent tube with scale); the rate $v = V/s$ (in which V is the volume rate and s is surface area) was read by means of the scale. In later tests the level was kept constant, as in [3], where the burning tank was coupled to a store tank directly and to two metering tanks, the system being controlled by a float gauge and contact system. The level in the store tank fell as the liquid burned: the float closed a contact, which energized a solenoid valve to allow the liquid from one

metering tank to enter the store until the original level was restored. The metering tanks were fitted with sight tubes to read the consumption. The level fluctuated only over a range of 5 mm in this system, as was shown by the readings of a thermocouple placed at the surface.

2. It is found that the rate of combustion rises at first and then remains constant, if the liquid is sufficiently deep [1,3,4], as Fig. 21 shows (curve 1). The steady rate of change of h is taken as the burning rate.

A mixture whose level is not maintained may show a continuous fall or rise in the rate (curves 2 and 3); a fall occurs with ethanol-propanol mixtures, and in many other cases, when burners are used. A rise occurs, for example, when toluene-rich ethanol-toluene mixtures are used.

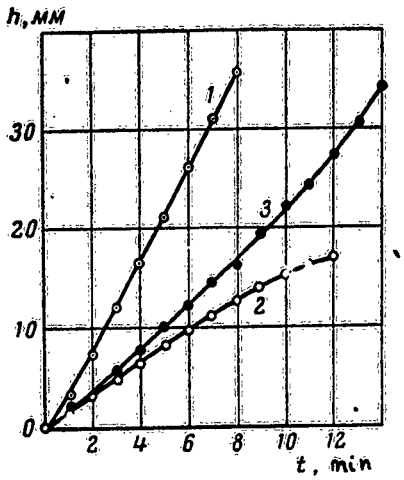

Fig. 21. Depth of fuel as a function of time.

The initial rise in rate is caused by the heating-up; the later changes are caused by alterations in composition.

We give below some results for burners and tanks of various materials and of wall thicknesses δ from 0.5 to 1 mm [1-17].

Heavy fuel oil: d of 1300, 2600, and 22 900 mm gave respectively v of 1.5, 2.3, and 2.2 mm/min.

Diethyl ether: d of 300, 800, 1390, and 2640 mm gave respectively v of 2.1, 2.7, 4.7, and 6.1 mm/min.

The tables below show that there is a wide spread in the v for $d < 10$ mm but good agreement for $d > 10$mm. A careful study of the results for any one liquid (say, benzine) shows that v is dependent on δ and on the material; the v are nearly equal if $\lambda\delta$ is constant (λ is the thermal conductivity), as Fig. 22 shows for d constant (10 mm) and $\lambda\delta$ variable (glass, stainless steel, and copper). Here v falls fairly rapidly at first but eventually tends to a limit. This effect has received detailed study [1,3,10]; Fig. 23 shows v against d for isoamyl alcohol, in which the open circles are for glass burners of δ about 1 mm and the half-filled ones are for stainless-steel ones having δ of 0.4 mm. Clearly, v falls as λ increases. The effect has been observed for other liquids, but its extent varies. In general,

the effect of δ becomes less as d increases.

4. The v as averaged for burners of closely similar $\lambda\delta$ show a clear relation of v to d; Fig. 24 illustrates this for kerosene. The v(d) curve is the same for all liquids; there is first a rapid fall, then a minimum, and finally a tendency to approach a limit (there is no great variation in v for d between 1 and 22.9 m). Thus there are, in effect, three ranges of d each having its own form for v(d).

Observations and photographs show that the flame from a burner (small tube) is laminar, whereas that in a wide tank is

Table 2.10

Benzine [1,3]

d, mm	v, mm/min	d, mm	v, mm/min	d, mm	v, mm/min
				[11]	
5,1	17,6				
6,5	10,4	5,7	5,5	3,3	11,6
9,8	6,0	10	2,9	5,2	6,3
11,7	4,8	21,4	1,6	8,7	3,9
16,2	3,8	32	1,6	12,6	2,3
20,0	3,0	41	1,6	14,6	2,2
24,4	2,3	84	1,7	20	2,1
34,5	2,1	9,8	3,7	25	1,7
47	1,8	15,6	2,4	54	1,3
62	2,0	20	2,3	101	1,3
81,5	1,9	28	1,3	150	1,9
106	2,0	40	1,3	200	2,2
148	1,6	65	1,0	250	2,2
300	2,4			300	2,7
495	3,8			800	3,6
1300	4,1			1390	4,0
8600	3,8			2640	4,5
22900	3,7				

Table 2.11

Tractor Kerosene [3,5,16]

d, mm	v, mm/min
3,7	12,0
5,0	7,5
6,0	6,4
7,1	4,8
11	3,2
20	1,9
30	1,4
47	1,4
80	0,9
148	1,2
150	1,1
300	1,9
500	2,8
800	3,4
1300	4,0
2600	4,2

turbulent. This gives an indication why v(d) shows the above behavior; v falls as d increases in the laminar range but shows little variation with d in the turbulent range. A reasonably exact relation for the laminar range is [3-5,10]

$$v = a + bd^{-n}, \qquad (2.43)$$

in which a and b are factors that vary from one liquid to another; a may be interpreted as the v for $d = \infty$, if the burning were to remain laminar. Table 2.18 gives a and n for liquids in burners

of stainless steel and glass; these show that n is about 1.5, while a varies from 0.5 to 1.4 mm/min.

The results for d between 1 and 23 m are few and not very precise, but some valuable conclusions can be drawn. There is hardly any variation of v with d, and the v for the various liquids differ much less than they do for smaller d, although these v are larger than those for d > 15 mm. The region is, of course, one of turbulent combustion.

5. The Re for the vapor stream from the liquid is of

Table 2.12

Kerosene

d, mm	v, mm/min	d, mm	v, mm/min
[3]		[11]	
3,7	10,3	3,3	6,2
5,0	6,2	5,2	4,0
6,0	6,0	8,7	2,0
7,1	3,3	12,6	1,5
11	1,9	14,6	1,4
20	1,3	20	1,05
30	1,0	25	0,8
47	1,0	54	0,8
80	0,9	101	1,0
148	0,9	150	1,5
300	1,6	200	1,6
00	3,0	250	1,6
22900	3,6	300	1,8
		800	2,3
		1390	2,6
		2640	2,7

Table 2.13

[3,5,16]

d, mm	v, mm/min		
	Diesel oil	Solar oil	Transformer oil
3,7	6,9	9,3	4,9
5,0	5,0	5,1	3,7
6,0	4,2	4,1	3,3
7,1	3,5	3,3	2,7
11	2,5	2,4	1,8
20	1,7	1,1	1,1
30	1,3	0,6	0,7
47	1,1	0,6	0,7
80	0,6	0,6	—
148	0,7	0,6	0,5
300	—	0,8	0,8
500	1,8	1,7	1,8
800	2,7	—	—
1300	3,3	—	—
2600	3,5	—	—

interest; the following are some values for benzine:

d, mm	6,0	7,1	11	20	30	47	80	148	300	98
Re, 10³	0,15	0,12	0,08	0,09	0,08	0,1	0,26	0,92		98

The Re for the cold streams produced in small burners are much below the critical Re; the usual critical value is exceeded for d = 500 mm. (Much the same is found for other liquids [2,5].) These results indicate that turbulence should set in at or below 500 mm, but the observations above on the pulsations in flames show that the velocity profile is such as to initiate turbulence for Re well below 2000, and perhaps at 300-400. The

latter range is reached for d ... about 15 cm, and, in fact, benzine burning in a vessel of diameter 15 cm (Fig. 1) does have a randomly pulsating flame. This means that the rate of turbulent combustion at first increases with d, but later remains constant over a wide range.

The transition region is associated with the onset of pulsations, which begin at a d dependent on the nature of the liquid; the bulk burning rate V is the controlling factor. Figure 1, and many similar results, would indicate that this region, which corresponds to the part around the minimum on the curve of v against d, starts for d of about 20 mm.

6. The start of the transition region can be deduced in another way. The theory of the laminar flame shows that $V/\delta \approx D$,

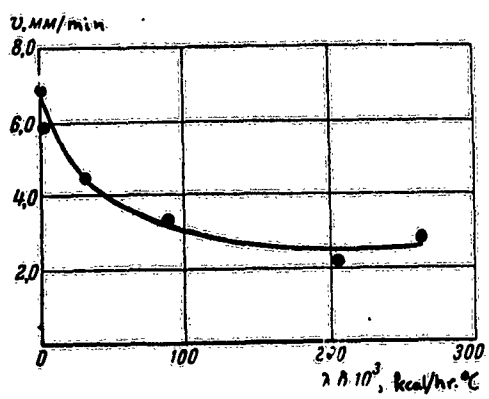

Fig. 22. Relation of v to for benzine.

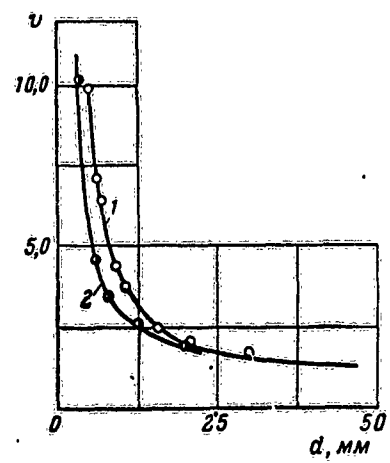

Fig. 23. Relation of v to d for isoamyl alcohol: 1) glass; 2) steel.

in which D is the diffusion coefficient for oxygen; V/δ remains constant for laminar burning. Table 2.19 gives the apparent D (divided by 10) for various fuels as functions of d; these show that V/δ remains constant up to d of 2-3 cm and that the apparent D has increased by a factor 10 for d = 15 cm.

7. This relation of v to d for laminar flow may be explained as follows. The rate is governed by the heat q received by the liquid from the flame in unit time. But

$$q = \pi R^2 \rho v q_0,$$

in which R is d/2, ρ is the density of the liquid, and q_0 is the amount of heat needed to bring 1 g of the liquid to the

evaporation temperature and then to evaporate it.

The liquid receives heat by radiation and conduction, in part through the wall of the vessel. Let q_1, q_2, and q_3 be the amounts of heat received in these various ways; then

$$q = q_1 + q_2 + q_3. \qquad (2.44)$$

A laminar flame is conical, with the vessel as its base. Now

$$q_1 = 2\pi R\gamma\lambda\frac{d\vartheta}{dn},$$

in which λ is the thermal conductivity of the gas between the flame and the liquid, $d\vartheta/dn$ is the temperature gradient, and γ is the width of the zone in which heat enters the liquid. are not dependent on d, then

$$q_1 = a_1 R,$$

in which a_1 is a factor independent of d.

We can also find q_2 approximately if we assume that only the combustion zone radiates. The liquid receives from a ring of width Δr and radius r an amount of heat

$$dq_2 = 2\pi r\Delta r\varepsilon\omega\, dz,$$

(Fig. 25), in which ω is the solid angle subtended by the surface at the ring, ε is the radiating capacity of the flame, dz is the height of the ring, and z is its distance from the surface. As a measure of ω we use the angle as seen from the

Table 2.14

Crude Petroleum [11]

d, mm	v, mm/min	
	Bibi Eibat	Karachukhur
3,3	2,4	2,0
5,2	1,2	1,3
8,7	0,8	0,7
12,6	0,6	0,5
14,6	0,6	0,5
20,0	0,5	0,4
25,0	0,5	0,4
54,0	0,5	0,4
101,0	0,45	0,4
150,0	0,7	—
300,0	0,9	0,8
800,0	1,5	1,4
1390,0	1,6	1,4
2640,0	1,6	1,55

If we assume that γ and $d\vartheta/dn$

Table 2.15

Quartz Burner, d = 106 mm [15]

Liquid	mm/min
Benzine grade I	2.2
" " II	1.8
Kerosene	1.0
Paraffin oil	0.65
Transformer oil	0.5
VM-4 oil	0.2
Heavy fuel oil after 3 hours' burning	0.4
MS oil	0.2
Glycerol	0.4
Amyl alcohol	1.0
Butanol	1.0
Methanol	0.9
Acetone	1.3

Table 2.16

Quartz Burner, d = 62 mm [1]

Liquid	mm/min	Liquid	mm/min
Avtol	0.6	Amyl alcohol	1.3
Machine oil	0.7	Isoamyl alcohol	1.4
Petroleum ether	2.4	Butanol	1.1
Benzene fraction	3.3	Isobutanol	1.1
Benzene	3.1	CS_2	1.7
Toluene	2.7	Methyl propyl ketone	1.4
Xylene	2.0	Dimethylaniline	1.5
Skipidar	2.4	Solar oil	0.8
Acetone	1.4	Kerosene	1.0
Methanol	1.2	Green oil	1.3
Diethyl ether	2.9	Automobile benzine	1.7
Aceloacetic ester	1.3	Aviation spirit	2.1

same height on the axis:

$$\omega = 2\pi \frac{h'}{l},$$

in which h' and l are as shown. But

$$h' = l - (\delta - h).$$

so

$$\omega = 2\pi\left(1 - \frac{\delta - h}{l}\right).$$

But

$$\frac{r}{h} = \frac{R}{\delta} \quad , \quad h = \delta - z,$$

so

$$dq_2 = a'' \frac{R}{\delta}(\delta - z)\left(1 - \frac{z}{\sqrt{R^2 + z^2}}\right)dz, \quad a'' = 4\pi^2 \varepsilon \Delta r.$$

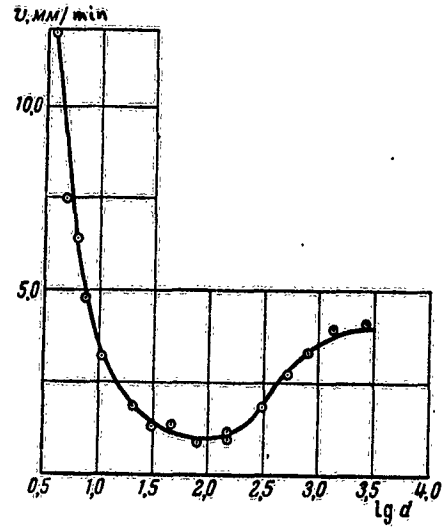

Fig. 24. Relation of v to d for tractor kerosene.

The integral from 0 to δ, with $\theta = R/\delta$, is

$$q_2 = 2\pi^2 \varepsilon \Delta r R^2 \frac{f(\theta)}{\theta}.$$

in which

$$f(\theta) = 1 + 2\theta - \sqrt{1 + \theta^2} - \theta^2 \ln \frac{1 + \sqrt{1 + \theta^2}}{\theta}.$$

Table 2.

Ethyl		Butyl and Isoamyl,	Butyl,	Isoamyl,
d, mm	v, mm/min	d, mm	v, mm/min	v, mm/min
Alcohols, glass burner [10]				
4,9	8,9	3,0	22,5	—
6,3	6,3	3,6	21,0	20
7,0	5,8	5,2	12,0	9,9
7,7	4,6	6,3	—	7,1
9,3	4,1	7,0	8,0	6,4
10,7	3,4	9,3	4,6	4,4
15,3	2,5	10,5	4,5	3,8
20,7	1,9	15,5	3,0	2,5
24,4	2,0	20,7	2,4	2,1
30,0	1,6	30,0	1,8	1,8
36,2	1,4	—	—	—
46,8	2,2	—	—	—

Alcohols, Steel Burner

d, mm		4,0	6,0	8,2	12,7	20
Ethyl	mm/min	14,0	6,2	4,3	2,9	2,1
Butyl	. . . . .	12,8	5,4	3,6	2,8	2,0
Isoamyl	. . . . .	10,2	4,6	3,5	2,7	2,0

Alcohols, Copper Burner, d = 10mm

	v, mm/min
Ethyl	2,7
Butyl	2,2
Isoamyl	2,05

... $f(\theta)/\vartheta$ varies little with θ, so we may say that

$$q_2 = a_2 R^2,$$

... which a_2 is a constant for a given liquid

The ... received from the wall is

$$q_3 = 2\pi R l_c \alpha \Delta\vartheta,$$

... which l_c ... length of the heated part, α is the heat-transfer ... and $\Delta\vartheta$ is the temperature difference, ... $l_c \alpha \Delta\vartheta$ is a ... function of ϑ, and we may assume [18] that

$$Nu = B\,(GrPr)^n,$$

... which ... a constant and n lies between 0 and 1/3. ...

GrPr, which in future we denote by Ra (Rayleigh's criterion), contains R^3, while l_c and $\Delta\vartheta$ vary little with R in the range of interest to us; then

$$l_c \alpha \Delta\vartheta \propto R^{3n-1},$$

and $0 < n < 1$. Then

$$q_3 = a_3 R^{3n}.$$

We insert these various q in (2.44) to get that

$$v = b_0 + b_1 R^{3n-2} + bR^{-1}, \qquad (2.45)$$

in which $b_0 = a_3/\pi\rho c$ and $(a - 1) > (3n - 2) > -2$.

Rough calculations show that v falls as d increases on account of the reduced contributions from conduction via the wall and the flame; (2.45) is in general agreement with experiment. Experiment [4] shows that conduction through the wall does play a major part; here a copper ring of the diameter of the burner (9.4 mm) was placed between the burner and the flame. This ring was made of wire 0.8 mm in diameter and was joined to a copper tube, which was cooled by water; there was a gap of 0.7 mm between ring and burner. Ethanol having its surface at the top edge of the burner had a v of 3.7 mm/min without the ring and 1.1 mm/min with it. The only reason for the difference must be that the ring prevented heat from reaching the wall of the burner.

Table 2.18

Liquid	a	n
Automobile benzine	1.4	1.73
Tractor kerosene	1.1	1.61
Illuminating kerosene	0.9	1.51
Solar oil	0.5	1.54
Diesel oil	0.8	1.31
Transformer oil	0.5	1.5
Ethanol	1.0	1.5
Butanol	1.3	1.5
Isoamyl alcohol	1.3	1.5
Glass Burners		
Ethanol	1.0	1.5
Butanol	1.0	1.5
Isoamyl alcohol	1.0	1.5

Also, v is much dependent on $\lambda\delta$, for the area of wall heated by the flame increases with $\lambda\delta$, and with it the loss of heat to the surroundings. The relative contribution of the heat from the wall decreases as d increases, so the effect of $\lambda\delta$ becomes smaller.

Formula (2.45) shows that v increases if the radiation from the flame becomes more important, so a liquid giving a luminous

Table 2.19

	d, cm											
	0,37	0,50	0,60	0,71	1,1	2,0	3,0	4,7	8,0	15	30	130
Automobile gasoline	—	—	0,5	0,5	0,5	0,5	0,6	1,0	—	—	18	182
Tractor kerosene	0,3	0,3	0,3	0,3	0,3	0,4	0,5	0,8	1,1	3,1	--	255
Diesel oil	0,3	0,3	0,3	0,3	0,3	0,4	0,5	0,7	—	—	—	200
Solar oil	0,3	0,3	0,3	0,3	0,3	0,3	0,3	0,5	—	3,1	6	—

Ethanol	d, mm	4,6	7,7	9,4	15,1	21,4	36,2	46,8	
	$m^* \cdot 10^4$	11	12	12	12	12	12	13	
Butanol	d, mm	3,0	3,6	5,2	7,0	10,2	15,5	20,7	30,0
	$m \cdot 10^4$	8	8	8	9	9	10	9	8

* $m = v\rho/6$.

flame should burn more rapidly than one with a nonluminous flame, other conditions being the same.

Relation of Laminar Burning Rate to Composition

1. The v for a binary mixture is dependent on the composition [4]; Fig. 26 gives results for mixtures in which ethanol was the first component, the second being butanol (curve 1), toluene (curve 2), or benzene (curve 3). Here g_x is the proportion of the second component by weight. The signs denote experiments with burners whose d ranged from 6.7 to 29 mm. The values are relative to the v for the first component (the origins of the curves are not the same). In each case, the v for the second component was higher. The points for the various d all lie close to a single $v(g_x)$ curve. Curve 1 is characteristic of nearly ideal miztures, such as those between lower alcohols; there is a monotonic rise.

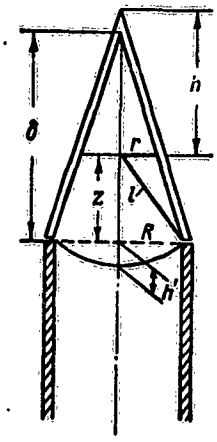

Fig. 25. Calculation of the rate of laminar burning of a liquid.

Curves 2 and 3 relate to imperfect mixtures; the g_x for the azeotropic mixture of toluene with ethanol is 0.32, and that for benzene with ethanol is 0.68. The inflections on the curves lie at the azeotropic compositions g_{xa}, and these divide the region $0 \leq g_x \leq g_{xa}$ (which shows one type of variation) from the region $g_{xa} \leq g_x \leq 1$ (which shows

another). The excess of either component over that for g_{xa} can be considered as a solution of that component in the azeotropic mixture.

The effects can be described mathematically, for g_x affects the radiation from the flame and also q_0. Simple calculations give

$$v = \frac{1}{(\alpha g_x + \beta)\rho}, \qquad (2.46)$$

in which ρ is the density of the liquid and α and β are constants for a given pair of liquids if d is constant; (2.46) fits the results of Fig. 26 quite well.

2. Mixtures of oil products give some interesting results. The following figures [4] for v (in mm/min) relate to aviation spirit used in glass burners of diameters 22 and 24.4 mm:

Volume concn.:	0	25	50	75	100
Benzine + kerosene (24.4)	2.6	2.4	2.3	2.1	1.9
" + solar oil (22)	2.8	2.6	2.4	1.7	1.5
" + transformer oil (24.4)	2.6	2.4	1.8	1.4	1.2

Here the volume concentrations are $100w_2/(w_1 + w_2)$, in which w_2 is the volume of the second component. The v after 3-4 min has been used if v varies with burning time. There is a regular fall in v as the proportion of benzine (the component of higher v) falls.

Figure 27 gives results for d = 24.4 mm for these products; an approximate relation is

$$v = A - B\rho,$$

in which A and B are functions of d. (The densities of the benzine, kerosene, solar oil, and transformer oil were respectively 0.73, 0.81, 0.87, and 0.88 g/cm^3.) The same trend in v with has been reported by others.

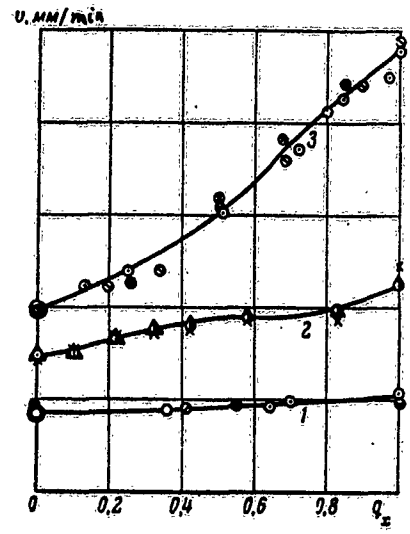

Fig. 26. Relation of v to composition for mixtures.

It is sometimes supposed that this trend is a result of variation in the calorific value Q, but this is not so, for the v for

oil products range from 1.5 to 4.5 mm/min [6], while the corresponding Q range from 10.5 to 11.0 kcal/kg (a factor 3 as against a change of 5%), so Q cannot be the decisive factor. The Q for the above oil products are virtually identical. A more likely assumption is that the fall in v is caused by an increase in q_0 (the amount of heat needed to evaporate 1 g starting from the cold liquid); now the boiling point increases regularly with ρ (although the latent heat of evaporation q falls somewhat), and so q_0 increases with ρ.

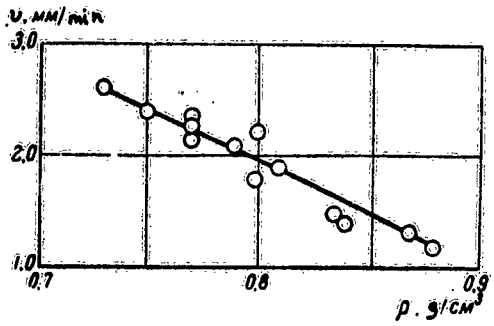

Fig. 27. Relation of v to density for oil products.

Table 2.20

	ρ, g/cm³	ϑ_r, °C	q, cal	q_0, cal	$vq_0 \cdot 10^{-2}$
Gasoline	0.73	100	70	104	73
Kerosene	0.82	180	57	129	73
Solar oil	0.89	230	52	146	74

Table 2.20 gives approximate q_0; the q are from [19], and the specific heats of all are 0.45. Here ϑ is the surface temperature of the burning liquid. We see that q_0 changes by 40% when ρ changes from 0.73 to 0.89 g/cm³ (by 0.16 g/cm³). The v show much the same range, and so the product vq_0 should be constant, as the above assumption would imply. This is actually so.

3. Interest also attaches to mixtures in which one component is incombustible; we have done tests in which ethanol was used with water and CCl_4, benzine with CCl_4, and benzene and kerosene with water, but we give here only the results for mutually soluble liquids. The ethanol-water mixtures were used in a burner with d = 7.7 mm; here v was constant if the proportion of alcohol was over 0.7, but mixtures with 0.62, 0.45, and 0.39 parts of alcohol showed gradually decreasing v. The initial depths were 50 mm; the 0.45 mixture burned for 16.5 min, the 0.39 one for 14 min, and a 0.30 one for 7.5 min. In all cases the residual liquid contained 26% of alcohol. Drops of water often appeared on the outside of the burner when the water-rich mixtures were used.

The following results are for such mixtures in burners of

diameters 7.7 and 21.9 mm. Steady v were reached for the 0.92 and 0.80 compositions; the v for the three lowest alcohol contents were taken as those after 2 min:

Wt. parts ($d = 7{,}7$ мм)	0,96	0,92	0,80	0,62	0,45	0,39
v, мм/min	4,6	3,9	3,0	2,4	2,2	1,9
δ, мм	24	18	13	10	5	—
Wt. parts ($d = 21{,}9$ мм)	0,96	0,85	0,73	0,54	0,45	
v, мм/min	2,0	1,5	1,2	1,0	0,6	

The vapor differed little from the liquid for the alcohol-rich mixtures, but the difference was very great for the others (Fig. 16), so the surface layers became very much depleted; the density increased, and the layer sank. The stirring caused the composition to alter; no stirring was observable for mixtures containing over 70% of alcohol, because the changes in composition were slight. Here v falls continuously with g_x, because q_o increases, so the flame temperature falls.

Ethanol-CCl_4 mixtures showed an unusual effect, which the following results illustrate:

$d = 9{,}0$ мм	g_x	0	0,22	0,40	0,55	0,61	0,65	0,67	0,69	0,72
	v, мм/min . . .	4,3	4,3	4,3	4,4	4,3	4,4	3,0	3,0	0
$d = 16$ мм	g_x	0	0,40	0,57	0,67	0,71	0,75			
	v, мм/min . . .	2,5	2,9	3,1	3,4	0	0			

(g_x is for CCl_4). Here v is constant or even increases up to g_x of 0.65 or 0.67; then there is a rapid fall, and the mixture with $g_x = 0.72$ will not ignite. Mixtures near this composition were also difficult to ignite.

This behavior of v for low g_x is caused by variation in the emissivity of the flame; pure alcohol gave a flame of very low luminosity, whereas the luminosity increased rapidly with g_x. Soot was produced for $g_x > 0.55$. These tests illustrate the importance of radiative transfer.

The following results are for benzine mixed with CCl_4 in burners with d = 9 mm:

g_x	0	0,23	0,41	0,49	0,56	0,62	0,64	0,68	0,73
v, мм/min . . .	7,2	7,1	6,0	5,4	4,0	2,7	2,6	0	0

Here v falls as g_x increases, expecially at the higher g_x; the mixture does not burn away completely even when g_x is small. The higher g_x, the more difficult the mixture was to ignite; much soot was deposited. The CCl_4 does not increase the number of radiating particles, but it increases q_o and so lowers the temperature of the flame.

Suspended water has an interesting effect on v; oil products such as benzine, kerosene, and mazut (heavy fuel oil) are of interest here. Figure 28 [6] shows the effects of water on the burning of mazut (the liquid was not kept topped up). The initial v is very low, but after a delay it increases sharply to a fixed value. The delay is the longer the greater the water content. Direct-distillation mazut will burn only if the water content is less than 0.6-0.7%, while emulsion crude will burn with up to 10% [20]. The suspended water retards the heating; it also affects the temperature at the surface and in the bulk [20]. The effect on v is ascribed to the heat lost by evaporation , but the process is actually rather complicated, and evaporation is only one aspect. The surface temperature and the dilution of the vapor by the steam are also important. The drying is prolonged, because convection currents are present.

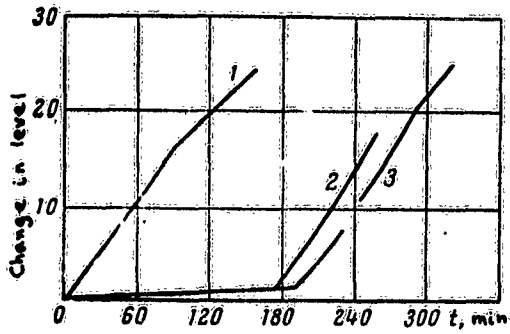

Fig. 28. Change in level with time for heavy fuel oil in a tank 80 cm in diameter; water contents: 1) 0.1 %; 2) 0.4%; 3) 0.56%.

Effects of Oxygen Concentration on the Burning Rate

Very little is known here, and such information as we have is largely qualitative. Some results [22] are as follows. Diesel oil and benzine were burned in an atmosphere whose oxygen concentration c_0 differed from that of air (Fig. 29). Here B is a cylindrical stainless-steel burner (d = 47 mm), S is a metal cylinder, O is a glass observation port, F is a burette carrying the fuel, C is a container for mixing the incoming gases, T is a thermocouple, and A is a galvanometer.

The air, oxygen, and nitrogen pass through rheometers into C and then through a layer of small stones at the bottom of S. The flow rate was 33 l/min in all cases. The gas was analyzed to ensure that c_0 was as calculated from the rheometer readings and was the same at all points in S. Figures 30 and 31 show results, in which ϑ is the surface temperature and c_0 is in %. Clearly, v increases with c_0; the liquids will not burn if c_0 is less than 15%. Further, ϑ increases with c_0, especially near the lower limit; much soot is produced, and the liquid starts to

boil, if $c_O > 21\%$. These effects are caused by the increase in the temperature and emissivity of the flame.

Effects of Air Movement on the Burning of Liquids in Tanks

It has long been known that the burning rate for an oil product in a tank is governed by the wind speed [3]; Blinov and Khudyakov made the first systematic measurements [16] on steel tanks of diameters 150, 300, 490, and 500 mm, whose heights were respectively 800, 1800, 2000, and 4000 mm. The 500 mm tank was fitted with a cooling jacket.

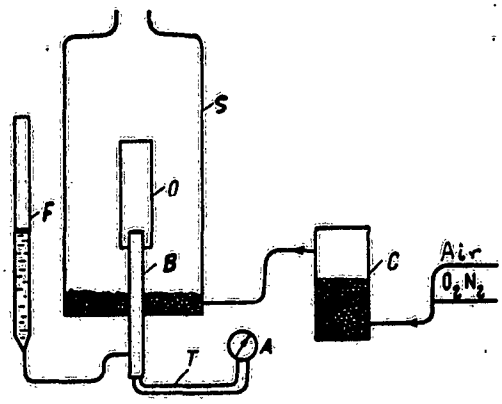

Fig. 29. Apparatus for measuring the rate of burning in an atmosphere having a known oxygen content.

A flow of air was directed onto the flame; this was produced by a large fan in the open, and by the air line in the laboratory. This flow was usually horizontal, but in some cases the angle with the vertical was 70° or 109°. Vertical screens were used in the open to eliminate the natural wind. Sometimes there was a horizontal screen to prevent the flames from touching the sides of the tank. This screen was of stainless steel and had a circular hole whose diameter equalled the outside diameter of the tank. The level of the liquid was kept fixed; the runs lasted from 2 to 5 hr. The fuels were diesel oil, tractor kerosene, and automobile gasoline.

The flame was vertical in the absence of any wind, which deflected the flame and caused it to touch the sides. This was the more so the greater the wind speed w. The area of contact with the sides decreased if w was greater than a critical speed w_c, while the flame was blown out at very high speeds.

Figures 32 and 33 show that v increases with w and tends to a limit v_∞, though mazut shows very little effect for w between 0 and 2.8 m/sec. The results fit

$$v - v_0 = (v_\infty - v_0)(1 - e^{-\beta w}), \qquad (2.47)$$

in which v_0 is v for w = 0 and β is a scale factor. The lines have been drawn in accordance with (2.47).

We can put (2.47) in another form if we put $u = v/v_0$:

$$u - 1 = (u_\infty - 1)(1 - e^{-2w}). \tag{2.48}$$

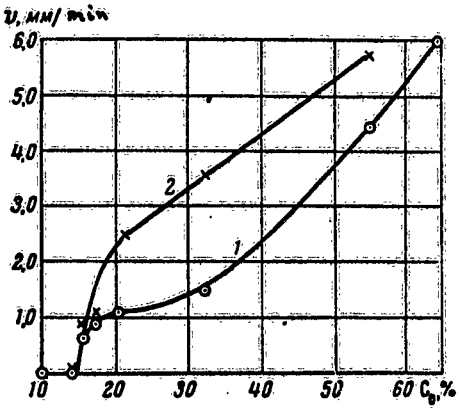

Fig. 30. Relation of v to c_0: 1) diesel oil; 2) benzine.

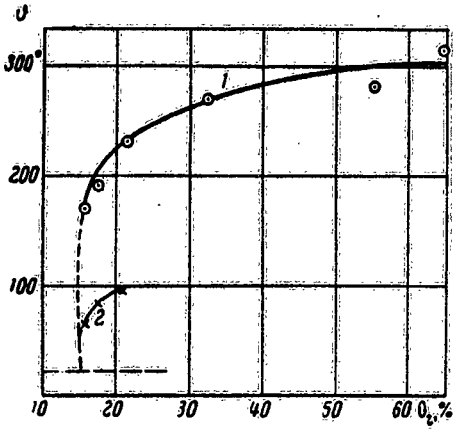

Fig. 31. Relation of surface temperature to c_0 for 1) diesel oil; 2) benzine.

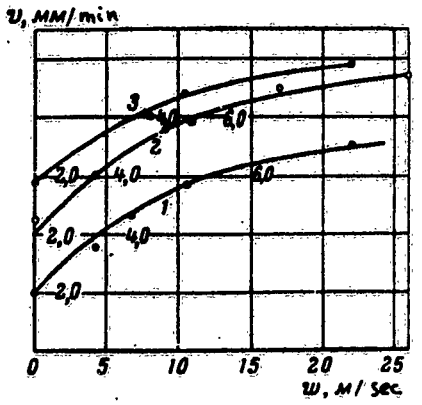

Fig. 32. Relation of v to wind speed: 1) tractor kerosene, d = 300 mm; 2) the same, d = 490 mm; 3) diesel oil, d = 490 mm.

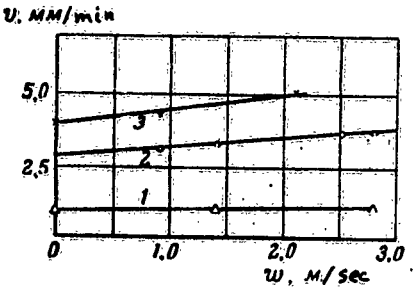

Fig. 33. Relation of v to w for d = 130 cm: 1) mazut; 2) diesel oil; 3) benzine.

If $\beta w \ll 1$,

$$u - 1 = (u_\infty - 1)\,\beta w = \nu w,$$

in which

$$\nu = (u_\infty - 1)\,\beta.$$

This ν is a measure of the initial rate of increase of u with w.

The experiments were worked up to yield v_0, u_∞, β, and ν (Table 2.21); the values for the tank 150 mm in diameter were

Table 2.21

	d, mm	v_0, m/sec	u_∞	β, sec/m	ν, sec/m
Diesel oil	150	0,6	4,0	1,0	3,0
	490	1,8	3,5	0,10	0,24
	1300	2,85	—	—	0,11
Tractor kerosene	150	1,1	3,0	0,98	1,95
	300	1,8	4,2	0,10	0,33
	490	2,0	3,9	0,10	0,29
Gasoline	150	1,4	4,5	1,85	0,65
	1300	3,9	—	—	0,14

not very exact, for here the range in w was small. The range of u_∞ in these tests was 3.0 to 4.5, with a mean of 3.9; the ν for diesel oil and benzine fit a single curve, which reflects the general behavior of $\nu(d)$ for oil products, for ν at first falls rapidly, then slowly, and is about 0.1 sec/m for d = 1300 mm. The ν for these three fuels increase only by 30-40% when w increases from 0 to 3 m/sec for $d \geqslant 1300$ mm, while ν for mazut does not alter at all.

It is impossible for v to increase indefinitely with w, for the flame is blown out for $w > w_c$; the w_c for tractor kerosene in a 300 mm tank is slightly above 22 m/sec, whereas that for this kerosene in a 490 mm tank is not reached at 26 m/sec.

The results for the 150 mm tank show that v is dependent on the wind direction as well as on the size of w; Table 2.22 shows that $(v - v_0)$ increases with α (the angle between the wind direction and the vertical). Further, the horizontal screen produces a certain reduction in v.

Table 2.22

	Kerosene			Diesel oil				
	$w = 1{,}8$ m/sec			$w = 2{,}6$ m/sec			$w = 1{,}1$ m/sec	
α	70	90	109	70	90	109	90	109
$v - v_0$	1,3	1,8	3,2	1,3	1,6	1,8	1,1	1,5

Valuable results were obtained with the 500 mm tank, which was cooled by a water jacket; the v for tractor kerosene at moderate wind speeds was 2.1 mm/min with the cooler working but 3.3 mm/min with it inoperative. In the first case, the kerosene absorbed 50 kcal/min, and in the second 120 kcal/min; the flowing water removed about 60 kcal/min.

The cause of the relation of v to w is that the wind tends to increase the flow of heat from the flame to the liquid; any factor that does this must tend to increase v. The above results may be analyzed as follows. The radiation from the flame and the flow of heat through the wall both tend to increase with w and so tend to raise v. The following figures [3] illustrate the effect of w on flame temperature for benzine in a 1300 mm tank:

w, m/sec	0	0.8	1.0	2.1
T, °C	1120	1120	1180	1190

Here the (natural) wind raised the temperature by 70° when its speed rose from 0 to 2 m/sec; this is equivalent to an increase of about 20% in the radiation flux, and so it must imply an increase in v.

The other important source is the flow of heat through the wall, which can be large, as the following argument shows. The equation of heat flow here is

$$q_1 = \alpha \Delta\vartheta s,$$

in which α is the heat-transfer factor, $\Delta\vartheta$ is the difference of temperature as between liquid and wall, and s is the area of the wall. For convective transfer [18]

$$Nu = c\,(Ra)^n. \tag{2.49}$$

in which Nu is Nusselt's number and Ra is Rayleigh's criterion:

$$Ra = GrPr = \frac{\rho^2 c \beta g l^3 \Delta\vartheta}{\eta\lambda} = b l^3 \Delta\vartheta, \tag{2.50}$$

in which ρ, c, η, g, and λ have their usual meanings, β is the thermal expansion coefficient, l is the length of heated wall, and b is the convection modulus, which is of the order of ten thousand for these oil products.

Experiment gives for benzine that $\Delta\vartheta = 20°$ for $l = 10$ cm, so $Ra = 10^9$; the c of (2.49) may be taken as 0.135, and n = 1/3 [18]. If only a quarter of the wall is heated, we have, for R = 25 cm, that

$$q_1 = 250\,\pi x l = 340 \text{ cal/sec}.$$

The v_o for this case is 3.5 mm/min, so

$$q_2 = 1000 \text{ cal/sec}.$$

Thus the heating of the wall by the flame makes a major contribution to the heat flow and thus to v; moreover, q_1 increases with w, because $\Delta\vartheta$ increases. The relative importance of q_1 decreases as R increases, which in part explains why ϑ decreases as d increases.

These arguments also explain why v for mazut is independent of w between 0 and 2.8 m/sec; Ra is dependent on η, as (2.50) shows, and η for mazut is many times that for benzine, so α (and hence the heat flux from the wall) is very much smaller for mazut.

The v for benzine and kerosene also show a regular trend with w for a quartz burner 30 mm in diameter; (2.47) applies. The flame is very much deflected; the temperature rises, and the radiation becomes much more intense. Ethanol shows no variation of v with w for this same burner, because its flame is of low luminosity.

Rate of Burning as a Function of Level in Tank

The level h (distance from the edge) affects not only v but also sometimes the mode of burning as well. Tables 2.23 and 2.24 give some results, which show that v decreases as h increases, the flame going out at a certain h, which we denote by z_o. The flame is laminar for all h if d is small, and there are no oscillations; the flame stays at the top of the burner, which it does not enter as the level falls. The pulsations set in as d increases, but they stop if $h \geq h_c$, in which h_c is a critical value. The base of the flame always lies above the edge of the burner. The pulsations persist as d increases further, but the flame starts to enter the burner when h becomes large. The larger d, the sooner the flame enters.

The surface temperature ϑ_s at first stays almost constant as h increases, as Fig. 34 shows for benzine, ethanol, and butanol in burners of diameters 11 and 23 mm. The behavior of $\vartheta_s(h)$ and

v(h) serve to explain this; Fig. 35 shows these curves for benzine. Here v falls continuously, although $_s$ at first is constant, because the greater distance implies a lower concentration gradient, so the rate of arrival of fuel is lower. This ultimately affects $_s$, which in its turn reduces the gradient and so reduces v further.

Figure 36 shows a selection of the results for diesel oil in tanks of diameters 307, 500, and 950 mm (change in level as a function of burning time). The burning ceases when the appropriate z_0 is reached. Here the flame enters the tank, and is

Table 2.23

		$d = 5{,}2$ мм					$d = 10{,}9$ мм					
Ethanol	h, мм	0	2,5	4,5	6,5	8,5	0	0,5	2,5	4,5	6,5	8,5
	$V \cdot 10^2$ см³/мин	—	15	11	6,6	2,1	33	29	23	16	9,0	3,7
	v, мм/мин	—	7,1	5,2	3,1	1,0	3,6	3,1	2,5	1,7	1,0	0,4
	δ, мм	—	15	10	8	3	31	29	20	15	10	5
	$V/\delta \cdot 10^3$	—	10	11	8	7	11	10	11	11	9	—
	Osc.	None										
Butanol	$V \cdot 10^2$	26	18	9,2	4,5	—	38	34	30	17	9,3	3,1
	v	12,4	8,6	4,4	2,2	—	4,1	3,7	3,2	1,8	1,0	0,3
	δ	40	28	14	7	—	60	60	48	25	13	5
	$V/\delta \cdot 10^3$	6,5	6,4	6,6	6,5	—	6,3	5,7	6,2	6,7	7,1	6,4
	Osc.	None										
Kerosene	$V \cdot 10^2$	19	13	4,5	—	—	31	26	22	12	3,4	—
	v	9,0	6,2	2,1	—	—	3,3	2,8	2,4	1,3	0,4	—
	δ	59	41	15	—	—	92	82	60	36	11	—
	$V \cdot 10^3/\delta$	3,2	3,2	3,0	—	—	3,4	3,2	3,7	3,3	3,1	—
	Osc.	None										
Benzine	$V \cdot 10^2$	—	33	20	12	5,1	60	—	50	32	17	8,8
	v	—	15	9,4	5,7	2,4	6,4	—	5,4	3,5	1,9	0,9
	δ	—	73	61	35	16	119	—	121	102	165	32
	$V \cdot 10^3/\delta$	—	4,5	3,3	3,3	3,2	5,0	—	4,1	3,1	2,7	2,8
	Osc.	No					Yes		No			

largely contained within the tank when h is large. The results for h as a function of t fit the relation

$$h = kt^n, \qquad (2.51)$$

in which n varies from 0.55 to 0.75. Some values of n are as

follows:

d, mm	80	307	500	950
Automobile benzine	0.70	0.60	0.55	0.62
Tractor kerosene	0.75	0.72	0.67	-

Figure 37 shows z_0 as a function of d (Khudyakov), both being here in mm. The results for d < 50 mm fit

$$z_0 = ad^{0.63}, \tag{2.52}$$

and those for d > 50 mm

$$z_0 = 0{,}055\, d^{1.7} \tag{2.53}$$

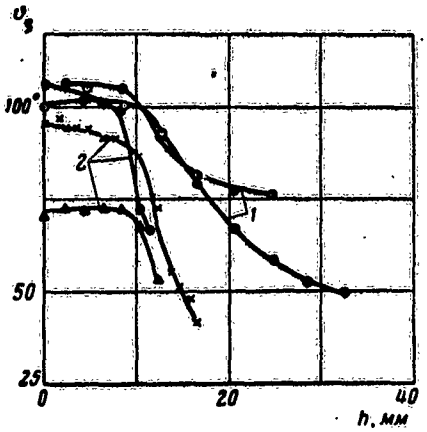

Fig. 34. Relation of ϑ_s to change in level: ⊙ and x, benzine; Δ, ethanol; + and ◑, butanol; 1) d = 23 mm; 2) d = 11 mm.

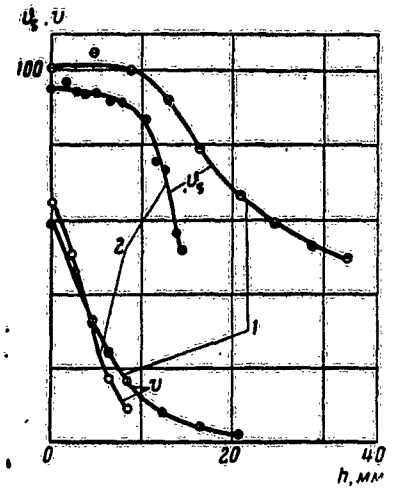

Fig. 35. Relation of ϑ_s to v and h for benzine in burners of d: 1) 23 mm; 2) 11 mm.

Further, a is dependent on the nature of the liquid for small d, so z_0 varies with the liquid for a given d. All the z_0 lie on a common curve if d > 50 mm, so the nature of the liquid is unimportant.

This behavior of $z_0(d)$ reflects differences in the processes. The flame enters a wide vessel freely, and the burning always occurs not far from the free surface; it lies above the edge and enters somewhat only at the very end if d is small. Convection is responsible for bringing in the oxygen in a wide vessel near the limiting h.

The z_0 for wide vessels are very large, and the flame does not go out in a real vessel if (2.53) applies. For example,

the z_0 for d = 5 m is 11 m, and is 34.5 m for d = 10 m.

Table 2.4

		$d = 22{,}6$ мм									
Ethanol	h, мм	0	0,5	2,5	4,5	6,5	8,5	12,5	16,5	20,5	24,5
	$V \cdot 10^3$, см³/min	80	69	56	39	25	18	8,9	5,3	5,5	
	v, мм/min	2,0	1,7	1,4	1,0	0,6	0,45	0,2	0,1	0,1	
	δ, мм	102	55	42	30	20	15	8	4	—	
	$V \cdot 10^3/\delta$	7,8	13	13	13	12	12	11	13	—	
		Osc.			No osc.			Flame in burner			
Butanol	$V \cdot 10^3$	92	72	56	39	26	17	7,2	5,0	5,0	
	v	2,3	1,8	1,4	1,0	0,6	0,4	0,2	0,1	0,1	
	δ	150	157	110	65	44	25	11	—	—	
	$V \cdot 10^3/\delta$	6,1	4,6	5,1	6,0	5,9	6,8	6,5			
		Osc.			No osc.			Flame in burner			
Kerosene	$V \cdot 10^3$	76	69	50	33	22	13	6,0	4,4	—	
	v	1,9	1,7	1,2	0,8	0,55	0,3	0,15	0,1	—	
	δ	170	158	134	98	61	47	—	—	—	
	$V \cdot 10^3/\delta$	4,4	4,4	3,7	3,4	3,6	—	—	—		
		Osc.			No osc.			Flame in burner			
Benzine	$V \cdot 10^3$	116	—	92	64	46	31	15	7,4	5	6
	v	2,9	—	2,3	1,6	1,2	0,8	0,4	0,2	0,1	0,1
	δ	200	—	180	148	110	95	49	10	—	—
	$V \cdot 10^3/\delta$	5,8	—	5,1	4,3	4,1	3,3	3,1	7,4	—	—
		Osc.					No osc.	Flame in burner			

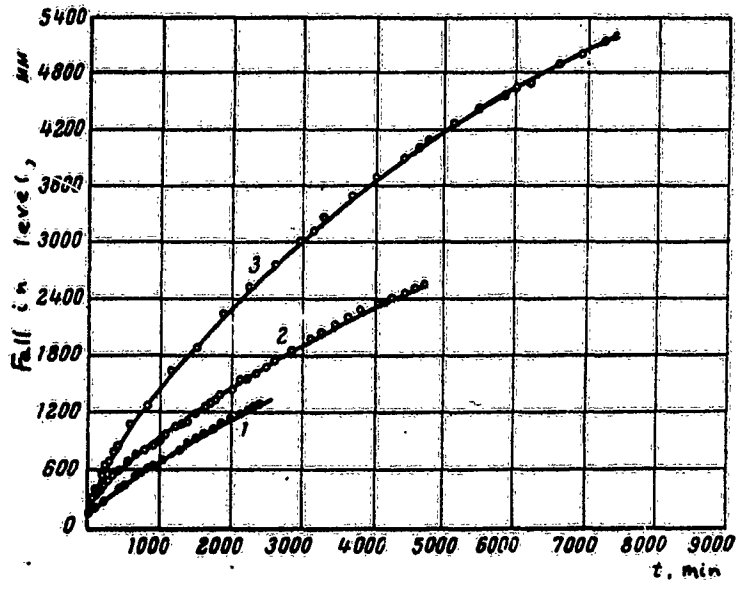

Fig. 36. Change in level of diesel oil as a function of time:
1) d = 307 mm, H = 1800 mm, extinction at v = 0.25 mm/min;
2) d = 500 mm, H = 3000 mm, extinction at v = 0.33 mm/min;
3) d = 950 mm, H = 5800 mm, extinction at v = 0.33 mm/min.

Variation of the Rate of Burning over the Free Surface

Experiments [22] on this were performed with sets of coaxial cylinders having their top edges in a common plane. The cylinders were filled with the liquid, and each was coupled to its own burette; the levels were kept at the top edge throughout the experiment. One set of experiments was done with a quartz outer tube (d = 30 mm) within which was a glass tube (d = 17 mm); others were done with tanks 300 and 800 mm in diameter with four sections each [22].

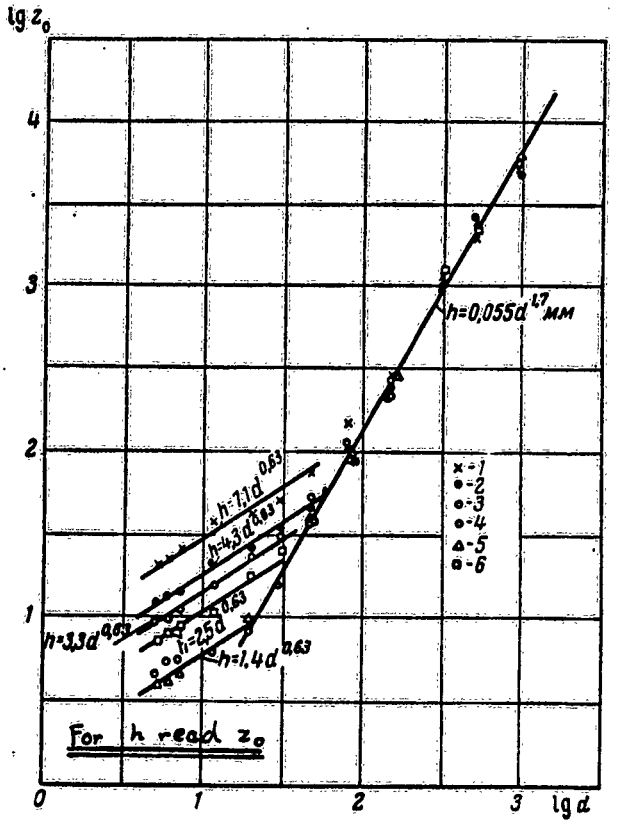

Fig. 37. Relation of z_0 to d for various fuels: 1) automobile benzine; 2) tractor kerosene; 3) illuminating kerosene; 4) transformer oil; 5) solar oil; 6) diesel oil.

Figure 38 gives results for benzine from the first apparatus; the circles relate to the annulus, and the crosses to the inner tube. The rate of burning at the periphery is clearly much higher. The following v were also recorded with this double burner:

Liquid	Edge	Center
Benzine	3.4	1.2
Kerosene	1.7	0.7
Benzine + water	3.2	-

The edge v is about three times the central v, so the heat flux at the edge must be much higher; this is not unexpected, for

it is caused by the base of the flame, which lies near the edge.

In some cases, water was placed in the inner tube, and benzine (or kerosene) in the annulus. The v for the benzine was reduced. In the case of kerosene, the water in the inner tube boiled over and extinguished the kerosene. These results are much as one might expect and need no special explanation.

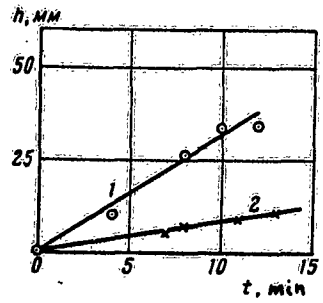

Fig. 38. Rates of burning for peripheral and central areas; v (mm/min): 1) 3.3; 2) 1.1.

Table 4 gives results from the tanks, in which 1 denotes the central section and 4 the outermost one. Here there is little variation between sections, the highest v being at the center, there being a fall towards the wall followed by a rise at the wall itself. Here the conditions of heat transfer were different from those in the small burner, for flames in tanks of diameters 300 and 800 mm are turbulent. The ratio of circumference to area is also much smaller, so the heat flowing in from the edge was of minor importance. This explains the major change in the pattern of burning rates.

Table 2.25

Liquid	d, мм	Sections and v, мм/мин			
		1	2	3	4
Benzene	300	3,6	3,5	3,2	4,4
Gasoline	300	4,3	3,9	3,5	4,3
Tractor kerosene	300	2,6	2,2	1,9	2,0
..	800	2,8	2,3	2,5	2,7
Diesel oil	800	3,8	2,0	2,7	2,8

References

1. G. N. Khudyakov. Vygoranie zhidkosti so svobodnoi poverkhnosti (Burning of a Liquid from a Free Surface). Izv. Akad. Nauk SSSR, OTN, No. 10-11, 1945.
2. V. I. Blinov. O yavlenii vybrosa goryuchei zhidkosti pri gorenii (Boiling-over of a Burning Combustible Liquid). Ibid., No. 2, 1955.
3. V. I. Blinov, G. N. Khudyakov, and I. I. Petrov. Izuchenie

goreniya nefteproduktov v rezervuarakh (A Study of the Burning of Oil Products ... Tanks). Trudy ENIN i TsNIIPO, 1955.
4. V. I. Blinov and G. N. Khudyakov. Issledovanie protsessa goreniya nefteproduktov v rezervuarakh razhchnykh diametrov (A study of the Burning of Oil Products in Tanks of Various Diameters). Repor. of ENIN, Academy of Sciences, 1955.
5. V. I. Blinov. O skorosti goreniya binarnykh smesei zhidkostei (Rates of Burning of Binary Liquid Mixtures). Trudy LIAP (Transactions of the Leningrad Institute of Aviation Instrumentation), No. 7, 1954; Inform. sbornik TsNIIPO (Bulletin of the Central Research Institute for Fire-Fighting), Moscow, publ. MKKh, 1955.
6. V. I. Blinov and G. N. Khudyakov. O nekotorykh zakonomernostyakh diffuzionnogo goreniya zhidkostei (Some Laws in the Diffusion Burning of Liquids) Dokl. Akad. Nauk SSSR, 113, No. 5, 1957.
7. P. P. Pavlov and A. M. Khovanova. O gorenii neftei i nefteproduktov so svobodnoi poverkhnosti (Burning of Oil and Oil Products from a Free Surface). Baku, 1955.
8. Idem. O teploperedache v nefteproduktakh pri gorenii ikh so svobodnoi poverkhnosti (Heat Transfer in Oil Products During Burning from a Free Surface). Inform. sbornik TsNIIPO (Bulletin of the Central Research Institute for Fire-Fighting), Moscow, publ. MKKh, 1954.
9. Idem. Gorenie sinteticheskogo dietilovogo efira sv svobodnoi poverkhnosti v rezervuarakh (Burning of Synthetic Diethyl Ether from a Free Surface ... Tanks). Inform. sbornik TsNIIPO (Bulletin of the Central Research Institute for Fire-Fighting), Baku, 1957.
10. J. H. Burgoyne and A. Katan. Burning of Petroleum Products in Open Tanks. J. Inst. Petroleum, 33, No. 279, 1947.
11. V. I. Blinov. O laminarnom gorenii zhidkostei v rezervuarakh (Laminar Burning of Liquids in Tanks). Trudy LIAP (Transactions of the Leningrad Institute of Aviation Instrumentation), No. 14, 1956.
12. P. P. Pavlov and A. M. Khovanova. Vliyanie razmera rezervuara na skorost' vygoraniya i rezhim goreniya neftei i nefteproduktov (Effects of Tank Size on the Burning Rate and Mode of Burning for Oil and Oil Products). Inform sbornik TsNIIPO (Bulletin of the Central Research Institute for Fire-Fighting), Baku, 1957.
13. A. Kruger and R. Radusch. Character of Combustion of Liquid Fuels in Storage Tanks. Erdöl und Kohle, 8, No. 7, 1955.
14. Inform. sbornik TsNIIPO (Bulletin of the Central Research Institute for Fire-Fighting), 1951.
15. G. N. Khudyakov. Yavlenie vybrosa tyazhelogo zhidkogo topliva pri gorenii ego so svobodnoi poverkhnosti (Boiling-over for Heavy Liquid Fuel Burning from a Free Surface).

Izv. Akad. Nauk SSSR, OTN, No. 5, 1950.
16. Idem. O temperaturnom pole zhidkosti, goryaskchei so svobodnoi poverkhnosti, i o fakele nad nei (Temperature Distribution in a Liquid Burning from a Free Surface and the Flame above the Liquid.) Ibid., No. 7, 1951.
17. V. I. Blinov and G. N. Khudyakov. O vliyanii vetra na skorost' vygoraniya nefteproduktov v rezervuarakh (Effects of the Wind on the Rate of Burning of Oil Products in Tanks). Inform. pis'mo No. 8, ENIN Akad. Nauk SSSR, 1958.
18. V. I. Blinov. O trekh rezhimakh goreniya zhidkostei v rezervuarakh (Three Modes of Burning of Liquids in Tanks). Izv. Akad. Nauk SSSR, OTN, No. 4, 1956.
19. M. A. Mikheev. Osnovy teploperedachi (Principles of Heat Transfer). Moscow-Leningrad, publ. Gosenergoizdat, 1947.
20. S. S. Nametkin. Khimiya nefti (Petroleum Chemistry), publ. Acad. Sci. USSR, 1955.
21. P. P. Pavlov and A. M. Khovanova. Gorenie emul'sionnykh neftei so svobodnoi poverkhnosti (Burning of Emulsified Crude Petroleum from a Free Surface). Inform. sbornik TsNIIPO (Bulletin of the Central Research Institute for Fire-Fighting), Baku, 1957.
22. Ya. B. Zel'dovich. K teorii goreniya neperemeshannykh gazov (Theory of the Burning of Unmixed Gases). Zh. Tekh. Fiz., 19, No. 10, 1949.
23. V. I. Blinov and G. N. Khudyakov. O nekotorykh zakonomernostyakh, kotorym podchinyaetsya gorenie nefteproduktov v rezervuarakh. Sb. "Issledovanie protsessov goreniya" (Some Laws Governing the Burning of Oil Products in Tanks. Coll. 'Study of Combustion Processes'), publ. Acad. Sci. USSR, 1958.
24. J. H. Burgoyne and J. F. Richardson. Extinguishing Burning Liquids by the Application of Noninflammable Gases and Liquids. Fuel, 28, No. 7, 150, 1949.

Temperature Distribution in a Burning Liquid

The temperature distribution has some special features; it plays a very important part in extinction, and there are many papers on it [1-13]. A single adjustable thermocouple is commonly used with narrow burners; a series of fixed couples may be used in wider vessels. The level is sometimes kept constant by feeding in fresh fuel at the bottom; replenishment was not used by Hall, Burgoyne, or Pavlov, and the l...l changed continuously throughout the process.

Surface Temperature of a Burning Liquid

The surface temperature ϑ_s^g rises rapidly when the liquid is ignited; it tends to a definite limit for a pure liquid and for certain mixtures. There is usually a slow rise in ϑ_s^g after the first rapid rise in the case of a mixture (Fig. 39). Ethanol very rapidly reaches a steady temperature; solar oil shows a very slow subsequent rise, while benzine mixed with solar oil shows a very rapid rise that is followed by a fairly slow approach to the value for solar oil. Table 2.26 lists the limiting ϑ_s^g for various liquids in burners of various materials and diameters, and also gives the boiling points $\vartheta^{g'}$, which are somewhat above ϑ_s^g. This occurs because the surface is covered by a layer of the saturated vapor, whose pressure π is governed by ϑ_s^g, which cannot exceed the $\vartheta^{g'}$ for the existing atmospheric pressure p_o; any such excess would cause π to exceed p_o, and so the vapor would be pushed away rapidly. The resulting rapid boiling would soon cool the liquid.

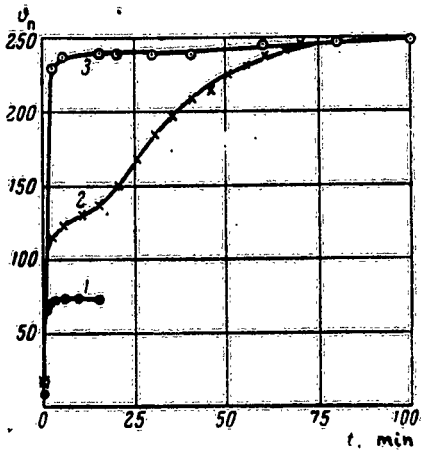

Fig. 39. Surface temperature as a function of time: 1) ethanol, d = 2.7 mm; 2) benzine + solar oil, d = 30 mm; 3) solar oil, d = 30 mm.

Table 2.27 gives ϑ_s^g for some binary mixtures of combustible liquids [6]; the burners were of glass, and the first component was ethanol. Here g_x is the proportion of the second component by weight and ϑ_o' is the initial boiling point of the mixture. The limiting ϑ_s^g are below ϑ_o', except in the case of isoamyl alcohol. We have seen above that g_x tends to change as combustion

proceeds; in fact, the top layer in the mixtures containing isoamyl alcohol became enriched to $g_x = 0.86$, whereas the propanol

Table 2.26

	Material*	d, mm	ϑ_s, °C	ϑ', °C
Ethanol	C	47	71	78
	»	12	71	78
	A	44	71	78
	»	21	69	78
	K	106	105	117
Butanol	C	36	104	117
	»	9	104	117
Amyl alcohol	K	106	120	129
Acetone	»	106	55	56

*C = glass; A = aluminum; K = quartz

mixture with $g_x = 0.50$ initially gave a top layer with $g_x = 0.68$ (0.85 in the case of the mixture initially of $g_x = 0.74$). Table 2.27 also lists ϑ', the actual boiling points of these surface layers; we see that $\vartheta_s \approx \vartheta'$.

Table 2.27

Second component	g_x	d, mm	ϑ_s, °C	ϑ_0', °C	ϑ', °C
Isoamyl alcohol	0.50	9.4	95	88	108
	0.50	36	95	88	108
Propanol	0.50	9.4	84	85	88
	0.74	9.4	89	90	92
Water	0.31	36	68	80	—
	0.27	21	72	79	—
	0.15	21	71	78	—

These results enable us to estimate the surface temperature during burning from the composition of the surface layer. Some measurements have been made on ϑ_s for oil products burning in tanks [2,4,6-8,11]; Table 2.28 gives mean surface temperatures for some [8]. Here ρ is the initial density, ϑ_0' is the initial boiling point during distillation, and c is the proportion distilling off up to the temperature shown in parentheses. The values

of $\nu\ell_s$ enclosed in parentheses relate to cases in which a homothermal layer appeared. Table 2.29 is from [7].

Table 2.28

	ρ, g/cm³	ϑ, °C	c, %	d, cm: 2.0	3.0	4.7	8.0	15	30	50	130
				ϑ_s, °C							
Automobile benzine	0,74	57	30 (100)	98	90	95	91	99	103	108	(90)
Tractor kerosene	0,72	105	25 (200)	177	[illegible]	168	177	192	—	—	—
Illuminating kerosene	0,82	170	14 (200)	—	—	—	204	222	—	—	—
Diesel oil	0,84	180	36 (240)	230	231	237	221	241	—	—	—
Solar oil	0,89	—	—	—	277	285	283	314	340	345	—
Transformer oil	0,89	—	—	—	—	—	—	—	343	337	—
Crude	0,88	—	—	238	213	215	205	—	—	—	(130)
Heavy oil	1,01	—	—	—	—	—	—	—	—	—	(230)
	1,01	—	—	—	—	—	—	—	—	—	290

Table 2.29

	ρ, g/cm³	ϑ, °C	c, %	d, cm: 30	80	140	260
				ϑ_s, °C			
Automobile benzine	0,76	50	30 (100)	—	100	—	—
Bibi Eibat crude	0,88	179	37 (305)	—	320	340	330
Karachukhur crude	0,89	184	30 (290)	—	350	350	230
Artemovo crude	—	—	—	—	200	—	—
Direct-dist. fuel oil	0,94	—	—	—	200	—	—
Diethyl ether	0,73	36	—	36	36	36	40

Khudyakov's results [4] for a quartz burner of diameter 106 mm are as below:

Liquid	ρ, g/cm³	$\nu\ell_s$	Liquid	ρ, g/cm³	$\nu\ell_s$
Benzine	0.73	108	VM-4 oil	0.89	347
Kerosene	0.81	220	Glycerol	1.25	239
Paraffin oil	0.87	287	MS oil	0.89	392
Transformer oil	0.88	293			

These results show that ϑ_s^{ℓ} for benzine is 90-110°, for tractor kerosene 170-200°, for illuminating kerosene 230-240°, for diesel oil 230-240°, for solar oil 280-340°, for transformer oil 290-340°, and for crude petroleum 130-350°. These ϑ_s^{ℓ} are always above ϑ_0^{ℓ}; the surface layers are depleted of volatile fractions. Moreover, the ϑ_s^{ℓ} for a given product vary from one tank size to another; for example, the ϑ_s^{ℓ} for benzine and crude for d = 130 cm and 260 cm are lower than those for d < 130 cm. In particular, Artemovo crude has a ϑ_s^{ℓ} for a 260 cm tank some 120° below the ϑ_s^{ℓ} for small tanks.

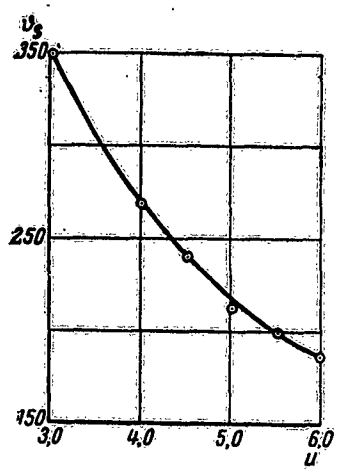

Fig. 40. Surface temperature in relation to the rate of increase in the depth of the homothermal layer for crude petroleum.

The homothermal layer, which shows vigorous convection, is responsible for these effects; its thickness increases as time passes, and the greater the rate of increase u, the lower ϑ_s^{ℓ}, because fresh cold liquid is introduced. This layer is absent if d < 130 cm, which explains the ϑ_s^{ℓ} of Table 2.27; the u for Artemovo crude are 3.1 mm/min (d = 80 cm), 3.2 (d = 140 cm), and 6.5 (d = 260 cm).

Experiments with emulsified crude [9] confirm this; ϑ_s^{ℓ} and u were found to be very much dependent on the water content. Figure 40 shows the relation of ϑ_s^{ℓ} to u, in which the line corresponds to

$$\vartheta_s = \vartheta_0 + \frac{b}{u}, \qquad (2.54)$$

This equation may be deduced as follows.

Let q be the heat received from the flame, q' the heat lost to the surrounds, q_0 be the latent heat of evaporation, ϑ_0^{ℓ} the initial temperature, c the specific heat, and s the free surface area. Now

$$q = q^1 + vsp q_0 + uscp(\vartheta_s - \vartheta_0).$$

We assume that v, q', and q are not affected by slight changes of water content, in which case (2.54) is found directly. A fuller treatment of the relation of ϑ_s^{ℓ} to u is to be found in [24].

Although the homothermal layer reduces r_s^{ℓ}, it does not affect v, which may even increase somewhat; the reason is that the homothermal layer contains a higher proportion of the volatile fraction, so the flow of vapor remains adequate in spite of the lower r_s^{ℓ}. The following calculation illustrates this.

The oil product may be assumed to be represented roughly by a binary system of mutually soluble components, one much more volatile than the other; to these we apply (2.41), which gives us that

$$g_y = g_{0,x} + (g_{0,x} - g_x)\varphi, \quad \varphi = \frac{u}{v},$$

in which u and v are as usual. Thus g_y is essentially dependent on φ, as is g_x; $g_y = g_{0x}$ if $\varphi = 0$, and $g_x = g_{0x}$ if $\varphi = \infty$ (g_y would be infinite in the latter case if this were not so, whereas the limiting g_y is 1).

The following detailed example illustrates the variations in g_y and g_x with φ. We assume that the mixture is ideal; α is the ratio of the vapor pressures of the two components. The theory of solutions shows that, for an ideal mixture,

$$g_y = \frac{g_x}{1 - (\alpha - 1) g_x}.$$

This g_y is substituted into (2.41) to give

$$(\alpha - 1)\varphi g_x + [\alpha + \varphi - (\alpha - 1) g_{0,x}] g_x - g_{0,x}(\varphi + 1) = 0.$$

The solution to this gives us the g_x for the top layer. Let us suppose that $\alpha = 2$ and $g_{0x} = 0.5$; the results then are:

φ	g_x	g_y
0	0,33	0,50
1,0	0,41	0,58
2,0	0,44	0,61
4,0	0,46	0,63
∞	0,50	0,67

We see that g_x and g_y at first increase rapidly with φ, but the rates of increase soon become very low.

The slight variations in r_s^{ℓ} for conditions under which the homothermal layer is absent are caused by slight errors in the positions of the thermocouples, for the temperature gradients are

very high; it is impossible to keep the thermocouples always exactly at the surface while burning proceeds. The slow change in τ_s^{ℓ} is caused by gradual alteration in the composition of the surface layer.

The above results show that the surface temperature of a mixture is dependent on the combustion conditions; it is not a constant, although it is dependent on the composition.

Horizontal Variation in the Temperature of a Burning Liquid

The temperature varies in any horizontal plane drawn within the liquid [8], as the following results show. Here l is the distance from the axis of the tank, whose radius R is 25 cm:

l/R	0	0.28	0.60	0.91	1.0
Transformer oil	166	—	171	217	260
Solar oil	—	188	188	—	270
Tractor kerosene	108	123	133	143	168
Lighting kerosene	111	113	—	121	168

The temperature rises towards the wall, where it is highest; the differential between axis and wall ranges up to 100°. The same effect is observed, but with smaller differences, for d < 50 cm, and with larger differences for d > 50 cm.

The following results are for tractor kerosene in a tank 260 cm in diameter; measurements were made at three points (1, 2 and 3) in planes 12, 22, and 50 cm below the edge of the tank. The points had angular separations with respect to the axis of 120°:

z	12	22	50
θ_1	149	74	33
θ_2	168	141	41
θ_3	230	109	41

These figures show that the wall temperature varies from point to point in any given plane. The same pattern is found with all oil products in tanks of diameters 130 and 260 cm.

These variations were caused by the need to operate in the open air with these large tanks, so there was interference by the wind, which deflected the flame and caused the wall to be heated unevenly. The effect is seen whenever the wall is exposed to air currents. These differences are bound to cause convection within the liquid.

Temperature Variations in a Burning Liquid

The temperature distribution is established gradually, as Fig. 41 shows for transformer oil, the z being the depths below the surface. In each case there is a rapid rise to a limit, which varies with z; the time taken to reach the limit in a metal vessel is much longer than that for a glass one.

Mixtures of benzine with solar oil show a different type of curve; there is first a very rapid rise in ϑ^{ℓ}, which is followed by a slower rise (at the surface and at some depth) to a limit corresponding to the initial composition of the mixture. Then there is a further rise, whose limit is close to that for solar oil. The latter rise is caused by alteration in the composition of the surface layer, and $\vartheta^{\ell}(t)$ gives an indication of the course of that alteration.

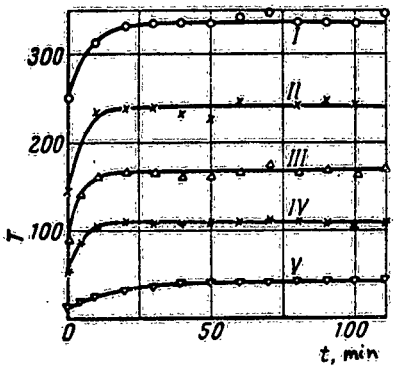

Fig. 41. Relation of ϑ^{ℓ} to time for transformer oil; z (mm): I) 0; II) 2; III) 5; IV) 9; V) 29.

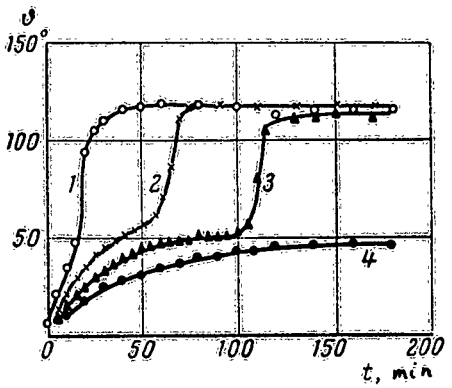

Fig. 42. $\vartheta^{\ell} = f(t)$ for benzine; z_0 (mm): 1) 60; 2) 100; 3) 130; 4) 195.

Kerosene, diesel oil, and solar oil show the behavior described for transformer oil; so do benzine and crude petroleum if d is small, but the $\vartheta^{\ell}(t)$ for these two for d large are very different, as Fig. 42 shows for benzine for d = 150 mm. The rise in the layer near the top is as for transformer oil at first, but then there is a fresh and very rapid rise to ϑ^{ℓ}_{s}. The second rise does not occur for layers at some depth. The effect of this second rise is to produce a layer of uniform temperature (the homothermal layer), whose thickness increases gradually as time passes.

This pattern of behavior was first observed for crude petroleum by Hall [1]; it was afterwards examined by Burgoyne and Katan [2] and by Khudyakov [4], and later by Pavlov and Khovanova

[7,9-11], Blinov and Khudyakov [12], and Blinov et al [8].

Vertical Variation in the Temperature of a Burning Liquid

1. Figure 43 shows $\vartheta^{\ell}(z)$ for tractor kerosene burning steadily in a vessel 150 mm in diameter; Fig. 44 does the same for butanol in a glass burner 36 mm in diameter. The temperature falls to the initial value within a few centimeters of the surface. This behavior is shown by tractor kerosene, diesel oil, solar oil, and transformer oil in all vessels, by benzine and crude petroleum in small vessels, and by all other mixtures we have used.

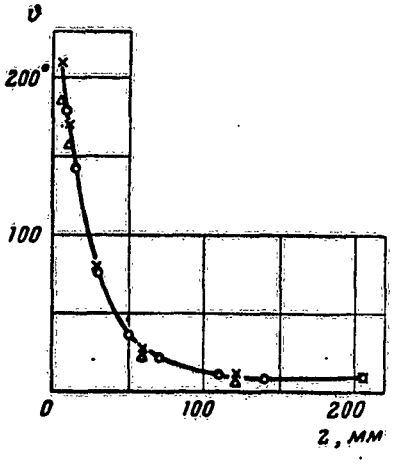

Fig. 43. $\vartheta^{\ell} = f(z)$ for tractor kerosene

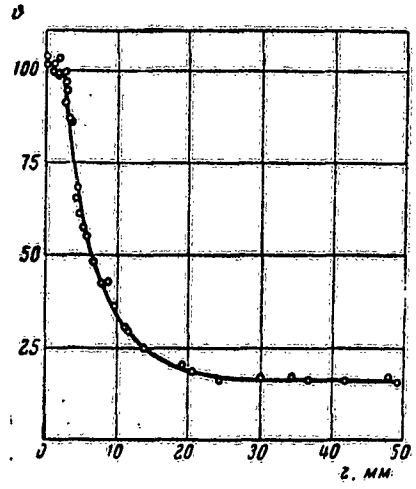

Fig. 44. $\vartheta^{\ell} = f(z)$ for butanol

The results can be represented by the equation

$$\vartheta - \vartheta_0 = (\vartheta_s - \vartheta_0)\, e^{-kz}, \qquad (2.55)$$

in which ϑ^{ℓ}_s and ϑ^{ℓ}_0 are as usual and k is a constant. The lines in Figs. 43 and 44 have been drawn up from (2.55), which fits the results well; this formula was proposed in 1949 [15] and has since been confirmed repeatedly [4,6,8,12].

2. Table 2.30 gives some values of k [4,6]. Some k for

oil products burning in steel tanks are as follows:

d, cm	8	14,8	30	50	80	130	260
Tractor kerosene	0,38	0,50	0,71	0,81	—	—	0,0
Illum. kerosene	0,52	0,52	1,09	0,98	—	—	—
Transformer oil	—	0,40	0,56	1,49	—	—	—
Diesel oil	0,50	0,56	—	—	0,24	0,08	0,09
Solar oil	0,36	0,46	0,63	1,19	—	—	—
Benzine	—	0,42	0,46	0,54	—	—	—
Crude petroleum	0,47	0,53	—	—	—	—	—

Table 2.30

Liquid*	Material**	d, mm	d_c mm	k, cm^{-1}	v, mm/min	$a_3 \cdot 10^4$, cm/sec
E	C	36	1	2,4	1,3	0,9
	»	10	1	3,0	3,6	2,0
	A	40	2	0,075	1,2	27
	M	10	1	0,085	2,2	43
B_1	C	36	1	2,0	1,6	1,3
	»	9,4	1	3,1	4,2	2,3
	M	10	1	0,075	2,4	53
	K	106	—	1,5	1,0	1,1
A_1	»	106	—	0,85	1,3	2,5
A_2	»	106	—	1,2	1,0	1,4
T	C	21	1	1,5	1,3	1,4
	K	30	1,6	1,1	0,9	1,4
	»	106	—	0,8	0,5	1,0
K	C	21	1	1,7	2,2	2,2
	K	30	1,6	1,3	1,3	1,7
	»	106	—	1,3	1,0	1,4
B_2		106	—	0,3	2,2	12
M_1	»	106	—	0,8	0,5	1,0
M_2	»	106	—	1,0	0,2	0,3
G	»	106	—	1,1	0,4	0,6

*E = ethanol; B_1 = butanol; A_1 = acetone; A_2 = amyl alcohol; T = transformer oil; K = kerosene; B_2 = benzine; M_1 = VM-4 oil; M_2 = MS oil; G = glycerol.

**C = glass; A = aluminum; M = copper; K = quartz.

Clearly, k varies widely. Moreover, although (2.55) fits tran-

sient states as well as steady ones, the k for the two types of state are not the same (k is a function of time for transient states). Figures 45 and 46 show k as functions of t for diesel oil and kerosene in tanks of diameters 130 cm (open circles) and 260 cm (half-filled circles) [16].

3. Further, k is dependent on d, on the material of the tank, and on the wind speed. Measurements [12] have been made with tractor kerosene and diesel oil in steel tanks whose d were 150, 300, 490, and 500 mm, and whose heights were correspondingly 800, 1800, 2000, and 400 mm. The 500 mm tank was fitted with a cooling jacket. Some use was also made of an asbestos-cement tank of outside diameter 330 mm, inside diameter 280 mm, and

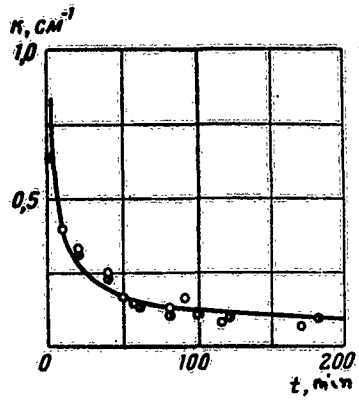

Fig. 45. Relation of k to t for diesel oil.

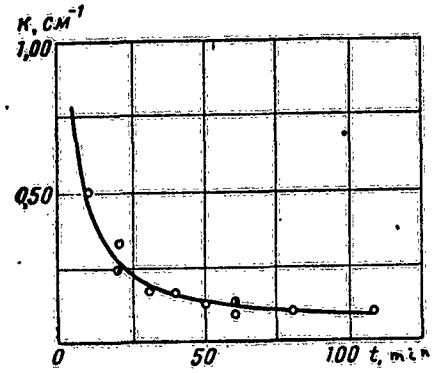

Fig. 46. Relation of k to t for kerosene.

height 1200 mm. Thermocouples were fixed to the walls and at various points within the liquid.

The flame was exposed to an air current, which was produced by a large fan (in the open air) or by the compressed-air line (in the laboratory). The air currents were usually horizontal, but in some cases they were directed at 70 or 109° to the vertical. Vertical screens were used to suppress interference from the wind out of doors; in some cases, the tank was fitted with a horizontal screen to prevent the flame from touching the sides. This screen was a sheet of stainless steel having a circular hole equal in diameter to the outside diameter of the tank; it was placed level with the top edge of the tank. The liquid level

was kept constant throughout the runs, which lasted 2-5 hr.

Tables 2.31-2.35 give the results; here h_o is the distance

Table 2.31

Tractor Kerosene, d = 150 mm, h_o = 10 mm

№	d_c, мм	w, м/sec	α, deg	v, мм/min	$k_ж \cdot 10^2$, $см^{-1}$	$a_s \cdot 10^2$, $см^2$/sec	$k_c \cdot 10^2$ $см^{-1}$	$\Delta\vartheta_{max}$, °C	τ, min	*Q, cal/sec
10	1	0	—	1,1	42	4,4	42	4	185	2,2
11	1	1,8	70	2,4	42	9,5	27	34	180	5,9
12	1	1,8	90	2,9	42	11	27	32	180	5,9
13	1	1,15	90	2,6	33	13	25	23	180	5,3
14	1	2,6	90	3,2	36	15	18	51	183	6,5
15	1	1,8	109	4,3	42	17	17	70	173	—
24	10	0	—	0,7	8,6	14	8,6	6	185	—
25	10	2,6	90	3,1	11	45	10,0	36	182	—
26	10	0,75	90	2,8	10	49	3,3	20	182	—
31	6	0	—	0,8	9	14	9,3	5	182	—
32	6	2,6	90	3,0	17	29	15	40	182	—
39	3	2,6	90	3,4	23	25	16	45	181	—
40	3	0	—	0,7	14	9	14	8	182	—

*Q is the rate of receipt of heat by the liquid.

Table 2.32

Tractor Kerosene, d = 300 mm

№	w, м/sec	v, мм/min	$k_ж \cdot 10^2$, $см^{-1}$	$a_s \cdot 10^2$, $см^2$/sec	h_0, мм	τ, min	Q, cal/sec
63	2	1,8	42	7,2	75	121	—
64	0	2,0	55	6	75	120	18,5
65	6,6	4,6	45	17	75	100	42
66	4,2	3,5	42	14	75	100	32
71_{ac}	6,6	4,7	24	39	40	300	43
75	22,0	7,0	45	26	30	182	65
76	10,5	5,7	31	30	30	180	53
77	4,2	3,5	22	27	30	180	32

from the rim to the liquid, w is the speed of the air current, and τ is the duration of the test. Subscript ⊃ denotes that the horizontal screen was used; subscript ac denotes the asbestos

Table 2.33

Tractor Kerosene, d = 490 mm

№	w, м/сек	v, мм/мин	$k_{ж} \cdot 10^3$, $см^{-1}$	$a_э \cdot 10^3$, $см^2/сек$	$k_c \cdot 10^3$, $см^{-1}$	h_0, мм	τ, мин	Q, кал/сек
47	0	2,5	28	15	28	80	180	65
48	10,8	5,8	25	39	4	80	240	150
49	26	7,4	26	20	—	80	235	192
50	0	2,5	15	27	8	80	240	65
51	9	5,6	19	48	—	80	240	144
61	7	4,1	38	18	28	115	210	106
62	1,2	2,0	23	14	12,5	110	190	52
73	4,2	4,0	20	33	6	60	180	104
74	17	7,0	50	23	6	60	180	182

Table 2.34

Diesel Oil, d = 150 mm, h_0 = 10 mm

№	d_c, мм	w, м/сек	α, deg	v, мм/мин	$k_{ж} \cdot 10^3$, $см^{-1}$	$a_э \cdot 10^3$, $см^2/сек$	$k_c \cdot 10^3$, $см^{-1}$	$\Delta\vartheta_{max}$	τ, мин
1	1	0	—	0,6	42	2,4	38	24	180
2	1	1,5	90	1,6	56	4,9	45	25	182
3	1	1,1	90	1,7	56	5,2	42	30	174
4	1	2,6	90	2,2	43	8,4	26	57	182
5	1	1,1	109	2,1	31	11,0	26	23	17
6	1	1,8	109	2,2	31	12,0	28	23	180
7	1	2,6	109	2,4	31	13,0	22	35	180
8	1	2,6	70	1,9	45	7,0	33	32	179
9	1	1,8	70	1,4	43	5,4	40	15	181
27	10	1,4	90	2,3	12	32,0	11	46	180
28	10	0	—	0,6	8,6	12,0	7	10	180
33	6	2,6	90	2,3	18	21,0	13	38	180
34	6	0	—	0,4	9,8	8,5	8	10	180
37	3	2,6	90	2,4	23	18,0	19	42	182
38	3	0	—	0,5	25	3,3	10	—	188

Table 2.35

Diesel Oil, d = 490 mm, h_o = 10 mm

№	w, m/sec	v, mm/min	$k_ж \cdot 10^3$, cm^{-1}	$a_э \cdot 10^3$, cm^2/sec	τ, min
42	22	5,8	—	—	—
43	10,4	4,8	—	—	—
44	22	5,8	—	—	240
45	0	1,8	36	8,4	270
46	8	4,0	31	21	180

tank. Here z_o' is the final value of z_o, subscript ж denotes the liquid, and subscript c the wall. In experiment 50, part of the wall was fitted with a wick system fed with kerosene, which heated that part of the wall. All results fit (2.55) well; k de-

Table 2.36

Diesel Oil and Tractor Kerosene, d = 500 mm, h_o = 10 mm

№	Fuel	Wind	w, m/sec	$k_ж \cdot 10^3$, cm^{-1}	$a_э \cdot 10^3$, cm^2/sec	u_0, mm/min	z_o', mm	τ, min	Q_1, cal/sec	Q_2, cal/sec
88	Diesel oil	Moderate	2,0	36	9,0	—	—	210	—	56
89a	»	Slight	1,7	55	5,1	—	—	140	46—79	48
89	»	»	1,9	42	7,6	—	—	160	—	54
90	»	Moderate	2,0	—	—	3,2	204	210	—	111
91	»	»	2,1	83	4,2	—	—	240	61	50
92	Tractor kerosene	»	3,3	104	54,0	3,8	180	200	—	120

Note. The cooling jacket carried diesel oil in run 88, water in runs 89a and 91, and no coolant liquid in run 89b. Runs 90-92 were performed with the jacket removed.

creases as the wall thickness d_c increases, as Fig. 47 shows for tractor kerosene. Here the open circles are for w = 0 and the half-filled ones for w = 2.6 m/sec. Diesel oil gives a similar pattern.

The asbestos tank gave similar results (No. 71); here v was as for the metal tank, but k was reduced to about half. Further, k is generally dependent on the level of the liquid; k is halved when the level is lowered from 30 cm (No. 77) to 75 cm (No. 60). This relation of k to h_o is seen in other cases;

v is almost unaffected by h_o within the limits used.

Figure 48 collects results for the effects of w on k for tractor kerosene; here the circles are for d = 490 mm and h_o of 60 and 80 mm, while the crosses are the k (halved) from runs 63,

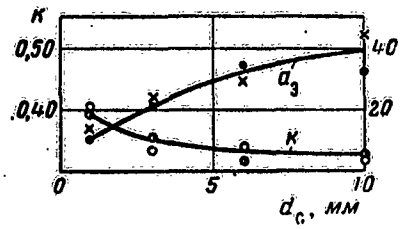

Fig. 47. Relation of k and a_3 to wall thickness for kerosene; d = 150 mm.

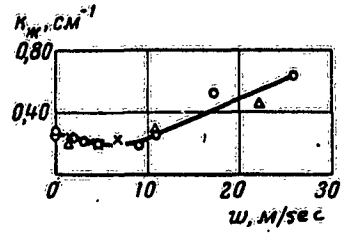

Fig. 48. Relation of k' to air speed w.

66, and 67. The triangles are the k from runs 75, 76, and 77. The points all lie near a common curve, which passes through a flat minimum near 8 m/sec. The results also indicate that k is dependent on α.

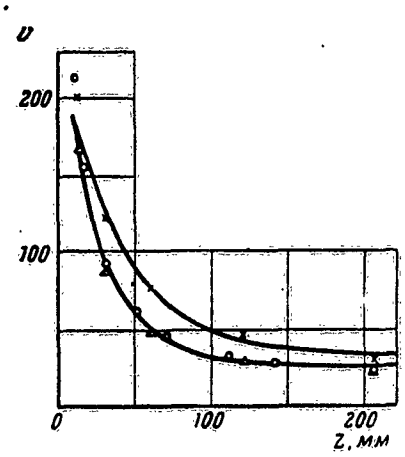

Fig. 49. Temperature distribution in the liquid and at the wall for kerosene; w = 1.8 m/sec.

Runs 47 and 50 indicate that the external fire on the wall had little effect on v, but k was nearly halved; the fire affected the temperature distribution very greatly. Further, in run 90 the cooler was inoperative, while in run 91 it carried running water. There was no effect on v, but $v(z)$ fitted (2.55) for run 91, whereas a homothermal layer was produced in run 90.

The wall temperature followed the temperature of the liquid closely and obeyed (2.55) well; results for the wall, where available, are shown as k_c (cm^{-1}). Figure 49 shows results for d = 150 mm for w of 0 and 1.8 m/sec; the circles denote the temperature at the axis, the crosses the temperature on the windward wall. The difference Δv^l between wall and liquid is small if w = 0, but the Δv^l for the lee side becomes considerable; it increases with w, and also with d. The wall temperature on the windward side is close to the axial temperature of the liquid. Figures 50

and 51 show $\Delta\vartheta^{\ell}$ for kerosene as a function of z, the distance from the rim, for several wind speeds and for two tanks. Diesel oil gives similar curves, which in many cases have a maximum. The position and height of this are dependent on w; for example, $\Delta\vartheta^{\ell}_{max}$ for kerosene for d = 150 mm and w = 1.15 m/sec is 22°, for 1.8 m/sec 32°, and for 2.6 m/sec 52°. Also, $\Delta\vartheta^{\ell}_{max}$ increases with d, for it is 32° for d = 150 mm and w = 1.8 m/sec, whereas it is 50° for d = 1300 mm and w = 1.4 m/sec. Some other results for kerosene [21] show that $\Delta\vartheta^{\ell} \approx 50°$ for d = 500 mm and 80° for d = 2600 mm.

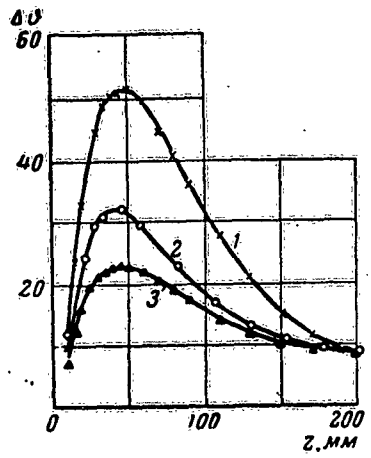

Fig. 50. $\Delta\vartheta^{\ell}(z)$ for tractor kerosene (d = 150 mm); w, m/sec: 1) 2.6; 2) 1.8; 3) 1.15.

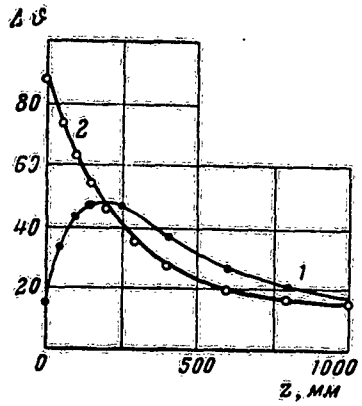

Fig. 51. $\Delta\vartheta^{\ell}(z)$ for kerosene (d = 1300 mm); w, m/sec: 1) 1.4; 2) 1.0.

$\Delta\vartheta^{\ell}(z)$ is governed by the $\vartheta^{\ell}(z)$ curves for wall and liquid; if (2.55) applies,

$$\Delta\vartheta = \vartheta_c - \vartheta_{ж} = b_0 + b_1 e^{-k_c z} - b_2 e^{-k_{ж} z}, \qquad (2.56)$$

in which

$$b_0 = \vartheta_{0,c} - \vartheta_{0,ж}, \quad b_1 = \vartheta \quad - \vartheta_{0,c}, \quad b_2 = \vartheta_п - \vartheta_0.$$

If $k_c = k_{ж} = k$,

$$\Delta\vartheta = b_0 + (b_1 - b_2)\, e^{-kz}$$

and the shape is then that of curve 2 in Fig. 51; usually, $k_c <$

$k_{\text{ж}}$, in which case (2.56) applies, and here the maximum lies at

$$z_{\max} = \frac{\ln(b_1 k_c) - \ln(b_2 k_{\text{ж}})}{k_c - k_{\text{ж}}}.$$

4. The temperature distribution represented by (2.55) arises as follows. It is asserted [1,5,7] that heat is transferred mainly by conduction in these cases; we must now test this. The flow of heat from the wall is negligible if d is large, whereupon the heat-conduction equation for a liquid burning at a rate v becomes

$$a\frac{\partial^2\vartheta}{\partial z^2} + v\frac{\partial\vartheta}{\partial z} = \frac{\partial\vartheta}{\partial t}, \tag{2.57}$$

in which a is the coefficient of molecular thermal diffusivity. We put $\vartheta = \vartheta_0^{\ell}$ at t = 0 and at $z = \infty$, and $\vartheta = \vartheta_s^{\ell}$ at z = 0; then the solution to (2.57) is [8,16]

$$\vartheta - \vartheta_0 = 4A\sqrt{\frac{a}{v^2}}\, e^{-\frac{vz}{2a}} \int_0^{\sqrt{v^2 t/4a}} \exp\left(-\psi^2 - \frac{b^2}{\psi^2}\right) d\psi,$$

in which A is a constant,

$$b = \frac{vz}{4a}, \quad \psi = v\sqrt{\frac{t-\tau}{4a}},$$

in which τ is a parameter. The steady-state result is found by putting $\tau = \infty$; the integral on the right then becomes

$$\frac{\sqrt{\pi}}{2}\exp\left(-\frac{vz}{2a}\right).$$

Then for the steady state

$$\vartheta - \vartheta_0 = (\vartheta_s - \vartheta_0)\exp\left(-\frac{vz}{a}\right). \tag{2.58}$$

This resembles (2.55); the two become identical if we put that

$$k = \frac{v}{a}. \tag{2.59}$$

Curve 1 of Fig. 52 shows $\vartheta(z)$ at the start; curve 2, from (2.58), does the same for t large, and the curve between 1 and 2 represents intermediate t. Curve 1 has $k = \infty$; (2.59) gives $k = 5.8\ cm^{-1}$ for curve 2 for $v = 3.5$ mm/min and $a = 0.001\ cm^2/sec$. These values of v and a are close to those for diesel oil for $d = 130$ cm; k should lie between ∞ and $6\ cm^{-1}$ (roughly) if conduction is the dominant process. But the results quoted previously show that k is much too small even for t small, so molecular conduction cannot be the main process (at least in those cases so far studied) when (2.55) is obeyed, apart from viscous liquids in narrow burners.

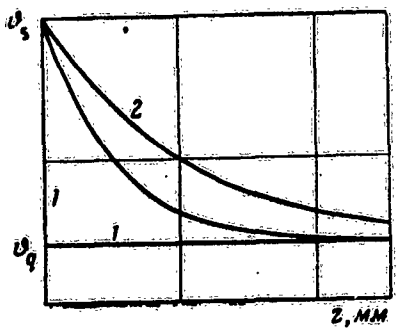

Fig. 52. Temperature distributions at the start and end of a run when the thermal conductivity governs the distribution.

Since $k > v/a$, convection must play a major part; this conclusion was drawn in 1949 [15] and has since been confirmed several times [8,12,13, 16].

The actual transport process is complex; it can [17] be represented as transfer by thermal conduction in a liquid of equivalent thermal diffusivity $a_э$, whereupon the equation retains the form of (2.58) and the limiting relations between k, v, and $a_э$ are still (2.58) and (2.59). Then we have that

$$\vartheta - \vartheta_0 = (\vartheta_s - \vartheta_0) \exp\left(-\frac{vz}{a_э}\right) \qquad (2.60)$$

and $k = v/a_э$. We determine k by experiment and so find $a_э$, and thence the convection factor

$$\varepsilon = a_э/a,$$

which gives an indication of the extent and nature of the convection.

5. Table 2.30 gives the $a_э$ for various liquids in burners of various materials having $d \leq 11$ cm. The following are some $a_э$ ($\times 10^3$, in cm^2/sec) for oil products in metal tanks:

d, cm	8	15	30	50	80	130	150
Tractor kerosene	3,5	3,7	4,0	6,2	—	—	78
Illum. kerosene	2,3	2,9	2,4	5,1	—	—	—
Transformer oil	—	2,1	2,2	2,1	—	—	—
Diesel oil	2,0	2,1	—	—	19	63	78
Solar oil	2,3	2,2	2,0	2,4	—	—	—
Benzine	—	6,3	9,0	—	—	—	—
Crude petroleum	2,1	2,5	—	—	—	—	—

The molecular thermal diffusivities a (in 10^3 cm^2/sec) for some liquids are as follows:

Ethanol	0.97	Acetone	1.0
Butanol	0.8	Glycerol	0.9
Amyl alcohol	0.7	Kerosene	0.9

All are close to 0.001 cm^2/sec, which we may take as an approximate value for the liquids of main interest. Then $\varepsilon = 1000a_э$; the above results show that $\varepsilon > 1$ for metal vessels, though $\varepsilon \leq 1$ for certain liquids in narrow burners of glass and quartz. In particular, the $a_э$ for glycerol and MS oil are low when narrow quartz tubes are used. These $\varepsilon > 1$ point to convection, for ε increases with the speed of the convection currents.

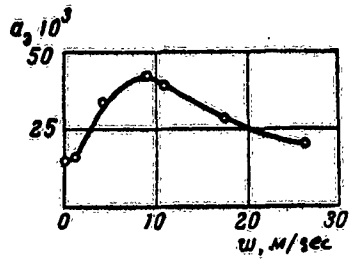

Fig. 53. Relation of $a_э$ to w for tractor kerosene.

Runs 71_{ac} (asbestos tank) and 65, together with Table 2.29, indicate that $a_э$ increases with d_c (wall thickness) and with λd_c; further, runs $61_э$ (with horizontal screen) and 51 (for the same wind speed) indicate that $a_э$ increases very greatly if the flame touches the side of the tank. This is confirmed by run 50 (with external flame); local heating increases $a_э$. Moreover, the increased heating of the wall is responsible for the rapid rise in $a_э$ in the series d = 80, 130, and 260 cm; these large tanks were used in the open, where the wind deflected the flame, whereas those with $d \leq 50$ cm were done in a building. Figure 53 illustrates the effects of w on $a_э$ for tractor kerosene in a metal vessel with d = 150 mm.

These results will be discussed further in relation to convective transfer in general and transfer from wall to liquid in particular; at this point we give results for benzine, crude petroleum, and other liquids that have homothermal layers.

Temperature Distribution in a Liquid Having a Homothermal Layer

1. We have seen above that benzine and other oil products give rise to layers whose temperature is ϑ_s at all points. The

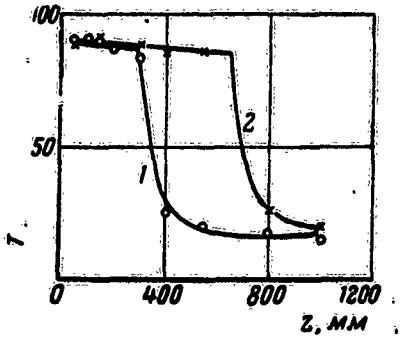

Fig. 54. Temperature distribution in burning benzine (d = 130 cm) after 1) 20 min; 2) 40 min.

depth of this layer increases with time, as Figs. 54 and 55 show (the circles denote the liquid in Fig, 55). The liquid consists effectively of two layers, upper and lower; the top (homothermal) layer has a very low gradient in ϑ, as for a material of very high thermal conductivity. The fall in ϑ in the lower layer is rapid; the distribution is as for an unstirred liquid. The two layers represent two distinct states of the liquid, and the gradual movement of the boundary represents the conversion from one state to the other, as in the freezing of soil. These layers will be termed liquid 1 (top) and liquid 2 (bottom) in what follows.

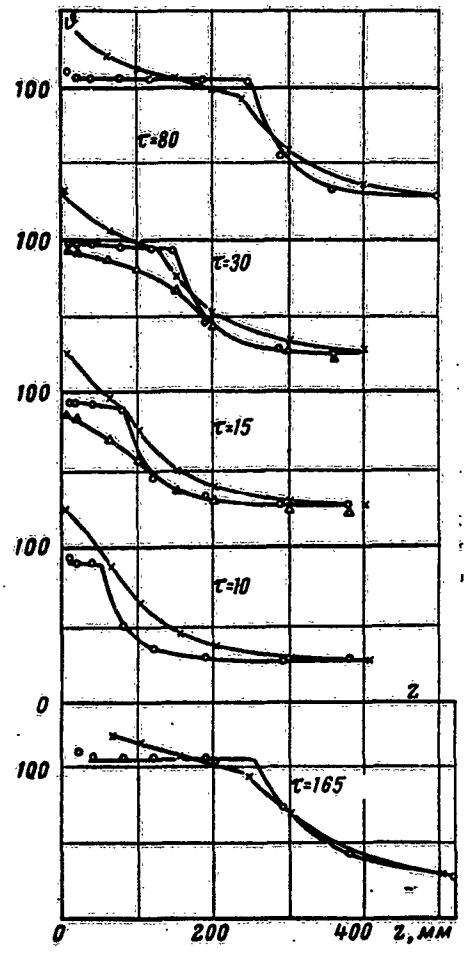

Fig. 55. Temperature distribution in the liquid and at the wall for automobile gasoline at various times: O liquid, x wall. The times τ are in minutes.

Liquids 1 and 2 differ in their a_ϑ; if we assume that the distribution in each is steady, we can readily deduce $\vartheta(z)$, which is sometimes called a distribution of the second kind, to distinguish it from the previous

(first) kind [8]. In fact, the $\vartheta^l(z)$ for liquid 1 is as for a length of wall z_0 (the depth of the layer) having a high conductivity. $\vartheta^l = \vartheta^l_s$ for $z = 0$ and $\vartheta^l = \vartheta^{l'}$ for $z = z_0$, so

$$\vartheta = \vartheta_s - \frac{\vartheta_s - \vartheta'}{z_0} z \quad \text{for} \quad 0 \leqslant z \leqslant z_0. \tag{2.60a}$$

in accordance with the conduction equation subject to the boundary conditions for liquid 1.

For liquid 2

$$a_2 \frac{d^2\vartheta}{dz^2} + u_c \frac{d\vartheta}{dz} = 0,$$

in which u_c is the speed of the interface; $u_c = v + u$, in which u is the rate of increase of z_0. Now $\vartheta^l = \vartheta^l_0$ at $z = \infty$, so

$$\vartheta = \vartheta_0 + (\vartheta'_s - \vartheta_0) \exp\left[-\frac{u_c}{a_2}(z - z_0)\right] \quad \text{for} \quad z_0 \leqslant z \leqslant \infty. \tag{2.60b}$$

The lines in Figs. 54 and 55 have been drawn in accordance with (2.60a) and (2.60b); they fit the experimental results well.

The ϑ for liquid 1 is found as follows. The heat transferred to the interface from the surface is

$$dQ = \lambda_e \frac{\vartheta_s - \vartheta'}{z_0} dt, \tag{2.61}$$

in which λ_e is the equivalent thermal conductivity of liquid 1. The heat received by liquid 2 is found as follows (Fig. 56). The temperature at time t is represented by abce, and at time $t + \Delta t$ by adfe; the heat entering liquid 2 in time Δt is

$$\Delta Q = c\rho \times (\text{area of bcfd}),$$

in which c is specific heat and ρ is density. But this area is simply that of bkmd, which is $(\vartheta^{l'} - \vartheta^l_0)\Delta z_0$, so

$$dQ = c\rho\,(\vartheta' - \vartheta_0)\, dz_0. \tag{2.62}$$

Then (2.61) and 2.62) give us that

$$\frac{dz_0}{dt} = u \frac{\lambda_e}{c\rho} \frac{\vartheta_s - \vartheta'}{z_0} \cdot \frac{1}{\vartheta' - \vartheta_0} = \varepsilon a \frac{\vartheta_s - \vartheta'}{z_0} \cdot \frac{1}{\vartheta_s - \vartheta'}.$$

so

$$\varepsilon = \frac{u}{a}(\vartheta' - \vartheta_0)\frac{z_0}{\vartheta_s - \vartheta'}. \qquad (2.63)$$

This u is simply the rate at which the liquid becomes heated.

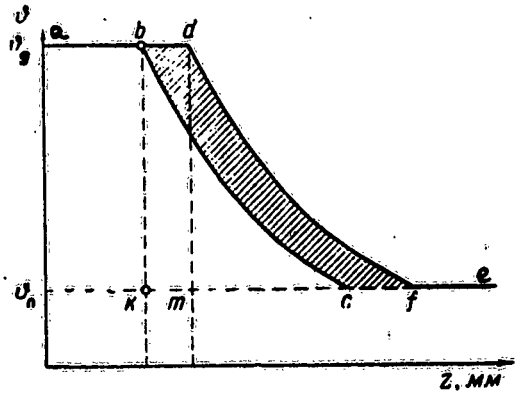

Fig. 56. Calculation of the heat transfer.

Results for automobile gasoline for d = 130 cm and u = 16.7 mm/min [8] give the temperature gradient in the top layer as 0.16 deg/cm, with $\vartheta' - \vartheta_0 = 50°$; then (2.63) gives ε as about 9000 and $a_э$ as 9, so λ_e is 3.6 cal/cm.sec.deg (four times the λ for copper). The ε found for benzine [10] is 10 000 to 11 000.

Now we consider ε for liquid 2; here $u_c/a_э = 0.17$ cm^{-1} and $u_c = 0.035$ cm/sec, so $a_э = 0.200$ cm^2/sec and $\varepsilon = 200$. This result is somewhat of an overestimate; Table 2.37 gives somewhat more precise values for d = 150 mm, h_0 = 10 mm, and $\alpha = 90°$, which show

Table 2.37

№	d_c, мм	w, м/сек	v, мм/мин	$k_ж \cdot 10^3$, $см^{-1}$	$a_э \cdot 10^3$, $см^2$/сек	u_0, мм/мин	z_0', мм	$\mu \cdot 10^3$, $мин^{-1}$	τ, мин	Q, кал
16	1	0	1,4	45	5,1	—	—	—	182	2,1
17	1	1,55	6,0	16	62	4,3	120	36	186	11,6
18	1	0,5	4,6	42	18	0,7	80	8,3	186	7,4
23	1	2,6	6,2	—	—	6,4	102	62	182	13,2
29	10	0	1,4	19	10	1,0	120	8,6	185	2,7
30	10	2,6	4,2	10	73	8,2	280	29	186	11,2
35	6	0	1,5	10	25	1,2	38	31	363	—
36	6	2,6	6,2	21	49	8,5	144	59	361	—
41	3	0	1,6	14	19	—	10	—	240	—
42	3	2,6	5,5	19	48	—	50	—	242	—

that $a_э$ ranges from 0.01 to 0.062 cm^2/sec. An interesting point is that ε shows a regular upward trend with w and with d_c.

These ε show that convection occurs in both layers when the

distribution is of the second kind; it is very strong in the top layer, for λ_e is many thousand times the molecular conductivity and even exceeds the λ for copper. It is much less strong, but still important, in the lower layer.

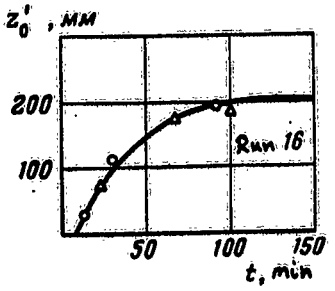

Fig. 57. Relation of z_0 to time.

2. Figure 57 shows that z_0 is at first proportional to t; the rate u_0 is given above, and also in Tables 2.38 to 2.43. This rate is dependent on the liquid and on the conditions; diethyl ether and benzine give the highest u_0. This rate does not persist, especially if the tank is tall, and z_0 tends to a limit z_0 (Fig. 58). The behavior is described well by

$$z_0 = z_0' (1 - e^{-\mu t}); \qquad (2.64)$$

in which μ is a constant and t is reckoned from the onset of formation of the top layer. The lines in Figs. 57 and 58 have been drawn in accordance with (2.64), which shows that this initial rate u_0 is related to z_0' and μ by

$$u_0 = z_0' \mu.$$

Tables 2.37, 2.40, 2.42, and 2.43 give u_0, μ, and z_0' derived from experiments with benzine [12].

It is simple to prove (2.64). The amount of heat received by the lower layer in unit time is proportional to $R^2(dz_0/dt)$, in which R is the radius of the vessel; if the liquid in the top layer moves at a speed v, it removes a quantity of heat $q \propto vR^2$ from the surface each second. The wall loses heat at a rate proportional to Rz_0. Now

$$\frac{dz_0}{dt} = av - \frac{b}{R} z_0,$$

We assume that a, b, and v are constant, and introduce the symbols

$$z_0' = \frac{avR}{b}, \quad \mu = \frac{b}{R},$$

which give us that

$$z_0 - z_0' = Ae^{-\mu t}.$$

Table 2.38

		d, cm				
		130			260	
Automobile benzine	Run	20	21	—	19	34
	u_0, mm/min	17	12	—	16	19
Bay Tugon crude	Run	22	23	24	25	26
	u_0, mm/min	5.4	4.7	4.6	10	10
Mazut 80	Run	13	14	15	10	—
	u_0, mm/min	4.0	1.8	2.7	7.1	—

Table 2.39

	d, cm	u_0, mm/min (limits)	Source
Light crude, dry	70	6—15	[1]
Ditto, moist	70	7—21	»
Heavy crude, dry	70	1—9	»
Ditto, moist	70	5—21	»
Crude, 0.25% water	56	4	[2]
Bibi Eibat crude	80	3,2	[5,7]
Ditto	140	3,7	» »
Karachukhur crude	80	3,1	» »
Ditto	140	3,2	» »
Ditto	260	6,5	» »
Gasoline	80	12	» »
Ditto	80—260	8—17	» »

Table 2.40

Automobile Benzine, d = 300 mm

№	w, m/sec	v, mm/min	$k_{ж} \cdot 10^3$, cm^{-1}	$a_э \cdot 10^3$, cm^2/sec	u_0, mm/min	$z_{от}$, mm	$\mu \cdot 10^3$, min^{-1}	τ_0, min	τ, min	h_0, mm	Q, cal/sec
67	0	2,2	—	—	6	220	28	29	195	75	28
68	4.6	4,0	—	—	11	180	59	9	194	75	50
69	6,6	4,4	—	—	11	174	62	4,5	190	75	53
$70_э$	6,6	4,5	38	19	—	25	—	—	185	75	27
$72_{ас}$	6,6	4,4	—	—	6	440	13	—	300	40	41
$73_{ас}$	0	1,9	—	—	5	520	10	—	300	40	35

Table 2.41

Diethyl Ether

	d, cm						
	30		80	139	264		
Wind speed w, m/sec	2.1	3.8	3.8	3.9	4.5	4.1	1.8
Initial depth of layer, cm	20	20	53	96	58	58	52
Mean v, mm/min	2.1	2.0	2.7	4.7	5.1	6.5	5.8
Mean u, mm/min	12	12	14	18	13	13	13
ϑ_s, °C	36	36	36	36	40	40	40
τ, min	76	122	260	207	121	83	89

Table 2.42

Automobile Benzine, d = 490 mm

№	w, m/sec	v, mm/min	$k_{\text{ж}} \cdot 10^2$, cm^{-1}	$a_s \cdot 10^3$, cm^2/sec	u_0, mm/min	z_0^*, mm	$\mu \cdot 10^3$, min^{-1}	τ_0, min	τ, min	h_0, mm	Q, cal/sec
54	4	3.6	—	—	15	900	17	—	190	60—131	154
56_s	4.3	2.6	—	—	13	500	26	46	240	130	125
58_s	18.6	7.3	—	—	7	210	31	6	240	130	161
59_s	7.0	4.7	45	17	—	—	—	—	210	130	76
60_s	0	3.2	—	—	7	200	31	—	190	130	94

Table 2.43

Automobile Benzine, d = 500 mm

№	Wind	v, mm/min	$k_{\text{ж}} \cdot 10^2$, cm^{-1}	$a_s \cdot 10^3$, cm^2/sec	u_0, mm/min	z_0^*, mm	$\mu \cdot 10^3$, min^{-1}	Q, cal/sec
85	Gusty to strong	4.2	14	50	—	—	—	155
86	Strong	—	—	—	12	350	50	55
87	Moderate	4.0	25	27	—	—	—	133

Note. The cooler contained no liquid in run 85; the benzine was thickened; the cooler was removed in run 86 (also with thickened benzine). The cooler carried running water in run 87, and the benzine was not thickened.

Formula (2.64) is reached if we calculate the time from the onset of formation of the layer and determine A.

The above results, together with Fig. 59, enable us to evaluate the effects of the various factors on u_0, μ, and z_0'; we see that u_0 increases with w, which points to the wind as a major factor in producing the homothermal layer. Results for benzine in iron tanks (Table 2.44) confirm this; here mode 1 indicates experiments to which (2.55) applies, mode 2 indicates a distribution of the second kind, and z_0 relates to the end of the experiment.

The top layer is always present, but z_0 is very small in small tanks for w = 0 (it then appears very quickly); z_0 is also

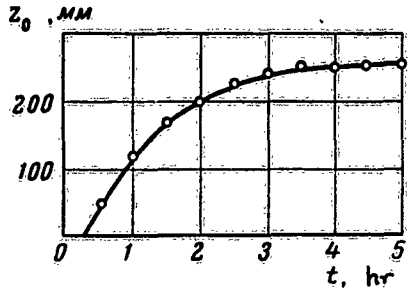

Fig. 58. Curve of $z_0(t)$ for crude petroleum

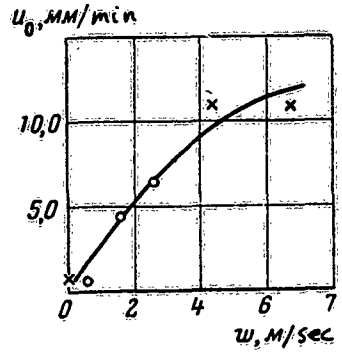

Fig. 59. Curve for $u_0(w)$.

small for large d if w = 0. A finite w always increases z_0, especially for d ≥ 176 mm, and increases u_0 as well in the latter case. For example, T-1 kerosene in a 176 mm tank had a large z_0 in the presence of a wind, but u_0 was only 2-3 mm/min.

The tests with the horizontal screens also demonstrate that the wind accentuates the top layer; for example, runs 54 and 56 show that the screen reduces z_0, the z_0' for these two runs being respectively 900 and 500 mm. Again, z_0 in run 69 was large, whereas in run 70 (same w, but with the screen) it was very small.

There is also some evidence that z_0' increases with d, but this aspect has not yet been examined in detail.

Runs 72_{ac} and 78_{ac} (for the asbestos-cement tank) show that the homothermal layer occurs even in a tank of low conductivity. Here z_0' is much greater than for the metallic tanks, although u_0 is somewhat lower.

The effects of a thickening agent (1.3% of aluminium naphthenate) were examined in run 86 (with benzine); v was not affected appreciably. Table 2.35 shows that a homothermal layer was still formed, except when a cooling jacket (free from liquid) was fitted; the jacket screened the wall from the flame.

3. Cooling the wall affected the temperature distribution very much; in run 87 (Table 2.35) the cooling jacket was supplied with running water, and here no appreciable homothermal layer appeared even in 2 hr. This result has been confirmed by others [10] for benzine in tanks of diameters 80, 139, and 264 cm. In one series the tank was cooled by water trickling from holes in a

Table 2.44

d, mm	Wind	Mode	$k \cdot 10^2$	v, mm/min	u_0, mm/min	$a_0 \cdot 10^4$, cm²/sec	ϑ_0, °C	τ, min	z_0, mm	No. of runs
12	No . .	1	66	4,8	—	12	89	93	9	2
20	» . . .	1	73	2,9	—	6,6	92	80	8	3
37	» . . .	1	50	2,0	—	7,0	101	110—210	3—7	6
37	Yes . .	1	67	3,9	—	9,7	92	160	9—16	6
176	No . .	1	38	2,9	—	11	109	120	—	2
176	Yes . .	2	49	4,0	4,8	30	85	37—56	200	3
176	» . . .	2	—	5,9	9,6	—	87	120	330	2
300	No . .	1—2	50	—	1,9	19	100	99	60	1
300	Yes . .	2	54	3,6	7,4	35	88	72—120	290	2

tube running around the top outer edge; no cooling was used in other runs. The temperature distribution in the first case was as for diesel oil and kerosene; ε varied from 6 to 12, and the temperature fell rapidly away from the free surface. In the second case there was a homothermal layer; ε was 11 000. A series was run [10] in which the cooling was not used at first; the development of the homothermal layer was recorded. After 29 min, when z_0 was 12 cm, the cooling was turned on; z_0 then gradually decreased and after 90 min was only 1.5 cm.

Petrov and Gerasimov [22] have also examined the effects of water cooling on benzine in two identical tanks 130 cm in diameter. The levels were kept constant during the runs; one tank was cooled by water flowing from a cooling pipe fitted to the outer top edge. The two tanks were used simultaneously in order to eliminate effects from the wind, air temperature, and so on. The flow of water V' was varied; so was h, the distance from the edge to the surface (Table 2.45). Figure 60 shows the mean rate of

heating $\bar{u}$ as a function of V' for h = 700 mm; there is an initial rise, followed by a rapid fall for V' near 1.2 l/sec per m. No homothermal layer was formed for V' > 1.2. The effects for h = 70 mm were very different; no layer arose even when V' was small, and u for the uncooled tank was 13 mm/min (as against 4 mm/min for h = 700 mm).

These results show that the cooling produces results dependent upon the conditions; it may accelerate or retard the heat-

Table 2.45

h, mm	Wall cooled				Uncooled		
	v^1, l/sec	z_0, mm	τ_1, min	$\bar{u}_1$, mm/min	z_0, mm	τ_2, min	$\bar{u}_2$, mm/min
700	1.0	400	37	11	400	80	5
700	1.2	0	74	0	100	57	2
700	1.2	0	159	0	300	107	3
700	0.6	300	30	10	300	54	6
700	0.3	400	38	10	400	63	6
700	1.2	300	53	6	300	80	4
70	0.9	0	38	0	400	30	13
70	0.25	0	41	0	400	28	14
70	0.1	0	41	0	400	32	12

ing. In the first case (h large, V' < 1.2), the water becomes heated before it reaches the level of the surface and so heats the liquid instead of cooling it; the flow is adequate to cool

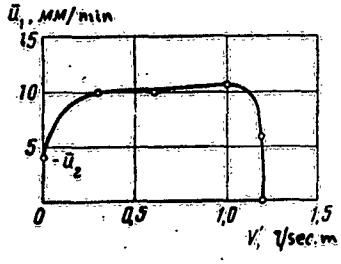

Fig. 60. Relation of $\bar{u}$ to water flow rate for benzine.

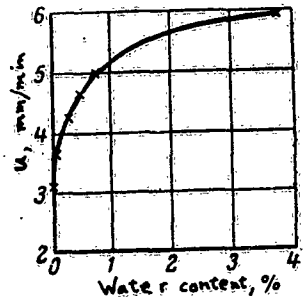

Fig. 61. Relation of u to water content for crude oil.

the benzine only for V' > 1.2. In the second case, the water flows only over the part of the tank containing the benzine.

It has several times been observed that the water content of an oil product is important [5,7,9]; fairly full results are a-

vailable for emulsion petroleum [9]. Here u is found to increase with the water content (Fig. 61), although ν_s^{ℓ} falls at the same time. The temperature distribution is dependent on the water content in some cases; Pavlov and Khovanova have shown that (2.55), with k large, applies to 'dry' machine oil, whereas 'moist' machine oil gives rise to a temperature distribution much as for benzine [5]. Further, they have shown that a distribution of the first kind applies to mazut containing not more than 0.1% of water, and one of the second kind if the content exceeds 0.5% [7].

4. Figure 55 shows the temperature distribution in benzine (open circles), at the lee wall (crosses), and at the windward wall (triangles). Here there is a substantial $\Delta\vartheta$ as between wall and axis; at first, the temperature on the lee side is eve-

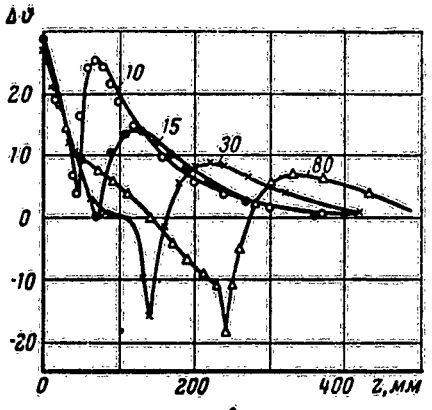

Fig. 62. $\Delta z^{\ell}(z)$ for benzine for various times (run 30).

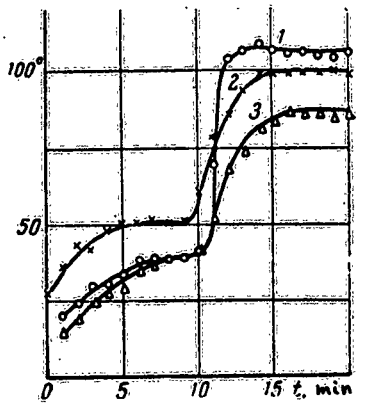

Fig. 63. Temperature vs. time for points in the same plane in benzine: 1) in liquid; 2) lee wall; 3) windward wall.

rywhere above that in the benzine, but later is is so only within and slightly below the homothermal layer. The Δz^{ℓ} below the layer decreases as time passes, eventually becoming zero.

Figure 62 shows $\Delta z^{\ell}(z)$ for 10, 15, 30, and 80 min; the lowest point on each curve corresponds to the bottom of the homothermal layer. Figure 63 shows the temperatures at the two sides for points in the same plane; this indicates that the second rapid rise in temperature is associated with the onset of a rapid rise in the wall temperature.

Heat Exchange Between Wall and Burning Liquid

1. We have seen above that the wall is not at the temperature of the liquid; a liquid that varies in temperature or concentration from point to point can be in mechanical equilibrium only if certain conditions are complied with. Any deviation

from those conditions results in convection, which tends to eliminate the differences. It is not usual for a burning liquid to comply with these conditions, so convection is present. Temperature differences are the main cause of convection, so we need to examine convective heat transfer.

Fairly detailed studies have been made on transfer of heat from a wall to liquid, but these mostly relate to pure substances, whereas oil products are usually complex mixtures, which may contain much suspended water. Blinov et al [13] have examined liquids of this type; their results are given below.

2. The transfer from a wall to a liquid free to move can be described by a general curve for all liquids and for bodies of various shapes [17,18]. Here the principal criterion is

Table 2.46

Liquid	ρ, g/cm³	ν, cm	ϑ	ϑ_0	θ_0	Distilled up to			
			°C			100°	140°	195°	200°
1. Ethanol	0,79	1,0	80	19	—				
2. Benzene	0,87	0,6	80	18	—				
3. 1 + 2	0,82	0,8	69	20	—				
4. Toluene	0,87	0,6	109	20	—				
5. 2 + 4	0,87	0,6	90	18	—				
6. Gasoline	0,74	0,8	—	20	78	32	89	97	—
7. Diesel oil	0,85	4,8	—	20	—	—	—	—	—
8. Mixture of 6 + 7	0,80	1,0	—	20	88	5	34	48	—
9. Tractor ker.	0,83	2,0	—	20	138	—	—	—	20
10. Paraffin oil	0,87	51	—	20	—	—	—	—	—
11. Crude	0,88	23	—	20	80	3	10	24	—

GrPr = Ra, which we have considered above. The shape of the body is of secondary importance, so tanks or other bodies of convenient shape can be used in the experiments.

Spirals were used in transfer measurements with binary mixtures and with oil products; the spiral was the filament from a lamp (40 w), which was placed in a vertical glass cylinder containing the liquid. This spiral was 0.64 mm in diameter and 24 mm long; it was placed horizontally. The resistance was measured as a function of temperature in calibration experiments, and so the resistance (ratio of voltage to current) under the working conditions gave the temperature. The current and voltage were allowed 4-5 min to settle down after any alteration; readings were taken every minute near the boiling point.

The first measurements were made on individual liquids

(benzene, toluene, ethanol, and mixtures of these; the ethanol-benzene mixture was 65:35 (by volume), and the benzene-toluene one was 50:50. The latter mixture is close to ideal, whereas the other is not. The same applies to the ethanol-toluene mixture.

The main measurements were made with automobile benzine, diesel oil, a mixture containing equal volumes of these, paraffin oil (dry and wet) tractor kerosene, crude petroleum (not specially moistened; also containing 3.6 and 12% water). The water was mixed with the oils by means of a very small centrifugal sprayer coupled to the water line and immersed in the oil. The mixture was used after it had been allowed to stand for some time (when the large droplets had settled out). The water content was determined by analysis.

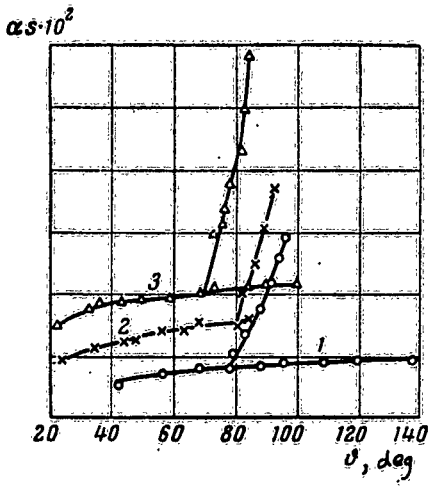

Fig. 64. Curves for $\alpha s = f(\vartheta^l)$ for 1) benzene; 2) ethanol; 3) benzene + ethanol.

Table 2.46 gives the parameters of these liquids in cgs units (ρ, density; ν, kinematic viscosity; ϑ_s^l, boiling point; ϑ_0^l, initial temperature; ϑ_0, initial distillation temperature) and also the proportion (%) distilling up to certain specified temperatures.

3. Figure 64 shows some of the results. Here ϑ^l is the temperature of the spiral, α is the heat-transfer factor, and s is the surface area of the spiral (only one was used); αs is in w/deg. The values are the means of several readings. The temperature of the liquid varied from 18 to 20°.

The $\alpha(\vartheta^l)$ curves for pure liquids, binary mixtures, and oil products (dry or moist) are all of the same general form; the points lie on two curves. One (curve A) rises slowly over a large range; the other (curve B) rises steeply, but sometimes has a less steep part later. The B curves cover only a small range in ϑ^l, in which α becomes much larger. The two curves result from two different transfer mechanisms [17,18]; curve A corresponds to free convection, while curve B corresponds to nuclear boiling. We consider convective transfer first.

4. Free convection is governed by

$$Ra = GrPr = \frac{\rho^2 c\beta g l^3 \Delta\vartheta}{\eta\lambda} = bl^3\Delta\vartheta,$$

in which ρ is density, c is thermal capacity, β is expansion coefficient, η is viscosity, and λ is thermal conductivity; l is the governing dimension (here the diameter of the spiral), g is the acceleration due to gravity, $\Delta\vartheta$ is the temperature difference, and b is the convection modulus:

$$b = \frac{\rho^2 c\beta g}{\eta\lambda}.$$

Nusselt's number ($Nu = \alpha l/\lambda$) is related to Ra [17] by

$$Nu = C\,Ra^n, \qquad (2.65)$$

in which C and n are functions of Ra, though they can be taken as constants (1.18 and 1/8 respectively) for Ra between 0.001 and 500, and also for Ra between 500 and 2×10^7 (then 0.54 and 1/4). Other C and n can be used to give a better fit in (2.65) if the range in Ra is smaller.

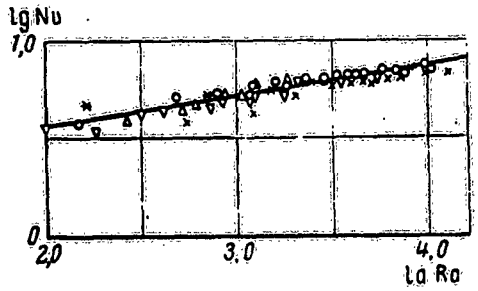

Fig. 65. Relation of Nu to Ra for toluene, benzene, ethanol, automobile benzine, tractor kerosene, and diesel oil.

Figure 65 shows results [13] for various liquids, which indicate that oil products obey (2.65) satisfactorily. The line drawn on the figure fits

$$Nu = 1{,}23\,\beta\,Ra^{0{,}16}, \qquad (2.66)$$

in which $\beta = 1.4$ if the surface area is calculated from

$$s = 2\pi r l',$$

in which r is radius and l' is length.

The range of Ra here is 10^2 to 10^4, so some of the results fall in the region in which n = 1/8 and in some in that in which n = 1/4. The Nu given by (2.66) for $Ra = 10^4$ and by $Nu = 0.54Ra'$ are in the ratio β, because the true surface area s' is greater than $2\pi r l'$. A spiral having turns in close contact gives $s'/s = 1.57$, which is close to β (1.4); the active area s_a is somewhat less than s', so we may take β as s_a/s. If we replace s by s_a,

we have

$$Nu = 1{,}2\,Ra^{0.16} \qquad (2.67)$$

The above results [17] agree well with other published values, so oil products obey the laws for pure substances. Formula (2.65) is applicable to mixtures not represented in Fig. 65, as the following shows. The two quantities appearing in Ra that are the most affected by ϑ^{ℓ} are $\Delta\vartheta^{\ell}$ and η; the relation of α to $\Delta\vartheta^{\ell}$ for any given liquid may be put as

$$\alpha = K(\Delta\vartheta^{\ell}/\eta)^{n} \qquad (2.68)$$

in which K is dependent on the liquid and on the dimensions of the heated surface, while n is as in (2.65).

Line A in Fig. 64 has been drawn in accordance with (2.68), which fits the results well in every case, so we may conclude that mixtures not represented in this way will obey the same laws as the others.

5. The B curves give α that vary with ϑ^{ℓ} (or, strictly, with $\Delta\vartheta^{\ell}$) as in

$$\alpha = \zeta(\Delta\vartheta)^{m}. \qquad (2.69)$$

The following values, although not very precise, do show that α increases very rapidly with $\Delta\vartheta^{\ell}$ once boiling sets in, especially for benzine:

Liquid	m
Automobile benzine	4.0
Benzine + diesel oil	4.0
Tractor kerosene	2.5
Moist paraffin oil	3.0
Crude petroleum	3.5

These m are much larger than the powers in Kutateladze's [23] proposed formula.

6. The intersection of the A and B curves defines ϑ^{ℓ}_{k}, the temperature of onset of boiling; boiling proper usually starts somewhat above ϑ^{ℓ}_{k}, because there is often a degree of superheating (sometimes considerable). This ϑ^{ℓ}_{k} is of great interest; Table 2.47 [13] gives values, as well as the boiling point ϑ^{ℓ}_{ku} and the temperature of the start of distillation θ for the oil products. These ϑ^{ℓ}_{k} agree with previously published values for pure compounds and binary mixtures, apart from toluene, whose ϑ_{k} is several degrees above the published values. The discrepancy is caused by impurities. The benzene-toluene mixture is of the nearly perfect type, while that with ethanol is of imperfect type. Both types behave as do pure substances. The

agreement between ϑ_k^l and ϑ_{ku}^l for the pure substances and binary mixtures confirms that ϑ_k^l is the temperature of onset of boiling.

Table 2.47 shows that $\vartheta_k^l = \theta$ for kerosene but $\vartheta_k^l > \theta$ for benzine and crude oil (especially the latter). The reason is that the crude oil contains only a very small proportion of the light fractions; only 3% distils over up to 100°, and only 10% up to 140°. The precise value of $\vartheta_k^l - \theta$ is dependent on the composition of the oil product.

Table 2.47

Liquid	ϑ_k	ϑ_{ku}	θ
	°C		
1. Ethanol	80	80	—
2. Benzene	79	80	—
3. 1 + 2	69	69	—
4. Toluene	103	111	—
5. 2 + 4	87	90	—
6. Gasoline	89	—	78
7. Diesel oil	176	—	—
8. 6 + 7	120	—	—
9. Tractor kerosene	137	—	137
10. Paraffin oil	260	—	—
11. Ditto, moist	100	—	—
12. Crude	160	—	78
13. Crude, 3.6% water	100	—	—
14. Crude, 12% water	100	—	—

The ϑ_k^l for the mixture of diesel oil with benzine is 120°, which lies between the ϑ_k^l for the components. This is to be expected, for the two mix in all proportions; the solutions are not ones giving a maximum or minimum on the vapor-pressure curve. The theory of solutions shows [24] that the boiling points of such mixtures lie between those of the components.

The moist paraffin oil has $\vartheta_k^l = 100°$, whereas the dry oil has a ϑ_k^l of over 250°. This is to be expected, for the water behaves as an insoluble liquid in relation to the oil; a mixture of this kind has

$$p = p_1 + p_2, \tag{2.70}$$

in which p is the total vapor pressure, while p_1 and p_2 are the saturation vapor pressures of the two components. Formula (2.70) implies that the boiling point of such a mixture should lie below that of the more volatile component. Now p_1 (water)

is much larger than p_2 (oil), so $p \approx p_1$, and the boiling point is very close to that of water, as is found. The same explanation is applicable to the crude oil containing 3.6 and 12% water; t_k is 100°, whereas t_k for the dry crude is 160°.

Conclusions

1. The wall temperature in a tank differs from the temperature of the liquid; the difference increases with the air flow rate; the same applies to narrow burners, although here Δt^ℓ is only 1-2° (Table 2.48). This difference gives rise to convection currents, whose vigor is indicated by Ra; the currents

Table 2.48

Ethanol [6]

	Aluminium, $d = 40$ mm					Glass, $d = 36$ mm			
z, mm	10	40	80	150	240	2	9	17	28
ϑ (center), °C	52	45	38	30	22	64	28	16	14
ϑ (wall), °C	53	46	39	31	23	66	31	18	15

arise when Ra exceeds a limit Ra_1, which is 1000 for vertical layers of liquid and 1600 for parallel plates, but much smaller for unbounded liquids. We may assume that convection currents are bound to be present if Ra > 1600, although Ra is also dependent on b, the convection modulus, which is dependent on the nature of the liquid. Some values are as follows:

Liquid	°C	b, 1/cm³·°C
Ethanol	27	126 000
"	50	142 000
Acetone	27	360 000
Automobile benzine	20	150 000
Tractor kerosene	20	60 000
Diesel oil	20	30 000
Glycerol	27	440

In general, b is small if η is large; it increases rapidly as the temperature rises. Convection in diesel oil sets in if $l^3 \Delta t^\ell > 0.05$, and in ethanol and automobile benzine if $l^3 \Delta t^\ell > 0.012$ cgs units.

A liquid in a narrow burner may be considered as a liquid layer; here $l = r$. A liquid in a tank is effectively unbounded horizontally, especially if d is large. The critical Ra is exceeded for diesel oil in a burner 8 mm in diameter if $\Delta t^\ell > 0.8°$, and for kerosene, benzine, and alcohol for even smaller Δt^ℓ.

Now Ra increases rapidly with d, so we may assume that convection is always present if $d > 8$ mm; on the other hand, convection does not occur even in ethanol if $d < 5$ mm, so here only conduction occurs. But v decreases as d increases, which means that heat received from the wall plays a significant part; this source becomes negligible under normal conditions if $d > 80$ mm.

2. The a_3 (equivalent thermal diffusivities) for liquids in metal tanks are much smaller than those for glass burners. The following are some a_3: copper, 900; aluminium, 500; iron, 150; glass, 1.7; quartz, 3.3. That for copper is some 500 times that for glass; the metal burners heat up in a manner distinct from that for glass and quartz. The depth of the layer heated by convection is much greater for a metal burner, which is one reason for the great difference in the a_3 of the liquids.

3. The l in the Rayleigh criterion equals the height of the part of the wall that is hotter than the liquid (for tanks); here $Ra \gg Ra_1$, and convection currents are present.

The maximum difference Δt^{ℓ}_{max} between lee wall and liquid increases with w, the wind speed; Ra increases with Δt^{ℓ}_{max}, so convection becomes more vigorous, and a_3 increases with w. However, the wall loses more heat, and the extent of the contact between wall and flame decreases, so ther is also a tendency for a_3 to decrease as w increases. Factors that tend to increase Δt^{ℓ} accentuate convection and increase a_3, as the results from run 50 show; the wall became heated. This explains why artificial cooling (with screens) reduces a_3, and why a_3 increases with wall thickness.

4. The flow near the wall is laminar for $Ra > Ra_1$, but it becomes turbulent if $Ra > Ra_2$ [17,19], the latter limit being higher; natural convection about a plane becomes turbulent if $Ra > 2 \times 10^9$ [19]. In general, Ra_2 is less than 10^9.

The Ra for some of the above tests are as follows. For run 12 (tractor kerosene), $l = 20$ cm and $\Delta t^{\ell} = 15°$; Ra is 7×10^9, which exceeds Ra_2, so the convection is turbulent. In fact, ϵ is about 11. In one of the runs for diesel oil in the 1300 mm tank, w was 0.4 m/sec; Δt^{ℓ} was 20° for a length of 25 cm above the liquid on the lee side, and here Ra was 9×10^9 ($> Ra_2$); ϵ was about 60. Tractor oil in a 150 mm tank, with no wind, gave $\Delta t^{\ell}_{max} = 8°$; the wall was hotter than the liquid for a length of 5 cm. Here Ra was several orders of magnitude lower; convection was vigorous but not turbulent, and ϵ was about 4.

These examples show that vigorous convection occurs at the wall of a tank containing a burning liquid; this may be turbulent under suitable conditions. Here a_3 is always greater than the molecular thermal diffusivity. Calculations show that ϵ

never exceeds 100, even when the convection at the wall is very vigorous.

Causes of the Homothermal Layer

Some oil products, and diethyl ether, give rise to such layers, which may be of considerable depth; kerosene, diesel oil, and solar oil do not give these layers. We have seen above that a_3 for the homothermal layer in benzine is higher than the thermal diffusivity of copper and also much higher than the a_3 for benzine itself when this layer is absent. This layer is vigorously mixed by convection, which also causes a rapid transfer of heat to the lower boundary of the layer.

Many different explanations have been proposed for the convection in this layer. It has been supposed that the upper part becomes depleted of light fractions, increases in density, and so sinks; Hall, who demonstrated the existence of this layer, first put forward this hypothesis [1]. However, measurements and calculations show that the density at the actual temperature is less than that of the cold initial material, so any such effect must be of minor importance. On the other hand, one might suppose that fresh material at the lower boundary is heated and rises; but then this new material rapidly becomes mixed with the already heated layer, so any density difference cannot persist. Again, differential boiling of fresh material cannot be invoked, for diethyl ether (a pure substance, which cannot give differential distillation) gives such a layer [11].

It has also been supposed that the temperature difference $\Delta\vartheta$ between wall and liquid is on of the main causes of the circulation in the layer [8]; all oil products give rise to substantial $\Delta\vartheta$, and Ra exceeds Ra_1 (and sometimes Ra_2 also), so convection (perhaps turbulent) is present. This motion occurs in kerosene, which does not give a homothermal layer, so $\Delta\vartheta$ alone cannot be the main cause of the layer.

Another suggestion is that distillation occurs at the bottom of the layer [2] or within the body of it [1]; the vapor bubbles rise and so stir the layer. However, nuclei are needed to cause normal boiling; vapor is seldom formed within the body of a liquid, and the process is explosive when it does occur.

The experiments with benzine (Fig. 55) serve to solve the problem; here the circles give ϑ for the liquid, and the crosses ϑ for the lee wall. Clearly, the latter ϑ is above 100° over m much of the region covered by the homothermal layer and is 80-90° at the lower edge of that layer. Benzine starts to boil at 89°, and direct observation shows that a considerable ridge (indicating a vigorous rising current) occurs at the lee wall. Now the wall always provides an adequate supply of nuclei, so normal

boiling can occur there. In fact, the benzine is boiling in this region, and the rising bubbles of vapor cause the vigorous stirring.

The homothermal layer arises with liquids of low boiling point (ϑ_k^l is about 90° for benzine and 35° for ether); mazut and machine oil also give such layers, although their ϑ_k^l are high, but only when they contain water. The dry materials give temperature curves that fit (2.55); ϑ_k^l falls to about 100° when water is present, so the liquids become effectively ones of low ϑ_k^l.

Crude petroleum gives a different type of distribution; it usually contains water, which is largely responsible for the homothermal layer. It is stated [7] that dry curde gives no such layer, the distribution being such as to fit (2.55). Kerosene, diesel oil, and so on are products that do not contain water and that have fairly high ϑ_k^l (137 and 176° for kerosene and diesel oil).

These results show that appreciable homothermal layers occur only for liquids whose ϑ_k^l are less than a limit θ_k not far from 100°; no such layer is formed under normal conditions if $\vartheta_k^l > \theta_k$, although one may form under special conditions.

The origin and growth of the layer in benzine are as follows. Figure 55 shows that $\Delta\vartheta$ is everywhere positive when the benzine has been burning for a few minutes, but then the wall temperature at the lower boundary of the homothermal layer becomes the same as that of the liquid at that point; subsequently, it falls below it. The liquid begins to boil when the wall has become hot enough; the rising bubbles stir the liquid, and the motion gives rise to the homothermal layer. At the same time, this layer is depleted of its light fractions. The heated layer of liquid facilitates the heating of the wall near the lower boundary of the layer; the curve for ϑ at the wall shows a kink, and boiling starts at the bottom level, which intensifies the circulation and introduces fresh liquid. The process of boiling gradually extends down the wall, and so on. In fact, the heated layer facilitates the heating of the wall, and the resulting boiling tends to increase z_0. The explanation for liquids other than benzine is, of course, much the same. The process can occur only in a liquid of low ϑ_k^l; the relation of z_0 to t fits (2.64), as experiment shows.

Conditions that favor boiling at the wall also favor the production of the layer; this explains run 87 (in which the tank was cooled by flowing water), when there was no homothermal layer, and also other experiments [10,22] in which the walls were washed by water.

Now the effects of the screen and the wind become explicable. The wind deflects the flame onto the wall, which becomes hot and

so causes more vigorous boiling; the layer arises more rapidly and is deeper. The horizontal screen prevents the flame from touching the wall, so the layer appears only slowly.

It may be that a very large tank containing only a very low level of liquid would not give rise to this layer, for the ratio of circumference to area would be very small.

The layer appears in benzine even in tanks made of poor conductors; the reason here is simply that the heat received by the inside wall from the liquid is not readily lost to the surroundings, so it migrates down the wall and causes the layer to develop fairly rapidly.

The best method of suppressing or minimizing this layer is to cool the tank with water, which prevents the liquid from boiling, but the process is effective only if performed properly. Petrov and Gerasimov's experiments show that incorrect treatment can actually accelerate the growth of the layer. Proper treatment can be highly effective for benzine, ether, crude petroleum, and so on.

References

1. Hall. Boiling-over of Crude Petroleum Burning in Tanks. Mech. Eng., 47, No. 7, 1925.
2. Burgoyne and Katan. The Burning of Petroleum Products in Open Tanks. J. Inst. Petroleum, 33, No. 279, 1947.
3. G. N. Khudyakov. Vygoranie zhidkosti so svobodnoi poverkhnosti (Burning of a Liquid from a Free Surface). Izv. Akad. Nauk SSSR, OTN, No. 2, 1955.
4. Idem. O temperaturnom pole zhidkosti, goryashchei so svobodnoi poverkhnosti, i o fakele nad nei (The Temperature Distribution in a Liquid Burning from a Free Surface, and the Flame Above). Ibid., No. 7, 1951.
5. P. P. Pavlov and A. M. Khovanova. O teploperedache v nefteproduktakh pri gorenii ikh so svobodnoi poverkhnosti (Temperature Distribution in an Oil Product Burning from a Free Surface). Inform. sbornik TSNIIPO (Bulletin of the Central Research Institute for Fire-Fighting), Moscow, publ. MKKh, 1954.
6. V. I. Blinov. O yavlenii vybrosa goryuchei zhidkosti pri gorenii (Boiling-over of a Burning Liquid). Izv. Akad. Nauk SSSR, OTN, No. 2, 1955.
7. P. P. Pavlov and A. M. Khovanova. O gorenii neftei i nefteproduktakh so svobodnoi poverkhnosti (Burning of Petroleum and Petroleum Products from a Free Surface). Baku, 1955.
8. V. I. Blinov, G. N. Khudyakov, and I. I. Petrov. O raspredelenii temperatury v nefteproduktakh, sgorayushchikh v rezervuarakh (Temperature Distribution in an Oil Product

Burning in a Tank). Inform. sbornik TSNIIPO (Bulletin of the Central Research Institute for Fire-Fighting), Baku, 1957.

9. P. P. Pavlov and A. M. Khovanova. O faktorakh, vliyesyushchikh na voznikovenie konvektsii v nefti i nefteproduktakh pri ikh gorenii v rezervuarakh (Factors Affecting Convection in Oil Products Burning in Tanks). Ibid., Baku, 1957.
10. P. P. Pavlov and A. M. Khovanova. Gorenie sinteticheskogo dietilovogo efira so svobodnoi poverkhnosti v rezervuarakh (Burning of Synthetic Diethyl Ether from a Free Surface in a Tank). Ibid., Baku, 1957.
11. V. I. Blinov and G. N. Khudyakov. K voprosu o raspredelenii temperatury v nefteproduktakh, sgorayushchikh v tsilindricheskikh rezervuarakh (Temperature Distribution in an Oil Product Burning in a Cylindrical Tank). Inform. pismo Energ. In-ta Akad. Nauk SSSR (Newsletter of the Power Institute, Academy of Sciences), No. 7, 1958.
12. V. I. Blinov, G. N. Khudyakov, and L. A. Volodina. O obmene teplom mezhdu stenkoi rezervuara i nefteproduktom (Transfer of Heat Between the Wall of a Tank and an Oil Product), Ibid., No. 9, 1958.
13. S. S. Kutateladze. Osnovy teorii teploobmena (Principles of Heat-Exchange Theory). Moscow-Leningrad, publ. Mashgiz, 1957.
14. V. I. Blinov. Issledovanie goreniya binarnykh smesei zhidkostei (A Study of the Burning of Binary Liquid Mixtures). Otchet LIAP (Report of Leningrad Institute of Aviation Instrumentation), 1949.
15. V. I. Blinov, G. N. Khudyakov, and I. I. Petrov. O mekhanizme tusheniya goreniya nefteproduktov v rezervuarakh putem peremeshwaniya ikh vozdukhom (Mechanism of the Extinction of an Oil Product Burning in a Tank by Means of Stirring with Air). Inform. sbornik TSNIIPO (Bulletin of the Central Research Institute for Fire-Fighting), 1958.
16. M. A. Mikheev. Osnovy teploperedachi (Principles of Heat Transfer), Moscow-Leningrad, publ. Gosenergoizdat, 1947.
17. S. S. Kutateladze. Teploperedacha pri kondensatsii i kipenii (Heat Transfer in Condensation and Boiling), Moscow-Leningrad, publ. Mashgiz, 1952.
18. R. L. Bosworth, Heat Transfer Processes. Moscow, publ. Gostekhizdat, 1957.
19. Tablitey fizicheskikh konstant, pod redaktsiei akademika A. F. Ioffe (Tables of Physical Constants, edited by A. F. Ioffe).
20. V. I. Blinov, G. N. Khudyakov, and I. I. Petrov. Izuchenie goreniya nefteproktov v rezervuarakh (A Study of the Burning of Oil Products in Tanks). Inform. sbornik TSNIIPO

(Bulletin of the Central Research Institute for Fire-Fighting), 1955.
21. I. I. Petrov and V. A. Gerasimov. Tushenie pozharov nefteproduktov v rezervuarakh vaspylennoi vodoi (Extinction of Fires of Oil Products in Tanks with Water Sprays). Inform. sbornik TSNIIPO (Bulletin of the Central Research Institute for Fire-Fighting), Baku, 1957.
22. L. D. Landau and E. M. Lifshits. Mekhanika sploshnykh sred (Mechanics of Continuous Media), Moscow, publ. Gostekhizdat, 1954.
23. V. I. Blinov. O nekotorykh voprosakh, otnosyashchikhsya k goreniyu i tusheniyu plamen nefteproduktov. Novye sposoby i sredstva tusheniya plamen nefteproduktov (Some Aspects of the Burning and Extinction of Oil Products. New Methods and Agents for Extinguishing Oil Products), publ. Gostoptekhizdat, 1960.

Boiling-Over of a Burning Liquid

1. Crude petroleum and certain oil products sometimes boil over when they burn in tanks; this makes the fire much more difficult to contain, and the burning liquid presents a serious hazard. Large volumes of burning material may be thrown high in the air; for example, in tests with crude petroleum in a 260 cm tank, depths of up to 4 m of oil have been thrown 12 m into the air, the spilled oil then covering an area of 1000 m^2 [3]. These boil-overs often cause great damage and loss of life; a fire at Baku in the early years of this century ignited a workers' settlement, with many deaths [12].

Much attention has been given to the effect, the first experiments being Hall's of 1925 [1], which numbered over 100. He found that a homothermal layer is produced in crude petroleum and that boil-overs occurred only when there was water under the oil. His conclusion was that the boil-over occurs when the high-temperature front reaches the surface of the water; the water must be removed in order to suppress the effect. Some of his conclusions were incorrect, though; for example, he believed that homothermal layers occur only in crude petroleum, not in products.

Hall's discovery of this layer gave rise to numerous studies on its rate of development; some of the results were published by the American Oil Institute [2]. Burgoyne and Katan [2] made a detailed study of heat transfer in burning oil products in 1947;

this showed that homothermal layers can occur in certain oil products. In the USSR, Pavlov and Khovanova have made measurements on outdoor equipment, while Khudyakov [4] and Blinov [5] have made laboratory studies. These last gave the best indication of the cause; they are dealt with below.

2. The laboratory studies were made on an apparatus resembling that used for measuring burning rates. A glass or quartz burner contained a liquid at a fixed level; in one series the liquid filled the entire burner, in a second there was mercury under the liquid, and in a third water. The depth of the layer of combustible liquid was measured with a cathetometer.

Liquids of low boiling point (acetone, benzene, ethanol) and

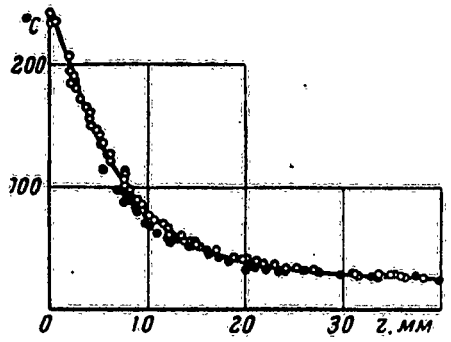

Fig. 66. Temperatures in solar oil for a glass burner 21 mm in diameter.

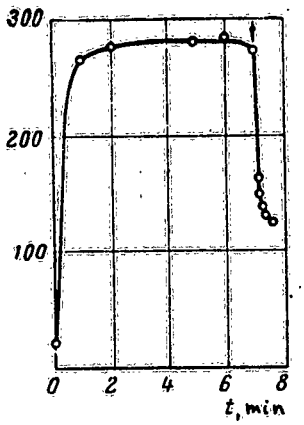

Fig. 67. Surface temperature of transformer oil floating on water containing floating particles.

of high boiling point (transformer oil) were used in the first series; in no case was the liquid ejected. The same applies to the second series, but the liquids (kerosene, solar oil, transformer oil) were ejected in the third series. This occurred when the residual layer was shallow; usually there were several cycles of boiling, in which part of the combustible liquid was ejected. A noise of explosive type occurred during the ejection. The underlying water did not eject the fuel if it had not previously been boiled; previously boiled water ejected the fuel during the third and fourth runs, unless it was left to stand several days between runs, when it boiled normally.

Several experiments were made in order to establish the temperature at the surface of the water, as well as the distribution

in the filled burner. The temperature at the interface was measured as a function of time. Figure 66 shows results for solar oil; the open circles relate to the solar oil, and the filled ones to the underlying water. The two liquids were at the same temperature at the interface; the same result was obtained with kerosene, so these results are probably applicable to other fuels.

The surface temperature v' of the water was above 100° when boiling or ejection occurred; v' not less than 120° were needed to cause boiling followed by ejection, and ones in excess of 140° were needed to cause direct ejection. These temperatures were the same for kerosene, solar oil, and transformer oil, but the depths of fuel at which they occurred vary from one liquid to another.

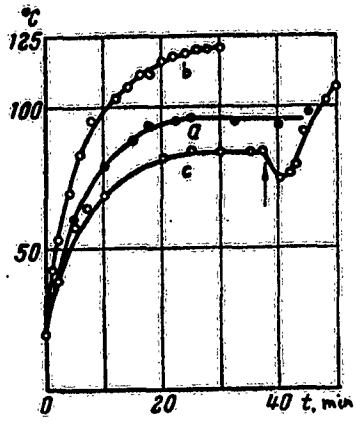

Fig. 68. Surface temperature of water heated from above with oil present initially or at a later stage.

Cork dust floating at the interface caused vigorous boiling to set in at a certain point; the temperature then fell rapidly to about 100°, and so did v_s' (Fig. 67). This was so for all the liquids; the boiling is simply that of water at 100°. The ejection effects are caused by superheating in water lying under the immiscible oil. Water is readily superheated under these conditions, as the following experiment shows. A wide test-tube was wound with 15 turns of constantan. The tube was filled with kerosene, which was heated slowly by a current passing through the coil. A drop of water was run in from a fine tube, and next to it was placed the bulb of a thermometer. The drop was observed under a microscope. A faint crackling was heard at 120-150°, and a small gas bubble detached itself from the drop, which also broke away from the tube. The drop also shrank gradually at temperatures above 100°, but no steam jacket was formed even at 140-150°.

A further experiment (on a tube wound with 12 turns) was performed with water that had been boiled for a long time; this was covered with transformer oil. The water began to boil smoothly at 100° if the surface was above the top of the spiral; bubbles were formed at the wall. But, if the water lay entirely below the coil, the temperature of the water rose above 100°, and the oil was ejected if the superheating was considerable.

A beaker was partly filled with water, which was exposed to radiation from above (from an arc lamp). Figure 68 shows the surface temperature as a function of time; a is for water alone, b is for water covered by a thin layer of solar oil, and c is for water initially alone but coated with oil at the point marked by the arrow. Clearly, the solar oil causes the surface temperature of the water to rise above the boiling point, which does not occur if the surface is free.

This also confirms that the boiling-over is caused by the strong superheating of water under a layer of oil. The effects are best understood by reference to the literature on the boiling of liquids [6-11].

3. Boiling is the production of vapor within the liquid; this does not occur below the boiling point. Superheating can occur, and the state is thermodynamically metastable; it can persist until a nucleus of the new (vapor) phase appears, whereupon it is converted to the stable state. Bubbles of vapor are generated and grow in the process. The usual nuclei for these vapor bubbles are particles of dust and minute gas bubbles, for a highly pure liquid allows of considerable superheating. Water that has been freed from air by prolonged boiling can be heated to 130° in a tube before it boils; pure water in a carefully cleaned glass vessel boils explosively at 137°. (Krebs heated water very carefully freed from air to nearly 200° without causing boiling.)

The abnormally elevated boiling point is very rapidly normalized if sand or any other solid with a substantial surface is added, for bubbles are formed on it at once. A liquid can be superheated within a second liquid having the same density; water droplets floating in a mixture of two oils can be heated to 178° without vaporizing [7].

The bubbles of vapor must be larger than a certain critical radius r_k, which is determined by the condition that the pressure must be the same on both sides of the interface. Then

$$p + \frac{2\alpha}{r_к} + h\rho\, g = p_s - \frac{2\alpha}{r_к}\frac{\rho'}{\rho}, \qquad (2.71)$$

in which p is atmospheric pressure, p_s is the saturation vapor pressure of the liquid, α is the surface tension, g is the acceleration due to gravity, h is the distance from the surface to the bubble, ρ is the density of the liquid, and ρ' is the density of the vapor. The bubble is eliminated by the external pressure if $r < r_k$ but can grow and move upwards if $r > r_k$. Now $p_s = p$ and $r_k = \infty$ at the boiling point, so suitable inclusions are needed

to cause boiling; but $p_s - p > 0$ for a superheated liquid. The r_k for a slightly superheated liquid is still large, so the inclusions are still necessary, but r_k falls very rapidly as the temperature increases, and the probability of the spontaneous production of bubbles soon becomes appreciable. At high temperatures suitable nuclei can arise from phase fluctuations; the theory [9-11] shows that the probability of producing a nucleus of critical size is

$$w \propto \exp\left(-\frac{16\pi\alpha^3 v^2 T_0}{3qk(\Delta T)^2}\right), \qquad (2.72)$$

in which v and q are the volume change and latent heat of the transition, T_0 is the boiling point, $\Delta T = T - T_0$, and T is the actual temperature. This w increases rapidly with ΔT.

The rate of production of vapor in normal boiling is governed by Q, the rate of intake of heat. Here

$$Q = n\nu m q_0,$$

in which n is the number of points at which bubbles are formed, ν is the number of bubbles formed per sec at each point, m is the amount of vapor in a bubble, and q_0 is the latent heat of evaporation.

Heat flowing in through a free surface accelerates evaporation at that surface but does not cause boiling. The effects discussed for oil products occur when the product prevents the water from evaporating, the heat arriving mainly via the oil. The water becomes heated above 100° if there are no nuclei at the surface; steam bubbles appear in the liquid at higher temperatures, and these expand rapidly. The expansion may be sufficiently violent to eject the oil if the temperature is high. The superheated water contains a large amount of stored heat, which is

$$Q = \int_0^{z_0} c\rho\,(\vartheta - \vartheta_k)\,s\,dz,$$

in which c, ρ, and ϑ_k are the thermal capacity, density, and boiling point, z is the distance from the free surface, ϑ is the temperature at that distance, z_0 is the thickness of the layer in which $\vartheta > \vartheta_k$, and s is the cross-section of the layer.

Ejection occurs when z_0 is small in laboratory tests, because the temperature in a burner varies rapidly with depth in a burner, as (2.55) shows. Large quantities of liquid may be ejected from storage tanks; here the homothermal layer causes a rapid

downward transfer of heat to the boundary, which superheats the water when the boundary reaches that liquid. Here the layers are very much thicker, but the phenomena are essentially the same as for burners.

Superheating of the water is certainly the cause of ejection for oil products; the water must be removed or prevented from becoming superheated. The latter is possible if suitable nuclei are introduced in good time, for normal boiling can commence when the boiling point is reached, so superheating and ejection are prevented. Special studies are needed to establish the best type of material to use for nuclei in each particular case.

The surface temperature of the burning liquid is somewhat below the boiling point, and the temperature decreases with depth, so a homogeneous liquid cannot become superheated and boil over. These effects can occur when a second (largely insoluble) liquid of much lower boiling point lies underneath. Suspended water in an oil product has pronounced effects on the rate of combustion, the surface temperature, and the development of the homothermal layer. This suspended water may cause the oil to boil over the side of the tank.

Fig. 69. Evaporation of a drop of water in very hot machine oil.

Blinov's experiments of 1956 illustrate the behavior of water droplets in hot oil. A glass tube (vertical) 5 cm in diameter and 70 cm long was used; the middle part was fitted with an external heater, and the tube was filled with machine oil, which was heated to 140-180°. Small drops of water were allowed to enter the oil, where they fell slowly. At 140-150°, some of these evolved a train of small bubbles, as shown in Fig. 69. The number of drops doing this increased with the temperature; this caused the oil to overflow at the top of the tube. This type of slop-over is found with oil products (including benzine) and crude petroleum.

References

1. Hall. Boiling-over of Crude Petroleum Burning in Tanks. Mech. Eng., 47, No. 7, 1925.
2. Burgoyne and Katan. The Burning of Petroleum Products in Open Tanks. J. Inst. Petroleum, 33, No. 279, 1947.
3. P. P. Pavlov and A. M. Khovanova. O gorenii neftei i nefteproduktakh so svobodnoi poverkhnosti (Burning of Petroleum and Petroleum Products from a Free Surface). Baku, 1955.
4. G. N. Khudyakov. Yavlenie vybrosa tyazhelogo zhidkogo topliva pri gorenii ego so svobodnoi poverkhnosti (Ejection of a Heavy Liquid Fuel Burning From a Free Surface). Izv.

Akad. Nauk SSSR, OTN, No. 5, 1950.
5. V. I. Blinov. O yavlenii vybrosa goryuchei zhidkosti pri gorenii (Boiling-over of a Burning Liquid). Izv. Akad. Nauk SSSR, OTN, No. 2, 1955.
6. M. A. Leontovich. Vvedenie v termodinamiku (Introduction to Thermodynamics), Moscow, publ. Gostekhizdat, 1950.
7. O. D. Khvol'son. Kurs fiziki (Textbook of Physics), vol. 3, 1919.
8. E. I. Nesis. Kipenie v real'nykh usloviyakh (Boiling under Real Conditions). Zh. Tekh. Fiz., 23, No. 9, 1952.
9. Ya. I. Frenkel', Obshchaya teoriya geterofaznykh fluktuatsii i predperekhodnykh yavlenii (General Theory of Heterophase Fluctuations and Pretransition Effects). Zh. Eksper. Teoret. Fiz., 2, 952, 1939.
10. L. Landau and E. Lifshits. Statisticheskaya fizika (Statistical Physics). Moscow, publ. Gostekhizdat, 1951.
11. V. G. Levich. Vvedenie v statisticheskuyu fiziku (Introduction to Statistical Physics). Moscow, publ. Gostekhizdat, 1950.
12. A. O. Yurkov. Vybrosy goryachikh nefteproduktov v svyazi s nakhozhdeniem v nikh vody (Ejection of Burning Oil Products in Relation to the Presence of Water). Neftyanoe Khozyaistvo, 1927.
13. G. M. Mamikoyants and N. K. Paul'. Prichiny vskipaniya i vybrosa goryashchei nefti iz rezervuara i bor'ba s nimi (Causes of Boiling-Over and Ejection of Burning Crude Petroleum in a Tank and Methods of Dealing with them). Ibid., No. 10, 1926.
14. R. F. Larson. Factors Affecting Boiling in Liquids. Ind. Eng. Chem., 37, No. 10, 1945.

Part Three

EXTINCTION OF FLAMES FROM LIQUIDS IN VESSELS

A burning liquid can be extinguished by acting on the liquid or on the flame. The liquid will cease to burn if its surface temperature falls below the ignition temperature; there is no need to cool the whole bulk of liquid. It may be sufficient to stir the liquid, as only a heated surface layer is involved; alternatively, the surface may be sprayed with water.

The flame dies away if the supply of vapor decreases; the supply is reduced if the hot liquid is covered with a thin layer of an incombustible one, for the diffusion coefficient for a vapor in a liquid is very low. A very thin film of liquid may be sufficient to extinguish the flame. A foam can act in this way, as we shall see, though often rather poorly.

The burning may cease if heat from the flame is prevented from reaching the liquid, but the method is of little practical interest, for it has been found [20] that the temperature of the liquid has scarcely altered 10 min after the flame is extinguished. Even if the flow of heat is stopped, the hot liquid will continue to evaporate and support the flame for a fair time.

The burning may stop if the normal conditions are disrupted, though this is practicable only in certain cases where a fine spray of water may be used; the droplets evaporate and cool the flame, while the steam dilutes the reactants, the result being that the flame goes out.

The above are the general methods of extinguishing flames, which are considered in detail below.

Extinction by Stirring

1. In 1903 Loran [1] concluded that the combustion of a liquid can be retarded or stopped by stirring, but the method did not find practical application at that time; it was not tested until about fifteen years ago [2-6]. A jet of air may be used to stir the liquid. The first application was to oil products in tanks [2], in which an air jet was used in the first series of trials, and a jet of the liquid itself in the second. The air or liquid was admitted through packing at the bottom of the tank. In some cases the flame was extinguished with liquid drawn from the lower levels and sprayed from above. The various methods were equivalent in their effects. These tests served to establish the conditions under which the fire could be put out, although the mechanism was discussed only in general terms.

Sukhov and Kozlov [4] made tests on the extinction of burning oil products with air jets at TsNIIPO in 1953; tanks 80 and 260 cm in diameter were used. The time to extinction was measured as a function of air flow, depth of liquid, and packing (size, amount, and position). The results were not analyzed, and no deductions as to the mechanism were made. Further tests on the new method were done on large tanks at the same institute in 1954; the report contains a discussion of the motion induced by the stirring. It was considered that the vortices set up by the air jet can be taken as confined to a cone whose vertex angle α is dependent on the viscosity, the method being successful if $R \leq h\tan(\alpha)$, in which h is the depth of the liquid and R is the radius of the tank.

In 1956 Pavolov and Sukhov [5] published results obtained in 1954 in Baku; here an attempt was made to deduce from theory the extinction conditions for oil products as functions of depth and diameter. Pavlov has since continued this work [6-8].

In 1958 there appeared studies [9,10] of the stirring produced by jets of air and liquid, with results on the extinction times for some oil products. These times T were defined as those necessary to reduce the temperature of the surface layer below the flash point; a relation between T, H, and the air flow rate V was demonstrated. These studies have been extended [11-15], and fresh evidence has been obtained on the hydrodynamics of the process, with special attention to the critical conditions for extinction. It was found that heat transfer from flame to liquid plays a major part, that the result is governed by the mean speed of the liquid at the free surface (i.e., by the time τ for an element of liquid to pass from the

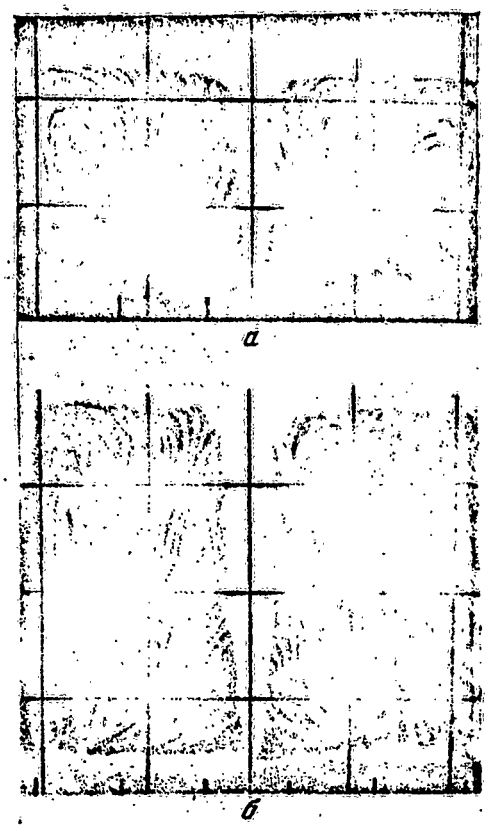

Fig. 1. Movement in a liquid stirred by a jet of liquid: a) h = 25 cm, q = 25 l/min, d = 1 mm; b) h = 40 cm, q = 2.5 l/min, d = 1 mm.

center to the edge), and that the flame was extinguished only when $\tau < \tau_c$ (the critical time). The numerous experimental results were examined in the light of the theory of similitude to derive an empirical relation between τ, V, h, and d (the diameter). It was shown that τ_c does not depend on the method of mixing; it depends only on ϑ_0, the initial temperature, and on the nature of the liquid. There are effects of h and d on T, but the critical conditions remain unchanged if τ is constant.

Now we turn to details of the hydrodynamic aspect, especially for stirring by means of a jet of the same liquid.

2. The motion was examined by means of an open plexiglas cylinder 50 cm in diameter and 110 cm high, which was contained in a lucite tank 50 x 50 x 110 cm. This was used in order to avoid distorting the pattern of movement in the cylinder. In the bottom there was a vertical tube fitted with a gauze. The vessels were filled with water, which was used in all tests of this type; the water contained a little sawdust, whose density was close to one. A projector illuminated a thin vertical layer passing through the axis.

The water entering through the tube entrained the particles; the pattern was photographed every 1-2 sec (Fig. 1). The inflow gave rise to a conical flow pattern; the vertex angle of the cone was constant at about 10°. Complex vortex patterns lay between the jet and the wall.

Quantitative studies were made with a tank 260 cm in diameter; this was filled with diesel oil, and a jet of the same oil entered through a grid at the bottom. The speed at points in the tank was measured with a Burtsev gauge.

3. The observations showed that the behavior was very nearly that of a turbulent jet entering a body of fluid of the same nature, so we shall use the main concepts relating to such jets [17].

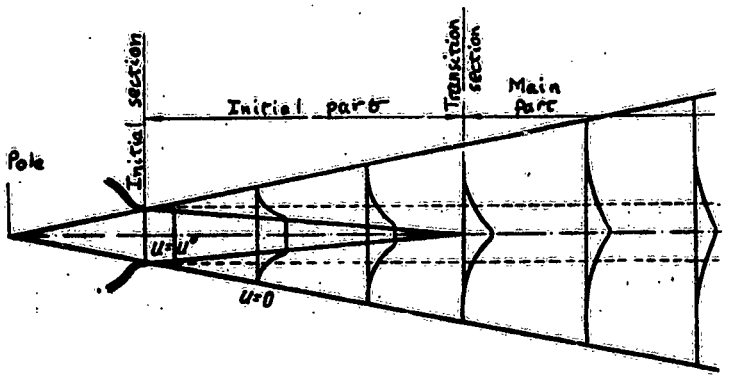

Fig. 2. Jet entering a body of fluid.

Such a jet is termed free and enclosed if it enters an unbounded medium having the same physical properties. A turbulent jet contains random vortex motions that travel beyond the limits of the jet and entrain the surrounding fluid. The particles leaving the jet are replaced by ones from outside, which retard the outer layers; there is a transfer of momentum from the jet to the body of fluid, with the result that the mass and width of the jet increase and the velocity at the boundary falls.

Figure 2 represents some features of such a jet. The boundaries of the divergent surface meet at the pole; the constant-speed core becomes narrower as the nozzle is left behind and finally vanishes at the transition section. The space between the nozzle and the transition section is called the initial part; that beyond, the main part. The jet spreads out in the latter part, and its speed falls. The distance h_o (from the initial section to the pole) is related to s_o (the length of the initial part) and to the angle α by

$$\frac{h_0}{R_0} \approx 4{,}0;\ \frac{s_0}{R_0} \approx 10{,}0;\ \alpha \approx 14°,$$

in which R_0 is the radius of the nozzle.

The velocity distribution takes the same form in all sections of the main part; the ratio of the velocity u to the velocity at the axis u_m (the dimensionless velocity) is the same at all similar points. Further, we use the ratio of the distance r from the axis to the width of the jet b; r/b is the same for similar points. Figure 3 shows the velocity distribution in terms of these parameters.

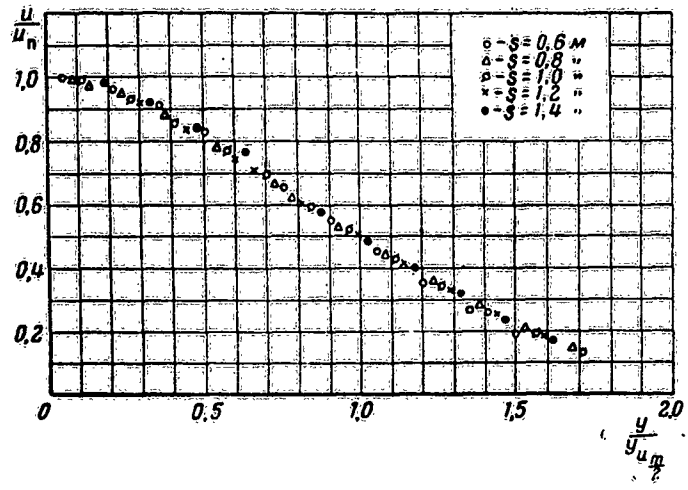

Fig. 3. Velocity distribution in the initial part of a turbulent jet of circular cross-section.

The relation of u_m to s (the distance from the nozzle in the main part) is found by assuming that the momentum remains constant in all cross-sections; then

$$\int_0^m u\,dm = \int_0^\sigma \rho u^2 d\sigma = \text{const},$$

in which dm is the mass of liquid flowing through the cross-

section in unit time, ρ is density, and $d\sigma$ is the area of an element in the cross-section. The condition for the conservation of momentum in an axially symmetric jet may be put as

$$u_m^2 x^2 \int_0^{b/x} \left(\frac{u}{u_m}\right)^2 \frac{r}{x} \frac{dr}{x} = \text{const.} \qquad (3.1)$$

in which x is the distance to the pole. Now u/u_m is a function of r/x alone, by virtue of the above:

$$\frac{u}{u_m} = f\left(\frac{r}{x}\right). \qquad (3.2)$$

so

$$\int_0^{b/x} \left(\frac{u}{u_m}\right)^2 \frac{r}{x} \frac{dr}{x} = \text{const.} \qquad (3.3)$$

Then the velocity at the axis is

$$u_m = \frac{\text{const}}{x}. \qquad (3.4)$$

It is usual to use the above s instead of x, in which case the dimensionless axial velocity may be put as

$$\frac{u_m}{u_0} = \frac{0{,}96}{\frac{as}{R_0} + 0{,}29} = \frac{0{,}96R_0}{ax}, \qquad (3.5)$$

in which a is a constant whose value varies with the structure of the flow in the initial section, being 0.07-0.08 for a circular nozzle; u_0 is the velocity in this section.

Now we calculate V, the flux at any cross-section of the main part:

$$V = \int_0^b u.2\pi r dr = 2\pi b^2 u_m \int_0^1 \frac{u}{u_m} r' dr'.$$

But

$$\frac{b}{R_0} = \frac{x}{h_0}, \qquad \int_0^1 \frac{u}{u_m} r'\, dr' = 1{,}14,$$

so (3.5) gives us that

$$V = 2{,}28\pi \left(\frac{x}{h_0}\right)^2 R_0 u_0 \frac{0{,}96 R_0}{ax}. \qquad (3.6)$$

In conclusion, we must point out that the above results relate to turbulent gas flows.

4. The main ideas for free jets can be applied to the confined jets used in stirring burning fuel. The results in this application are as follows. Figure 4 [16] shows the velocity distribution in terms of the distance from the axis of the tank (abscissa) and the vertical component of the velocity (u) or the distance to the inlet (h). Here we find two types of

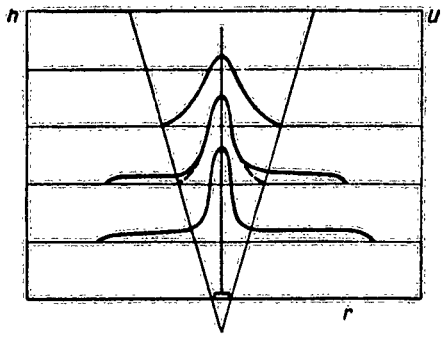

Fig. 4. Velocity distribution in a jet of liquid confined in a liquid.

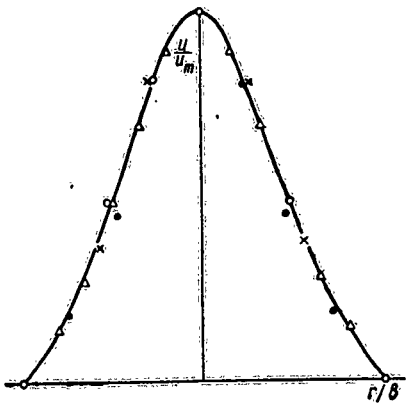

Fig. 5. Velocity profile in a jet.

curve, one which falls rapidly to zero and the other which falls rapidly at first but then runs parallel to the abscissa for a long way. The sharply falling parts in both cases relate to the motion in the jet, while the other parts are the result of interaction between the jet and the walls.

Figure 5 shows u/u_m against $r' = r/b$; the various symbols relate to various experiments on the main part of the jet, while the full line relates to a free jet [17]. The two velocity profiles are clearly similar, and u/u_m is a function of r' only:

$$\frac{u}{u_m} = f(r'), \qquad (3.7)$$

in which f(r') is almost the same for both types of jet. The pole of the confined jet is defined by the boundaries of the cone, but the considerable uncertainty in these causes the pole to be located only roughly. The α for this case is about 10°, though this tends to be low, on account of poor sensitivity in the velocity gauge.

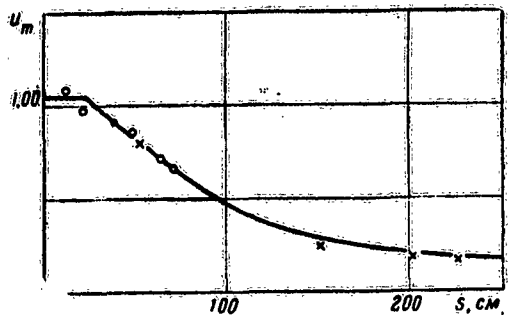

Fig. 6. Relation of u_m to s.

Figure 6 shows u_m as a function of s; u_m remains constant (as in a free jet) near the nozzle, the behavior for the main part being described by

$$u_m = \frac{b_0}{b_1 s^{3/2} + 1}, \qquad (3.8)$$

in which b_0 is a function of V_0, the rate of influx. This shows that the axial speed falls off more rapidly with s, which is a result of gravitational forces (these oppose the upward motion of the liquid). The flow, including the entrained liquid, is given by

$$V = \int_0^b 2\pi r u dr = u_m b^2 I,$$

in which

$$I = \int_0^1 \frac{u}{u_m} 2\pi r' dr'.$$

This I is the same for all sections and is close to one; there is very little error if we put that

$$V = u_m b^2. \qquad (3.9)$$

This, with (3.8), shows that the flow increases with s, but not very rapidly.

5. Petrov and Reutt have measured τ (the traversal time) for tanks 50, 260, and 2240 cm in diameter; the liquids were water, kerosene, and diesel oil. A rotameter measured the surface speed v as a function of r; Fig. 7 shows the results from one run. Here

$$\tau = \int_0^R \frac{dr}{v(r)}, \qquad (3.10)$$

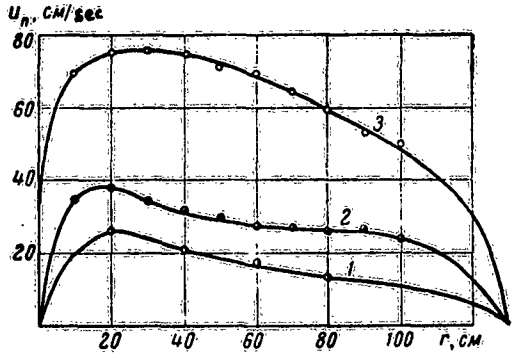

Fig. 7. Flow rate at the surface of a stirred liquid; vessel diameter: 1) 6.5 mm; 2) 13 mm; 3) 26 mm.

in which R is the radius of the tank. Graphical integration was used. In some cases, τ was measured with a stopwatch and cork; the method is not very precise, for the values show a large spread, and at least 50 measurements must be made for each point.

This τ is a function of u_0 (the speed at the inlet), the diameter of the inlet d_c, the diameter of the tank d, and the depth h:

$$\tau = f(h, u_0, d, d_c).$$

These five parameters may be formed into the three dimensionless quantities

$$\frac{u_0 \tau}{d}, \quad \frac{h}{d}, \quad \frac{d_c}{d}.$$

The jet is turbulent, so viscous friction may be neglected; τ is then independent of the nature of the liquid to a first approximation, and

$$\frac{u_0\tau}{d} = \varphi\left(\frac{h}{d}, \frac{d_c}{d}\right). \qquad (3.11)$$

This means that $u_0\tau/d$ must be constant for given h/d and d_c/d.

Figure 8 shows results for the tank 260 cm in diameter for the three liquids for three inlets; clearly, τ is not dependent on the nature of the liquid, but it does vary greatly with u_0 and d_c.

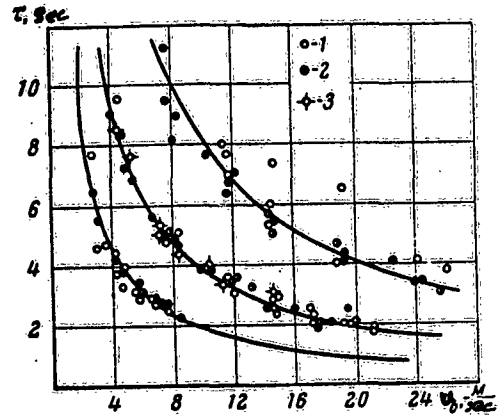

Fig. 8. Relation of τ to u_0; d_c (mm): 1) 26; 2) 13; 3) 6.5.

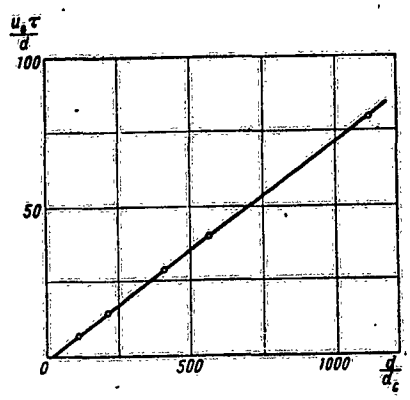

Fig. 9. Relation of $u_0\tau/d$ to d/d_c.

There is no effect of h/d on τ. Further, Fig. 9 shows that $u_0\tau/d$ is proportional to d/d_c; the results give

$$\tau = a\frac{d^2}{u_0 d_c}, \qquad (3.12)$$

in which a is 0.0725. This is applicable for d from 50 to 2240 cm for $h/d \geq 0.2$ and $d_c/d \geq 0.0018$; it is stated that (3.12) is applicable for any injection system if d is replaced by the equivalent diameter d_e.

6. The hydrodynamic picture is more complex if air is used; here we have a two-phase jet, which does not follow the laws for a single-phase jet, although there are certain points of resemblance. Several studies have been made of the hydrodynamics of the process [9,11-13]; the main results are as

follows.

The velocity distribution in the liquid has been examined [9] by means of the transparent model described above; the general pattern was very much that shown in Fig. 1. The angle of the cone was constant at about 10°. The jet showed strong pulsations; the height and position of the raised area at the surface varied rapidly. The motion in the space between the jet and the wall was also complicated; this was of toroidal type and encompassed all the liquid if $h \leq R$, but the toroid was confined to the upper part if $h > R$, the thickness of this part being constant and roughly equal to R. Complicated movements occurred between the bottom and the toroid; the center of the left part of the toroid would fall, and the right would rise, whereupon the water flowed downwards on the left under the

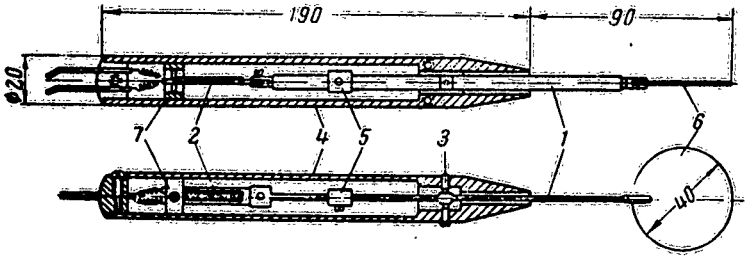

Fig. 10. Instrument for recording pulsations in a flow.

toroid, upwards at the wall on the right, and then, at the boundary of the toroid, back to the axis. Then the two halves would change positions, and so on. Sometimes vortices arose briefly in the lower part. These jets were, of course, turbulent.

Petrov and Reutt [12] have examined the motion within the jet by means of the special strain-gauge device shown in Fig. 10; here 2 is a steel plate bearing the wire strain gauge. One end of the plate is held by the rod 1, the other bearing on the needle in the support ring 7. Rod 1 is joined to the disc 6 and can perform small movements about its axle, which is held in the bearings 3 within the body 4. The rod and disc are balanced by the weight 5. This instrument detects large-scale pulsations, which contain most of the energy; it records flow rates from 10-15 cm/sec upwards. The motion is recorded on a narrow paper strip by an MPO-2 oscillograph.

Studies were made on diesel oil in a tank 2.6 cm in

diameter; h was 208 cm and d_c was 26 mm (axial). The disc was set at right angles to the flow direction. Most of the measurements were made on the axis of the jet; Fig. 11 shows recordings for a flow rate of 3.3 l/sec. The type of fluctuation is clearly very much dependent on s, for there were regular oscillations whose amplitude and frequency were functions of flow rate at distances of 10, 20, and 30 cm. The motion became more random at large distances, few regular features being apparent at 80 cm, although two frequencies (one low, one high) persist at 80 and 120 cm.

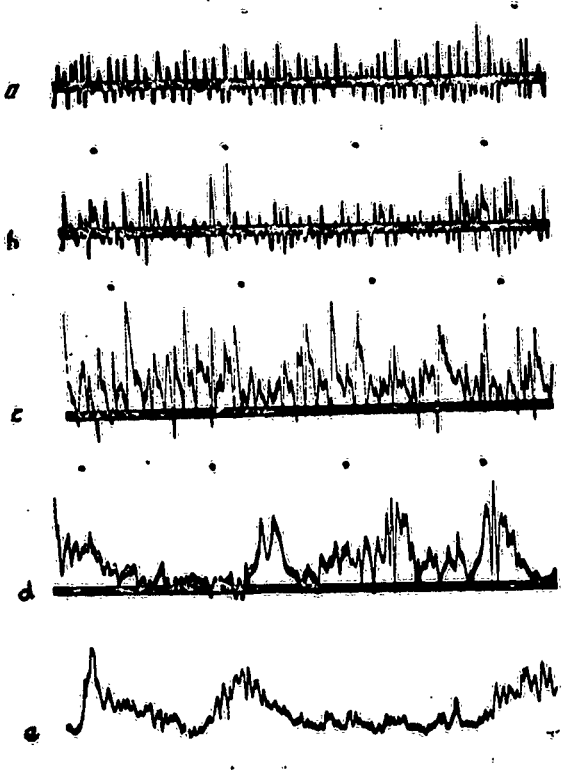

Fig. 11. Pulsations at distances from the inlet (cm) of; a) 10; b) 20; c) 30; d) 80; e) 120. The points are time marks at intervals of 2 sec.

Photographs of the inlet show that a large air bubble is formed near the inlet; the upper part is struck by the jet of incoming air, and this gives rise to many small bubbles. The cavity enlarges and expands upwards; the number of small bubbles increases, but these soon break away in a body to leave the bubble as it was at the start (Fig. 12). The frequency of this process increases somewhat with the flow rate. The groups of bubbles entrain liquid; they gradually disperse. The motion in the jet becomes highly irregular, partly on account of oscillation of the axis of the jet about its mean position. The bubbles are also unevenly distributed within the jet. The low-frequency oscillations are caused by the groups of bubbles; the high-frequency ones, by the individual bubbles.

Blinov et al [9] have derived some empirical laws for the

velocity distribution in such jets; a Burtsev rotameter was used with water in a tank 2.6 m in diameter. Figure 13 shows the results from one series, the velocities being the vertical velocity distribution in such jets; a Burtsev rotameter was used with water in a tank 2.6 m in diameter. Figure 13 shows the results from one series, the velocities being the vertical components for the heights shown. The curves are comparable with those of Fig. 4, and here again we find two types. The composite curves contain parts related to the jet and to the liquid between jet and wall. The parts for the jet alone are shown by broken lines at the flanks. These curves show that the boundaries of the jet lie on straight lines that meet at an effective pole, which lies below the inlet. The angle α between the axis and any such line is 13°, no matter what V_o (the flow rate) may be, provided this is less than 1 l/sec.

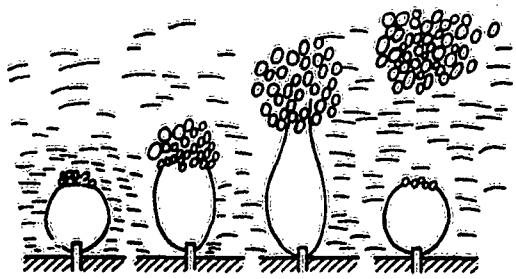

Fig. 12. Pulsation of the air cavity at the inlet.

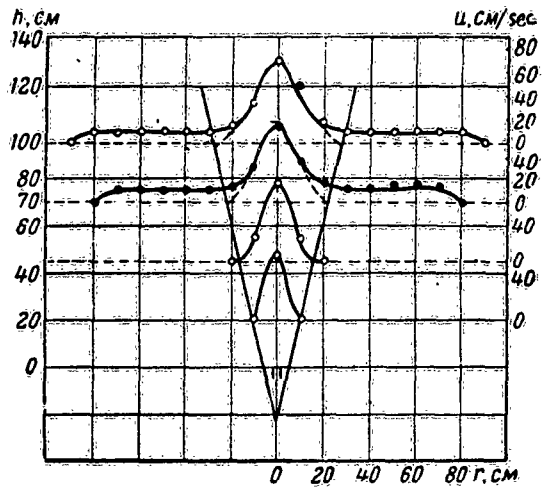

Fig. 13. Velocity profiles for a vertical air jet in a liquid; h = 1.25 m, d_c = 25 mm, q = 2.1 l/sec.

Figure 14 shows the velocity as a function of distance from the axis; the signs relate to the various experiments.

Representation in dimensionless terms shows clearly that here we have that

$$u' = \frac{u}{u_m} = f(r'),$$

in which f(r') is the same for all runs. The profile is very similar to that for a single-phase unconfined jet.

Figure 15 shows how u_m varies with s; for s > 50 cm, u_m is constant. This is very different from the behavior of a free jet;

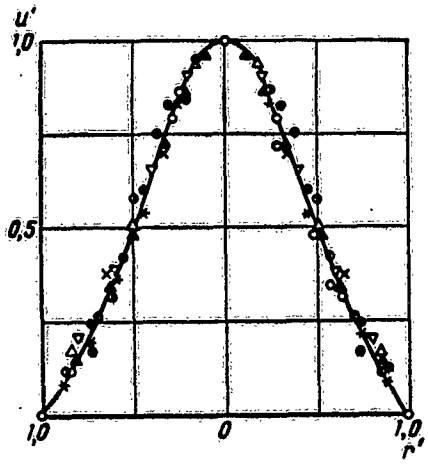

Fig. 14. Velocity profile across the jet when a liquid is stirred with air.

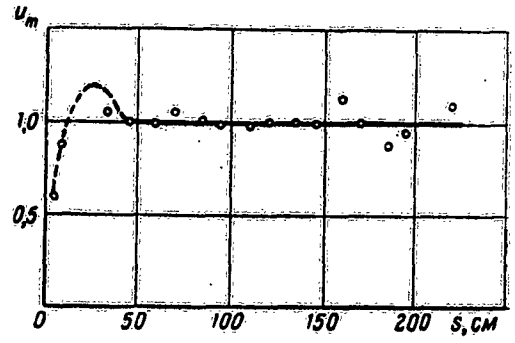

Fig. 15. Velocity at the axis as a function of distance from nozzle.

u_m is constant on account of the lift provided by the air bubbles. Now

$$\bar{u}_m = a\sqrt[3]{\frac{V_0}{h}g},$$

in which h and g are as above, and a is independent of V_0 and h but is a function of d_c. The flow of liquid is

$$V = \bar{u}_m r_m^2 \int_0^1 2\pi r' f(r')\, dr' = \bar{u}_m r_m^2 I,$$

in which I represents the integral, which is found to be 1.03, so we may put that

$$V = \bar{u}_m r_m^2 = (s + h_0)^2 \tan^2 \alpha\, a \sqrt[3]{\frac{V_0}{h}g}.$$

Measurements have been made of the horizontal velocity component 1 m from the axis in the top layer, which gives the flow G in that layer (Figs. 16 and 17); here G' is G for V = 6 l/sec. The points fit the curve of Fig. 16 well; $G(V_0)$ is the product of two functions, one containing only h and one containing only V_0:

$$G = \varphi(h)\,\psi(V_0).$$

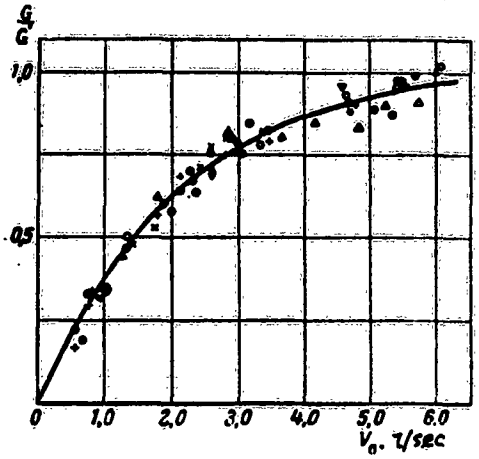

Fig. 16. Flow of liquid in top layer as a function of air flow.

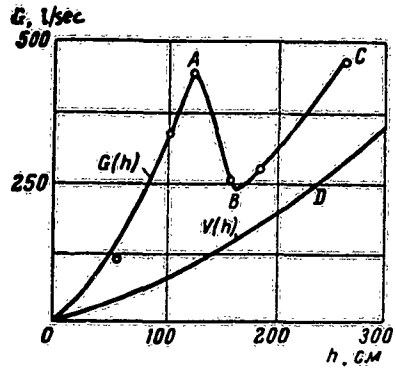

Fig. 17. Flow of liquid in top layer for a constant air flow.

To a first approximation

$$\psi(V_0) \propto V_0^{3/4}.$$

A more accurate expression for $G(V_0)$ is

$$G = \varphi(h)\,(1 - e^{-\beta V_0}).$$

Figure 17 shows that G(h) has an intermediate maximum; $G > V$ at all times, because the flow at the surface includes liquid taking part in the vortex motion between jet and wall. Also, $G \propto V$ over sections OA and BC, so

$$\varphi(h) = b\frac{(h+h_0)^2}{\sqrt[3]{h}},$$

in which b is a constant.

Petrov and Reutt have made many measurements of τ [19]; results [11,13] have been worked up by means of the method of dimensions. Reutt's main results [11] were used in conjunction with boundary conditions and hydrodynamic equations to deduce a system of dimensionless parameters; Reutt has shown that this same system can be derived from general arguments. We may assume that the mean speed at the surface (i.e., τ) is a function of h, d, V_0, g, σ (surface tension), and $\Delta\rho$ ($= \rho - \rho'$), ρ being the density of the liquid and ρ' that of air. If we take d as the main parameter, we get the dimensionless quantities

$$\frac{u^2}{gd}, \quad \pi = \frac{\sigma}{d^2\Delta\rho}, \quad Q = \frac{V_0^2\rho'}{gd^3\Delta\rho}, \quad H = \frac{h}{d}.$$

These may be related as in

$$\frac{u^2}{gd} = f(\pi, Q, H) \tag{3.13}$$

Now the quantity on the left is simply Fr, while π is Weber's number We; Petrov and Reutt [13] introduced τ into Fr to derive the relation

$$\frac{d}{g\tau^2} = A\left(\frac{h}{d}\right)^m\left[\frac{\sigma}{d^2\Delta\rho}\right]^{-n}\left\{B + \left(\frac{gd^3\Delta\rho}{V_0\rho'}\right)^k\right\}^{-1}, \tag{3.14}$$

in which A, B, m, n, and k are found empirically as 1.26×10^6, 0.81×10^{10}, 1.53, 0.42, and 0.83. The results are worked up to give

$$\frac{d}{g\tau^2} = (A' + B'H_0)(CH_0^{-m} + Q^{-n})^{-1}. \tag{3.15}$$

Here A' and n vary with the liquid; B', C, and m are the same for water, kerosene, and diesel oil, while H_0 is given by

$$H_0 = \frac{h^2}{d}\sqrt[3]{1 + \frac{\rho h}{p_0}},$$

in which p_0 is the atmospheric pressure.

Equation (3.15) is applicable even when the air is fed in at the side or through several tubes.

It is no accident that the viscosity does not appear in (3.14), for the viscosity is assumed to have no great effect; a mixture of crude oil with diesel oil has about four times the viscosity of diesel oil, but τ is unaffected, while Pavlov [8] finds that a 100-fold increase in viscosity demands only 60% more air to produce extinction. This work of Pavlov's deals principally with the effects of viscosity in this method; extensive experimental results are given. Unfortunately, lack of certain vital details prevents us from using these results.

The above relationships are cumbrous; moreover, the viscosity does have a certain effect. We now examine whether a simpler equation incorporating the viscosity can fit the results. Blinov's results in this context are as follows.

The formula must contain dimensionless combinations of h, τ, V_0, d, $\Delta\rho$, η, g, and d_c, e.g.

$$\tau\sqrt{\frac{g}{l}},\quad \frac{h}{\zeta},\quad \frac{d^3}{V_0}\sqrt[3]{\frac{g^2}{\nu}},$$

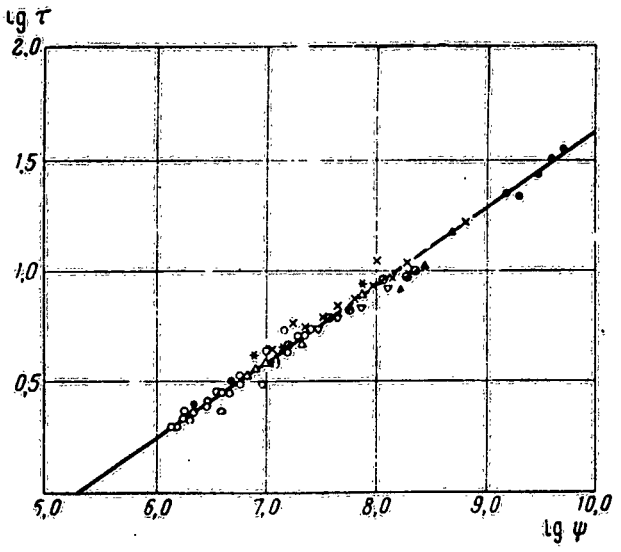

Fig. 18. Relation of log τ to log φ.

in which l is a linear dimension, $\nu = \eta/\rho$ (the kinematic viscosity), and η is the viscosity. (The density of air is neglected relative to the density of the liquid.) Petrov and Reutt's results show that

$$\psi = \frac{d^5}{V_0 l^2}\sqrt[3]{\frac{g^2}{\nu}},$$

and that

$$\tau = f(\psi).$$

Figure 18 shows results from thirteen runs with water, kerosene, diesel oil, and crude oil mixed

with diesel oil for tanks of diameters 2.6 and 22.4 m (central air feed). No points have been omitted; V_0 varied from 0.3 to 300 l/sec, and φ by four orders of magnitude. The straight line is

$$\lg \tau = 0{,}345\,(\lg \psi - 5{,}30).$$

The results give a good fit to

$$\tau = \left(\frac{\psi}{2 \cdot 10^5}\right)^{0{,}345}. \qquad (3.16)$$

The results for d = 130 cm deviate systematically from the above line, the deviation (upwards) increasing with h; (3.16) is not applicable for $d < 2.6$ m. The walls may have a pronounced effect in small tanks.

Equation (3.16) is also inapplicable if the air is fed in from the sides, though the results are satisfactory if the inlets are symmetrically placed and if the equivalent diameter is used. Six inlets in a 22.4 m tank give an equivalent diameter of 0.7d, so several such inlets are more economical than one central one.

The τ of (3.16) should be replaced by $\tau(g/l)^{1/2}$, although this l is not d or d_c; perhaps the mean size of the bubbles is involved. The lack of suitable results prevents us from deciding on this point, so (3.16) for the present remains unchanged.

7. Consider a rigid parallelepiped of volume dv moving over the surface with the mean speed of the liquid; the liquid inside is in continuous exchange with that outside, and so the internal temperature will vary continuously from ϑ_0 (initial) to some final value. This last is governed by the heat received from the flame and by the heat lost as a result of the turbulence; it may be above a critical limit if τ is large, so the flame will not go out. Extinction occurs only for $\tau < \tau_c$, the critical time.

This conclusion [14,15] is confirmed by tests; some results for kerosene are given below for an 8.6 m tank having a central air inlet.

h, m	1,8	3,1	3,3	3,4	4,4	4,6	1,3
V, l/sec	51	58	53	50	26	58	47
τ, sec	8	5,2	5,2	5,2	5,4	4,0	10
Result	—	+	+	+	+	+	—

Extinction occurs if $\tau < 8$ sec. Fuller results were obtained by measuring the time to extinction, the results being extrapolated to the critical V for a given h; the τ for this V_c was calculated from the formulas. Table 3.1, and later tables, give the results.

Table 3.1

2.6 m Tank Stirred with Air

Перемешивание воздухом $d = 2{,}6$ м

h, м	V_c, м/sec	v_0, °C	τ_c, sec	Fuel, air inlet
2,08	0,34	29	7,2	Diesel oil, central
1,54	0,54	39	7,5	Ditto
2,34	0,77	31	7,6	Diesel oil, side
1,76	1,0	22	7,8	Ditto
2,08	0,4	15	7,0	Kerosene, central
1,30	0,65	9	7,0	Ditto

Here we must add that the τ_c for kerosene in a 22.4 m tank is less than 15 sec. The method of mixing, the depth, and d_c all have no effect on τ_c; d has a slight effect, but ϑ_0 is the most important parameter. Figure 19 shows $\tau_c(\vartheta_0)$ for diesel oil and kerosene; clearly, τ_c falls rapidly, especially as the critical limit ϑ_{0c} is approached. Stirring does not extinguish the flame if $\vartheta_0 > \vartheta_{0c}$.

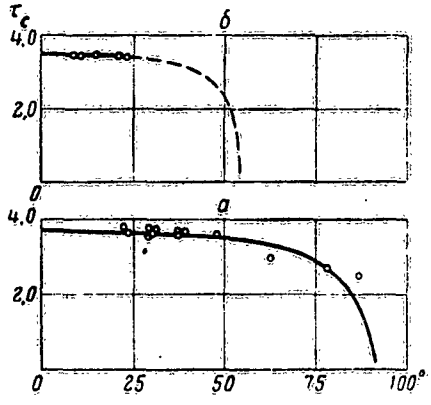

Fig. 19. Relation of τ_c to ϑ_0 a) for diesel oil and b) for kerosene.

The relation of τ_c to d_c may be found as follows [98]. Consider the parallelepiped dv as before; let the time taken to traverse a radius be τ_c, so the temperature when it reaches the wall is ϑ_c (critical). The burning ceases in this case.

The heat received is $dq = \rho c(\vartheta_c - \vartheta_0)dv$; of this, $dq_1 = \varepsilon a T^4 \tau_c ds'$ is received from the flame and $dq_2 = \alpha(\vartheta_n - \vartheta)\tau_c ds''$

is received from the adjacent liquid. Here ε and a are parameters of the emission from the flame (temperature T), ds' is the area that receives the radiation, α is the heat-transfer factor, $\bar{\vartheta}_n$ and $\bar{\vartheta}$ are the mean temperatures of the liquid under and in dv, and ds" is the area available for heat transfer. The law of conservation of energy gives us that

$$dq = dq_1 + dq_2\,;\quad \rho c\,(\vartheta_c - \vartheta_0)\,dV = \varepsilon a T_\varphi^4 \tau_c\,ds' + \alpha\,(\bar{\vartheta}_n - \bar{\vartheta})\,\tau_c\,ds''. \qquad (3.17)$$

But

$$\bar{\vartheta} = \frac{\vartheta_n + \vartheta_c}{2}. \qquad (3.18)$$

These two give us that

$$\tau_c = \left[b_1 + \frac{b_2}{\vartheta_c - \vartheta_0}\right]^{-1}, \qquad (3.19)$$

in which b_1 and b_2 are constants dependent on the properties of the liquid, the flame, and the conditions generally; they vary little with d for large tanks of equal burning time. The full line in Fig. 20 is for (3.19), which fits experiment well.

8. The flame does not go out if $\tau > \tau_c$; the extinction is the more rapid the smaller τ if $\tau < \tau_c$. The condition $\tau = \tau_c$ divides the two states; if air is used, we must have

$$\psi = \psi_c = \frac{d^5}{V_0 h^2}\sqrt{\frac{g^2}{\nu}} \qquad (3.20)$$

We may assume that ψ_c is independent of d for $d \geq 2.6$ m, from which we may draw some interesting conclusions. Here (3.20) gives us that

$$\frac{h}{d} = \text{const}\sqrt{\frac{d^3}{V_0}} = \text{const}\sqrt{\frac{d}{V_s}}, \qquad (3.21)$$

in which V_s is the specific flow (the flow per unit surface area); then h/d is clearly a function of V_s and d, and is not a constant, although this is commonly assumed to be the case [8].

The critical conditions give us that

$$\frac{d^6}{V_0 h^2} \text{ or } \frac{d^3}{V_s h^2} = \text{const} \; ; \; V_{sc} = \text{const}\frac{d^3}{h^2}, \tag{3.22}$$

or, if d is constant,

$$V_0 h^2 = \text{const} \; ; \; h = \frac{\text{const}}{\sqrt{V_0}}. \tag{3.23}$$

These relationships are only approximate, being empirically derived from numerous experiments.

The boundary condition for extinction by a jet of liquid is

$$\frac{d^2}{u_0 d_c} = \text{const}.$$

This gives us a relation between critical values:

$$V_s = \frac{u_0 d_c^2}{d^2} = b' d_c, \tag{3.24}$$

in which b' is a constant for a given liquid; this implies that V_{sc} is dependent only on d_c (within the range in d_c that has been examined).

These relationships are not applicable if h is small, for a fountain may form, air channels may arise, and so on [15]. The constants of (3.20) and (3.24) are, of course, functions of ϑ_0.

9. It is usual to measure the time T to extinction; the relation of T to τ is important, for the two are not equal, though they have a unique functional relation $T = f(\tau)$. Now $T = \infty$ for $\tau = \tau_c$, and $T \to 0$ as $\tau \to 0$; these requirements are satisfied by

$$T = \frac{a}{\left(\frac{\tau_c}{\tau}\right)^m - 1}, \tag{3.25}$$

in which a and m are parameters.

Consider first the use of air; (3.16) is inserted in (3.25), whereupon we have

$$T = \frac{a_1}{\frac{1}{\psi^m} - \frac{1}{\psi_c^m}}, \quad a_1 = \frac{a}{\psi_c^m}.$$

or

$$T = \frac{a_2}{(V_0h^2)^m - (V_0h^2)_c^m}, \qquad (3.26)$$

in which a_2 varies with the liquid. Unfortunately, we have few results on T for d > 260 cm, so (3.26) cannot be tested thoroughly, but such results as there are for T [10, 19] we shall use. Figure 20 shows T for diesel oil and d = 260 cm [10]; the crosses denote results for oil that had been burning

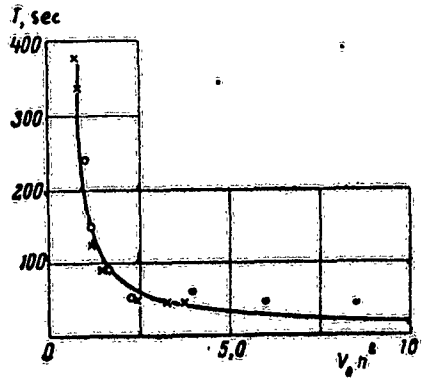

Fig. 20. Relation of T to h^2V_0.

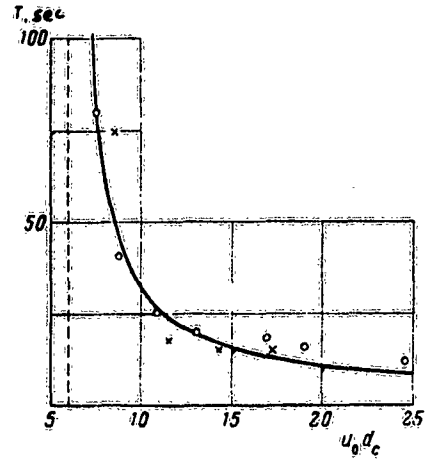

Fig. 21. Relation of T to air flow rate.

for 2 min, while the circles denote 0.4T for oil that had been burning for 30 min. The line is from (3.26), with m = 2/3. The points all lie near the curve, some of the deviations being the result of errors in T and of variation in ϑ. Further, a_2 increases with the time for which the liquid has been burning. If h is constant, we can replace (3.26) by

$$T = \frac{a_3}{V_0^{3/2} - V_c^{3/2}}, \qquad (3.27)$$

and if V is constant, by

$$T = \frac{a_4}{h^{4/3} - h_c^{4/3}}. \qquad (3.23)$$

Experiment confirms (3.27); the line in Fig. 21 (for T against V_0) represents (3.21), the points being from [20]. Further, (3.27) is the same as a formula given previously [18] while (3.28) is very similar to another one [18].

The existing data do not allow us to relate the a_2 of (3.26) to d.

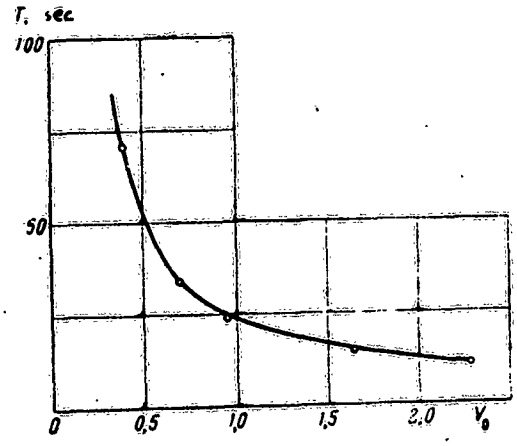

Fig. 22. Relation of T to $u_0 d_c$.

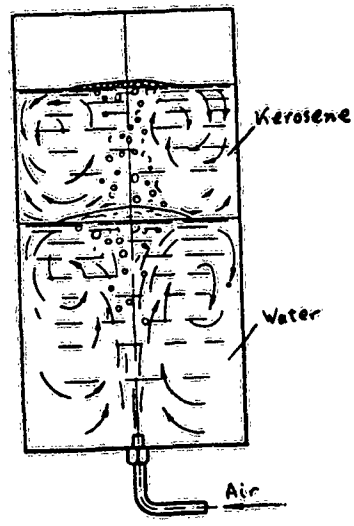

Fig. 23. Motion when two immiscible liquids are stirred.

10. The above discussion, in conjunction with (3.12), enables us to put for liquid-jet extinction that

$$T = \frac{b'}{(u_0 d_c)^n - (u_0 d_c)_c^n}; \quad b' = \frac{b''}{(u d_c)_c^n}. \qquad (3.29)$$

The only experimental results are those of [19]; Fig. 22 shows T against $u_0 d_c$, the curve being from (3.29) and the various signs being for the different runs. Here n has been taken as 2/3; (3.29) fits the points well.

11. The experiments on extinction by stirring confirm

the theoretical picture. The cold liquid from the bottom flows over the surface, where it mixes with the hot liquid and is heated by the flame. If $\vartheta' < \vartheta_c$ (the latter being the ignition temperature), the flame goes out. The cold liquid, as it were, shields the hot part from the flame. This point must be stressed, for it is sometimes incorrectly supposed that the extinction occurs when the mixing has proceeded sufficiently to reduce the temperature of the hottest part below the flash point.

12. The above experiments relate to tanks containing the combustible liquid alone; in practice, there may be another liquid (such as water) under the fuel. Our picture of the process is far from complete; only qualitative observations have been made on kerosene floating on water [16] in the above transparent tank. Figure 23 illustrates the pattern, which shows that each liquid is stirred separately; the mechanism is as for a single liquid, but the stirring is reduced for a given air flow.

References

1. Kanavtsev, G. I. Sposoby penotusheniya neftyanykh pozharov (Methods of Extinguishing Oil Fires with Foam). Baku, publ. Azneft'izdat, 1935.

2. J. H. Burgoyne and L. L. Katan. Fires in Open Tanks of Petroleum Products: Some Fundamental Aspects. J. Inst. Petroleum, 33, 158 (1947).

3. Resinger. A New Method of Extinguishing Flames. World Petroleum, No. 2, 1952.

4. Ya. V. Sukhov and A. V. Kozlov. Tushenie nefteproduktov s pomoshch'yu szatogo vozdukha. Otchet TsNIIPO, 1953. Izyskanie naibolee effektivnykh sposobov tusneniya pozharov nefteproduktov. Otchet TsNIIPO, 1954. (Extinction of Oil Products with Compressed Air; Report of TsNIIPO, 1953. The Search for the Most Effective Methods of Extinguishing Oil-Product Fires. Report of TsNIIPO, 1954.)

5. P. P. Pavlov and Ya. V. Sukhov. Tushenie v rezervuarov nefteproduktov putem peremeshivaniya poslednikh s pomosh-ch'yu szhatogo vozdukho (Fire Extinction in Oil-Product Tanks by means of Stirring with Compressed Air). Baku, Trudy Azerbaidzhanskogo industr. in-ta (Trans. Azerbaijan Industrial Inst.), 1956.

6. P. P. Pavlov. Gorenie i tushenie nefteproduktov metodom peremeshivaniya tem zhe nefteproduktom i ikh svyaz' s fiziko-khimicheskimi kharakteristikami nefteprodukta (Combustion and Extinction of Oil Products by Mixing with the Same Product, and Relation to the Physico-Chemical Characteristics of the Product). Inform. sbornik TsNIIPO (Bulletin of the Central Research Institute for Fire-Fighting), Baku, 1957.

7. P. P. Pavlov and B. A. Kulikov. Tushenie pozharov nefteproduktov v podzemnykh emkostyakh metadom peremeshivaniya s pomoshch'yu szhatogo vozdukha (Extinction of Oil Products Burning in Underground Tanks by means of Stirring with Compressed Air). Ibid., 1957.

8. P. P. Pavlov. Vliyanie vyazkosti nefteproduktov na ikh tushenie metodom peremeshivaniya (Effects of Viscosity on the Extinction of an Oil Product by Stirring). Ibid., 1957.

9. V. I. Blinov, G. N. Khudyakov, I. I. Petrov, and V. Ch. Reutt. O dvizhenie zhidkosti v rezervuare pri peremeshivanii ee struei vozdukha (Motion of the Liquid in a Tank in Response to Stirring with an Air Jet). Inzh.-Fiz. Zh., 1, No. 11, 1958; Inform. sbornik TsNIIPO (Bulletin of the Central Research Institute for Fire-Fighting), M., Publ. MKKh, 1958.

10. V. I. Blinov, G. N. Khudyakov, and I. I. Petrov. O mekhanizme tusheniya goreniya nefteproduktov v rezervuarakh putem peremeshivaniya ikh vozdukhom (Mechanism of Extinction by means of Stirring with Air for Oil Products Burning in Tanks). Inform. sbornik TsNIIPO (Bulletin of the Central Research Institute for Fire-Fighting), M., publ. MKKh, 1958.

11. V. Ch. Reutt. Primenenie metodov teoriya podobiya i razmernosti pri izucheniya gidrodinamiki protsessa peremeshivaniya zhidkosti v rezervuarakh (Use of the Theory of Similitude and the Method of Dimensions in Studies on the Hydrodynamics of the Stirring of a Liquid in a Tank). Ibid., 1959.

12. I. I. Petrov and V. Ch. Reutt. O kharaktere dvizheniya pri peremeshivanii zhidkosti v rezervuare s pomoshch'yu vozdukha (Motion of a Liquid Stirred with Air in a Tank). Ibid., 1959.

13. Idem. Nekotorye zakonomernosti gidrodinamiki peremeshwaniya zhidkosti v rezervuarakh (Some Hydrodynamic Laws in the Stirring of a Liquid in a Tank). Ibid., 1959.

14. Idem. Kriticheskie usloviya potukhaniya plameni nefteprodukta pri ego peremeshivanii v rezervuare (Critical Extinction Conditions for the Flame of an Oil Product Stirred in a Tank). Ibid 1959.

15. Idem. Raschet parametrov sistemy tusheniya nefteproduktov v rezervuarakh metodom peremeshivaniya (Calculation of the Parameters of the Extinction System for Stirring an Oil Product in a Tank). Ibid., 1959.

16. V. I. Blinov, G. N. Khudyakov, and I. I. Petrov. Issledovanie mekhanizma tusheniya plameni nefteproduktov s pomoshch'yu starykh i novykh ognegasitel'nykh sredstv (A Study of the Mechanisms of Extinction of Burning Oil Products by Means of Old and New Extinguishing Agents). Trudy ENINA and TsNIIPO, 1956.

17. G. N. Abramovich. Turbulentnye svobodnye strui zhidkosti i gazov (Turbulent Free Jets of Liquid and Gases). Moscow, publ. Gosenergoizdat, 1948.

18. V. I. Blinov. O nekotorykh voprosakh, otnosyashchikhsya k goreniyu i tusheniyu plameni nefteproduktov. Iz kn. "Novye sposoby i sredstva tusheniya plameni nefteproduktov" (Some Problems in the Burning and Extinction of Oil Products. In 'New Methods and Agents for Extinguishing Oil Products'). Publ. Gostopizdat, 1960.

19. I. I. Petrov and V. Ch. Reutt. Tushenie pozharov nefteproduktov v rezervuarakh metadom peremeshwaniya (Extinction of Burning Oil Products in Tanks by Stirring). Otchet TsNIIPO (Report of the Central Research Institute for Fire-Fighting), 1957.

20. V. P. Losev and M. P. Kazakov. O mekhamizme tushashchego deistviya pen pri gorenii jefteproduktov v rezervuarakh (Mechanism of Extinction by Foam for Oil Products Burning in Tanks). Inform. sbornik TsNIIPO (Bulletin of the Central Research Institute for Fire-Fighting), M., publ. MKKh, 1958.

Extinction of Flames from Liquids by Means of Foam

The Russian engineer Loran proposed the use of foams in fires caused by liquids in 1904; the method is now in common use. Up till about 1940 or so, it was generally believed that the foam extinguishes the liquid by preventing access of air; in 1938 Bogdanov [1] argued that the foam 'acts by isolating the liquid from the influx of heat' and that 'the foam acts as an insulator, for it has a low thermal conductivity and does not transmit the heat', which inhibits the evaporation, so the

flame goes out. These conclusions were not tested by experiment.

In 1951 Khudyakov [2] showed that Bogdanov's conclusions were incorrect for volatile liquids; the cooling action of the foam stops the burning only if the top layer of liquid is cooled to the ignition temperature. He stated that 'it is clear that the foam retards the transfer of heat from the flame to the liquid and also cools the top layer, but these effects only reduce the rate of evaporation; the flame continues, for the flow of vapor is sufficient to maintain it. It may be that the foam also retards the evaporation'. His experiments on the evaporation of benzene, xylene, and the benzene fraction from coal tar were made on surfaces coated with foam and also on uncoated ones; the foam reduced the rate of evaporation very greatly. He concluded that 'the foam acts mainly by preventing the hot liquid from evaporating'.

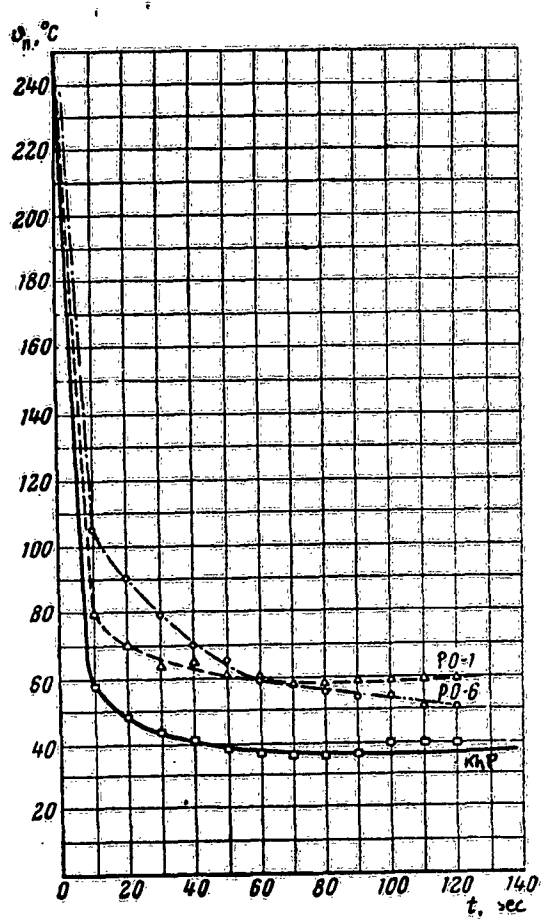

Fig. 24. Surface temperature of kerosene during the extinction of the flame by foam.

Other important studies on foams are Losev and Kazakov's [3] and Blinov and Khudyakov's [4]. The first two workers (from the Central Research Institute for Fire-Fighting) used a tank 130 cm in diameter and 150 cm high, which was fitted with thermocouples at many points. The fuels used were tractor kerosene, diesel oil, benzine, and raw crude oil.

1. The kerosene tests showed that the foam caused a

sharp fall in surface temperature in the first 20 sec, the subsequent fall being slow (Fig. 24). Foams PO-1 and PO-6 suppressed the burning completely when the surface temperature reached 50-60°; the chemical foam required 30°. Figure 25 shows the temperature distribution during and after the burning; the foam has cooled a thin upper layer of the liquid, but under this there lies a hotter layer.

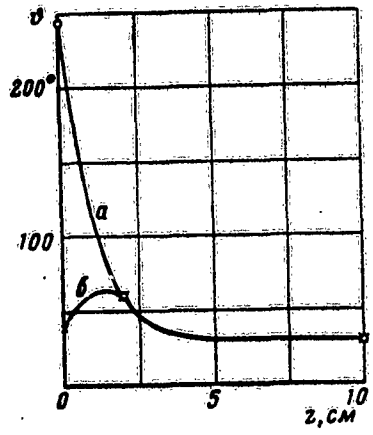

Fig. 25. Temperature distribution in kerosene a) before the start of extinction and b) at the end; extinction time 180 sec.

2. Some tests were done with diesel oil (surface 20 cm below the top of the tank). Table 3.2 shows that PO-1 foam produced extinction at a surface temperature of 100°, while KhP (chemical) foam required 40-70°.

3. Numerous tests were done with benzine; PO-1 and chemical foam were used. Benzine gives rise to a homothermal layer, whose thickness increases with time; the foam was applied when this layer had reached thicknesses of 10, 20, 35, 65, and 80 cm. Figure 26 shows the results from one run; the foam lowers the surface temperature and alters the

Table 3.2

Foam Layer 2.5 cm Deep

Foam	Surface temperature, °C		Mult. of foam	Foam flow rate l/sec. m²	Rate of run-off l/sec. m²	Extinction time, sec	
	Start	End				Main	Complete
PO-1	170	93	8,0	0,5	0,23	—	72
PO-1	280	98	8,0	0,5	0,15	—	60
KhP	250	40	4,1	0,5	0,61	55	108
KhP	230	70	4,1	0,5	0,36	55	75

distribution in the homothermal layer (a submerged hot layer is formed). The temperature in this layer gradually falls; the convection in this layer does not stop during the extinction.

The cooling would be more rapid, of course, if there were no convection. The extinction time increases with the burning time, because the hot layer becomes thicker. The burning ceases when the surface temperature is somewhat above 20°, which is well above the flash and ignition points. Much the same is found for crude petroleum.

4. The extinction is associated with pronounced cooling of the top layer, which depresses the vapor pressure; for example, the vapor pressure of kerosene at 30° is [5] 20-30 mm Hg and at 50° is 30-40 mm Hg. The foam reduces the vapor pressure by about a factor 15.

In some cases, the temperature reached is below the ignition temperature; for example, chemical foam on kerosene produces 37-40°, or on diesel oil 40-70°, both of which are below the ignition temperatures. It has been found [6] that the ignition temperature is decisive to extinction in other cases also. Other foams produce extinction with surface temperatures above the ignition temperature; here the cooling is still important, but the retardation of evaporation also plays a major part. Clearly, the balance between cooling and retardation varies, with some part played by screening from the flame.

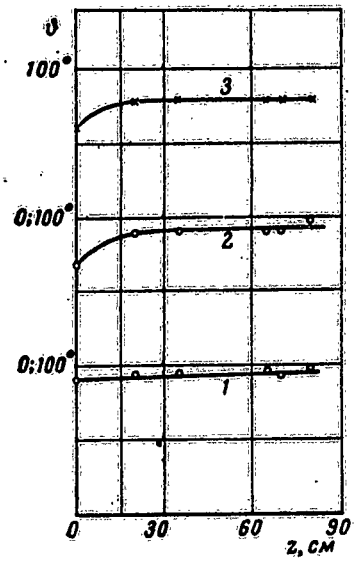

Fig. 26. Temperature in benzine during foam extinction: 1) start; 2) after 60 sec; 3) after 360 sec.

A liquid that gives a homothermal layer is difficult to extinguish, largely because convection brings up the heated layer even during the extinction time. Clearly, a burning liquid would be much more readily extinguished if the top layer could first be cooled in some way.

5. The retardation by foam has been studied [4] in the laboratory. Two crystallizing dishes 144 mm in diameter and 68 mm high were placed on sensitive laboratory scales; one was partly filled with the liquid, and the loss in weight was recorded every 5 min. This gave the rate of free evaporation. Then the two dishes were filled with foam and the readings were repeated; the two dishes eliminated any correction for

evaporation of the foam. A special soap foam was used as being highly stable; a layer 6 cm deep had broken up only partly after several weeks at room temperature. The experiment was performed in a fume cupboard providing a good current of air. All tests

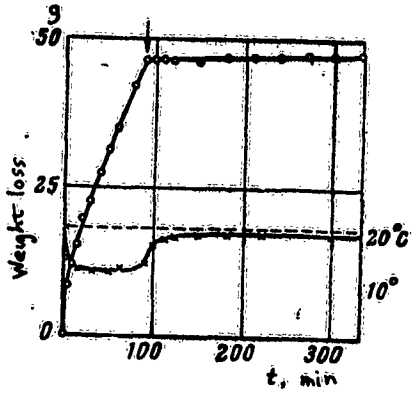

Fig. 27. Evaporation of benzine with and without foam.

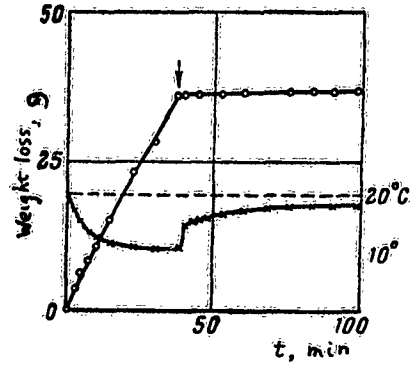

Fig. 28. Evaporation of benzene with and without foam.

were done at room temperature. Figures 27 and 28 give some results, in which the circles denote weight and the crosses temperature of the liquid. The arrows denote the points when the foam was applied. The evaporation rate fell at first and then remained constant until the foam was applied; the foam reduced the rate greatly and raised the temperature somewhat.

Table 3.3

h	$M \cdot 10^4$	$M' \cdot 10^4$	ϑ_k	$\Delta\vartheta$	$\Delta\vartheta'$
53	2,6	4,6	19,5	8	2
52	1,8	1,0	19,5	7	2,5
54	1,5	0,6	18,5	5	1,5
53	0,7	1,5	20	3	1,5
55	1,8	2,3	19	6	1
54	2,7	5,6	23	9	2
50	1,6	7,4	27	6	1

Table 3.3 gives detailed results for benzene; here M is the specific evaporation rate for the free surface in $g/cm^2 min$, M' is the same for the covered surface ϑ_k is room temperature, $\Delta\vartheta$ is the fall caused by the evaporation from the free surface, $\Delta\vartheta'$ is the same for the covered surface, and h is the depth of the foam layer (mm). These results show that the foam reduces the rate by a factor of 55 for benzene and by a factor of 150 for benzine. Similar results were obtained with carbon tetra-

chloride and toluene.

6. The evaporation of a liquid is a rather complex process; some insight into it may be gained as follows. Let us suppose that the rate of evaporation in the above experiments was governed by diffusion through the layer of air in the dish, which is described by an effective diffusion coefficient D'. The process is virtually steady, and the dish was surrounded by an air current, so we may assume that the concentration at the upper edge was zero, that at the surface being c_0, which corresponds to the saturation vapor pressure at the temperature of the liquid.

Then

$$M = D' \frac{c_0}{h}, \tag{3.30}$$

in which h is the distance from the surface to the upper edge. But

$$c_0 = \mu \frac{p}{RT}, \tag{3.31}$$

in which p is saturation vapor pressure, R is the gas constant, T is absolute temperature, and μ is the molecular weight of the liquid. These together give us that

$$D' = \frac{M}{\mu} h \frac{RT}{p}. \tag{3.32}$$

The D' of (3.32) enables us to judge the mechanism of removal from the free surface. The application to benzene is as follows. The mean M is 3×10^{-5} g/cm^{2}sec for h = 5.3 cm; p for 15° is 60 mm Hg. Then (3.32) gives us that D' = 0.62 cm^2/sec; the published [5] D for benzene in air is 0.09 cm^2/sec, and so D' is some seven times D*. Now we turn to the effects of the foam; here M' was 5.5×10^{-7} g/cm^{2}sec, the foam being 5.3 cm deep. We take the concentration at the upper surface as zero, in which case (3.32) gives us D' as 0.009 cm^2/sec, which is only a tenth of D. This D' we denote by D'*. Table 3.4 shows that similar relations apply to other liquids.

These D' differ from D because there are always air currents over the free surface, which remove the vapor, while

---

* The effective D for evaporation from a free surface will in future be denoted by D".

the air within the foam is stagnant. This last feature is one of the factors that reduce the evaporation rate, but it cannot be the only one, for then D'* would equal D, whereas in fact it is much lower. The liquid films in the foam also retard the diffusion; the D for vapors in liquids are thousands of times smaller than those for air, so even thin films of liquid retard evaporation very greatly. The D for the liquids of Table 3.4 are about 0.1 cm^2/sec, whereas those for vapors in liquids are [7] around 10^{-5} cm^2/sec. A film of liquid 60 μ thick would be sufficient to reduce the evaporation rate for benzene at 20° to 5.5×10^{-7} $g/cm^2 sec$; a film 12 μ thick would reduce the rate to 9×10^{-7}, and one of only 5 μ would be as effective as 5 cm of stagnant air. Soap films are a few μ thick, and there are several such films on the route to the surface. This set of films is responsible for much of the retardation; the greater the total thickness of these, the smaller M'.

Table 3.4

Liquid	Diffusion coeff., cm²/sec		
	D	D''	D'*
Benzene	0.09	0.62	0.009
Toluene	0.08	0.21	0.04
CCl_4	0.14	0.50	—
Benzine (automobile) . . .	0.09	0.2	0.003

The diffusion coefficients for vapors in liquids increase rapidly with temperature, being roughly inversely proportional to the viscosity of the liquid. The viscosity of water at 100° is a quarter of that at 20°, so we may expect D'* to vary in the same way. Even so, the films of liquid in the foam still cause most of the retardation.

The results for benzine may serve to illustrate some conclusions here. The burning rate for large vessels is 4 mm/min; a layer of foam 5 cm deep and of temperature close to 100° should reduce the evaporation rate to about 0.1 mm/min (by a factor of 30-40). But experiment shows that the flame cannot persist at this evaporation rate, so the burning ceases. The flame can persist only if the vapor breaks through the foam or if not all the surface is covered by the foam.

7. Finally, we deal with some other aspects of the effects of liquid films. If these form bubbles or a foam, the trapped air takes no part in the convection, so the rate of removal of vapor is much reduced, for the rate of diffusion

through the liquid is some four orders of magnitude lower.

Sometimes a thin film of one liquid on the surface of another will suppress evaporation more or less completely. For example, a layer of 1 mm of oil on water in a crystallizing dish allows virtually no evaporation even in a period of two years. Even the thinnest films retard the evaporation of water very greatly. For example, it has been proposed to eliminate evaporation from reservoirs in Australia in this way, and also to alter the climate over extensive areas of the world.

These films depress evaporation very greatly, especially if the film material is insoluble, for the concentration of the main liquid in the bottom part of the film is very low, so the concentration gradient across the film is also low. But Fick's law states that the amount diffusing across 1 cm^2 in 1 sec is proportional to D and to the concentration gradient; thus the loss is very small indeed if D and the gradient are small.

Floating insoluble thin films could be used to suppress evaporation from burning liquids, especially oil products; such films would provide a rapid and reliable means of extinction, which would solve a very serious problem. We may expect that the problem will be solved in the near future; there are already indications that thin films of certain fluorine compounds can depress the evaporation of benzine substantially [8].

Lastly, it has been claimed in the foreign press that an artificial plastic foam can reduce the evaporation of oil products [9]; Standard Oil of Ohio has used hollow spheres (made of substituted phenols and formaldehyde or furfural) which were filled with nitrogen and were of mean diameter 30 μ. These pack with a density of 0.013 g/cm^3, and a layer 19-25 mm thick of these microspheres reduced the evaporation of volatile products on average by 80%. The layer was stable; in two years of use, the density and mean diameter did not alter. However, our tests with microspheres have not given the remarkable results claimed abroad; sometimes they facilitate evaporation rather than suppress it, for the layer causes the liquid to rise by capillary action. The spheres would have to be repellent to the liquid in order to suppress evaporation.

A layer of microspheres differs very considerably from an ordinary foam; it may reduce the evaporation rate by minimizing the free surface, whereas a foam retards evaporation by virtue of the slow diffusion through the walls of the bubbles.

References

1. L. L. Bogdanov. Mekhanizm ognegasyashchego deistviya peny (Mechanism of the Extinguishing Action of a Foam). Pozharnaya Tekhnika, No. 5, publ. MKKh RSFSR, 1938.

2. G. N. Khudyakov. Usloviya, narushayushchie protsess vygoraniya zhidkosti. Otchet ENIN AN SSSR (Conditions that Interfere with the Combustion of a Liquid. Report of ENIN, Academy of Sciences of the USSR). 1951.

3. V. P. Losev and M. V. Kazakov. O mekhanizme tushashchego deistviya pen pri gorenii nefteproduktov v rezervuarakh (Mechanism of the Extinguishing Action of Foam for Oil Products Burning in Tanks). Inform. sbornik TsNIIPO (Bulletin of the Central Institute for Fire Research), Moscow, publ. MKKh, 1958.

4. V. I. Blinov and G. N. Khudyakov. O mekhanizme tusheniya plameni zhidkostei v rezervuarakh s pomoshch'yu peny (Mechanism of the Extinction of a Liquid Burning in a Tank by Means of Foam). Ibid., 1958.

5. A. S. Irisov. Isparyaemost' topliv dlya porshnevykh dvigatelei i metody eye issledovanie (Evaporation of Fuels for Piston Engines and Methods of Studying it). Moscow, publ. Gostopizdat, 1955.

6. I. I. Petrov and V. Ch. Reutt. Kriticheskie usloviya potukhaniya plameni nefteprodukta pri ego peremeshivaniya v rezervuare (Critical Extinction Conditions for an Oil Product Stirred in a Tank). Inform. sbornik TsNIIPO (Bulletin of the Central Institute for Fire Research), Moscow, publ. MKKh, 1959.

7. Tekhinicheskaya entsiklopediya. Spravochnik fizicheskikh, khimicheskikh i tekhnicheskikh velichin (Technical Encyclopedia. Handbook of Physical, Chemical, and Technical Quantities). Vol. 7, Moscow, publ. OGIZ, 1931.

8. Ind. Eng. Chem., 66, 1954, p. 17a.

9. L. Gubina. Umenshenie ispareniya nefteproduktov pri pomoshchi iskusstvennoi peny iz plastmassy (Reduction of the Evaporation of Oil Products by Means of an Artificial Plastic Foam). Tyl i snabzhenie Sovetskoi Armii (Support and Supplies of the Soviet Army), No. 11, 1955.

Extinction of Burning Liquids with Water Sprays

1. Water sprays have long been used to extinguish oil products burning in tanks [1,2]; at the beginning of this century, Vermishev campaigned vigorously for serious work on the method and made several attempts to demonstrate by experiment that the method is effective with crude oil. Until recently, fine water sprays have not been extensively used to extinguish oil products; the work of the last decade has revealed the main principles of the method.

The major papers here are Khudyakov's [3] and Rasbash and Rogowski's [4]. Khudyakov has used several oil products in a tank 30 cm in diameter; he finds that sprays consisting

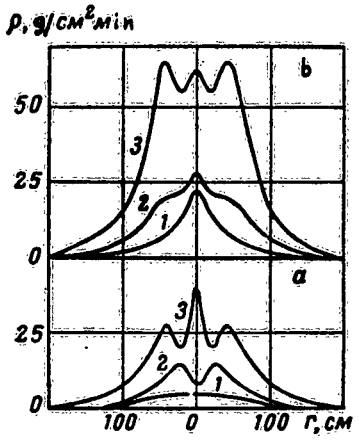

Fig. 29. Relation of flow density to distance from axis of spray for jets of d_c equal to 1, 2, and 3 mm: a) p = 3 atm; b) p = 10 atm.

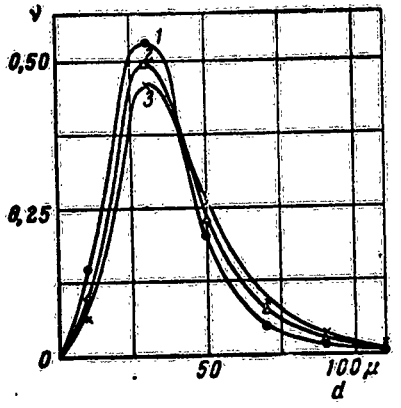

Fig. 30. Droplet size distributions for the centrifugal sprays; p: 1) 10 atm; 2) 6 atm; 3) 3 atm.

of large drops do not cool the flame appreciably but do cool the top layer of liquid. This cooling soon extinguishes heavy oil products, for the surface temperature falls below the flash point. Sprays of very small droplets can extinguish light oil products as well: 'the spray evaporates in the combustion zone and lowers the flame temperature; the steam reduces the concentrations of oxygen and fuel' [3].

Rasbash and Rogowski also used several liquids in a small tank; the extinction time was measured as a function of burning time and of droplet size. They conclude that coarse sprays are effective for liquids of high boiling point, whereas the

formation of steam in the flame (rather than cooling of the liquid) is the significant feature for benzene and other volatile liquids.

Work at the Central Fire Research Institute has shown that fine water sprays can extinguish benzine burning in tanks of large diameter [5]. The most detailed study of fine sprays [6] has recently been supplemented by some work [11] on the extinction of benzine; the earlier study was concerned with diesel oil, kerosene, crude petroleum, and automobile benzine in tanks of diameters 80, 130, and 260 cm. The water was sprayed by centrifugal and pneumatic devices; the flow from any one jet was small, so sets of jets were used. Each of centrifugal sprays consisted of 19 jets arranged on a spherical surface; the diameters d_c of the outlets were 1, 1.5, 2, and 3 mm. Use was also made of a set of 151 jets each of diameter 1.5 mm. The flow V is related to the pressure p by

$$V = A\sqrt{p},$$

in which A is dependent on the size of the spray nozzle, being related to d_c by

$$A = 0{,}17\, d_c^{1{,}25}.$$

The A for the 151-jet device was 2.32 l.cm/sec.kg$^{1/2}$. The cone covered by the sprays had a vertex angle of nearly 180°. Figure 29 shows the flow density ρ in g/cm^2.min at 1 m.

The pneumatic sprays were used in sets of seven, with one in the center and the other six uniformly spaced on a circle. The droplet size was measured by allowing the spray to fall on a plate coated with soot; the droplets left tracks, which were photographed. The diameters d were measured on enlarged prints [7,8]. Figure 30 shows the size distributions for several pressures for the centrifugal system. Nearly all of the d were less than 100 μ, and the position of the peak scarcely varied with pressure. The most probable size was 30 μ, and the mean d was independent of d_c, although it did vary with pressure as $\sqrt[3]{p}$ [9,10]. The pneumatic system did not give such uniform droplets, and the most probable size fell as the pressure increased, as did the mean d (here denoted by $\bar{d}$).

2. The pneumatic sprays were used only with benzine in the 80 cm tank; the sprays were started when the fuel had been burning for 2 min. Figure 31 gives the results in terms of water pressure (abscissa) and air pressure (ordinate); a minus sign in the circle means that the flame did not go out, and a

plus that it did. The extinction succeeds if the pressures lie within the extinction region, which is shown hatched.

3. Many tests (more than 100) were done with the centrifugal pumps in the 130 and 260 cm tanks. The product was left to burn for a set time, then the spray head was inserted. The flame at first became much bigger, then shrank greatly, and finally either went out or became localized under the spray. The

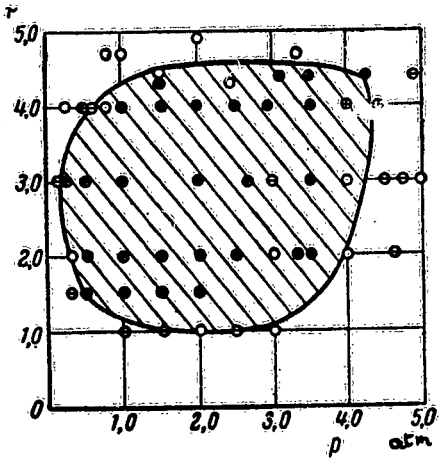

Fig. 31. Extinction of benzine by water from pneumatic sprays.

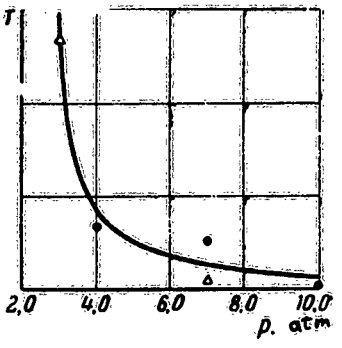

Fig. 32. Extinction time as a function of p for d = 260 cm, d_c = 3 mm.

temperature was measured at points on the axis and at the wall; flow measurements were made, and the distance of the spray head from the surface was recorded, as were the burning and extinction times. The fuel was supplied continuously to keep the level constant in most cases; alternatively, the initial level was set a little high, and the spray was started when the desired level had been reached. Several different oil products were used; the results are given below.

Diesel oil. The extinction time T is related to the water pressure p, and the fire cannot be extinguished if p is below a certain limit, as Fig. 32 shows. Here the ordinate is T', the ratio of T to the T for p = 7 atm. The signs denote experiments done under identical conditions (only p was varied) with d_c = 3 mm. The line corresponds to the formula

$$T' = \frac{b}{p - 2{,}5}.$$

The limiting p for d_c = 3 mm was 2.5 atm (4 atm for d_c = 2 mm; there is a general inverse relation between the two). The flow V for the limiting p was 1.06 l/sec for d_c = 3 mm and 0.81 l/sec for d_c = 2 mm; the smaller flow in the second case implies that the droplet size is the important quantity, rather than the flow, for the smaller the droplets the less the limiting V and the smaller the limiting p. Table 3.5 shows that T falls as V increases; this is especially clear for d = 260 cm.

Table 3.5

d, cm	d_c, mm	t, min	h, cm	H, cm	p, atm	v, l/sec	T, sec
130	1	26	50	74	4	0.2	7
130	2	26	50	74	4	0.8	4
260	1	60	35	75	10	0.5	120
260	3	60	35	75	10	2.1	5

Table 3.6 illustrates the effect of droplet size for the 130 cm tank; $\bar{d}$ and T tend to increase together. Further, T increases with the burning time t and is somewhat dependent on the height H of the spray above the surface, as well as on h, the distance from the surface to the edge of the tank; Table 3.7 gives results for d_c = 2 mm and d = 130 cm. The heated walls play a major part in suppressing the flame, for T decreases as h increases.

The surface temperature at extinction (ϑ') is as follows:

	d=130 H=74 cm						d=260 H=75 cm					
p, atm. .	10	7	4	10	7	4	10	7	10	7	4	7
t, sec. .	5	5	7	3	4	5	16	29	5	24	37	17
ϑ', °C. .	138	123	130	87	100	148	29	53	80	42	47	37

	d=130 H=55 cm	d=130 H=30 cm
p, atm. . .	4	10
t, sec . . .	—	—
ϑ', °C . . .	37	41

The surface temperature during burning (240° for diesel oil) falls sharply as soon as the spray is turned on. ϑ' was well above the ignition temperature when T was short but did not exceed that temperature when T was long; this has an important

Table 3.6

d_c, mm	t, sec	h, cm	H, cm	p, atm	V, l/sec	$\bar{d}$, μ	T, sec
2	21	8	92	3	0.8	55	70
1	17	8	92	10	0.5	44	30
2	27	50	74	4	0.8	55	5
1	27	50	74	10	0.5	44	5

Table 3.7

t, min	h, cm	H, cm	p, atm	T, sec	t, min	h, cm	H, cm	p, atm	T, sec
21	8	92	4	70	21	8	92	10	20
27	50	74	4	5	26	50	74	10	3

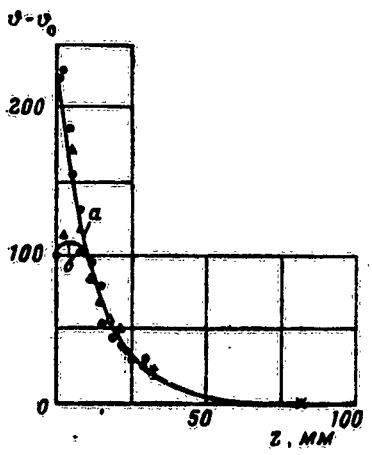

Fig. 33. Temperature distribution in diesel oil before and during extinction.

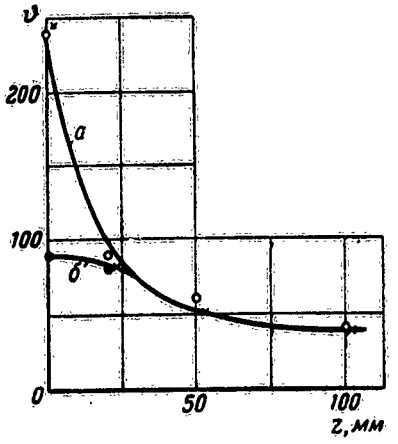

Fig. 34. Temperature distribution in kerosene a) before and b) during extinction.

bearing on the mechanism of extinction. Moreover, the surface temperature during the extinction was somewhat higher at the

edge than at the center.

Figure 33 shows the temperature as a function of depth z; curve a relates to the period before the spray was started, and curve b to the start of extinction. The signs denote several different runs. Clearly, the onset of extinction affects the distribution substantially; the surface is cooled by the water, but the temperature increases with depth for a certain distance and is unaffected by the water at a depth of a few centimeters. The surface temperature ϑ falls continuously during the extinction, while the peak moves to larger z.

Table 3.8

d_c, mm	z_0, cm	t, min	p, atm	V, l/sec	T, sec
1	10	20	10	0,5	60
1	20	15	10	0,5	430
2	5	8	7	1,1	15
2	10	26	7	1,1	28
2	20	21	7	1,1	30
2	5	13	4	0,8	23
2	20	18	4	0,8	60
1	10	20	10	0,5	60
2	10	32	10	1,3	15
1	20	15	10	0,5	430
2	20	20	10	1,3	37
1	10	14	7	0,4	—
2	10	26	7	1,1	28
1	20	22	7	0,4	125
2	20	21	7	1,1	30

Kerosene (flash point about 40°) gave similar results, of which we give here only those for the temperature distribution before and during the extinction (Fig. 34) and those for ϑ'. Here again, ϑ' is above the flash point if T is short but is below it if T is long.

Now we turn to the results for automobile benzine, which gives rise to a homothermal layer. Table 3.8 gives results for d = 130 cm, h = 35 cm, and H = 56 cm; these show that T increases with z_0 (the depth of the homothermal layer) but decreases as V increases. Table 3.9 (for the same dimensions) shows that T increases with $\bar{d}$ even though there is some increase in V. Further, T increases as p decreases, and the flame cannot be extinguished at all if p is below a certain limit. It has been found [6,11] that T and the limiting p

decrease as h increases. Finally, the flame begins to be quenched when ϑ exceeds the flash point, as the following results show:

ϑ', °C	29	36	36	40	43	13	39	16	35	12
T, sec	70	37	30	60	∞	40	30	65	25	135

Figure 35 shows the temperature distribution before (curve a) and during the extinction; the numbers on the curves are the times (in sec) from the start of spraying. The water

Table 3.9

d_c, mm	z_0, cm	i, mm/min	p, atm	V, l/sec	$\bar{d}$, μ	T, sec
1	5	25	10	0,5	44	20
2	5	13	4	0,8	55	23
1	10	20	10	0,5	44	60
2	10	16	4	0,8	55	75

cools the entire heated layer, but the surface is cooled somewhat more rapidly. Table 3.10 and Figs. 36 and 37 give results [12] for tanks 130 cm in diameter; here ϑ is as before, h_x is the thickness of the cold layer at the start, h' is the thickness of the hot layer, t is the spraying time, ϑ' is the final temperature, and u is the mean rate of increase in h'. Figure 36 shows ϑ as a function of time for various depths; Fig. 37, as a function of depth for various times. The hot layer is cooled, but the cool layer is heated, because the water carries heat from the hot layer down to the cool one, which increases the thickness of the hot layer quite rapidly.

It has been found that water sprays can extinguish automobile and aviation benzines in tanks up to 860 cm in diameter*; the extinction times range from 15 to 30 sec.

The results for crude petroleum are largely the same as those for benzine.

4. Before we discuss the above results, we must consider some aspects of the behavior of water droplets in flames

* The benzine may overflow in the process; care must be taken to keep the level of liquid below the top edge of the tank.

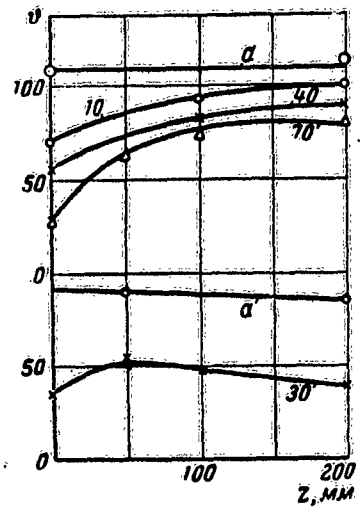

Fig. 35. Temperature distribution in benzine before and during spraying with water.

and in oil products. First we consider the motion.

There have been many studies on droplets in various media, which have been surveyed by Levich [13] and Fuks [14]; some later results [6] derive from cinematographic measurements, which show that droplets falling on an immiscible liquid may break up, in which case complex effects comparable with those at solid surfaces can occur [8,25,26]. Drops that enter the liquid soon attain a steady speed; the motion of a drop is more complex than that of a solid sphere, for the shape can alter. Moreover, surface-active materials can impede movement in the surface of the drop, which then moves as a solid sphere of radius r whose limiting velocity v for small Re is given by Stokes's law as

$$v = \frac{2}{9}\frac{\rho - \rho'}{\eta} g r^2, \qquad (3.33)$$

in which ρ and ρ' are the densities of drop and medium respectively, η is the viscosity of the medium, and g is the acceleration due to gravity. If, on the other hand, the surface of the drop is fully mobile, we have that

Table 3.10

ϑ_0, °C	ϑ, °C	h_x, cm	h', cm	V, mm/sec	d, μ	t, sec	ϑ', °C	u, mm/sec
32	120	35	35	0.2	50—100	500	70	0.6
46	130	40	30	0.5	»	240	70	1.7
50	120	40	30	1.0	»	180	65	2.2
48	140	40	30	0.2	»	600	75	0.7
30	110	40	30	0.2	200—300	550	70	0.7
25	85	35	35	0.5	»	210	52	1.7
30	110	40	30	1.0	»	160	60	2.5

$$v = \frac{2(\rho - \rho')}{3\eta} \cdot \frac{\eta + \eta'}{2\eta + 3\eta'} gr^2, \qquad (3.34)$$

in which η' is the viscosity of the drop; (3.34) becomes (3.33) if $\eta' = \infty$. The latter formula gives the higher v, but both are in close agreement with experiment if $Re \ll 1$. The two are applicable to droplets in flames and oil products provided that the diameter does not exceed 150 μ, which is so for almost all the droplets produced by the above devices.

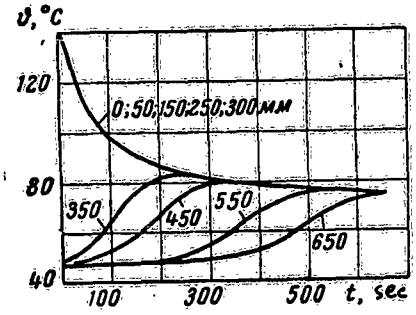

Fig. 36. Temperature as a function of time for various depths in benzine sprayed with water.

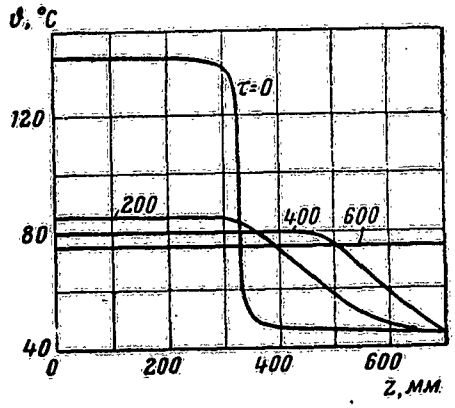

Fig. 37. Temperature as a function of depth for various times during the spraying of benzine with water.

Of course, impure water is used on fires, so Stokes's formula should be used.

5. Consider now the temperature of a drop falling through a flame; the drop is heated and starts to evaporate. In the nearly steady state, the influx of heat q is balanced by evaporation:

$$q = 4\pi r^2 \alpha (\vartheta - \vartheta') = -c^x \frac{dm}{dt} = 4\pi r^2 \alpha_m c^x (\pi' - \pi), \qquad (3.35)$$

in which α and α_m are the coefficients of heat and mass transfer respectively, ϑ and ϑ' are the temperatures of medium and drop, π and π_c are the vapor pressure of water in the flame and the

saturation vapor pressure at temperature ϑ', $c^{\varkappa}$ is the latent heat of evaporation, and m is the mass of the drop.

It is found [13, 15-18] that

$$\alpha = \alpha_0 \varphi(r, v), \quad \alpha_m = \alpha_{0m} \varphi(r, v), \tag{3.36}$$

in which α_0 and α_{0m} are independent of r and v; then (3.35) and (3.36) give us that

$$\vartheta - \vartheta' = \beta(\pi' - \pi). \tag{3.37}$$

This β is also independent of r and v.

Formula (3.37) has long been used for determining atmospheric humidity by reference to wet- and dry-bulb thermometers [24]; it implies that ϑ' is a function of ϑ and π but not of r and v. Fedoseev and Polishchuk [19] have shown that (3.37) is applicable to drops in gases heated to 700°. The following results are for π = 12 mm Hg; they derive from (3.37) and the paper quoted:

ϑ, °C	400	500	600	700	800	900	1000	1100
ϑ', °C	65	70	75	78,5	82	86	88,5	91

Of course, ϑ' alters if π changes. These figures indicate that the droplets reaching the hot oil product should have temperatures not exceeding 90°.

Now we turn to the heating and evaporation in the flame. Let c be the specific heat of the drop, whose initial temperature and radius are ϑ_0 and r_0; let τ and τ' be the times of heating and evaporation. Further, let ϑ_φ, λ, η, and ν be respectively the temperature, thermal conductivity, viscosity, and kinematic viscosity of the gases in the flame, t being time. If we assume that the drop is heated but does not evaporate, we have that

$$\frac{4}{3}\pi r_0^3 \rho c \frac{d\vartheta'}{dt} = 4\pi r_0 \alpha (\vartheta_\Phi - \vartheta').$$

But ρ and c are unity for water, and $\vartheta_\varphi \gg \vartheta'$, so the integral of the equation for time τ is

$$\tau = \frac{1}{3} \frac{\vartheta' - \vartheta_0}{\vartheta_\phi \alpha} r_0. \tag{3.38}$$

Next, the evaporation time for a drop of temperature ϑ' is given by

$$-\rho c^x \frac{dr}{dt} = \alpha \vartheta_\phi, \tag{3.39}$$

in which α is a function of v and r. Sokol'skii and Timofeeva [16] give that

$$\alpha = \frac{\lambda}{r}(1 + 0{,}08\,\mathrm{Re}^{1/2}). \tag{3.40}$$

If now v is given by Stokes's law, and if $r < 100\ \mu$, we have $0.08\mathrm{Re} \ll 1$, so $\alpha = \lambda/r$. The integral of (3.39) is then

$$\tau' = \frac{c^x}{2\lambda\vartheta_\phi} r_0^2; \tag{3.41}$$

$$\frac{\tau'}{\tau} = \frac{3}{2} \frac{c^x}{\vartheta' - \vartheta_0}. \tag{3.42}$$

But (3.42) implies that τ'/τ is independent of r; this is readily shown to be so if v is not governed by Stokes's law but $0.08\mathrm{Re} \ll 1$. Now c^x is 540 cal/g; if $\vartheta' - \vartheta_0 = 60°$, then $\tau'/\tau = 13.5$.

This justifies us in assuming (as is usual) that the evaporation takes place in two stages; first the drop is heated (evaporation being negligible), and then the drop evaporates at constant temperature.

We may also determine τ and τ' approximately by means of (3.38) and (3.41). We put ϑ_ϕ as 1000° and $\Delta\vartheta$ as 60°, with λ as the value for air at the appropriate temperature (2×10^{-4} cal/cm·sec·deg for 1000°). Then $\tau' = 1350 r_0^2$ and $\tau = 100 r_0^2$; if $2r_0 = 0.01$ cm = 100 μ, $\tau = 2.5$ msec, $\tau' = 34$ msec, and $\tau + \tau' = 36$ msec.

We can find τ in another way. The apparatus with 19 jets each with $d_c = 3$ mm had a V of 2.1 l/sec at 10 atm; the

jets emerged at 16 m/sec. We assume that the droplets move with this speed; then $\alpha = \lambda(1 + 12r_o)/r_o$. If $r_o = 50\ \mu$, $\alpha = 1.35\ /r_o$, in which case τ and τ' come out as 1.35 times the values given above. Stokes's formula gives the v for $r = 0.005$ cm as about 10 cm/sec, so a change in v from 10 to 1600 cm/sec alters τ and τ' by only a factor 1.35. But 16 m/sec must be much more than the terminal speed of a drop, and the above r_o is the maximum used in the experiments, so the true τ and τ' must be very close to those given by (3.38) and (3.41) with $\alpha = \lambda/r_o$.

Although τ and τ' vary little with v within the above limits, the times t spent in the flame do vary greatly, for $t = h/v$, h being the distance from jet to liquid. For example, $t = 63$ msec if $h = 100$ cm and $v = 16$ m/sec; $t = 10$ sec if the steady-state v is used and $r_o = 50\ \mu$, or 2.5 sec if $r_o = 100\ \mu$ (both for $h = 100$ cm). A drop with $r_o = 50\ \mu$ would evaporate completely even for $v = 16$ m/sec, whereas one with $r_o = 100\ \mu$ would evaporate partly at 16 m/sec but completely at the steady-state speed; the life of a drop is a function of v and r_o. Large drops pass through the flame and reach the surface; the limiting radius for which this is possible decreases as the flame temperature falls.

These results show that most of the drops evaporate before they reach the liquid, but that the proportion surviving increases as the flame cools. That proportion is clearly dependent also on h.

7. Consider now the drops that do reach the liquid. These soon reach a steady speed, which is given by Stokes's law if r is small. The solubility of water in oil products is very low, so r may be taken as constant. (The drops are merely heated.) Let us suppose that the top layer is a homothermal layer of temperature ϑ_c and that this layer is free from convection. The heat received in time dt is

$$dq = 4\pi r^2 \alpha\,(\theta_c - \theta)\,dt = \tfrac{4}{3}\pi r^3\,d\theta.$$

The integral to this, with $z = vt$ and $\vartheta = \vartheta_0$ at $z = 0$ is

$$\frac{\theta_c - \theta}{\theta_c - \theta_0} = e^{-\beta z},\quad \beta = 3\frac{\alpha}{rv}. \tag{3.43}$$

Formula (3.43) shows that ϑ increases rapidly at first,

until ϑ_c is approached, the rate of approach increasing with β. The heat transfer factor α determines β; it is given by (3.40), but the second term on the right in (3.40) is small relative to the first if $r < 100\ \mu$, and so we have that

$$\alpha = \frac{\lambda}{r} \qquad \beta = \frac{3}{v_0 r^4} = \frac{\beta_0}{r^4}, \tag{3.44}$$

$$v_0 = \frac{2}{9} \frac{\rho - \rho'}{\eta'} g;$$

in which ρ is the density of water, ρ' is the density of the oil product, and η' is the viscosity.

(3.43) and (3.44) show that the distance needed to attain the temperature ϑ_c increases very rapidly with r, as does the thickness of the layer so cooled. For example, a drop with $r = 100\ \mu$ attains the temperature of benzine within 1 cm, whereas one with $r = 50\ \mu$ does the same in a few mm.

The heated drops then enter a layer having the initial temperature of the liquid; here they are cooled in accordance with

$$\frac{\vartheta - \theta_0}{\theta_s - \theta_0} = e^{-\beta z},$$

which is comparable with (3.43). The temperature of the layer will become uniform if convection is present.

Consider now the temperature of a drop entering an oil product whose temperature is given by

$$\frac{\theta - \theta_0}{\theta_s - \theta_0} = e^{-hz}. \tag{3.45}$$

(this applies for diesel oil, kerosene, solar oil, and certain other products). Now

$$4\pi r^2 \alpha (\theta - \vartheta)\, dt = \frac{4}{3} \pi r^3 d\vartheta,$$

so

$$d\vartheta = \beta (\theta - \vartheta) dz,$$

and the problem is that of solving

$$\frac{d\vartheta}{dz} = \beta\,(\theta_s - \theta_0)\,e^{-kz} + \beta\,(\theta_0 - \vartheta).$$

We introduce a new variable y defined by

$$\theta_0 - \vartheta = ye^{-kz}.$$

Transferring from ϑ to y, we have

$$\frac{dy}{dz} = -\beta\,(\theta_s - \theta_0) + (k - \beta)\,y.$$

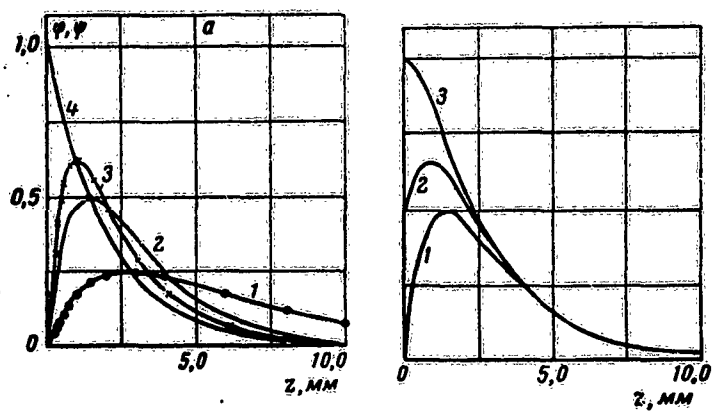

Fig. 38. Temperature as a function of distance from the surface for a drop moving in an oil product; a) φ and ψ as functions of z for β of 1) 0.25; 2) 1.0; 3) 2.0; 4) ψ = f(z) for k = 0.5; b) temperature as a function of z for φ_0 of 1) 0, 2) ½, 3) 1. (β = 1.0, k = 0.5).

The integral of this is

$$\vartheta = \theta_0 - \beta\,\frac{\theta_s - \theta_0}{k - \beta}\,e^{-kz} - Be^{-\beta z},$$

in which B is a constant of integration. But $\vartheta = \vartheta_0$ at z = 0 and $\vartheta = \theta_0$ at z = ∞, so

$$\frac{\vartheta - \theta_0}{\theta_s - \theta_0} = \frac{\beta}{k - \beta}\,(e^{-\beta z} - e^{-kz}) + \frac{\vartheta_0 - \theta_0}{\theta_s - \theta_0}\,e^{-\beta z}. \qquad (3.46)$$

Consider the particular case $\Theta_0 = \vartheta_0$. Then

$$\frac{\vartheta - \vartheta_0}{\vartheta_s - \vartheta_0} = \frac{\mu}{k - \beta}(e^{-\beta z} - e^{-kz}).$$

Figure 38 shows the relation of ϑ to z in terms of φ and ψ.

$$\psi = \frac{\vartheta - \vartheta_0}{\vartheta_s - \vartheta_0}, \quad \varphi = \frac{\vartheta - \vartheta_0}{\vartheta_s - \vartheta_0}.$$

The curves have been constructed on the assumption that k = 0.5 cm^{-1}, with β of 0.25, 1.0, and 2.0 cm^{-1} (β decreases as r increases). The curves show that the temperature $\vartheta(z)$ passes

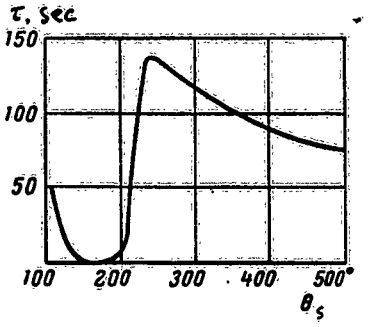

Fig. 39. Evaporation time as a function of surface temperature for drops on a solid.

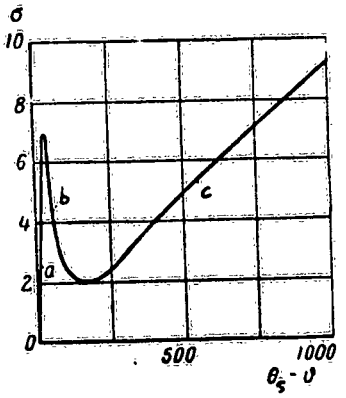

Fig. 40. Heat flux density from heated wall to drop.

through a maximum if (3.46) defines the temperature of the oil; the position z_m of this maximum is dependent on r for a given k, for z_m increases with r. For example, $\beta = 2$ if $z_m = 1$ and $k = 0.25$ cm^{-1}; (3.46) then gives $r = 200$ μ.

Figure 38b shows that the shape of $\varphi(z)$ is governed by ϑ_0, for the peak rises and moves to the left as ϑ_0 increases. Figure 38 indicates that the water cools the top layer and warms the lower layers; the precise effect is dependent on ϑ_0, but, in any case, the result is not the same as that of stirring the liquid.

8. Some of the spray falls on the hot wall, so we must examine the effects there.

The evaporation time τ for a drop on a solid is dependent

on the surface temperature ϑ_s [20,21], as Fig. 39 shows for drops of water of radius 2.3 mm [20]. At first α falls as ϑ_s increases, but a maximum is reached at 240°. This behavior is a result of the spheroidal state, which occurs when ϑ_s exceeds some critical value ϑ_c, which is well above the boiling point (Rebinder and Pletneva find that this state occurs with water when $\vartheta_s \geq 250°$). This ϑ_c is independent of r. In this state the drop is separated from the surface by a thin layer of vapor, which impedes the transfer of heat.

Figure 40 [20] shows the relation of the heat flux σ to the temperature difference $\vartheta_s - \vartheta$. Branch a corresponds to boiling in which distinct bubbles of vapor are formed; this is replaced by film boiling when $\vartheta_s > \vartheta_c$, and here the heat flux is much lower. The following experiment illustrates the interaction between a water spray and a heated wall. A thick brass disc was fixed to an electric hotplate, and the temperature was brought to the desired value. The disc was then exposed to a spray from a miniature centrifugal sprayer. Photographs showed that drops falling on the unheated disc did not evaporate; some rebounded, but the surface became very wet. Steam was produced vigorously at 110°, and the amount increased up to 250°, but further increase produced less steam. Similar results were obtained with single drops falling on a horizontal disc; at room temperature they broke up and wetted the disc, whereas at higher temperatures they still broke up, but the disc rapidly dried off. No wet spots were observable at 210°, and the drops did not wet the disc at all at about 250°. At 315° and above, the droplets produced by fragmentation bounced over and off the surface; very small ones evaporated.

These observations are in accordance with the general trends described above; the process as a whole is complex.

9. The above results and deductions give us a fairly complete picture of the mechanism whereby a water spray extinguishes a burning liquid.

The burning ceases sometimes (always, for volatile liquids) when the surface temperature is well above the ignition temperature; this shows that processes in the flame are mainly responsible, not the effects on the liquid. Cooling of the surface plays the main part only when the surface temperature approaches the ignition temperature.

The processes in the flame are as follows. Droplets less than 100 μ in size (the vast majority of all droplets from the sprayers) evaporate completely in the flame if the path from sprayer to surface is reasonably long; larger drops evaporate only partly. This evaporation produces much steam in

the flame, which is cooled and ''luted; moreover, the steam tends to prevent the air from reaching the surface. Very rapid evaporation may cool and disrupt the flame so greatly that it can no longer persist; the steam and vapor, together with some air, form a rapidly moving flow, whose speed is partly the result of the low density of steam (less than that of air by a factor 1.7). This flow makes the ''me much taller; the effect is always observed at the start of extinction. The flame soon shrinks and vanishes if steam is formed sufficiently rapidly. A sufficient inflow of wate. .pray will extinguish even a very volatile liquid. No standard method is as powerful and flexible as this; even better results might be obtained if the water were mixed with some very volatile but incombustible liquid, as Petrov and Tsygan [28] have recently shown.

The larger drops evaporate in part during the initial phase; the residual parts of them cool the liquid somewhat and so depress the evaporation, but the effect is comparatively minor.

9. If the flow of spray is insufficient to put the flame out rapidly, the burning is at first only heavily depressed; the result is that the lower temperature allows more drops to enter the liquid, which is thereby cooled, so the evaporation rate falls. The flame becomes still cooler, even more drops enter the liquid, and so on. The flame goes out in some areas, but the continuing flow of water cools the liquid further, and eventually the flame is extinguished entirely.

Figure 38 illustrates the effects of the water on the temperature distribution in the liquid. Of course, the flame is extinguished in this case only when Θ_s falls below the ignition temperature, so this method takes longer than the previous one; moreover, it can work only for liquids of high ignition temperature, not for volatile ones. Here the evaporation in the flame plays a vital part. The flame is usually located under the spray after the initial period.

A poorly dispersed flow of inadequate density does not, in general, produce extinction.

10. A major part may be played by the steam formed at the heated wall, which may be at over 700° near the top, so the heat flow to the spray may be high. There can be no vigorous production of steam in this way if the liquid level is high, for the area is small and the temperature is low. Conditions are more favorable if the level is low; the flame is extinguished more readily and more rapidly. Of course, steam may be formed also at the surface of the liquid, if the drops of

water remain there.

These observations elucidate all the trends that have been reported in extinction studies. Some further trends deducible from the experiments are as follows.

The extinction time T is a function of H (the distance from sprayer to surface); the flame is not extinguished even when the water pressure p is high if H is small. For example, a p of 10 atm did not give extinction in one case, whereas much lower p did give extinction under other conditions. The reason was undoubtedly that the path was short and, moreover, only the central part of the tank was vigorously sprayed because H was small; the cooling at the edges was slight, and no steam was formed at the walls, so the flame did not go out. Again, the extinction was not so rapid for distances in excess of the optimum H, because part of the spray missed the burning area or was carried off by the wind.

Sometimes the burning did not stop although the surface temperature at the axis was below the flash point, because the edges are always hotter than the center. Clearly, here the edge temperature was too high and the spray density was too low. This illustrates the importance of the distribution of the spray, which is dependent on the design of sprayer, on the pressure, and on the position of the sprayer.

It is sometimes claimed that diesel oil and kerosene are better extinguished by coarse sprays, but our results do not confirm this, for the method is particularly effective at the higher pressures, which give fine sprays in sufficient volume. These fine sprays give rise to much steam, and the flame soon goes out; steam is not produced so vigorously if the drops are large, the process takes longer, and the cooling of the liquid becomes important.

11. Crude petroleum and benzine give rise to a homothermal layer, which steadily becomes deeper. This layer is the scene of vigorous turbulence. The temperature of this layer falls when the flame begins to be extinguished, and its thickness is increased by the stirring produced by the water. The convection dies away only towards the end of the extinction; it is a major impediment to the process.

Any measure that would suppress the development of this layer would assist the process; the layer does not develop [11,22,23] if the wall is cooled with water [11,23]. The process may be accelerated by cooling the part of the wall below the surface of the liquid; cooling above the surface depresses the production of steam and so retards the process.

12. Experience shows that burning benzine can be extinguished with water sprayed pneumatically, but the pressures must lie within the extinction region. Clearly, the need here is for an adequate amount of water in the form of a fine spray. Moreover, the air injected into the flame has an adverse effect. Extinction does not occur at low water flows, for the burning is not sufficiently depressed; moreover, low water pressures give coarse sprays, which are ineffective, for they do not produce steam rapidly. Large air flows give a fine spray, but extinction does not occur, for the air increases the combustion density and the rate of evaporation of the fuel. Here the air acts much as does the wind, in that it stimulates the flame. This means that pneumatic sprayers, which in any case demand special equipment for supplying the air, should not be used (apart from for certain special purposes).

Combined Extinction of Oil Products Burning in Tanks

We have seen above that a foam first cools the surface (and is thereby partly destroyed) and then covers the surface with a blanket that largely suppresses evaporation. The cooling action may be insufficient, and the foam may be rapidly destroyed, if the liquid has been burning for a long time.

A foam is far more effective if the surface is first cooled in some way; this means that several combined methods are possible [6,27-29], and these have been studied by Petrov and Tsygan [3,28] and by Petrov et al [12]. We consider here some of the results given in [28], which relate to benzine burning in a tank 130 cm in diameter; the fuel was first cooled with water sprayed from a special rotating sprayer and then was treated with foam:

h, cm	t, min	z_0, mm	V, l/sec·m²	t_0, min	V', l/sec·m²	T, min	Result
40	47	400	—	—	0,32	23	+
40	45	400	2,1	7	0,32	10	+
50	48	400	—	—	0,5	—	—
50	140	400	2,1	2	0,5	1,2	+

Here h is the distance from the surface to the edge of the tank, t is burning time, z_0 is the depth of the homothermal layer before the water was applied, V is the flow of water, t_{ox} is the duration of the water spray, V' is the flow rate of the foam, and T is the extinction time for the foam. This

preliminary cooling reduced T substantially and gave extinction when the foam alone was unable to do this.

In certain cases burning benzine or petroleum was stirred with an air jet before treatment with foam; this again was more effective than foam alone. Stirring is reasonably effective, of course, when the fuel has not become heated throughout most of its depth.

To conclude, we ma_ _.int out that diffusion burning of liquids in tanks has been studied for only two decades, but that much experimental evidence has been accumulated. This evidence demonstrates a number of important principles and gives us a reasonably clear picture of the processes of ignition, burning, and extinction. All the same, it must be considered as only the first stage in the construction of a detailed theory of the processes.

References

1. I. A. Vermishev. Ognegasitel'nye svoistva kipyashchei vody i poluchenie ee na pozhare pri pul'verizatsii kholodnoi vody. Doklad na zasedanii khimicheskogo otdelenie IRTO 26 marta 1903 (Extinguishing Properties of Boiling Water and the Production of it in the Fire by Atomization of Cold Water. Paper at the Meeting of the Chemical Section of IRTO 26 March 1903).

2. L. Ya. Tslaf and A. N. Zotikova. Tushenie legkovosplamenyashchikhsya zhidkostei v statsionarnykh nazemnykh emkostyakh raspylennoi vodoi. Otchet TsNIIPO, 1940 (Extinction of Readily Ignited Liquids in Fixed Storage Tanks with Water Sprays). Report of the Central Research Institute for Fire-Fighting, 1940.

3. G. N. Khudyakov. Usloviya, narushayushchie protsess vygoraniya zhidkostei. Otchet ENINa, 1951. (The Conditions that Interfere with the Burning of Liquids. Report of ENIN, 1951).

4. D. J. Rasbash and Z. W. Rogowski. The Extinction of Liquid Fires with Water Sprays. Chemistry and Industry, 24, No. 1, 1954; Combustion and Flame, No. 4, 1957.

5. N. M. Antonov and N. F. Lebedev. Issledovanie sposoba tusheniya pozharov nefteproduktov raspylennoi szhatym Vozdukhom (aerirovannoi) vodoi. Otchet TsNIIPO, 1956 (A Study of the Method of Extinguishing Oil-Product Fires with Water Dispersed [Aerated] with Compressed Air. Report of the Central Research Institute for Fire-Fighting, 1956).

6. V. I. Blinov, G. N. Khudyakov, and I. I. Petrov. O mekhanizme tusheniya goreniya nefteproduktov raspylennoi vody. Inf. sbornik TsNIIPO (The Mechanism of the Extinction of Burning Oil Products with Sprayed Water. Bulletin of the Central Research Institute for Fire-Fighting), Moscow, publ. MKKh, 1958.

7. N. N. Strulevich and Yu. F. Dityatkin. O sootnoshenie mezhdu diametrom kapli i ee otpechatkom na sloe saxhi. Tekhnicheskii byulleten' TsIAM (The Relation of Diameter to Imprint on a Soot layer for a Drop. Technical Bulletin of TsIAM), No. 2, 1949.

8. G. D. Salamandra and N. M. Naboko. Ulavlivanie na plastinku, pokrytuyu sloem sazhi, kak metod opredeleniya krupnosti raspylennniya topliva (Deposition on a plate coated with Soot as a Method of Determining the Droplet Size of Sprayed Fuel). Zh. Tekh. Fiz., 27, No. 3, 1957.

9. V. I. Blinov. O dispersnosti mekhanicheski raspylennoi vody (Droplet Sizes of Mechanically Sprayed Water). Moscow, publ. VTI, 1933.

10. I. I. Novikov. Zakonomernosti drobleniya zhidkostei v tsentrobezhnykh forsunkakh (Laws of Dispersion for Liquids in Centrifugal Pumps). Zh. Tekh. Fiz., 18, No. 3, 1948.

11. I. I. Petrov and V. Gerasimov. Tushenie pozharov nefteproduktov v rezervuarakh raspylennoi vodoi (Extinction of Oil-Product Fires in Tanks with Sprayed Water). Otchet TsNIIPO (Report of the Central Fire-Fighting Research Institute), 1957.

12. I. I. Petrov, V. Ch. Reatt, and V. P. Losev. Razrabotka prakticheskikh rekomendatsii po kombinirovannomu metodu tusheniya nefteproduktov v rezervuarakh (Development of Practical Notes on a Combined Method of Extinguishing Oil Products in Tanks). Ibid., 1958.

13. V. G. Levich. Fiziko-khimicheskaya gidrodinamika (Physico-Chemical Hydrodynamics), publ. Acad. Sci. USSR, 1952.

14. N. A. Fuks. Mekhnika aerozolei (Mechanics of Aerosols), publ. Acad. Sci. USSR, 1955.

15. Boussineque. J. de Mathematique, No. 285, 1905.

16. A. N. Sokol'skii and F. A. Timofeeva. O skorosti sgoraniya pyl. Sb. "Issledovanie protsessov goreniya natural'nogo topliva (Rate of Combustion of Dust. Coll.: 'Study of Combustion Processes for Natural Fuel'), Moscow, publ. Gosenergoizdat, 1948.

17. D. N. Vyrubov. Teplootdacha i isparenie kapel' (Heat Loss and the Evaporation of Drops). Zh. Tekh. Fiz., 9, No. 21, 1939.

18. N. A. Fuks. Isparenie i rost kapel' v gazoobraznoi srede

(Evaporation and Growth of Drops in a Gaseous Medium), publ. Acad. Sci. USSR, 1958.

19. D. I. Polishchuk. Isparenie kapel' pri temperaturakh sredy, prevyshayushchikh temperaturu kipeniya (Evaporation of Drops at Temperatures above the Boiling Point). Zh. Tekh. Fiz., 23, No. 12, 1953.

20. S. S. Kutateladze. Teploperadacha pri kondensatsii i kipenii (Heat Transfer in Condensation and Boiling), Moscow, publ. Mashgiz, 1952.

21. N. A. Pletneva and P. A. R[illegible]inder. Zakonomernosti ispareniya kapel' zhidkosti v sferoidal'nom sostoyanie (Laws of Evaporation for Drops of Liquid in the Spheroidal State). Zh. Tekh. Fiz., 20, No. 9, 1946.

22. P. P. Pavlov and A. M. Khovanova. Vliyamie okhlazhdeniya stenok rezervuara na gorenie i tushenie nefteproduktov (Effects of cooling the Walls of a tank on the Burning and Extinction of Oil Products). Inform. pis'mo bakinskoi laboratorii TsNIIPO (Newsletter of the Baku Laboratory of the Central Research Institute for Fire-Fighting), 1956.

23. V. I. Blinov and G. N. Khudyakov. K voprosu o raspredeleniya temperatury v nefteproduktakh, sgorayushchikh v tsilindricheskikh rezervuarakh (Temperature Distribution in an Oil Product Burning in a Cylindrical Tank). Informats. pis'mo No. 7 Energeticheskogo in-ta AN SSSR (Newsletter No. 7 of the Power Institute, Acad. Sci. USSR), 1958.

24. J. C. Maxwell. Collected Scientific Papers, vol. 11, p. 625, Cambridge, 1890.

25. Olliver. A Study of Capillarity. Ann. Chem. Phys., 10, 229, 1907.

26. V. I. Blinov and G. N. Khudyakov. Issledovanie mekhanizma tusheniya plameni nefteproduktov s pomoshch'yu starykh i novykh ognegasitel'nykh sredstv (A Study of the Mechanisms of Extinction of Oil Products by means of Old and New Extinguishing Agents) Otchet ENIN AN SSSR (Report of ENIN, Acad. Sci. USSR), 1956.

27. V. I. Blinov, G. N. Khudyakov, and V. I. Losev. Izuchenie mekhanizma tusheniya goreniya nefteproduktov penami (A Study of the Mechanism of Extinction of Oil Products by Foams). Ibid, 1956.

28. I. I. Petrov and S. M. Tsygan. Metody kombinirobannogo tusheniya pozharov nefteproduktov v rezervuarakh (Methods of Combined Extinction for Oil Products in Tanks) Otchet TsNIIPO (Report of the Central Research Institute for Fire-Fighting) 1957.

29. J. H. Burgoyne, L. L. Katan, and J. F. Richardson. Extinguishing Petroleum Fires. Fire Protection and Accident Prevention Review XI, 12, No. 109, p. 491-3, 1949.

30. G. N. Khudyakov. O sposobakh i ognegasitel'nykh sredstvakh pri bor'be s pozharami (Methods and Extinguishing Agents for Dealing with Fires) Inform. sbornik TsNIIPO (Bulletin of the Central Research Institute for Fire-Fighting), 1954.